

Evangeline G. Warmerdam

Advanced imaging and intervention in congenital heart disease



Advanced imaging and intervention in congenital heart disease

Evangeline G. Warmerdam

COLOPHON

Cover design:	James Jardine www.jamesjardine.nl
Layout:	James Jardine www.jamesjardine.nl
Print:	Ridderprint www.ridderprint.nl
ISBN:	978-94-6416-345-2

Copyright © Evangeline G. Warmerdam 2021. All rights reserved. No parts of this publication may be reproduced, stored in a retrieval system or transmitted in any form by any means without prior permission of the author.

Advanced imaging and intervention in congenital heart disease

Geavanceerde beeldvormende diagnostiek en interventie
in aangeboren hartafwijkingen
(met een samenvatting in het Nederlands)

P R O E F S C H R I F T

ter verkrijging van de graad van doctor aan de
Universiteit Utrecht
op gezag van de
rector magnificus, prof. dr. H.R.B.M. Kummeling,
ingevolge het besluit van het college voor promoties
in het openbaar te verdedigen op

donderdag 26 augustus 2021 des middags te 2.15 uur

door

Evangeline Gerdine Warmerdam

geboren op 10 september 1991
te Ede

Promotoren

Prof. dr. P.A.F.M. Doevendans
Prof. dr. T. Leiner

Copromotoren

Dr. M. Voskuil
Dr. H.B. Grotenhuis

Financial support by the Dutch Heart Foundation for the publication of this thesis is gratefully acknowledged.

Publication of this thesis was additionally supported by Pie Medical Imaging.

Werken en feesten vormt schoone geesten.

- Prof. dr. Johanna Westerdijk

Table of contents

Chapter 1	General introduction and thesis outline	9
Chapter 2	Three-dimensional and four-dimensional flow assessment in congenital heart disease	19

PART ONE: COARCTATION OF THE AORTA

Chapter 3	Abnormal aortic flow related to left ventricular mass and volume in coarctation: a four-dimensional flow CMR study	39
Chapter 4	Effect of stent implantation on blood pressure control in adults with coarctation of the aorta	59
Chapter 5	Safety and efficacy of stenting for aortic arch hypoplasia in patients with coarctation of the aorta	75

PART TWO: TETRALOGY OF FALLOT

Chapter 6	Percutaneous pulmonary valve implantation; current status and future perspectives	93
Chapter 7	Four-dimensional flow CMR in tetralogy of Fallot: current perspectives	125

PART THREE: TRANSPOSITION OF THE GREAT ARTERIES

Chapter 8	Head-to-head comparison between computational fluid dynamics and four-dimensional flow CMR of the pulmonary arteries in congenital heart disease	145
-----------	--	-----

Chapter 9	Head-to-head comparison of 4D flow CMR, 2D phase-contrast CMR and Doppler echocardiography for the detection of pulmonary artery stenosis in patients after the arterial switch operation	163
Chapter 10	Echocardiography and MRI parameters associated with exercise capacity in patients after the arterial switch operation	179
Chapter 11	Abnormal vortex formation in the right pulmonary artery after the arterial switch operation	199
Chapter 12	Impact of pulmonary haemodynamics on exercise performance in patients after the arterial switch operation	207
Chapter 13	General discussion and future perspectives	225

APPENDIX

Nederlandse samenvatting	239
List of publications	247
Review committee	251
Dankwoord	253
Curriculum vitae	259



Chapter 1

General introduction
and thesis outline

INTRODUCTION

Congenital heart disease (CHD) is defined as a structural cardiovascular anomaly, resulting from abnormal development of the heart, or blood vessels near the heart, before birth. It is the most common congenital defect, with an estimated prevalence of 8 per 1000 live births.¹ This means that in The Netherlands around 1500 children are born with CHD each year. Only several decades ago, a minority of patients with CHD reached adulthood and therapeutic options were limited. Due to major advances in diagnostics, surgical techniques, perioperative care and percutaneous techniques, the survival rate of patients with CHD has improved dramatically. Nowadays, 70% - 95% of patients survive into adulthood.² Unfortunately, the increase in survival goes hand in hand with an increase in morbidity. Patients with all types of CHD encounter late complications, such as heart failure, cardiac arrhythmias, and pulmonary hypertension.³ These sequelae usually arise either from the longstanding haemodynamic abnormalities or as a consequence of required intervention(s). The increase in survival combined with considerable morbidity results in a growing population of CHD patients that requires lifelong surveillance. Furthermore, a considerable number of patients will also require (repeat) interventions. This highlights the need for comprehensive non-invasive diagnostic techniques and minimally invasive treatment strategies.

Although diagnostic modalities available for evaluation of cardiac anatomy and function in CHD patients are ample, the modalities most frequently used – echocardiography, computed tomography (CT) and cardiac magnetic resonance (CMR) – are not able to provide an advanced evaluation of cardiovascular blood flow. In recent years, the role of altered blood flow in cardiac development and CHD has become a subject of interest. Patients with CHD often have abnormal blood flow patterns, either due to the primary cardiac defect or as a consequence of the surgical intervention(s). Research suggests that these abnormal blood flow patterns may contribute to diminished cardiac and vascular function.⁴ Since the majority of CHD patients require lifelong follow-up, there is a need for patient-friendly and non-invasive imaging modalities that can help acquire haemodynamic evaluation. Serial assessment of haemodynamic parameters in patients with CHD may allow for improved understanding of the often-complex haemodynamics in these patients and thereby potentially guide the timing and nature of interventions. In this thesis we investigated the value of three- and four-dimensional imaging in different CHD populations. In **chapter 2** we review the available literature on computational fluid dynamics (CFD) and four-dimensional flow CMR (4D flow CMR) to explore the additional value of these two modalities in patients with CHD.

Cardiac catheterization provides the opportunity for haemodynamic evaluation and percutaneous interventions in CHD patients. The major advantages of catheter interventions compared to surgery are its minimally invasive nature and the avoidance of the need for cardiopulmonary bypass. In the last decades many new imaging techniques and devices have become available, which means percutaneous treatment is now an option for a wide range of patients. The development of novel devices and use of advanced three-dimensional imaging techniques allows interventional cardiologists to perform interventions in patients previously thought to be too small or ill to treat, or in cardiovascular structures that were previously thought to be technically impossible. With the anticipated growth in number of adult CHD patients, the number of percutaneous interventions will grow in similar order to provide these patients with a favourable cardiovascular status. However, novel treatment strategies need to be assessed constantly for safety and efficacy to ensure optimal care for this complex and sometimes fragile patient population. In this thesis, we discuss several percutaneous intervention strategies for patients with CHD.

PART ONE - COARCTATION OF THE AORTA

Coarctation of the aorta (CoA) is a congenital narrowing of the proximal descending aorta, mostly in the juxtaductal position.⁵ CoA frequently occurs in combination with other cardiac defects, such as a bicuspid aortic valve, aortic arch hypoplasia, and ventricular septal defect (VSD). Its natural history carries a mean life expectancy of approximately 35 years, mainly resulting from hypertension-related complications such as left ventricular failure (28%), intracranial haemorrhage (12%), aortic rupture/dissection (21%) and premature coronary artery disease, but also from infective endocarditis (18%) or associated heart defects.⁵ CoA repair may be performed surgically (for infants) or percutaneous (for older children and adults). Even though initial repair is often performed with high degrees of anatomical success, up to two third of patients develop hypertension later in life⁶⁻⁸ and up to 10% develop recurrent CoA and require a reintervention.⁹⁻¹¹

Due to the risk of long-term complications, lifelong follow-up is warranted for patients with (repaired) CoA. Regular blood pressure evaluation and cardiac imaging are recommended. The preferred advanced imaging modalities for follow-up are CT or CMR. Since this often-young patient population needs repeated imaging follow-up, CMR may be preferred over CT since it prevents radiation exposure. However, the disadvantage of CMR compared to CT is the difficulty in visualizing stented aortic regions. Since 4D flow CMR is a non-invasive modality that can assess flow parameters currently used

in haemodynamic evaluation (i.e. flow volume, regurgitation fraction, peak velocity) but additionally provides a wide range of novel advanced flow parameters (i.e. energy loss, kinetic energy, vorticity, helicity, pressure difference) we thought it could be ideal for follow-up of CoA patients. Since it is non-invasive and there is no need for ionising contrast, the burden for patients is low, making it suitable for regular follow-up. Furthermore, the advanced flow parameters could provide us with novel insights into CoA haemodynamics and eventually even be used as indicators for intervention or to evaluate the result of interventions. In **chapter 3** we present the results of the 4D-FLOAT study (Four-Dimensional flow Cardiac Magnetic Resonance Imaging for the assessment of Coarctation of the Aorta). This was a 4D flow CMR pilot study in our centre, in which we investigated the relation between haemodynamics and LV functionality in patients with coarctation of the aorta.

There are several theories that may explain the difficulties in blood pressure regulation after successful CoA repair. First, it is hypothesized that CoA is not a focal problem, but rather a disease encompassing the entire aorta. Histological studies in humans have shown that proximal to the CoA, the stiffness of the aortic wall is increased, due to an increase in collagen and a decrease in smooth muscle cells and elastin.¹²⁻¹³ Aortic stiffness may lead to high systolic blood pressure by decreasing aortic compliance. Second, aortic arch hypoplasia and/or a gothic arch have been described to be a substrate for systemic arterial hypertension.^{5,14} Third, an altered baroreceptor function may contribute to persistent hypertension after successful CoA repair. The baroreceptors were used to operate at higher arterial pressure levels before the repair and have a reduced sensitivity to changes in arterial pressure.¹⁵ Furthermore, age of initial CoA repair is known to be an important risk factor for the development of late hypertension.¹⁶ Last, since recurrent CoA is not uncommon, development of hypertension after repair later in life could be sign of recurrent CoA and warrants further investigation. Hypertension in patients with (a history of) CoA should be abolished, regardless of its origin. When structural abnormalities (recurrent CoA, hypoplastic aortic arch) are thought to play a role, intervention should be considered. Only a handful of studies have investigated the effect of stent placement on blood pressure control in adult patients. In **chapter 4** we present a retrospective single centre study on the effects of stent placement on blood pressure control in adult patients with CoA. Around 10% of patients with CoA have a concomitant hypoplastic aortic arch. Both systemic hypertension and abnormal blood pressure response to exercise have been reported in patients with a hypoplastic aortic arch.^{6,17} This patient group might benefit from stent placement in the aortic arch. However, research on this procedure is limited. In **chapter 5** we investigate the safety and efficacy of stenting for aortic arch hypoplasia in patients with coarctation of the aorta.

PART TWO – TETRALOGY OF FALLOT

Tetralogy of Fallot (TOF) is the most common cyanotic CHD and accounts for 7-10% of all CHD.¹⁸ TOF consists of a combination of a ventricular septal defect (VSD), overriding of the aorta, right ventricular outflow tract (RVOT) obstruction, and right ventricular (RV) hypertrophy.¹⁹ Surgical repair, consisting of VSD closure and RVOT plasty, is usually performed during infancy. Nowadays, major advances in surgical techniques and perioperative care have resulted in survival rates of over 90% up to 20 years after surgical repair.¹⁹ Despite most patients now surviving well into adulthood, mortality rates continue to be high during the third and fourth postoperative decades.²⁰⁻²² These decreased survival rates are related to postoperative sequelae such as residual RVOT obstruction, pulmonary regurgitation (PR) and RV dilation or hypertrophy, ultimately leading into a negative cascade of RV dysfunction, congestive heart failure, arrhythmias and sudden cardiac death.²³

Surgical and percutaneous pulmonary valve replacement (PVR) are procedures which can lead to reduced RV volumes and improved symptoms^{24,25}, but emerging data show that, using current CMR criteria, they unfortunately do not prevent postoperative ventricular arrhythmia, heart failure, and sudden death.²⁶ Thus, more research into novel criteria for PVR, the timing of PVR and outcomes after PVR is warranted. In **chapter 6** we give an overview of the current status and future perspectives of percutaneous pulmonary valve implantation. Novel imaging modalities could provide insights into the complex haemodynamics of TOF and could possibly provide novel criteria for PVR. In **chapter 7** we provide a comprehensive review of available research on 4D flow CMR research in TOF patients. We discuss the potential role of 4D CMR in an improved timing for PVR, since this has been subject of academic debate for decades.

PART THREE – TRANSPOSITION OF THE GREAT ARTERIES

Transposition of the great arteries (TGA) is the second most common cyanotic CHD, accounting for 5-8% of all congenital heart defects.²⁷ In TGA, the aorta arises from the RV and the pulmonary artery from the left ventricle. For TGA, the arterial switch operation (ASO) is currently standard of care.²⁸ With the ASO, the normal arrangement of the circulation is restored by detaching the aorta and pulmonary arteries (PAs) from their roots and reattach them to the correct ventricle. Nowadays, ASO is combined with the LeCompte manoeuvre, bringing the main pulmonary artery (MPA) and the pulmonary bifurcation anterior to the aorta.²⁹ Although the ASO results in an excellent survival rate, frequent complications occur such as dilation of the ascending aorta and pulmonary

artery stenosis (PS).³⁰ Branch PS is the most common cause for reintervention after ASO, with an incidence of up to 20% of ASO patients.^{30,31} Stretching of the pulmonary arteries with the LeCompte manoeuvre, dynamic systolic compression, due to the close anatomical relationship with an often dilated ascending aorta, scar formation at the anastomosis site and atherosclerosis due to altered shear stress distribution are all thought to lead to PS after ASO.³² The degree of PS can be determined by the dimensions of the branch PAs, the flow distribution to left and right PA, and peak velocities in the PAs. The peak velocity and flow distribution can be determined by several imaging modalities: 4D flow CMR, two-dimensional phase-contrast (2D PC) CMR, and Doppler echocardiography. A lot of these patients undergo cardiac catheterization in the end to perform invasive haemodynamic assessment. The advantages of 4D flow CMR and CFD are that they can give an evaluation of the blood flow within an entire volume, instead of a single plane, which is the case in 2D PC CMR. Furthermore, both 4D flow CMR and CFD are non-invasive and do not require the administration of iodine contrast, which greatly reduces risks and burden for the patient, compared to CT and cardiac catheterization. In **chapter 8**, we present a head-to-head comparison of 4D flow CMR and CFD analysis in healthy pulmonary arteries and TGA patients. In **chapter 9** we compare peak velocities measured by 4D flow CMR with 2D PC CMR and Doppler echocardiography.

ASO patients with a smaller and stiffer pulmonary vascular bed may not be able to accommodate the increase in blood flow during exercise. Therefore, ASO patients often have a reduced exercise capacity when compared to their healthy peers.³⁰ In **chapter 10** we investigate which imaging parameters are associated with a reduced exercise capacity in patients late after ASO. In **chapter 11** we present a TGA patient with vortex formation in the right PA and decreased exercise capacity. In **chapter 12** we investigate which advanced 4D flow energetics are associated with exercise capacity in TGA patients after ASO. In **Chapter 13** we discuss the findings of this thesis, put these findings in a broader perspective and discuss future perspectives.

REFERENCES

1. Hoffman JIE, Kaplan S. The incidence of congenital heart disease. *J Am Coll Cardiol* 2002;39:1890–900.
2. Oster ME, Lee KA, Honein MA, et al. Temporal trends in survival among infants with critical congenital heart defects. *Pediatrics* 2013;May;131(5):e1502-8.
3. Warnes CA, Liberthson R, Danielson GK, Dore A, Harris L, Hoffman JI, et al. Task force 1: the changing profile of congenital heart disease in adult life. *J Am Coll Cardiol*. 2001; 37:1170–1175.
4. Vanderlaan RD, Caldarone CA, Backx PH. Heart failure in congenital heart disease: the role of genes and hemodynamics. *Pflugers Arch - Eur J Physiol* 2014;466:1025–35.
5. Torok RD, Campbell MJ, Fleming GA, Hill KD. Coarctation of the aorta: Management from infancy to adulthood. *World J Cardiol*. 2015 Nov 26;7(11):765-775.
6. Ou P, Bonnet D, Auriacombe L et al. Late systemic hypertension and aortic arch geometry after successful repair of coarctation of the aorta. *Eur Heart J*. 2004 Oct;25(20):1853-1859.
7. Lawrie GM, DeBakey ME, Morris GC, Jr, Crawford ES, Wagner WF, Glaeser DH. Late repair of coarctation of the descending thoracic aorta in 190 patients. Results up to 30 years after operation. *Arch Surg*. 1981 Dec;116(12):1557-1560.
8. Presbitero P, Demarie D, Villani M et al. Long term results (15-30 years) of surgical repair of aortic coarctation. *Br Heart J*. 1987 May;57(5):462-467.
9. Brown ML, Burkhart HM, Connolly HM, Dearani JA, Cetta F, Li Z, et al. Coarctation of the aorta: lifelong surveillance is mandatory following surgical repair. *J Am Coll Cardiol* 2013 Sep 10;62(11):1020-1025.
10. Hager A, Kanz S, Kaemmerer H, Schreiber C, Hess J. Coarctation Long-term Assessment (COALA): significance of arterial hypertension in a cohort of 404 patients up to 27 years after surgical repair of isolated coarctation of the aorta, even in the absence of restenosis and prosthetic material. *J Thorac Cardiovasc Surg*. 2007 Sep;134(3):738-745.
11. Anagnostopoulos-Tzifa A. Management of aortic coarctation in adults: endovascular versus surgical therapy. *Hellenic J Cardiol*. 2007 Sep-Oct;48(5):290-295.
12. Sehested J, Baandrup U, Mikkelsen E. Different reactivity and structure of the prestenotic and poststenotic aorta in human coarctation. Implications for baroreceptor function. *Circulation*. 1982 Jun;65(6):1060-1065
13. Trojnar O, Mizia-Stec K, Gabriel M et al. Parameters of arterial function and structure in adult patients after coarctation repair. *Heart Vessels*. 2011 Jul;26(4):414-420.
14. Ntsinjana HN, Biglino G, Capelli C, et al. Aortic arch shape is not associated with hypertensive response to exercise in patients with repaired congenital heart diseases. *J Cardiovasc Magn Reson*. 2013 Nov 12;15:101.
15. Beekman RH, Katz BP, Moorehead-Steffens C, Rocchini AP. Altered baroreceptor function in children with systolic hypertension after coarctation repair. *Am J Cardiol*. 1983 Jul;52(1):112-117.

16. Daniels SR. Repair of Coarctation of the Aorta and Hypertension: Does age matter? *The Lancet*. Volume 358, No. 9276, p89, 14 July 2001.
17. Ou P, Mousseaux E, Celermajer DS, et al. Aortic arch shape deformation after coarctation surgery: effect on blood pressure response. *J Thorac Cardiovasc Surg*. 2006;132:1105–11.
18. Villafane J, Feinstein JA, Jenkins KJ, et al. Hot topics in tetralogy of Fallot. *J Am Coll Cardiol* 2013;Dec;10;62(23):2155–66
19. Fallot E. Contribution a l'anatomie pathologique de la maladie bleue (cyanose cardiaque). *Mars Med*. 1888;25:77ff
20. Cuypers JAAE, Menting ME, Konings EEM, et al. Unnatural history of tetralogy of Fallot: prospective follow-up of 40 years after surgical correction. *Circulation*. 2014 Nov 25;130(22):1944–53. doi: 10.1161/CIRCULATIONAHA.114.009454.
21. Murphy JG, Bersh BJ, Mair DD, et al. Long-term outcome in patients undergoing surgical repair of tetralogy of Fallot. *N Engl J Med*. 1993 Aug 26;329(9):593–9. doi: 10.1056/NEJM199308263290901.
22. Nollert G, Fischlein T, Bouterwek S, et al. Long-term survival in patients with repair of tetralogy of Fallot: 36-year follow-up of 490 survivors of the first year after surgical repair. *J Am Coll Cardiol*. 1997 Nov 1;30(5):1374–83. doi: 10.1016/s0735-1097(97)00318-5.
23. Gatzoulis MA, Balaji S, Webber SA et al. (2000) Risk factors for arrhythmia and sudden cardiac death late after repair of tetralogy of Fallot: a multicentre study. *Lancet* 356:975–981
24. Alkashkari, et al. Transcatheter Pulmonary Valve Replacement: Current State of Art. *Curr Cardiol Rep*. 2018 Mar 15;20(4):27
25. Ferraz Cavalcanti PE, et al. Pulmonary valve replacement after operative repair of tetralogy of Fallot: meta-analysis and meta-regression of 3,118 patients from 48 studies. *J Am Coll Cardiol*. 2013 Dec 10;62(23):2227–43.
26. Bokma JP, et al. A Propensity Score-Adjusted Analysis of Clinical Outcomes After Pulmonary Valve Replacement in Tetralogy of Fallot. *Heart*. 2018 May;104(9):738–744
27. Brickner ME, Hillis LD, Lange RA. Congenital heart disease in adults. Second of two parts. *N Engl J Med* 2000;342:334–342.
28. Jatene AD, Fontes VF, Paulista PP, Souza LC, Neger F, Galantier M, et al. Anatomic correction of transposition of the great vessels. *J Thorac Cardiovasc Surg* 1976;72:364–370.
29. Lecompte Y, Neveux JY, Leca F, Zannini L, Tu TV, Dubois Y, et al. Reconstruction of the pulmonary outflow tract without prosthetic conduit. *J Thorac Cardiovasc Surg* 1982;84(5):727–731.
30. Ruys TP, Van der Bosch AE, Cuypers JA, et al. Long term Outcome and quality of life after arterial switch operation: a prospective study with a historical comparison. *Congenit Heart Dis*. 2013;May-Jun;8(3):203–10
31. Choi BS, Kwon BS, Kim BG, et al. Long-Term Outcomes After an Arterial Switch Operation for Simple Complete Transposition of the Great Arteries. *Korean Circ J* 2010;Jan;40(1):23–30
32. Morgan CT, Mertens L, Grotenhuis H, Yoo SJ, Seed M, Grosse-Wortmann L. Understanding the mechanism for branch pulmonary artery stenosis after the arterial switch operation for transposition of the great arteries. *Eur Heart J Cardiovasc Imaging*. 2017 Feb;18(2):180–185. doi: 10.1093/ehjci/jew046.



Chapter 2

Three-dimensional and four-dimensional flow assessment in congenital heart disease

Evangeline G. Warmerdam

Gregor J. Krings

Tim Leiner

Heynric B. Grotenhuis

Heart (British Cardiac Society) vol. 106,6 (2020): 421-426

ABSTRACT

Congenital heart disease (CHD) is the most common form of congenital defects, with an incidence of 8 per 1000 births. Due to major advances in diagnostics, perioperative care and surgical techniques, the survival rate of patients with CHD has improved dramatically. Conversely, although 70%–95% of infants with CHD survive into adulthood, the rate of long-term morbidity, which often requires (repeat) intervention, has increased. Recently, the role of altered haemodynamics in cardiac development and CHD has become a subject of interest. Patients with CHD often have abnormal blood flow patterns, either due to the primary cardiac defect or as a consequence of the surgical intervention(s). Research suggests that these abnormal blood flow patterns may contribute to diminished cardiac and vascular function. Serial assessment of haemodynamic parameters in patients with CHD may allow for improved understanding of the often complex haemodynamics in these patients and thereby potentially guide the timing and nature of interventions with the aim of preventing progression of cardiovascular deterioration. In this article we will discuss two novel non-invasive four-dimensional techniques to evaluate cardiovascular haemodynamics: four-dimensional flow cardiac magnetic resonance and computational fluid dynamics. This review focuses on the additional value of these two modalities in the evaluation of patients with CHD with abnormal flow patterns, who could benefit from advanced haemodynamic evaluation: patients with coarctation of the aorta, bicuspid aortic valve, tetralogy of Fallot and patients after Fontan palliation.

INTRODUCTION

Congenital heart disease (CHD) is the most common form of congenital defects, with an incidence of 8 per 1000 births.¹ Due to major advances in diagnostics, perioperative care and surgical techniques, the survival rate of patients with CHD has improved dramatically. Conversely, although 70%–95% of infants with CHD survive into adulthood,² the rate of long-term morbidity, which often requires (repeat) intervention, has increased.

Recently, the role of altered haemodynamics in cardiac development and CHD has become a subject of interest. Patients with CHD often have abnormal blood flow patterns, either due to the primary cardiac defect or as a consequence of the surgical intervention(s). Research suggests that these abnormal blood flow patterns may contribute to diminished cardiac and vascular function.³ Serial assessment of haemodynamic parameters in patients with CHD may allow for improved understanding of the often complex haemodynamics in these patients and thereby potentially guide the timing and nature of interventions with the aim of preventing progression of cardiovascular deterioration.

In this article we will discuss two novel non-invasive four-dimensional (4D) techniques to evaluate cardiovascular haemodynamics: 4D flow cardiac magnetic resonance (CMR) and computational fluid dynamics (CFD). This review focuses on the additional value of these two modalities in the evaluation of patients with CHD with abnormal flow patterns, who could benefit from advanced haemodynamic evaluation: patients with coarctation of the aorta (CoA), bicuspid aortic valve (BAV), tetralogy of Fallot (TOF) and patients after Fontan palliation.

CURRENT CLINICAL PRACTICE

Evaluation of CHD is currently done using echocardiography, CMR, CT and invasive angiography.^{4,5} Echocardiography, being cost-effective and non-invasive, is used for routine cardiac evaluation and provides information on anatomy and physiology, while flow assessment can be performed by colour Doppler. However, image quality is strongly dependent on the acoustic window and operator skills.^{6,7}

CMR provides a three-dimensional (3D) evaluation of cardiovascular anatomy, volume, and function. CMR has a high intraobserver and interobserver agreement and requires no ionising radiation.⁸ Blood flow can be analysed using two-dimensional (2D) phase-contrast (PC) CMR, while dynamic angiographic data can be acquired after administration of intravenous contrast. Unfortunately, CMR is costly and time-consuming. Furthermore,

it is hampered by the fact that the patient must remain immobile during image acquisition, which can prove difficult especially for young children. Thus, if a CMR is warranted in infants or small children, general anaesthetic is often required. Also, CMR measurements within stents are not possible due to susceptibility artefacts created by the presence of implants containing metal, and scanning of patients with certain types of pacemaker devices is contraindicated.^{4,5} In addition, shortly after cardiac surgery, CMR is often not possible due to temporary pacing wires and sternal wires. Furthermore, 2D PC CMR suffers from errors in flow quantification due to motion of the heart relative to the imaging plane and may give an incomplete assessment of blood flow patterns due to technical limitations, especially in complex CHD. The aforementioned issues and the expense, expertise and non-portable nature of the investigation are CMRs most relevant limitations.

Alternatively, CT provides a rapid tool for high-resolution imaging of the cardiovascular system and does not suffer from artefacts due to stents or prosthetic valves like CMR. However, CT requires ionising radiation and mainly produces anatomical information; routine CT currently provides no information on haemodynamics or blood flow.

Cardiac catheterisation (CC) allows for the measurement of blood flow and pressure inside the cardiovascular system. Its invasive nature and the use of ionising radiation are major drawbacks. Nevertheless, CC also provides the opportunity to intervene in the same instance when indicated. Due to the increase in treatment options with percutaneous closure devices and cardiac valves, the use of CC for diagnostic purposes is declining. Instead, CC is increasingly used as an interventional technique.⁴

4D FLOW CMR

4D flow CMR is the term used for time-resolved phase-contrast CMR with flow-encoding in all three spatial directions. 3D volumetric images are combined with 3D velocity encoding throughout the cardiac cycle. Using 4D flow CMR, qualification and quantification of flow over an entire volume can be obtained, in contrast to conventional 2D PC CMR by which only basic flow parameters can be measured in a single 2D plane in one direction. 4D flow CMR was first described and validated in the late 1990s, with the objective to provide a more comprehensive evaluation of haemodynamics.^{9,10} Only recently acquisition time, spatial resolution and time required for analysis of 4D flow CMR have reached acceptable levels for clinical application. Currently, 4D flow CMR acquisition requires approximately 10–15 min, and the time required for analysis greatly varies and depends on the software used, operator skills and desired measurements.

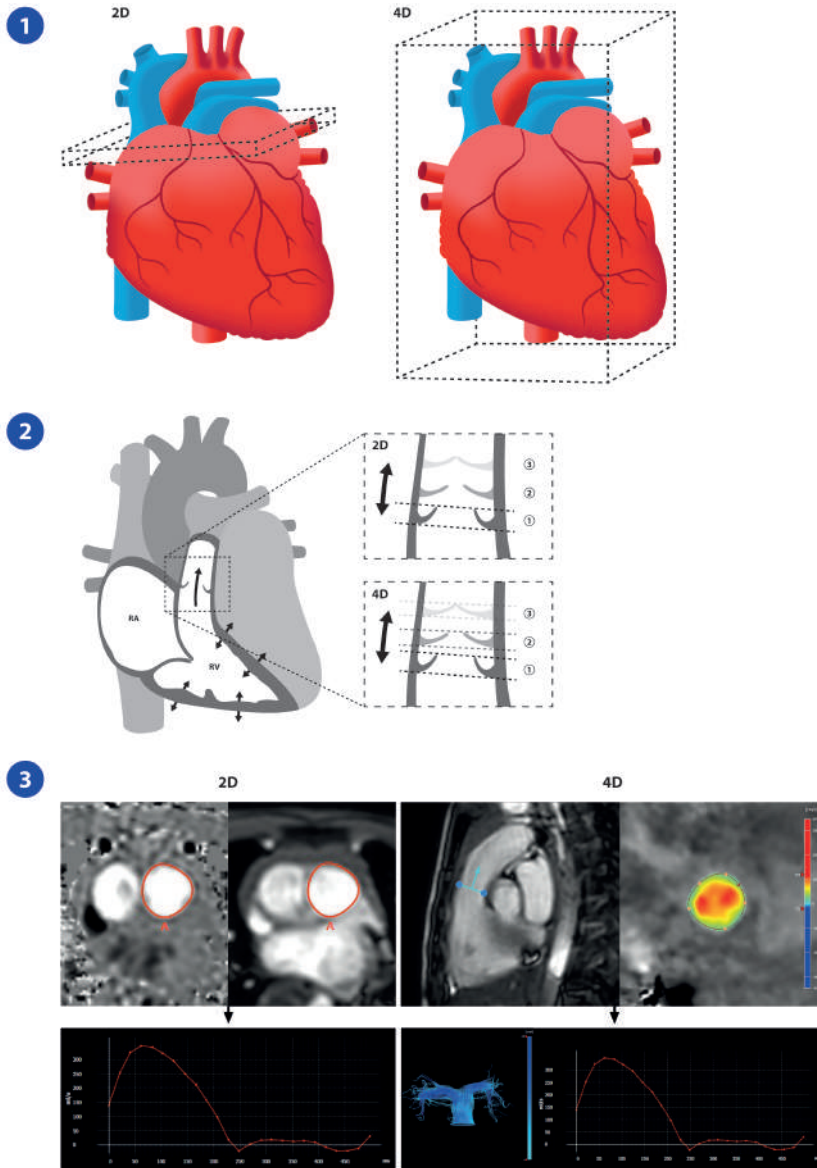


Figure 1. Valve analyses by 2D flow PC CMR versus 4D flow CMR. (A) For 2D PC CMR, imaging planes for flow measurements must be individually prescribed, and separate breath-holding scans need to be performed for each acquisition. For 4D flow CMR, all data are acquired in a single acquisition, so any plane of interest can be analysed retrospectively to study the haemodynamic status of the individual patient. (B) In 2D PC CMR, information on valvular blood flow has to be obtained from one static plane, so flow assessment is hampered by the through-plane motion of the valve during the cardiac cycle. 4D flow CMR provides retrospective valve tracking, making it more accurate than 2D PC CMR due to its ability to correct for valvular through-plane motion and flow angulation. (C) After identification of the valve area, both 2D PC CMR and 4D flow CMR provide information on basic flow parameters. However, 4D flow CMR can also visualise both the forward and, if present, backward flow over the valve. 2D, two-dimensional; 4D, four-dimensional; CMR, cardiac magnetic resonance; PC, phase contrast; RA, right atrium; RV, right ventricle.

Spatial resolution for 4D flow CMR is currently $1.5 \times 1.5 \times 1.5 - 3 \times 3 \times 3 \text{ mm}^{3,11}$ which implies that analysis of very small vessels or an important stenosis can be a challenge. Similar to 2D PC CMR measurements, 4D flow CMR measurements are reproducible and have a low intraobserver and interobserver variability.^{12,13} To obtain flow measurements with 2D PC CMR, each plane of interest for flow measurements has to be individually prescribed, and separate breath-holding scans have to be performed. With 4D flow CMR, all data are acquired in a single acquisition, so any location or plane of interest can be analysed retrospectively to study the haemodynamic status of the individual patient.

4D flow CMR has multiple applications beneficial for assessment of CHD. Visualisation of blood flow patterns is possible for the entire cardiovascular system, including the heart and major blood vessels. Flow direction and velocity can be easily assessed using colour-coded streamlines.¹⁴ Quantification of flow can be performed using retrospective valve tracking, which is a reproducible and reliable method to visualise and quantify blood flow over all four cardiac valves simultaneously (Figure 1). It is more accurate than 2D PC CMR due to its ability to correct for valvular through-plane motion and flow angulation.^{15,16} Relative pressure mapping over a stenotic blood vessel can provide pressure differences between two chosen planes in a vessel, which has shown good agreement with invasive catheter measurements in small patient cohorts.^{17,18} Furthermore, 4D flow CMR allows for kinetic energy measurements within the ventricle. Since kinetic energy reflects ventricular performance, it could potentially be a novel and advanced method for evaluation of the cardiac function.¹⁹ Intracardiac kinetic energy has been shown to be abnormal in patients with TOF, Fontan circulation, mitral regurgitation and heart failure.²⁰

COMPUTATIONAL FLUID DYNAMICS

CFD is a specialised area of mathematics and a branch of fluid mechanics often used in engineering to study complex flow patterns. In CHD, CFD can be performed by creating 3D models of the cardiovascular system of a patient, based on CMR, CT or 3D rotational angiography. A 3D mesh is made from the imaging data; subsequently, the Navier Stokes equation is solved for each cell within the mesh. Patient-specific haemodynamic parameters such as pressure, velocity or cardiac output at the start or inlet of the system are used as the so-called 'boundary conditions' for the analysis. Based on these boundary conditions, the blood flow throughout the model is calculated. Results of the analyses include, among others, velocity, pressure, direction of flow, wall shear stress (WSS) and pulse wave velocity. A major advantage of CFD is that it can be used to predict the haemodynamic effects of an intervention like stent placement or implantation of

heart valves (Figure 2). The quality of the CFD analysis depends on the accuracy of the geometric and haemodynamic boundary conditions. Due to the complex nature of the equations that need to be solved in a CFD analysis, it requires substantial computational power and can be time-consuming.

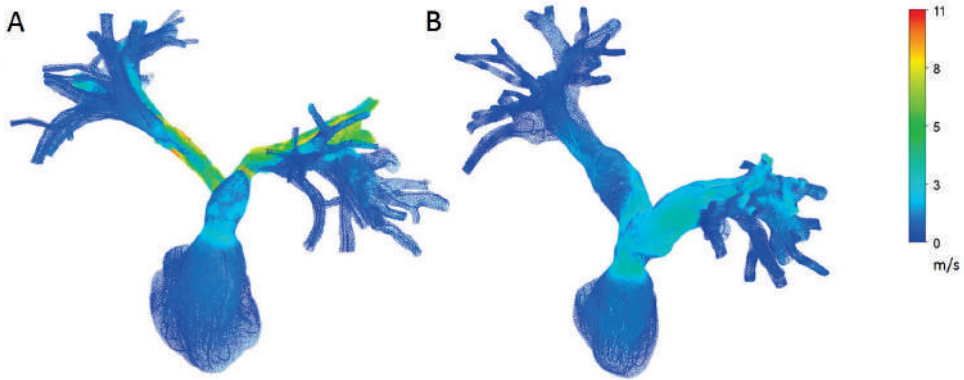


Figure 2. Visualisation of flow pathlines and vector fields of computational fluid dynamics analyses in a toddler with valvular and supra-valvular pulmonary stenosis. (A) The situation before Y-stent implantation: multilevel stenosis of the pulmonary arteries resulting in flow acceleration in both branches. (B) The situation after Y-stent procedure. An increase in vessel diameter results in reduction of flow velocities. Image courtesy of Maartje Conijn, University Medical Center Utrecht.

ADVANCED HAEMODYNAMIC ASSESSMENT

Both 4D flow CMR and CFD can provide flow visualisation and a broad range of parameters for flow quantification, including basic parameters such as (peak) velocity, pressure, volume, and direction of flow. In addition, important advanced blood flow parameters including WSS, pulse wave velocity and kinetic energy can also be determined. WSS is defined as the tangential force of the flowing blood on the vessel wall. Abnormal levels of WSS have been found to be related to the pathogenesis of atherosclerosis, aneurysm formation and intimal hyperplasia.^{11,21} Pulse wave velocity is the propagation velocity of the arterial pulse through the cardiovascular system and can be used as a marker for aortic stiffness, which is predictive of cardiovascular mortality.^{11,22} Kinetic energy is the mean energy content per mass unit in the blood flow. Kinetic energy measurements represent the amount of energy required for ventricular contraction and to what extent energy is lost due to turbulent flow. Kinetic energy measurements are therefore a good marker of ventricular efficiency.^{11,23}

CLINICAL APPLICATIONS IN CONGENITAL HEART DISEASE

Coarctation and bicuspid aortic valve

CoA is a narrowing of the upper descending thoracic aorta, most often distal to the origin of the left subclavian artery near the insertion of the ligamentum arteriosum. CoA accounts for approximately 5%–8% of all CHDs. Arterial hypertension and the associated cardiovascular complications are the most common long-term sequelae in patients with CoA. Surgery is usually performed in early childhood, while balloon dilatation and percutaneous stent placement are the treatment of choice for older patients.²⁴ The imaging modalities currently used in clinical practice can only provide dimensions, velocities, and pressure gradients, and therefore fail to give a comprehensive characterisation of the aortic blood flow and effects on the aortic wall. Furthermore, echo and 2D PC CMR are very limited in their abilities to visualise and quantify complex and turbulent blood flow at and around the site of aortic narrowing. According to the current guidelines, CC is the gold standard to determine the pressure gradient across the site of CoA, and intervention is usually performed when the blood pressure gradient exceeds 20 mmHg.²⁵ Patients are often anaesthetised during CC, resulting in systolic blood pressures that are lower than when the patient would be conscious. Pressure gradients measured in anaesthetised patients can therefore underestimate the severity of the CoA. Adrenergic drugs can be administered to artificially create a blood pressure similar to waking conditions or even exercising. Current limitations of the available diagnostic modalities to evaluate patients with CoA imply that our understanding of CoA and its effects on the entire cardiovascular system is incomplete. Both 4D flow CMR and CFD can provide more sophisticated and comprehensive haemodynamic parameters and consequently improve our understanding of this disease. 4D flow CMR provides visualisation and comprehensive quantification of blood flow in the left ventricle and the entire aorta. Furthermore, 4D flow CMR provides an alternative for CC pressure measurements as these could also be derived from blood flow velocities by CMR.^{17,18} From the time-resolved velocity fields acquired with 4D flow CMR, 4D pressure fields can be calculated by solving the pressure Poisson equation.^{17,26} This approach is more accurate than the simplified Bernoulli equation used with Doppler echocardiography, since the Bernoulli equation is highly dependent on the accuracy of the maximum velocity measurement due to the exponentiation hereof.²⁶ The validity of this technique has been evaluated in small phantom and human studies and showed good agreement with expected values and standard methods.²⁶ Furthermore, a recent cohort study of patients with CoA demonstrated that 4D flow CMR pressure gradients are in good agreement with invasively acquired pressure gradients.¹⁷ 4D flow CMR

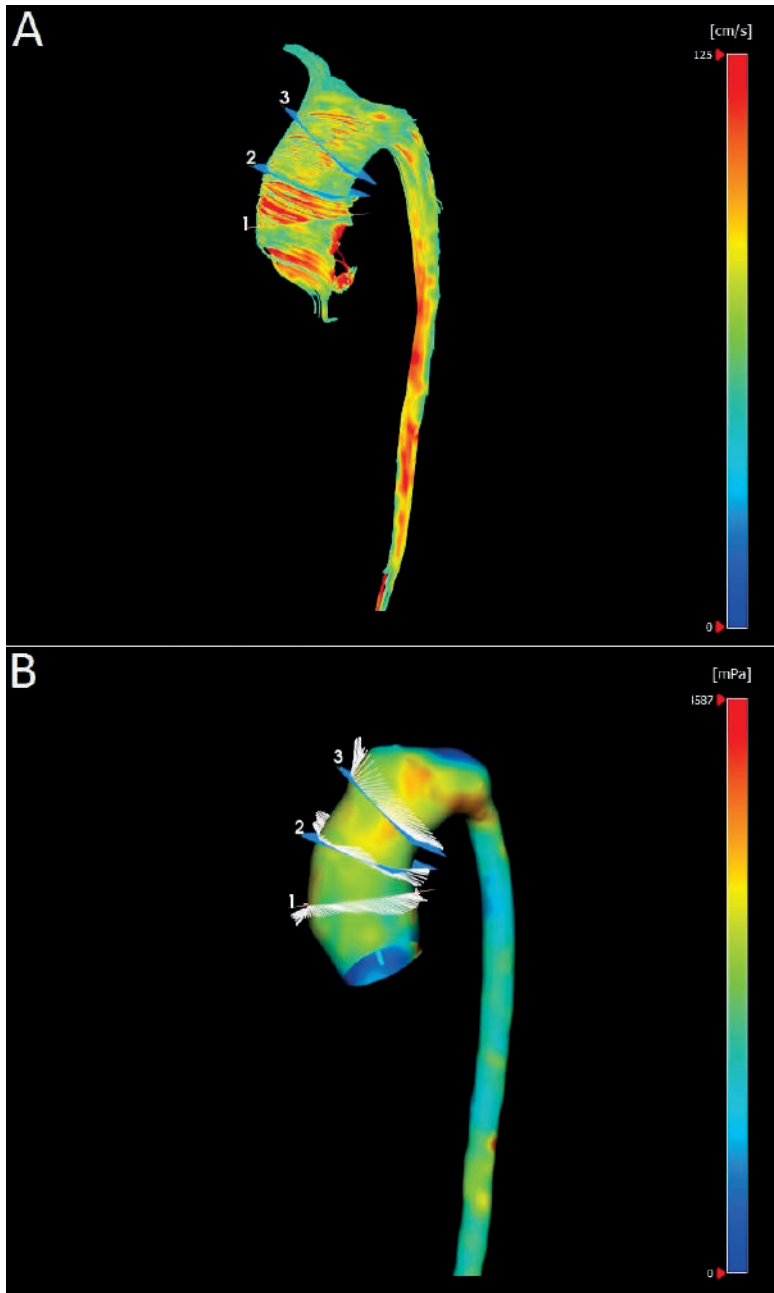


Figure 3. Velocity streamline image of 4D flow CMR-derived blood flow (A) and wall shear stress analysis (B) in a teenage patient with a bicuspid aortic valve (fusion of the right coronary cusp and the non-coronary cusp) and a dilated ascending aorta (33.6 mm, Z-score: +4.1). The velocity streamlines in A show an abnormal helical flow pattern and in B show abnormal high values of wall shear stress along the wall of the ascending aorta. 1, 2, and 3 represent the consecutive order in which the planes for analysis were created. 4D, four-dimensional; CMR, cardiac magnetic resonance.

could therefore potentially be used as a non-invasive technique to assess awake, resting pressure gradients in CoA, and to further refine clinical decision making especially in patients with CoA where indication for treatment is not clear-cut.

Up to 40% of patients with CoA have a BAV.²⁷ BAV is not only associated with dysfunction of the aortic valve, but also with aortic pathology such as aortic dilatation and even dissection.²⁸ The abnormal arrangement of the aortic valve leaflets in BAV generates an abnormal flow pattern in the ascending aorta which depends on the type of leaflet fusion (Figure 3). 4D flow CMR studies in BAV have demonstrated altered flow patterns in the ascending aorta and an aberrant distribution of aortic WSS. Alterations in aortic haemodynamics can provide a trigger for remodelling of the aortic wall, hence the frequently observed ascending aortic dilatation.^{29–33} CFD analyses comparing blood flow in BAV versus normal (non-dilated) aortas with tricuspid aortic valves show an altered WSS distribution in all different BAV fusion types.^{34,35} Both 4D flow CMR and CFD analyses show abnormal WSS distribution in patients with BAV even before aortic dilation occurs, suggesting that abnormal WSS could precede anatomical remodelling of the aorta. Serial monitoring of WSS in addition to routine aortic dimensions may allow early identification of young asymptomatic patients at risk of (progressive) aortopathy and may guide the surgeon to reinforce specific aortic sites at increased risk of aortic sequelae.

Tetralogy of Fallot

TOF, characterised by pulmonary stenosis, ventricular septal defect, overriding aorta and right ventricle (RV) hypertrophy, is the most common cyanotic type of CHD and accounts for 7%–10% of all CHDs.³⁶ Surgery is often required in the first year of life and results in high survival rates. As a consequence of widening the right ventricular outflow tract, a certain degree of pulmonary valve regurgitation (PR) is inherent to TOF surgery, which can result in RV volume and pressure overload over time. Blood flow analysis by 4D flow CMR in patients with TOF has demonstrated increased vortical flow in the right atrium, RV and in the pulmonary arteries (PAs).^{37–39} Abnormal vortical flow within the RV changes the blood flow pattern in an energetically unfavourable way. However, the relationship between vortex formation and myocardial changes or symptoms remains to be investigated in TOF. Vortex flow in the right atrium could be caused by tricuspid valve regurgitation or anatomical variants after surgical repair.³⁸ Abnormal vortical flow in the RV is thought to be the result of PR, directing inflow from the tricuspid valve towards the RV base and away from the RV outflow tract.^{37,38} PR is common in patients with TOF and is associated with impaired cardiac function.⁴⁰ PR could also play a role in the formation of vortex flow in PAs, although the aetiology is still poorly understood.

Flow vortices in general are associated with alteration in WSS and affect endothelial function.²¹ A comprehensive evaluation of the blood flow within the RV and pulmonary vascular bed can be performed using 4D flow CMR, helping to understand the interaction between the different (repaired) defects and study any negative arterial–ventricular interaction. Further research could potentially identify parameters suitable for the prediction of outcomes in patients with repaired TOF and refine timing of pulmonary valve replacement.

Fontan circulation

Patients with only a single functional ventricle undergo three consecutive palliative operations resulting in a total cavopulmonary connection (TCPC), also known as Fontan circulation. In the absence of a functional sub-pulmonary ventricle, the superior and inferior caval veins are connected to the PA. Assessment of the haemodynamic situation in Fontan circulation is highly complex due to the abnormal position and geometry of the systemic ventricle, the extent of the Fontan circuit and the passive nature of flow to the pulmonary circulation. Blood flow to the pulmonary circulation in Fontan patients is predominantly driven by the intrathoracic pressure changes during respiration, systemic venous pressure, systolic and diastolic performance of the systemic ventricle, and the peripheral muscle pump.⁴¹ Recent research suggests that energy loss within the TCPC is an important factor for Fontan haemodynamics and should be minimised if possible.⁴² Factors that could be of influence on energy loss in the TCPC are vessel size, anastomosis shape, total blood flow and pulmonary/caval flow distribution.⁴² Only a handful of 4D flow CMR studies investigating energy loss in the TCPC have been performed to date, since the limited spatial resolution can lead to underestimation of energy loss. In contrast, a substantial number of CFD studies have been reported,^{43–45} of which the largest study by Haggerty et al.⁴³ used CMR-based CFD to evaluate the haemodynamics in 100 Fontan patients, with a focus on power loss within the Fontan circuit. This study showed stenosis in the Fontan tunnel and undersized pulmonary arteries were associated with increased power loss, thereby have a clearly negative effect on Fontan haemodynamics.⁴³ Currently, there is no research available investigating the relation between energy loss and common complications in Fontan circulation, such as protein-losing enteropathy and liver cirrhosis.

Ejection fraction of the systemic ventricle, typically a good indicator of cardiac function, can be normal in patients with Fontan circulation, despite clinical signs of circulatory failure.⁴⁶ There are several reasons why ejection fraction is not representative of ventricular function in this patient group: the abnormal position and geometry of the systemic ventricle, the atrioventricular valve regurgitation that many patients with a

Fontan circulation have, and the fact that it is a load sensitive marker. The first exploratory studies suggest that kinetic energy assessment has the potential to provide novel information on ventricular dysfunction in the Fontan circulation and can lead to new insights into the physiology of this complex circulation. Further research is necessary to determine if kinetic energy assessment can provide information on early ventricular dysfunction and whether it is related to outcomes in Fontan patients.⁴⁷

CFD has been used for surgical planning in patients to aid surgeons and physicians in clinical decision making.⁴⁴ CFD analysis can provide insight into preoperative blood flow. However, the main advantage lies in the possibility of virtual surgery. Models of the patient's anatomy after several different types of surgery can be generated, and patient-specific boundary conditions can be used to assess the expected haemodynamics after surgery. This personalised approach to surgical planning can provide insight into possible complications and help to determine the best surgical strategy for the patient. At this point, the procedure is time-consuming and requires good collaboration between clinicians and engineers.⁴⁴ Although more research is needed, it is a very promising technique and would mean a great step forward in a complex and demanding process for both the clinician and the patient.

CONCLUSION

Patients with CHD often have abnormal blood flow patterns, either due to the cardiac defect or the required intervention(s). Since altered blood flow patterns can result in diminished cardiac or vascular function, it is important to have diagnostic tools to visualise and quantify blood flow in CHD in the entire heart and large vessels. The advances described in this review show the great potential of both techniques to evaluate a broad variety of haemodynamic parameters in a non-invasive manner to assess the haemodynamic status of patients with CHD. However, more research is warranted to determine the clinical significance of advanced haemodynamic parameters in CHD. Serial assessment with 4D flow CMR or CFD is likely to become of great importance to improve our understanding of complex CHD. Furthermore, it can help to optimise timing of interventions and prevent progression of cardiovascular deterioration.

REFERENCES

1. Hoffman JL, Kaplan S. The incidence of congenital heart disease. *J Am Coll Cardiol* 2002;Jun;39(12):1890-900.
2. Oster ME, Lee KA, Honein MA, et al. Temporal trends in survival among infants with critical congenital heart defects. *Pediatrics* 2013;May;131(5):e1502-8.
3. Vanderlaan RD, Caldarone CA, Backx PH. Heart failure in congenital heart disease: the role of genes and hemodynamics. *Eur J Physiol* 2014;466:1025.
4. Babu-Narayan SV, Giannakoulas G, Valente AM, et al. Imaging of congenital heart disease in adults. *Eur Heart J* 2016;Apr;37(15):1182-1195.
5. Prakash A, Powell AJ, Geva T. Multimodality non-invasive imaging for assessment of congenital heart disease. *Circ Cardiovasc Imaging* 2010;19:133-144
6. Chukwu EO, Barasch E, Mihalatos DG, et al. Relative importance of errors in left ventricular quantitation by two-dimensional echocardiography: insights from three-dimensional echocardiography and cardiac magnetic resonance imaging. *J Am Soc Echocardiogr*. 2008; 21: 990-997.
7. Lai WW, Gauvreau K, Rivera ES, et al. Accuracy of guideline recommendations for two-dimensional quantification of the right ventricle by echocardiography. *Int J Cardiovasc Imaging*. 2008; 24: 691-698
8. Bellenger NG, Davies LC, Francis JM, et al. Reduction in sample size for studies of remodelling in heart failure by the use of cardiovascular magnetic resonance. *J Cardiovasc Magn Reson* 2000;2:271-278
9. Wigström L, Sjöqvist L, Wranne B. Temporally resolved 3D phase-contrast imaging. *Magn Reson Med* 1996;36(5):800-3.
10. Wigström L, Ebbers T, Frynens A, et al. Particle trace visualization of intracardiac flow using time-resolved 3D phase contrast MRI. *Magn Reson Med* 1999;41(4):793-9.
11. Dyverfeldt P, Bissell M, Barker AJ, et al. 4D flow cardiovascular magnetic resonance consensus statement. *J Cardiovasc Magn Reson* 2015;17(1):72.
12. Stoll VM, Loudon M, Eriksson J, et al. Test-retest variability of left ventricular 4D flow cardiovascular magnetic resonance measurements in healthy subjects. *J Cardiovasc Magn Reson* 2018;20:15.
13. van Ooij, P, Powell AL, Potters WV, et al. Reproducibility and Inter-Observer Variability of Systolic Blood Flow Velocity and 3D Wall Shear Stress Derived From 4D flow MRI in the Healthy Aorta. *J Magn Reson Imaging* 2016;Jan;43(1):236-248.
14. Calkoen EE, Roest AA, van der Geest RJ, et al. Cardiovascular function and flow by 4-dimensional magnetic resonance imaging techniques: new applications. *J Thorac Imaging*. 2014 May;29(3):185-96
15. Roes SD, Hammer S, van der Geest RJ, et al. Flow assessment through four heart valves simultaneously using 3-dimensional 3-directional velocity-encoded magnetic resonance imaging with retrospective valve tracking in healthy volunteers and patients with valvular regurgitation. *Invest Radiol*. 2009;44:669-675].

16. Crandon S, Elbaz MSM, Westenberg JJM, et al. Clinical applications of intra-cardiac four-dimensional flow cardiovascular magnetic resonance: A systematic review. *Int J Cardiol*. 2017 Dec 15;249:486-493
17. Riesenkampff E, Fernandes JF, Meier S, et al. Pressure fields by flow-sensitive 4D, velocity-encoded CMR in patients with aortic coarctation. *JACC Cardiovasc Imaging* 2014;Sep;7(9):920-6
18. Rengier F, Delles M, Eichhorn J, et al. Noninvasive 4D pressure difference mapping derived from 4D flow MRI in patients with repaired aortic coarctation: comparison with young healthy volunteers. *Int J Cardiovasc Imaging*. 2015 Apr;31(4):823-30.
19. Carlsson M, Heiberg E, Toger J, Arheden H. Quantification of left and right ventricular kinetic energy using four-dimensional intracardiac magnetic resonance imaging flow measurements. *Am J Physiol Heart Circ Physiol*. 2012;302:H893-900.
20. Sjöberg P, Heiberg E, Wingren P, et al. Decreased Diastolic Ventricular Kinetic Energy in Young Patients with Fontan Circulation Demonstrated by Four-Dimensional Cardiac Magnetic Resonance Imaging. *Pediatr Cardiol* 2017;Apr;38(4):669-680
21. Paszkowiak JJ, Dardik A. Arterial wall shear stress: observations from the bench to the bedside. *Vasc Endovascular Surg* 2003;Jan-Feb;37(1):47-57.
22. Markl M, Wallis W, Breckencke S, et al. Estimation of global aortic pulse wave velocity by flow-sensitive 4D MRI. *Magn Reson Med* 2010 Jun;63(6):1575-82.
23. Dyverfeldt P, Sigfridsson A, Kvitting JP, et al. Quantification of intravoxel velocity standard deviation and turbulence intensity by generalizing phase-contrast MRI. *Magn Reson Med* 2006;Oct;56(4):850-8.
24. Ovaert C, Benson LN, Nykanen D, et al. Transcatheter treatment of coarctation of the aorta: a review. *Pediatr Cardiol* 1998;19:27-44
25. Mancia G, Fagard R, Narkiewicz K, et al. 2013 ESH/ESC Guidelines for the management of arterial hypertension: the Task Force for the management of arterial hypertension of the European Society of Hypertension (ESH) and of the European Society of Cardiology (ESC). *J Hypertens* 2013 Jul;31(7):1281-357.
26. Bock J, Frydrychowicz A, Lorenz R, et al. In vivo noninvasive 4D pressure difference mapping in the human aorta: phantom comparison and application in healthy volunteers and patients. *Magn Reson Med* 2011;Oct;66(4):1079-88
27. Warnes CA. Bicuspid aortic valve and Coarctation: two villains part of a diffuse problem. *Heart* 2003;Sep;89(9):965-6.
28. Ando M, Okita Y, Morota T, et al. Thoracic aortic aneurysm associated with congenital bicuspid aortic valve. *Cardiovasc Surg* 1998;Dec;6(6):629-34.
29. Hope MD, Hope TA, Crook SES, et al. 4D flow CMR in assessment of valve-related ascending aortic disease. *JACC Cardiovasc Imaging* 2011;Jul;4(7):781-7
30. Barker AJ, Markl M, Burk J, et al. Bicuspid aortic valve is associated with altered wall shear stress in the ascending aorta. *Circ Cardiovasc Imaging* 2012;5(4):457-66

31. Bissell MM, Hess AT, Biasioli L, et al. Aortic dilation in bicuspid aortic valve disease: flow pattern is a major contributor and differs with valve fusion type. *Circ Cardiovasc Imaging* 2013;6:499–507
32. Piatti F, Sturla F, Bissell MM, et al. 4D Flow Analysis of BAV-Related Fluid-Dynamic Alterations: Evidences of Wall Shear Stress Alterations in Absence of Clinically-Relevant Aortic Anatomical Remodeling. *Front Physiol* 2017;Jun;26:8:441
33. Meierhofer C, Schneider EP, Lyko C, et al. Wall shear stress and flow patterns in the ascending aorta in patients with bicuspid aortic valves differ significantly from tricuspid aortic valves: a prospective study. *Eur Heart J Cardiovasc Imaging* 2013;Aug;14(8):797–804
34. Cao K, Atkins SK, McNally A, Liu J, et al. Simulations of morphotype-dependent hemodynamics in non-dilated bicuspid aortic valve aortas. *J Biomech* 2017;Jan;4:50:63–70
35. McNally A, Madan A, and Sucosky P. Morphotype-dependent flow characteristics in bicuspid aortic valve ascending aortas: a benchtop particle image velocimetry study. *Front Physiol* 2017;Feb;1:8:44
36. Villafane J, Feinstein JA, Jenkins KJ, et al. Hot topics in tetralogy of Fallot. *J Am Coll Cardiol* 2013;Dec;10:62(23):2155–66
37. Francois CJ, Srinivasan S, Schiebler ML, et al. 4D cardiovascular magnetic resonance velocity mapping of alterations of the right heart flow patterns and main pulmonary artery hemodynamics in tetralogy of Fallot. *J Cardiovasc Magn Reson* 2012;Feb;7;14:16
38. Hirtler D, Garcia J, Barker AJ, et al. Assessment of intracardiac flow and vorticity in the right heart of patients after repair of tetralogy of Fallot by flow-sensitive 4D MRI. *Eur Radiol* 2016;Oct;26(10):3598–607
39. Geiger J, Markl M, Jung B, et al. 4D-MR flow analysis in patients after repair for tetralogy of Fallot. *Eur Radiol* 2011;Aug;21(8):1651–7
40. Frigiola A, Redington AN, Cullen S, et al. Pulmonary regurgitation is an important determinant of right ventricular contractile dysfunction in patients with surgically repaired tetralogy of Fallot. *Circulation* 2004;Sep 14;110(11 Suppl 1):II153–7
41. Hjortdal VE, Emmertsen K, Stenbøg E, et al. Effects of exercise and respiration on blood flow in total cavopulmonary connection: a real-time magnetic resonance flow study. *Circulation* 2003;108:1227–1231
42. Rijnberg FM, Hazekamp MG, Wentzel JJ, et al. Energetics of Blood Flow in Cardiovascular Disease: Concept and Clinical Implications of Adverse Energetics in Patients With a Fontan Circulation. *Circulation* 2018;May;29;137(22):2393–2407
43. Haggerty CM, Restrepo M, Tang E, et al. Fontan hemodynamics from 100 patient-specific cardiac magnetic resonance studies: a computational fluid dynamics analysis. *J Thorac Cardiovasc Surg* 2014;Oct;148(4):1481–9
44. Trusty PM, Restrepo M, Kanter KR, et al. A pulsatile hemodynamic evaluation of the commercially available bifurcated Y-graft Fontan modification and comparison with the lateral tunnel and extracardiac conduits. *J Thorac Cardiovasc Surg* 2016;151:1529–1536

45. Tang E, Restrepo M, Haggerty CM, et al. Geometric characterization of patient-specific total cavopulmonary connections and its relationship to hemodynamics. *JACC Cardiovasc Imaging* 2014;7:215–224.
46. Barron DJ, Kilby MD, Davies B, et al. Hypoplastic left heart syndrome. *Lancet* 2009;374;551–564
47. Wong J, Chabiniok R, Tibby SM, et al. Exploring kinetic energy as a new marker of cardiac function in the single ventricle circulation. *J Appl Physiol* 2018;Jan;25



PART ONE

Coarctation of the Aorta



Chapter 3

Abnormal aortic flow related to left ventricular mass and volume in coarctation: a four-dimensional flow CMR study

Evangeline G. Warmerdam

Julio Sotelo

Bart. W. Driesen

Sergio Uribe

Jos J.M. Westenberg

Tim Leiner

Gregor J. Krings

Heleen B. van der Zwaan

Michiel Voskuil

Heynric B. Grotenhuis

Submitted

ABSTRACT

Background. Even after successful repair for coarctation of the aorta (CoA) abnormal blood flow patterns can be expected due to aortic narrowing, a changed aortic geometry after repair, or generalized aortopathy, all of which may have a negative impact on left ventricular (LV) performance. The aim of this study is to investigate the relationship between aortic haemodynamics assessed by four-dimensional flow (4D flow) cardiac magnetic resonance imaging (CMR) and LV performance in CoA patients.

Methods. CoA patients with a clinical indication for CMR underwent additional 4D flow acquisition. Wall shear stress, oscillatory shear index, vorticity, viscous dissipation, energy loss, kinetic energy and velocity angle were assessed for several aortic segments at peak-systole. Global pulse wave velocity (PWV) was assessed for the entire aorta, as well as LV ejection fraction, volumes, and mass.

Results. A total of 17 CoA patients were included. Increased velocity angle in the ascending aorta was correlated with decreased LV mass ($p = 0.0445$). Energy loss at the CoA site and increased degree of vorticity in the descending aorta were correlated with increased LV end-diastolic and end-systolic volume ($p = 0.0499$, $p = 0.0461$, respectively). PWV was correlated with LV mass and LV end-systolic volume ($p = 0.0385$, $p = 0.0397$, respectively). Apart from energy loss the CoA site, all correlations remained significant after correction for age.

Conclusion. Adverse aortic-ventricular interaction in CoA patients was demonstrated by abnormal aortic haemodynamics by 4D flow assessment and was associated with impaired LV performance. 4D flow CMR may provide novel parameters to assess aortic-ventricular interaction in patients with CoA.

INTRODUCTION

Coarctation of the aorta (CoA) is characterized by a local narrowing of the proximal descending aorta, most common in the juxtaductal position. It accounts for approximately 5–8% of all congenital heart disease and frequently occurs in combination with other cardiac lesions, such as bicuspid aortic valve (BAV) and ventricular septal defect.^{1,2} The most common sequelae are hypertension-related complications such as left ventricular (LV) failure, intracranial haemorrhage, premature coronary artery disease.¹ Surgical correction is standard of care in infants with CoA, the treatment of choice for older children and adults is percutaneous stent implantation.

Despite successful CoA repair, a substantial number of CoA patients suffer from hypertension and impaired LV function later in life.^{4,5} Changed aortic arch geometry, frequent residual aortic narrowing, and the negative impact of generalized aortopathy on the Windkessel effect often result in an increased afterload in CoA patients.^{6–9} LV changes such as hypertrophy and hyperkinesia can then be expected as a result of adverse arterial-ventricular interaction.

Due to the risk of these long-term complications, lifelong follow-up is warranted for patients with (repaired) CoA. Regular blood pressure evaluation and cardiac imaging are recommended, for which cardiac magnetic resonance (CMR) is the preferred imaging modality.⁶ In recent years, the scope of CMR has been expanded with a novel technique: four-dimensional flow CMR (4D flow CMR). This technique allows for flow assessment over an entire volume. Previous studies investigating CoA patients using 4D flow CMR have shown abnormal flow phenomena in patients with CoA and after successful CoA repair.^{7–9}

In this study, we hypothesized that potentially abnormal aortic flow patterns could have a negative impact on the LV by adverse arterial-ventricular interaction. The aim was therefore to investigate if there is a relationship between potentially abnormal aortic haemodynamics as assessed by 4D flow CMR and LV performance as measured by routine CMR in patients with native or recurrent CoA.

METHODS

Patients

Patients aged > 7 years of age with (a history of) CoA who had an indication for routine CMR as determined by their treating physician at our centre were asked to participate. For this study, 4D flow acquisition was added to the routine CoA CMR protocol. Informed consent was obtained for all patients (and their guardians, if applicable). This study was approved by the local medical ethical committee (study number 16-197).

CMR acquisition

CMR imaging was performed on a 3.0 T scanner (Ingenia R5.6.1, Philips Healthcare, Best, The Netherlands). Routine LV dimensions, function and mass were assessed using a retrospective ECG-gated steady state free-precession cine pulse sequence with breath holds in multiple short-axis planes. The short-axis plane was perpendicular to the ventricular long-axis and contained 13-15 slices with a slice thickness of 8 mm covering the entire LV. Imaging parameters were as follows: pixel size = 0.94 mm^2 , FOV = $270 \times 270 \text{ mm}^2$, number of cardiac phases = 40, echo time = 1.5 mm, repetition time = 3.0 mm, flip angle = 45° , SENSE = 2.5. Scan times were typically 8-10 minutes per scan.

4D flow CMR acquisition was performed without administration of gadolinium contrast in a sagittal orientation covering the complete thoracic aorta using retrospective ECG gating and a respiratory navigator placed on the lung–liver interface. Imaging parameters for the 4D flow CMR were as follows: voxel size = $2.5 \times 2.5 \times 2.5 \text{ mm}$, FOV = $300 \times 300 \text{ mm}^2$ – $350 \times 350 \text{ mm}^2$, number of cardiac phases: 16-25, TE = 2.6 ms, repetition time = 4.4 ms, flip angle = 10° , fold-over direction = AP, VENC = 200-350 cm/s, TFE factor = 3, SENSE = 2.5 (AP) and 1.5 (RL). Scan times for 4D flow CMR were typically 8-12 minutes per scan.

CMR post-processing

Cine images of the LV were segmented using CAAS MR solutions version 5.1 (Pie Medical Imaging, Maastricht, The Netherlands) as previously described.¹⁰ Routine LV parameters collected for this study were: end diastolic (ED) LV mass indexed for body surface area (LV mass_i), LV ejection fraction (LVEF), LVED volume (LVEDV), LVES volume (LVESV), LVEDV indexed for body surface area (LVEDV_i), LVESV indexed for body surface area (LVESV_i), LV stroke volume (SV) and LV SV indexed for body surface area (LVSV_i).

Post-processing of 4D flow CMR images was performed using an in-house developed 4D flow CMR MATLAB toolbox.¹¹ The data processing includes four steps: a) the segmentation of the thoracic aorta using the angiographic image¹²; b) the generation

of the tetrahedral finite element mesh¹³ from the segmentation generated in (a); c) the interpolation of the velocities field to the tetrahedral finite element mesh, using a cubic interpolation (Figure 1).

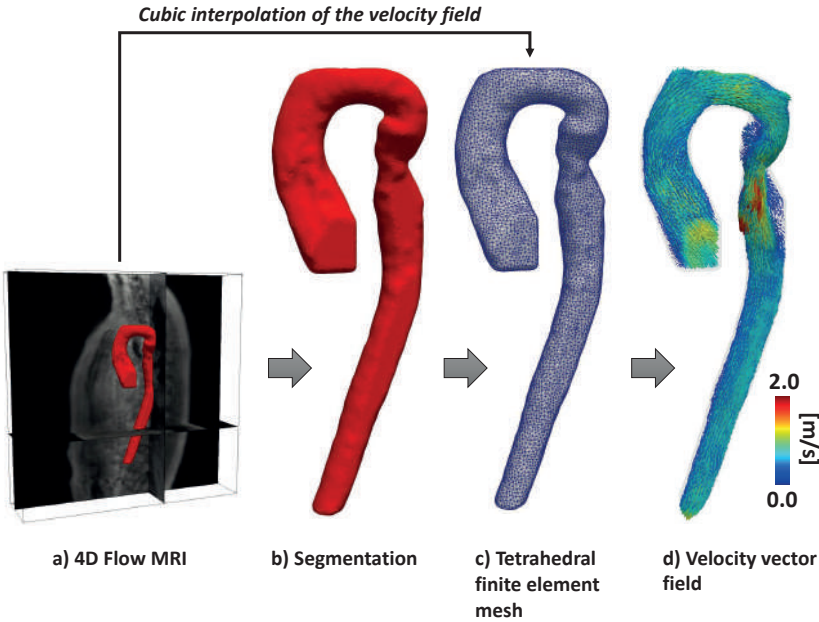


Figure 1. The steps for pre-processing of the four-dimensional flow cardiac magnetic resonance.

Once the velocity fields were interpolated to the tetrahedral finite element mesh, a global least square stress projection method was used to calculate the derivative value of the velocity field in each orthogonal direction (x , y , z), as previously described.^{14,15} Using this information the wall shear stress, oscillatory shear index, vorticity, viscous dissipation, energy loss, and kinetic energy were calculated at the nodal level. The equations and the three-dimensional maps of each haemodynamic parameter at peak systole are shown in Figure 2.

The velocity angle was calculated as the angle between the velocity vectors and the axial unit vector, in each point of the lumen of the vessel. The axial unit vectors are evaluated as the normalized gradient of the Laplace solution as described previously.¹⁶ The Laplace solution was also used to automatically calculate different level sets equally spaced (5 mm) along the vessel. In each level set the flow curve and the cross correlation

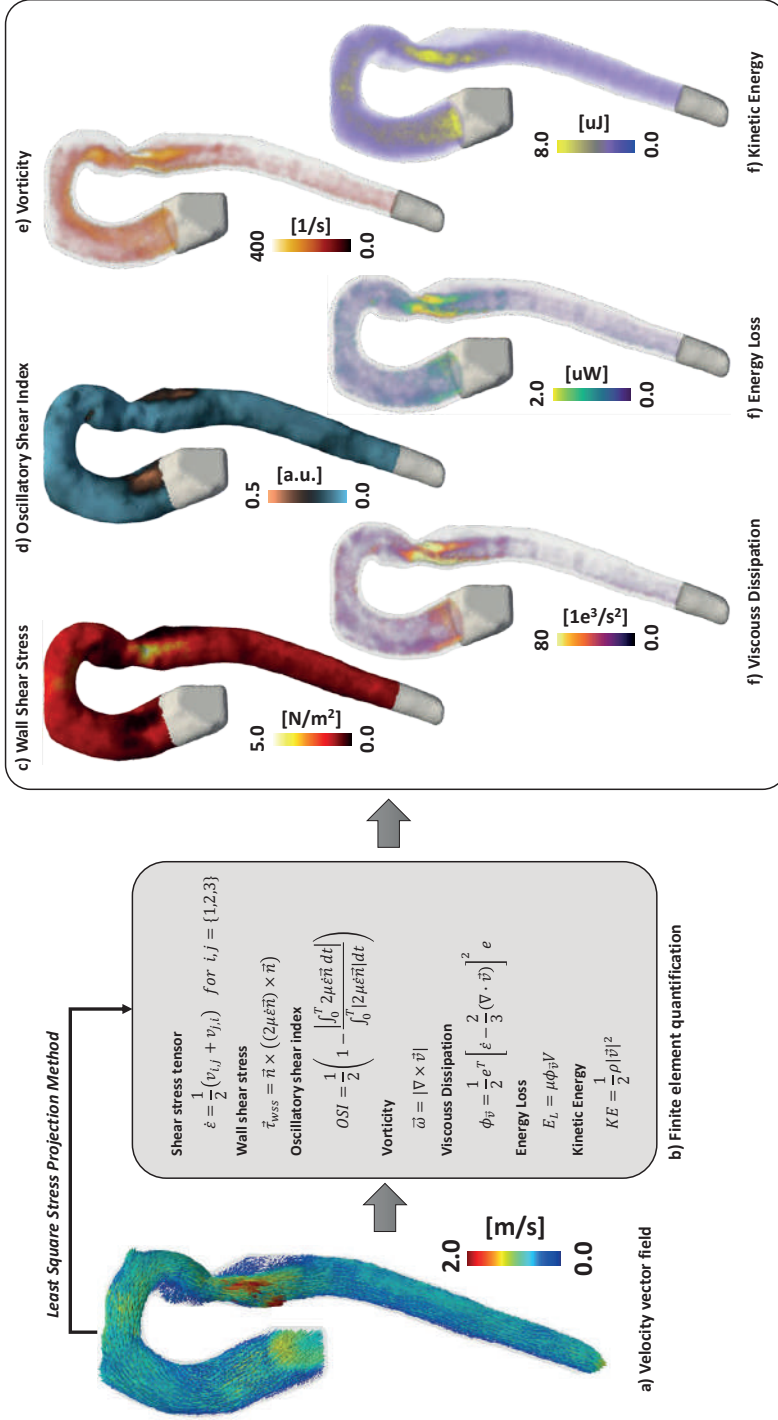


Figure 2. Formulas and required steps for the calculation of the different advanced 4D flow parameters (left) and examples of visualization of the different 4D flow parameters (right). Where is the velocity vector, is the derivative value of the component of with respect to . is the inward unit normal vector to the surface, is the dynamic viscosity, is the density of the blood, is the density of the blood, is the identity matrix. Parameters were calculated at the nodal level.

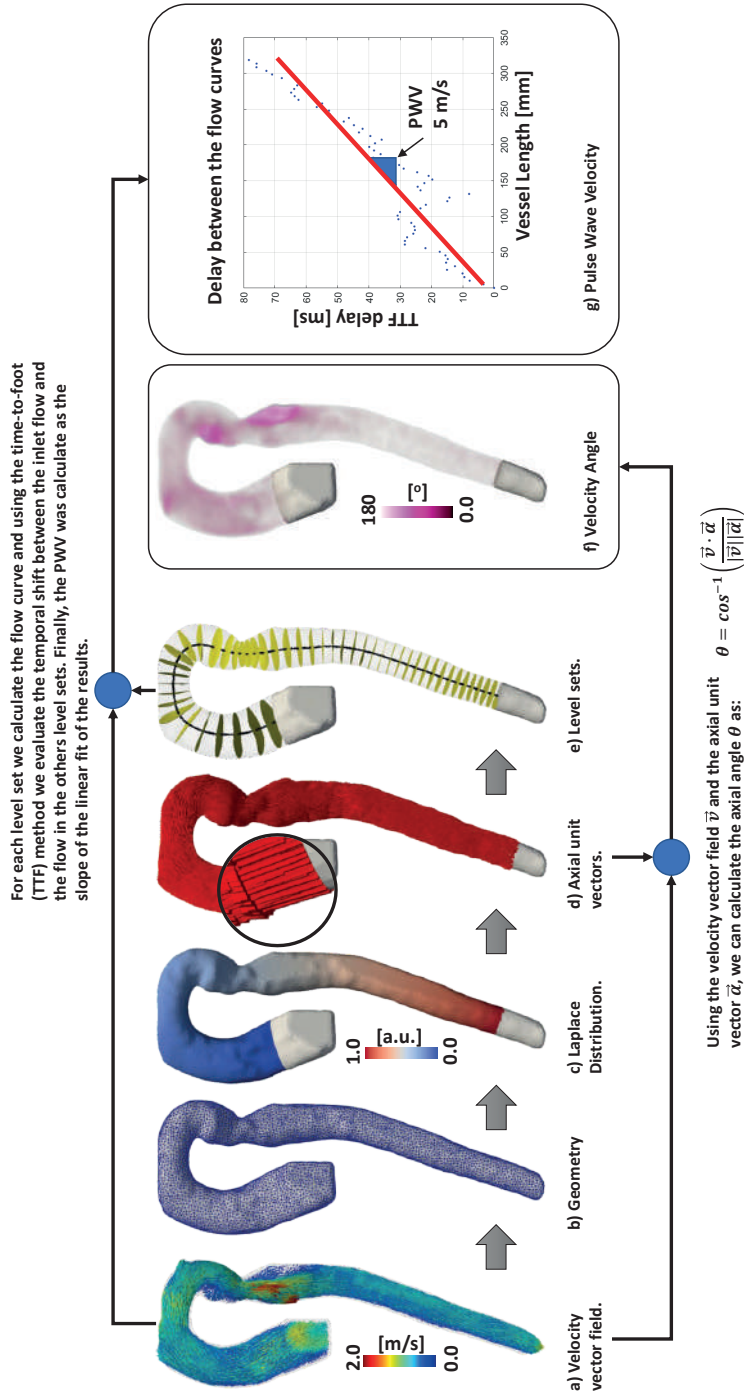


Figure 3. Steps required for calculation of the velocity angle and pulse wave velocity. Pulse wave velocity was calculated using the time-to-foot method.

was calculated and used to evaluate the temporal displacement with the inlet flow curve. Finally, the global pulse wave velocity (PWV) was calculated as the slope of the linear fit of the temporal displacement results (Figure 3), using the time-to-foot method.¹⁷

For the 4D flow post-processing, the aorta was divided into 7-10 segments, depending on the length of the aorta within the acquired volume. Subsequent 4D flow analysis was then performed for the following aortic segments: one segment for the ascending aorta, one at the site of the narrowest aortic diameter (CoA), and one for the descending aorta. For the ascending aorta, the mean and maximum values of wall shear stress, oscillatory shear index, kinetic energy, and velocity angle were collected. For the CoA segment, peak velocity, mean and maximum values of wall shear stress, oscillatory shear index, kinetic energy and velocity angle were collected. For the descending aorta, vorticity, viscous dissipation, and energy loss were collected.

Statistics

Statistical analysis was performed using R version 3.6.3.¹⁸ Descriptive statistics were used for demographic data. Quantitative data are presented as mean \pm standard deviation, median (interquartile range), or absolute number (percentage). Normality of continuous data was assessed using histograms, QQ-plots, and the Shapiro-Wilk test. Linear regression was used to test if there was a correlation between different continuous parameters. For 4D flow parameters with a statistically significant relation to LV parameters, age was subsequently added to the regression model to investigate whether results held up after correction for age. Comparison between groups was performed using the student's t-test or the Mann-Whitney U test, depending on normality. Results were considered statistically significant if the probability value (p-value) did not exceed or was not equal to 0.05. Due to the exploratory nature of this study, correction for multiple testing was not performed.¹⁹

RESULTS

A total of 17 patients were included, 7 patients (41%) were male, mean age was 28 ± 19 years. Thirteen (76%) of the patients with CoA underwent previous intervention; 3 underwent balloon angioplasty, 10 underwent surgical repair. Mean age at CoA intervention was 5 ± 6 years. Out of 17 patients, 4 (24%) patients had a native CoA. The most common associated defects were BAV and ventricular septal defect, both present in 5 (29%) patients. Data on outpatient blood pressure measurements were available for 15 (88%) patients. Mean systolic blood pressure was 142 ± 14 mmHg. Data on 24 hour blood pressure measurements were available for 10 (59%) patients: mean systolic blood

pressure during the day was 124 ± 16 mmHg, mean systolic blood pressure during the night was 112 ± 15 mmHg. Nine patients (53%) had systolic hypertension during their outpatient visit (> 140 mmHg), five patients (29%) used one or more antihypertensive drugs. After CMR acquisition seven patients (41%) underwent cardiac catheterization and three of them had a peak-to-peak gradient of > 20 mmHg over the CoA site and thus underwent percutaneous stent implantation. All baseline data are presented in Table 1.

Table 1. Baseline characteristics.

Characteristic	
Age (years)	28 ± 19
Male	7 (41%)
Height (cm)	170 ± 12
Weight (kg)	64 ± 15
Body mass index (kg/m^2)	22 ± 4
<i>Concomitant cardiac defect</i>	
Bicuspid aortic valve	5 (29%)
Ventricular septal defect	5 (29%)
Atrial septal defect	1 (6%)
Hypoplastic aortic arch	1 (6%)
Persistent ductus arteriosus	1 (6%)
<i>Previous coarctation repair</i>	
End-to-end anastomosis	7 (41%)
Patch angioplasty	1 (6%)
Surgery, type unknown	2 (12%)
Balloon dilatation	3 (18%)
None	4 (24%)
<i>Systolic blood pressure (mmHg)</i>	
Outpatient (n = 15)	142 ± 14
24 hours – average (n = 11)	121 ± 12
24 hours – daytime (n = 10)	124 ± 16
24 hours – night-time (n = 10)	112 ± 15
<i>Medication use</i>	
ACE inhibitor	2 (12%)
Angiotensin II receptor blocker	1 (6%)
Beta-blocker	3 (18%)
Calcium-channel blocker	1 (6%)
Diuretics	1 (6%)
None	12 (71%)

Data are presented as number (percentage) or mean \pm standard deviation.

Aortic haemodynamics and ventricular performance

Mean diameter of the ascending aorta was 28 ± 8 mm, mean CoA diameter was 16 ± 4 mm, and median diameter of the descending aorta was 18 (IQR: 15 - 20) mm. Mean peak velocity across the former CoA site was 239 ± 59 cm/s. CMR showed preserved biventricular function for all patients, expressed by a mean LVEF of $58 \pm 5\%$. LV dimensions were also normal with a mean LVEDV_i of 97 ± 16 ml/m², mean LVESV_i of 41 ± 10 ml/m², and mean LV mass_i of 51 ± 10 g/m². Mean global PWV throughout the complete aorta by 4D flow CMR was 561 ± 167 cm/s. A summary on 4D flow haemodynamics can be found in Table 3.

Table 2. Cardiac magnetic resonance parameters for the left ventricle and the aorta site.

CMR parameter	
LV mass _i (g/m ²)	51 ± 10
LVEDV _i (ml/m ²)	97 ± 16
LVESV _i (ml/m ²)	41 ± 10
LV Stroke volume _i (ml/m ²)	57 ± 9
LV Ejection fraction	58 ± 5
AoAsc peak velocity (cm/s)	118 ± 30
AoAsc diameter (mm)	28 ± 8
CoA peak velocity (cm/s)	239 ± 59
CoA diameter (mm)	16 ± 4
AoDesc peak velocity (cm/s)	112 ± 47
AoDesc diameter (mm)	18 (IQR: 15 - 20)
Pulse wave velocity (cm/s)	561 ± 167

Data are presented as mean \pm standard deviation or median (interquartile range). AoAsc: ascending aorta, AoDesc: descending aorta, CoA: coarctation site, ED: end-diastolic, ES: end-systolic, IQR: interquartile range, LV: left ventricle, LVEDV_i: left ventricular end-diastolic volume indexed for body surface area, LVESV_i: left ventricular end-systolic volume indexed for body surface area.

Arterial – ventricular interaction

Using linear regression analyses no significant relationship was found between CoA diameter, peak velocity at the (former) CoA site, systolic blood pressure and the LV parameters. Several significant associations were found between 4D flow parameters and LV volumes and mass (Table 4). For the ascending aorta maximum velocity angle, an expression of local flow orientation, was related to LV mass_i ($p = 0.0445$). For the (former) CoA site, maximum energy loss was correlated to LVEDV_i and LVESV_i ($p = 0.0499$, $p = 0.0426$, respectively). For the descending aorta, maximum vorticity was related to LVEDV_i ($p = 0.0461$). Global PWV for the aorta was found to have a significant relationship with

LV mass_i and LVESV_i ($p = 0.0385$, $p = 0.0397$, respectively). Apart from the correlations with maximum energy loss at the CoA site, these results remained significant after correction for age.

Since patients with BAV have abnormal flow patterns in the entire aorta, and especially the ascending aorta (Figure 1A), we analysed whether the maximum velocity angle in the ascending aorta, the maximum vorticity in the descending aorta and the PWV were different between patients with BAV and patients with normal aortic valves. No significant differences between these groups were found (Table 5).

Table 3. Four-dimensional flow cardiac magnetic resonance parameters for the aorta.

Location	4D flow parameter	Mean values	Maximum values
AoAsc	Wall shear stress (N/m ²)	1.18 (IQR: 0.99 – 1.78)	2.50 (IQR: 1.91 – 3.73)
AoAsc	Oscillatory shear index (a.u.)	0.11 (IQR: 0.09 – 0.15)	0.42 (IQR: 0.35 – 0.46)
AoAsc	Kinetic energy (μJ)	2.02 (IQR: 0.71 – 2.51)	9.81 (IQR: 4.02 – 11.92)
AoAsc	Velocity angle (°)	12.17 (IQR: 8.70 – 18.18)	78.72 (IQR: 52.29 – 118.36)
CoA	Wall shear stress (N/m ²)	1.28 (IQR: 0.96 – 1.89)	3.34 (IQR: 2.09 – 3.58)
CoA	Oscillatory shear index (a.u.)	0.06 (IQR: 0.04 – 0.11)	0.35 (IQR: 0.19 – 0.43)
CoA	Kinetic energy (μJ)	1.72 (IQR: 0.70 – 2.61)	97.17 (IQR: 60.49 – 150.92)
CoA	Energy loss (μW)	0.59 (IQR: 0.30 – 0.78)	1.78 (IQR: 1.13 – 3.98)
CoA	Velocity angle (°)	11.32 (IQR: 8.29 – 13.07)	97.17 (IQR: 60.49 – 150.92)
AoDesc	Vorticity (s ⁻¹)	48.49 (IQR: 30.95 – 57.11)	120.00 (IQR: 97.23 – 152.81)
AoDesc	Viscous dissipation (e ³ /s ²)	3.04 (IQR: 1.78 – 4.34)	14.93 (IQR: 9.55 – 25.74)
AoDesc	Energy loss (μW)	0.07 (IQR: 0.05 – 0.13)	0.32 (IQR: 0.28 – 0.39)

Data are presented as median (interquartile range). AoAsc: ascending aorta, AoDesc: descending aorta, CoA: coarctation site, IQR: interquartile range.

Table 4. Statistically significant results for linear regression analyses.

Location	4D flow parameter	LV parameter	Intercept	Coefficient	R	p-value
Ascending aorta	Maximum velocity angle (°)	LV mass _i	101.5664	-0.3207	0.4926	0.0445
Aortic coarctation	Maximum energy loss (μW)	LVEDV _i	88.6325	1.8864	0.4824	0.0499
Aortic coarctation	Maximum energy loss (μW)	LVESV _i	35.7114	1.2810	0.2465	0.0426
Descending aorta	Maximum vorticity (s ⁻¹)	LVEDV _i	78.1594	0.1248	0.4909	0.0454
Complete aorta	Pulse wave velocity (cm/s)	LV mass _i	33.373	3.3790	0.5571	0.0385
Complete aorta	Pulse wave velocity (cm/s)	LVESV _i	62.370	-3.658	0.5542	0.0397

ED: end-diastolic, LV: left ventricle, LVEDV_i: left ventricular end-diastolic volume indexed for body surface area, LVESV_i: left ventricular end-systolic volume indexed for body surface area.

Table 5. Comparison of flow parameters between patients with a bicuspid aortic valve and patients with a normal aortic valve.

Parameter	BAV (n = 5)	Normal AoV (n = 12)	p-value
Maximum velocity angle AoAsc (°)	107.1 (IQR: 52.3 - 118.4)	78.1 (IQR: 64.0 – 107.0)	0.7990
Vorticity AoDesc (s ⁻¹)	9.7 (IQR: 9.6 - 14.9)	18.5 (IQR: 10.7 - 42.4)	0.1946
Pulse wave velocity (cm/s)	659.5 (IQR: 645.2 – 697.9)	588.7 (IQR: 436.7 – 698.9)	0.3913

Data were presented as median (interquartile range). AoAsc: ascending aorta, AoDesc: descending aorta, AoV: aortic valve, BAV: bicuspid aortic valve, PWV: pulse wave velocity.

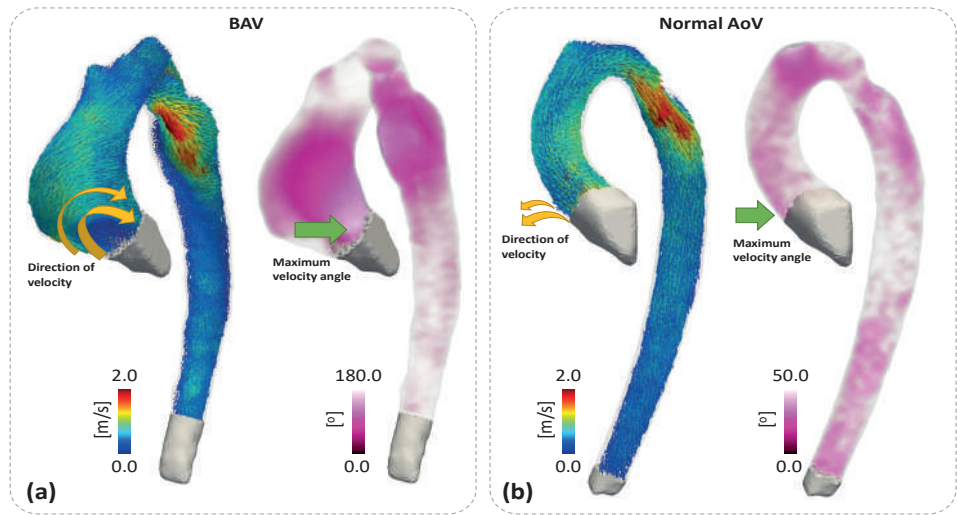


Figure 4. Visualisation of velocity angle in the ascending aorta in two patients. In (a) we show a coarctation patient with a bicuspid aortic valve with higher values of velocity angle in the ascending aorta generated by the abnormal rotational flow which is characteristic for bicuspid aortic valve patients. In (b) we show a coarctation patient with normal aortic valve, the maximum velocity angle in this case is also located in the proximal ascending aorta, given by small rotational flow at the sinuses of Valsalva.

DISCUSSION

Several 4D flow CMR studies have been performed in patients with (recurrent) CoA. The majority of these studies focussed on non-invasive pressure gradients and wall shear stress²⁰⁻²² or gave a qualitative analysis of vortices and helical flow.^{7,9,23} To the best of our knowledge, this study is the first to investigate the relationship between advanced 4D flow parameters and LV function, volume and mass and conveys the following findings:

1. Increased local flow rotation, as expressed by maximum vorticity, in the descending aorta is related to increased LVEDV_i.
2. Increased local flow orientation, as expressed by maximum velocity angle, in the ascending aorta is related to decreased LV mass_i.
3. Global PWV measured by 4D flow CMR is related to LV mass_i and LVESV_i.
4. 4D flow parameters correlated to LV parameters were not significantly different between patients with BAV and patients with normal AoV.

Our analyses show a significant correlation between maximum vorticity in the descending aorta and LVEDV. The presence of altered aortic flow and vortex flow in CoA patients has been previously described.^{7,16} Hope et al. found marked helical flow at peak systole in the descending aorta of patients with repaired CoA and an angulated aortic geometry that were not seen in healthy volunteers or patients with repaired CoA and normal aortic geometry.⁷ Furthermore, they reported vortex flow distal to mild narrowing of the aorta and in areas of post-stenotic dilatation.⁷ Frydrychowicz et al. also investigated flow patterns in patients with repaired and native CoA and healthy controls. They found that CoA patients were at greater risk of helical and vortex flow compared to healthy controls.²³

We found maximum velocity angle in the ascending aorta to be related to decreased LV mass_i. To the best of our knowledge, only one recent work by Sotelo et al.²⁴, analysed this parameter in the aorta in healthy volunteers and patients with transposition of the great arteries. They found a relationship between velocity angle and aortic root dilatation in patients with transposition of the great arteries. This is consistent with our results where this parameter increases in the proximal ascending aorta, caused by the turbulence generated in the sinuses of Valsalva in CoA patients with a normal aortic valve, and by the effect of dilatation of the ascending aorta in CoA patients with BAV (Figure 4). Both Hope et al. and Frydrychowicz et al. also found right-handed helical flow in CoA patients, exemptions being the patients with BAV.^{7,23} Thus, although there is evidence to suggest velocity angle may play a role in aortic dilatation, the relationship LV mass_i is still unexplained.

Patients with repaired CoA are known to have an increased PWV - a measure for aortic stiffness - late after repair.²⁵⁻²⁷ Our findings of a mean global PWV of 561 ± 167 cm/s are in line with previous research performed by Dijkema et al. who found a mean PWV in the aortic arch of 5.6 ± 1.9 m/s in a cohort of CoA patients aged 30 ± 10.6 years.²⁶ Other researchers found lower a lower PWV in CoA patients: Juffermans et al. reported a mean PWV of 4.8 ± 1.4 m/s in the proximal aorta and Ou et al. reported a mean PWV of 4.7 ± 1.3 m/s in the aortic arch.^{25,27} The lower PWV found in these studies is most likely do to the

differences in age of the cohorts; the cohort of Juffermans et al. had a mean age of 14 ± 3 years and the cohort of Ou et al. had a mean age of 12 ± 8 years. Since PWV increases with age, this is the most likely explanation for the differences in PWV between the studies.²⁸ The correlation between PWV and LV mass_i and LVESV_i in this study remained significant after correction for age. Increased aortic stiffness may result in hypertension, creating an increased afterload for the LV, which may ultimately lead to LV hypertrophy. PWV could therefore be a valuable parameter to follow-up in CoA patients.

Up to 40% of CoA patients have a BAV.²⁹ The abnormal arrangement of the aortic valve leaflets in BAV generates an abnormal flow pattern in the ascending aorta.^{30,31} To determine whether the correlations found in this study were not solely driven by the presence of BAV in five patients in our cohort, we performed a comparison of the values of 4D flow CMR parameters found to have a significant association with LV parameters for patients with BAV and normal, tricuspid, aortic valve. No significant differences were found between the two groups. However, since the two groups compared are small (5 versus 12), results of this comparison should be interpreted with caution.

Previous research on diagnostic parameters in CoA has mainly focussed on parameters such as the pressure gradient, peak velocity, PWV, and CoA diameter. Our results on vorticity and velocity angle suggest that other characteristics of the blood flow (i.e. rotation and orientation) could also be of importance. It gives a basis for further research into these parameters. This study is a first step towards unravelling the complex interaction between aortic haemodynamics and LV performance using 4D flow CMR. More studies in larger groups are warranted to determine the clinical relevance of advanced 4D flow parameters in CoA. In the future, these parameters could possibly be used for early detection of haemodynamic abnormalities or even to help in the clinical decision making for treatment of CoA.

LIMITATIONS

There are several limitations that need to be considered. First, the number of patients was limited and also heterogeneous due to the inclusion of patients with native and a (suspected) recurrent CoA. Regardless of the sample size, we were still able to detect several significant findings. Second, data on blood pressure and blood pressure gradient were acquired retrospectively, resulting in missing data. Third, the movement of the vessel was not considered in the segmentation process, only one segmentation was generated for all cardiac phases. Last, there was no control group available of healthy volunteers to compare with data from the CoA patients.

CONCLUSION

We show that multiple aortic 4D flow parameters in CoA patients have a relationship with LV performance: maximum velocity angle in the ascending aorta, maximum vorticity in the descending aorta and PWV of the entire thoracic aorta. Routine CMR parameters including vessel diameter and peak velocity demonstrated no relationship with LV function, volumes, or mass. Thus, 4D flow CMR may provide novel parameters to assess cardiovascular haemodynamics and the interaction between the aorta and the LV in patients with (recurrent) CoA. Further research in larger groups of patients is warranted to determine the clinical significance of these findings of adverse arterial-ventricular interaction.

REFERENCES

1. Torok R.D., Campbell M.J., Fleming G.A., and Hill K.D.: Coarctation of the aorta: management from infancy to adulthood. *World J Cardiol* 2015; 7: pp. 765-775
2. Warnes C.A.: Bicuspid aortic valve and Coarctation: two villains part of a diffuse problem. *Heart* 2003; 89: pp. 965-966
3. Dijkema EJ, Grotenhuis HB, Leiner T. Diagnosis, imaging and clinical management of aortic coarctation. *Heart*. 2017 Aug;103(15):1148-1155. doi: 10.1136/heartjnl-2017-311173.
4. Ou P, Celermajor DS, Jolivet O, et al. Increased central aortic stiffness and left ventricular mass in normotensive young subjects after successful coarctation repair. 2008 Jan;155(1):187-93. doi: 10.1016/j.ahj.2007.09.008. Epub 2007 Nov 19.
5. Crepez R, Pitscheider W, Oberhollenzer R, et al. Long-term follow-up in patients operated on for aortic coarctation. The echo-Doppler and MRI assessment of left ventricular function and the transisthmic gradient. *G Ital Cardiol*. 1993 Aug;23(8):767-76.
6. Brown ML , Burkhart HM , Connolly HM , et al. Coarctation of the aorta: lifelong surveillance is mandatory following surgical repair. *J Am Coll Cardiol* 2013;62:1020–5.doi:10.1016/j.jacc.2013.06.016
7. Hope MD, Meadows AK, Hope TA, et al. Clinical evaluation of aortic coarctation with 4D flow MR imaging. *J Magn Reson Imaging*. 2010 Mar;31(3):711-8. doi: 10.1002/jmri.22083.
8. Senzaki H Iwamoto Y Ishido H Masutani S Taketazu M Kobayashi Tet al. Ventricular-vascular stiffening in patients with repaired coarctation of aorta. *Circulation* 2008;118:S191–8.
9. Hope MD, Meadows AK, Hope TA, et al. Images in cardiovascular medicine. Evaluation of bicuspid aortic valve and aortic coarctation with 4D flow magnetic resonance imaging. *Circulation*. 2008 May 27;117(21):2818-9. doi: 10.1161/CIRCULATIONAHA.107.760124.
10. Prakken, NH, Velthuis, BK, Vonken, EJ, Mali, WP, Cramer, MJ. Cardiac MRI: standardized right and left ventricular quantification by briefly coaching inexperienced personnel. *Open Magn Reson J* 2008; 1:104–111.
11. Sotelo J, Mura J, Hurtado D, Uribe S. A novel MATLAB Toolbox for processing 4D Flow MRI data. *Proc Intl Soc Mag Reson Med* 27. 2019;1956
12. Bock J, Frydrychowicz A, Stalder AF et al. 4D phase contrast MRI at 3 T: effect of standard and blood-pool contrast agents on SNR, PC-MRA, and blood flow visualization. *Magn Reson Med*. 2010;63(2):330-8.
13. Qianqian F, Boas DA. 2009. Tetrahedral Mesh Generation from Volumetric Binary and Gray-Scale Images. In *Proceedings of the 6th IEEE International Conference on Symposium on Biomedical Imaging: From Nano to Macro*, Boston, Massachusetts, USA: 1142–1145.
14. Sotelo J, Urbina J, Valverde I, et al. 3D Quantification of Wall Shear Stress and Oscillatory Shear Index Using a Finite-Element Method in 3D CINE PC-MRI Data of the Thoracic Aorta. *IEEE Trans Med Imaging*. 2016;35(6):1475-87.
15. Sotelo J, Urbina J, Valverde I, et al. Three-dimensional quantification of vorticity and helicity from 3D cine PC-MRI using finite-element interpolations. *Magn Reson Med*. 2018;79(1):541-553.

16. Sotelo J, Dux-Santoy L, Guala A, Rodríguez-Palomares J, et al. 3D axial and circumferential wall shear stress from 4D flow MRI data using a finite element method and a laplacian approach. *Magn Reson Med*. 2018;79(5):2816-2823.
17. Wentland AL, Grist TM, Wieben O. Review of MRI-based measurements of pulse wave velocity: a biomarker of arterial stiffness. *Cardiovasc Diagn Ther*. 2014;4(2):193-206. doi:10.3978/j.issn.2223-3652.2014.03.04
18. R Core Team (2020). R: A language and environment for statistical computing. R Foundation for Statistical Computing, Vienna, Austria. URL <https://www.R-project.org/>
19. Bender R, Lange S. Adjusting for multiple testing--when and how? *J Clin Epidemiol*. 2001 Apr;54(4):343-9. doi: 10.1016/s0895-4356(00)00314-0.
20. Ebbers T, Wigstrom L, Bolger AF, Engvall J, Karlsson M. Estimation of relative cardiovascular pressures using time-resolved three-dimensional phase contrast MRI. *Magn Reson Med* 2001;45: 872-9
21. Tyszka JM, Laidlaw DH, Asa JW, Silverman JM. Three-dimensional, time-resolved (4D) relative pressure mapping using magnetic resonance imaging. *J Magn Reson Imaging* 2000;12:321-9.
22. Donati F, Figueroa CA, Smith NP, et al. Non-invasive pressure difference estimation from PC-MRI using the work-energy equation. *Med Image Anal*. 2015 Dec;26(1):159-72. doi: 10.1016/j.media.2015.08.012.
23. Frydrychowicz A, Markl M, Hirtler D, et al. Aortic hemodynamics in patients with and without repair of aortic coarctation: in vivo analysis by 4D flow-sensitive magnetic resonance imaging. *Invest Radiol*. 2011 May;46(5):317-25. doi: 10.1097/RLI.0b013e3182034fc2.
24. Sotelo J, Valverde I, Martins D, Bonnet D, Boddaert N, Pushparajan K, Uribe S, Raimondi F. Impact of aortic arch curvature in flow haemodynamics in patients with transposition of the great arteries after arterial switch operation. *Eur Heart J Cardiovasc Imaging*. 2021 Jan 31;jeaa416. doi: 10.1093/ehjci/jeaa416.
25. Ou P, Celermajor DS, Jolivet O, et al. Increased central aortic stiffness and left ventricular mass in normotensive young subjects after successful coarctation repair. *Am Heart J* 2008; 155: pp. 187-193
26. Dijkema EJ, Sliker MG, Leiner T, et al. Arterioventricular interaction after coarctation repair. *Am Heart J*. 2018 Jul;201:49-53. doi: 10.1016/j.ahj.2018.04.004.
27. Juffermans JF, Nederend I, van den Boogaard PJ, et al. The effects of age at correction of aortic coarctation and recurrent obstruction on adolescent patients: MRI evaluation of wall shear stress and pulse wave velocity. *Eur Radiol Exp*. 2019;3(1):24. Published 2019 Jun 20. doi:10.1186/s41747-019-0102-9
28. Diaz A, Tringler M, Wray S, et al. The effects of age on pulse wave velocity in untreated hypertension. *J Clin Hypertens (Greenwich)*. 2018 Feb;20(2):258-265. doi: 10.1111/jch.13167.
29. Warnes CA. Bicuspid aortic valve and Coarctation: two villains part of a diffuse problem. *Heart* 2003;Sep;89(9):965-6.

30. Meierhofer C, Schneider EP, Lyko C, et al. Wall shear stress and flow patterns in the ascending aorta in patients with bicuspid aortic valves differ significantly from tricuspid aortic valves: a prospective study. *Eur Heart J Cardiovasc Imaging* 2013;Aug;14(8):797-804
31. Barker AJ, Markl M, Burk J, et al. Bicuspid aortic valve is associated with altered wall shear stress in the ascending aorta. *Circ Cardiovasc Imaging* 2012;5(4):457-66



Chapter 4

Effect of stent implantation on blood pressure control in adults with coarctation of the aorta

Jennifer J. van der Burg
Evangeline G. Warmerdam
Gregor J. Krings
Folkert J. Meijboom
Arie P. van Dijk
Marco C. Post
Gerrit Veen
Michiel Voskuil
Gertjan Tj. Sieswerda

Cardiovascular revascularization medicine:
vol. 19,8 (2018): 944-950

ABSTRACT

Background. Stenting of coarctation of the aorta (CoA) generally results in good angiographic results and a decrease in trans-coarctation pressure gradient. However, effect on blood pressure control is less clear. The goal of the current retrospective analysis was to investigate the effects of CoA stenting on blood pressure control.

Methods. A retrospective analysis was conducted in consecutive adult patients with a CoA who underwent a percutaneous intervention at one of the three participating hospitals. Measurements included office blood pressure, invasive peak-to-peak systolic pressure over the CoA, diameter of the intima lumen at the narrowest part of the CoA and use of medication. The follow-up data were obtained, based on the most recent examination date.

Results. There were 26 patients with native CoA and 17 with recurrent CoAs (total $n = 43$). Seven of them underwent two procedures. Mean peak-to-peak gradient decreased from 27 mmHg to 3 mmHg ($p < 0.001$), and minimal diameter increased from a mean of 11 mm to 18 mm ($p < 0.001$). Mean systolic blood pressure decreased from 151 ± 18 mmHg to 135 ± 19 mmHg at first follow-up of 3.8 ± 1.9 months and 137 ± 22 mmHg at latest follow-up of 19.5 ± 10.9 months ($p = 0.001$ and $p = 0.009$, compared to baseline, respectively). The total number of hypertensive patients decreased from 74% to 27% at latest follow-up. No significant change in antihypertensive medication was observed.

Conclusion. A clinically significant decrease in systolic blood pressure of 16 mmHg was shown after (re)intervention in CoA patients, which sustained at follow-up. This sustained decrease of blood pressure can be expected to lead to less future adverse cardiovascular events.

INTRODUCTION

Aortic coarctation (CoA) is a congenital restriction of the lumen of the aorta, commonly occurring as stenosis in the juxtaductal position.¹ It accounts for 5–8% of all congenital heart disorders, but can also have an acquired cause (i.e. Takayasu).² CoA may be seen in isolation but frequently occurs in combination with other cardiac lesions like bicuspid aortic valve or ventricular septal defect.³ Its natural history carries a mean life expectancy of approximately 35 years, mainly resulting from hypertension related complications such as left ventricular failure (28%), intracranial haemorrhage (12%), aortic rupture/dissection (21%) and premature coronary artery disease, but also from infective endocarditis (18%) or associated heart defects.¹ Unrepaired CoA frequently causes problems in early infancy, with 60% of the untreated patients with symptomatic high-grade CoA and 90% of the patients with complicated CoA dying during the first year of life. CoA may be corrected surgically with a high degree of anatomical success, but patients typically show high rates of hypertension, may suffer from restenosis, and in up to 10% recurrent CoA occurs with the need of a re-intervention.^{4–6} Up to one third of the patients develop hypertension during follow-up.^{7–9}

As of the 1990s, invasive percutaneous treatment became widely accepted as a treatment option for CoA. Initially, percutaneous treatment only consisted of expandable balloon dilatation, and relatively high rates of complications such as restenosis and balloon rupture were observed.¹⁰ With the introduction of the Cheatham Platinum stent (NuMED, Hopkinton, NY, USA) a way to overcome these drawbacks was introduced. Placement of a balloon-expandable stent soon became standard of care. Percutaneous stent placement as treatment for CoA leads to fewer acute complications and acute angiographic and long-term results comparable with surgical repair.¹¹ Although the therapy virtually abolishes the risk of early left ventricular failure, even after relief of obstruction to a residual transaortic pressure gradient of < 10 mmHg, long-term blood pressure control proves to be suboptimal in many patients.¹¹ It is hypothesized that an underlying generalized arteriopathy is accountable for the persisting systemic hypertension even after treatment of the focal stenosis. Although not undebated, aortic arch hypoplasia and/or gothic arch have been described to be a substrate for systemic arterial hypertension.^{7,12} Furthermore, reduced baroreceptor sensitivity and residual arch gradients may also be contributing factors.^{13–15} Alternatively, a sub-optimal result of the (surgical or catheter) intervention may account for residual aortic obstruction resulting in reactive hypertension. Age of initial CoA repair is also known to be of great influence on the risk of long term hypertension.¹⁶ Regardless of its aetiology,

hypertension should be abolished, as it is associated with structural changes in the heart and blood vessels, leading to significant cardiovascular mortality and morbidity (i.e. stroke, acute myocardial infarction, aortic dilatation and dissection).¹⁷

Recently, we observed a rather striking improvement in systemic blood pressure regulation in several CoA cases that underwent (re-)intervention with stent placement. This observation supports the notion that blood pressure control may be more directly related to residual CoA relief than generally held. The aim of this study was to investigate the effects of stenting on blood pressure control in adult CoA patients.

METHODS

Patient population

We performed a retrospective observational chart review of all patients from the University Medical Center Utrecht, Radboud University Medical Center Nijmegen and St. Antonius Hospital Nieuwegein who underwent stent placement for CoA from 2009 to 2015. Data on demography, biometry, medication use, blood pressure, cardiac imaging parameters, and stent procedures were collected from the electronic patient file. Patients who underwent surgical repair or balloon dilatation without stent placement were excluded. Patients were divided in native CoA (no previous intervention), recurrent CoA, and patients with multiple interventions (interventions > 1 year apart).

Measurements

In accordance with the European Society of Cardiology (ESC) protocol¹⁸, blood pressure was measured by cuff sphygmomanometer on the right arm and leg. In case of arteria lusoria, the left arm was used. Hypertension was defined as systolic blood pressure > 140 mmHg on the upper limb, regardless of medication¹⁸; when reliable office measurements were not available, ambulatory blood pressure monitoring was analysed.¹⁸ A non-invasive arm-leg gradient of > 20 mmHg was considered suggestive of CoA.¹⁹ The echocardiographic parameters used to specifically assess presence of CoA were spectral and/or colour Doppler patterns in descending or abdominal aorta. Furthermore, left ventricle (LV) dimensions, LV systolic function and presence of LV hypertrophy were evaluated from 2D short and/or long-axis views. Non-invasive aortograms were obtained through Computed Tomography or Magnetic Resonance Imaging of the chest. The aortic lumen at the narrowest part of the CoA was measured and compared to the diameter of aorta at the diaphragm level. The presence and number

of collaterals was also assessed. To quantify the burden of the anti-hypertensive regime, Defined Daily Dose (DDD) index of the WHO²⁰ was calculated, both prior to intervention and at follow-up.

Indication for catheterization/stenting

As determined by the multidisciplinary Grown Up Congenital Heart disease team, CoA patients were considered candidate for intervention if either of the following was present: (a) upper-limb hypertension or significant LV hypertrophy and a significant trans-coarctation gradient (20 mmHg non-invasive, 15 mmHg invasive), (b) upper-limb hypertension or significant LV hypertrophy with an invasive gradient < 15 mmHg in the presence of extensive collateral formation and clear substrate, or (c) $\geq 50\%$ luminal narrowing at the CoA site as compared to the diaphragm level.¹⁹

Catheterization procedure

All patients underwent diagnostic catheterization for invasive pressure gradient measurements, (three-dimensional) angiography and, if indicated and deemed technically feasible, subsequent stent implantation. The procedures were performed under conscious sedation or general anaesthesia. Vascular access was achieved through the femoral artery using the standard Seldinger technique. Patients were heparinized (1.000 IE/10 kg). Using an open-end catheter, the gradient over the CoA was assessed. Stent placement was performed if the gradient was considered significant (> 15 mmHg) and/or in case of the presence of hypertension with a clear substrate. The required size of the stent was determined by measuring the angiographic diameter of the transvers aortic arch. In case of aortic arch hypoplasia stent target diameter was chosen to fit the descending aorta at level of diaphragm. In recent cases, three-dimensional rotational angiography was used. In general, covered stents were preferred if considered safe (i.e. side branch access). The stents that were used were the Cheatham Platinum (CP) covered and non-covered stent (NuMED, Hopkinton, NY, USA), Advanta V12 stent (Atrium, Mijdrecht, Netherlands), ev3 Max LD IntraStent (Covidien, Irvine, California, USA) and Andra Stent XXL (Andamed, GmbH, Reutlingen Germany). The stent was expanded on a Balloon-in-Balloon (BiB; NuMED, Hopkinton, NY, USA) and if deemed necessary post-dilated with a ultra-high-pressure balloon (Atlas; Bard Medical, Covington, GA). We prefer to flare the stent exit with the use of a Cristal Balloon (Balt, Montmorency, France). In case of severe narrowing (so called sub-atretic CoA), a relative under-expansion was accepted, to lower the risk of dissection and dilate to final diameter during second procedure.^{21,22} In case of intentional under-expansion, a staged procedure for optimal post-dilatation was performed with a second procedure approximately 4–6 months after the index procedure. Femoral arterial access was closed with the use of two Perclose

ProGlide suture-mediated closure systems (Abbott Vascular, Clonmel, Tipperary, Ireland). One day after the intervention, a Computed Tomography scan aortography was made to rule out dissection before discharge.

Multiple interventions

For this study, the catheterization procedures specifically planned for post-dilatation were considered an integral part of the index procedure; only after the post-dilatation procedure was performed, the index procedure was regarded as complete, and follow-up began. Only patients who underwent a catheterization for suspicion of re-CoA at least one year after the index procedure were considered to have had multiple interventions. For patients who underwent multiple interventions, data on PG, diameter and blood pressure were collected after the last procedure.

Follow-up

Patients received follow-up care based on advice from the Grown-Up Congenital Heart disease team and clinical protocol.¹⁹ Data were collected at two time points after stent implantation. The first was scheduled after approximately three months. For the second and latest follow-up, data on the most recent examination or hospital visit were used. At both time points, upper limb blood pressure was determined.

Statistical analysis

All data were entered in IBM SPSS Statistics 21 software. Descriptive statistics were used for demographic and other descriptive data. Quantitative data were expressed as mean \pm standard deviation or frequency (%). Paired or unpaired student's t -test was used for comparing group means. Wilcoxon signed rank test was used if indicated. Linear regression analyses were used to assess the relationship between continuous variables. A probability (p) value < 0.05 was considered to represent statistical significance.

RESULTS

Demographic data

We identified a total of 57 CoA patients who underwent an intervention between 2009 and 2015, of which 43 underwent balloon dilatation with stent placement. Data on first follow up (mean 3.8 ± 1.9 months) were available for 35 patients. Data on latest follow up (mean 19.5 ± 10.9 months) were available for 26 patients. Population characteristics are shown in Table 1.

Table 1. Baseline characteristics

Variable	N = 43
Age (years)	41 ± 15
Male	26 (60.5%)
Body Mass Index (kg/m ²)	25 ± 4.6
Classification	
Native CoA	26 (60.5%)
Recurrent CoA	17 (39.5%)
Early surgical repair	
Patch angioplasty	5 (11.6%)
End-to-end anastomosis	1 (2.3%)
Aorta graft prosthesis	1 (2.3%)
Complex procedure	6 (14%)
Unknown	8 (18.6%)
Associated cardiac anomalies	
Bicuspid aortic valve	22 (51.2%)
Patent ductus arteriosus	5 (11.6%)
Ventricular septal defect	3 (7%)
Comorbidities	
Turner syndrome	1 (2.7%)
Noonan syndrome	1 (2.7%)
Alagille syndrome	1 (2.7%)

Data are presented as mean ± standard deviation or absolute number (%)

Procedural data

A total of 50 interventions were performed; 43 were index procedures, 7 patients underwent two interventions. In the current study, procedural success, defined as a PG ≤ 10 mmHg, was achieved in 88% of cases. Stent implantation was performed in 3 out of the 7 of the unplanned procedures during follow-up. Eight patients had two stents implanted during the re-intervention.

There were no deaths related to the procedures. During 2 procedures (4%), tearing of the intimal lining of the aorta occurred. The ensuing local dissections were treated successfully with covered stent implantation without sequelae on subsequent imaging. One patient suffered an intra-cerebral haemorrhage several hours after the procedure. CT showed no circle of Willis anomalies, all haemostasis parameters were found to be

normal. The haemorrhage was most likely due to the combination of heparinization and hypertensive episodes during and after the procedure. Mild neurological deficits remained during follow up.

Peak-to-peak gradient

At baseline, the mean peak-to-peak pressure gradient (PG) was 27.5 ± 19.2 mmHg and decreased to a mean PG post intervention of 3.5 ± 5.0 mmHg ($p < 0.001$). Data are shown in Table 2. No significant relation was found between difference in systolic blood pressure and initial PG ($p = 0.07$; Figure 1).

Table 2. Mean PG and mean diameter pre- and post-intervention

	PG pre (mmHg)	PG post (mmHg)	p-value	Diameter pre (mm)	Diameter post (mm)	p-value
Total (n=43)	27.5 ± 19.2	3.3 ± 5.0	< 0.001	11.4 ± 3.7	17.6 ± 3.7	< 0.001
Native ¹ (n=26)	26.6 ± 17.4	1.9 ± 3.7	0.001	10.8 ± 4.1	18.4 ± 3.9	0.003
Recurrent (n=17)	22.6 ± 14.5	5.8 ± 6.3	0.003	12.2 ± 2.9	16.9 ± 2.9	< 0.001
Multiple interventions (n=7)						
First intervention	25.0 ± 14.2	4.7 ± 4.9	0.018	8.3 ± 4.7	14.5 ± 2.1	0.003
Second intervention	21.9 ± 10.9	9.2 ± 10.5	0.027	14.5 ± 2.1	17.7 ± 2.8	0.002

Values are expressed as mean \pm standard deviation.

¹: Concludes index procedure in case of second unplanned procedure.

Coarctation diameter

The mean luminal diameter of the CoA was 11.4 ± 3.7 mm at baseline and increased after stent implantation to 17.6 ± 3.4 mm ($p < 0.0001$). No significant relation was found between difference in systolic blood pressure and the initial CoA diameter ($p = 0.85$; Figure 2).

Effects on blood pressure regulation

Mean systolic blood pressure was 151 ± 18 mmHg at baseline and decreased to 135 ± 19 mmHg at first follow-up and 137 ± 22 mmHg at latest follow-up ($p = 0.001$, $p = 0.009$, compared to baseline, respectively; Figure 3). Mean diastolic pressure was 82 ± 12 mmHg and decreased to 73 ± 11 mmHg at first follow up and to 76 ± 10 mmHg at latest follow up ($p < 0.001$ and $p = 0.029$, compared to baseline, respectively). Data on mean systolic and diastolic blood pressure, mean arterial pressure, and mean pulse

wave are shown in Table 3. At baseline 76% of patients were hypertensive, declining to 22.9% at first follow up ($p < 0.001$) and 26.9% at latest follow up ($p = 0.001$, compared to baseline) (Table 4).

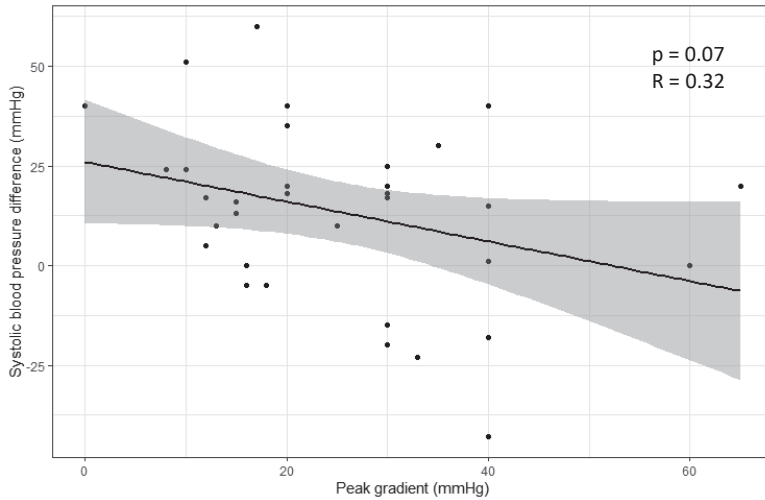


Figure 1. Linear regression for difference in systolic blood pressure and PG pre-stenting.

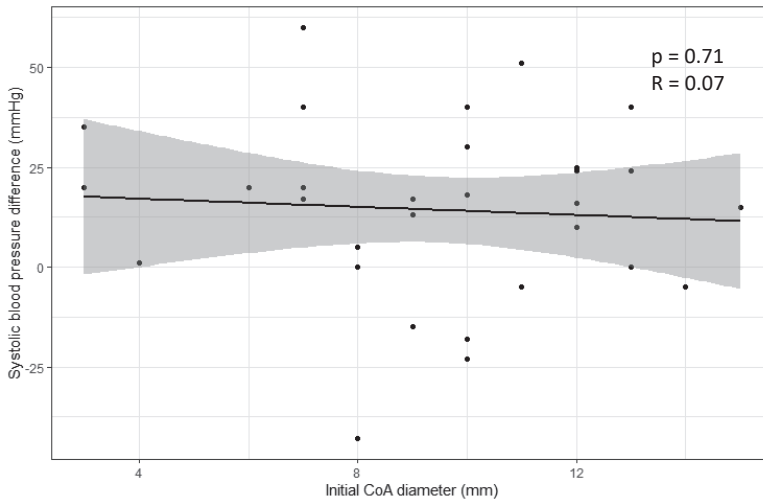


Figure 2. Linear regression result for difference in systolic blood pressure and original CoA diameter.

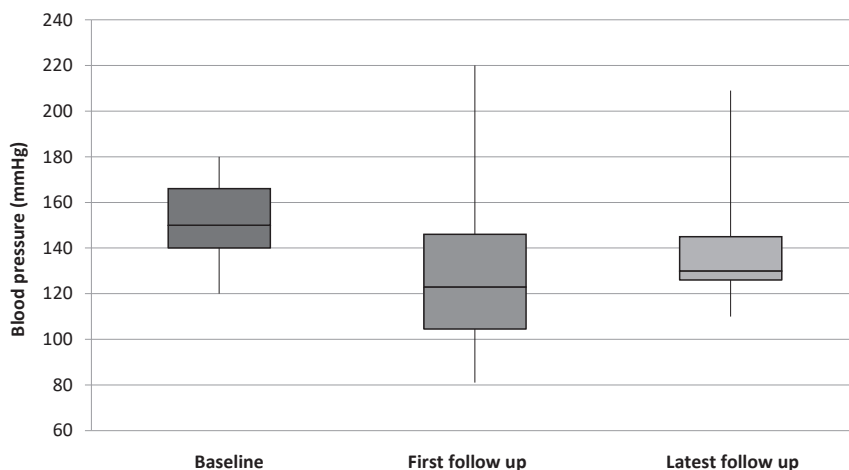


Figure 3. Systolic blood pressure at baseline, first follow-up and latest follow-up.

Need-for-treatment threshold and procedural success

Patients with a baseline PG < 20 mmHg ($n = 16$) had a mean systolic blood pressure of 154 ± 20 mmHg at baseline, 130 ± 19 mmHg at first ($p = 0.046$), and 136 ± 20 mmHg at latest follow-up ($p = 0.008$). Patients with baseline PG < 10 mmHg ($n = 4$) showed a decrease from a mean systolic blood pressure of 153 ± 18 mmHg at baseline to 133 ± 17 mmHg at first ($p < 0.001$) and 137 ± 16 mmHg at latest follow-up ($p = 0.146$).

Medication

The medication regime included diuretics, beta-blockers, angiotensin-converting enzyme inhibitors, angiotensin II receptor blockers, and calcium channel blockers. There was no significant difference in DDD of medication or number of pills taken per patient at baseline and first follow up post-intervention ($p = 0.117$ and $p = 0.642$, respectively). No significant association was found between medication and systolic blood pressure ($p = 0.396$). Data are shown in Table 5.

Table 3. Results on blood pressure measurements.

	Baseline	First FU	Latest FU	p-value (baseline – first FU)	p-value (baseline – latest FU)
Mean systolic blood pressure					
Total (n=43)	151 ± 18	135 ± 19	137 ± 22	0.001	0.009
Native ¹ (n=26)	150 ± 18	137 ± 15	135 ± 19	0.015	0.028
Recurrent (n=17)	153 ± 19	131 ± 24	141 ± 27	0.022	0.139
Multiple interventions (n=7)					
First intervention	151 ± 18	135 ± 13	144 ± 7	0.027	0.893
Second intervention	146 ± 6	137 ± 10	136 ± 25	0.144	0.285
Mean diastolic blood pressure					
Total (n=43)	82 ± 12	73 ± 11	76 ± 10	< 0.001	0.029
Native ¹ (n=26)	81 ± 12	76 ± 12	78 ± 10	0.021	0.362
Recurrent (n=17)	82 ± 13	69 ± 8	74 ± 12	0.007	0.024
Multiple interventions (n=7)					
First intervention	78 ± 10	63 ± 13	78 ± 9	0.144	0.343
Second intervention	81 ± 9	66 ± 8	69 ± 17	0.109	0.180
Mean arterial pressure					
Total (n=43)	104 ± 13	94 ± 12	97 ± 12	< 0.001	0.006
Native ¹ (n=26)	104 ± 13	96 ± 12	97 ± 11	0.005	0.133
Recurrent (n=17)	105 ± 13	91 ± 12	97 ± 14	0.012	0.021
Multiple interventions (n=7)					
First intervention	102 ± 12	86 ± 10	100 ± 8	0.043	0.345
Second intervention	102 ± 8	90 ± 9	91 ± 19	0.109	0.109
Mean pulse pressure					
Total (n=43)	69 ± 17	63 ± 17	63 ± 19	0.098	0.139
Native ¹ (n=26)	69 ± 20	62 ± 14	60 ± 15	0.147	0.196
Recurrent (n=17)	69 ± 20	63 ± 22	70 ± 24	0.138	0.400
Multiple interventions (n=7)					
First intervention	73 ± 12	69 ± 14	66 ± 5	0.686	0.496
Second intervention	65 ± 6	71 ± 4	67 ± 11	0.285	0.317

Data are presented as mean ± standard deviation. ¹ Concludes index procedure in case of second unplanned procedure, FU: follow-up.

Table 4. Data on the proportion of patients with or without hypertension.

	Hypertension Baseline	Hypertension First FU	Hypertension Latest FU	p-value (Baseline – First FU)	p-value (Baseline – Latest FU)
Total (n=43)	29 (74%)	8 (23%)	7 (27%)	< 0.001	0.001
Native ¹ (n=26)	17 (74%)	6 (29%)	5 (31%)	0.007	0.014
Recurrent (n=17)	12 (75%)	2 (12%)	2 (20%)	0.005	0.025
Multiple interventions (n=7)					
First intervention	5 (71%)	1 (17%)	2 (29%)	0.046	0.157
Second intervention	4 (57%)	1 (25%)	1 (14%)	0.276	0.317

Data are presented as absolute number of patients (percentage).¹ Concludes index procedure in case of second unplanned procedure, FU: follow-up.

Table 5. Data on medication use.

	DDD Pre- intervention	DDD Post- intervention	p-value	Number of pills pre- intervention	Number of pills post- intervention	p-value
Total (n=43)	1.5 ± 1.8	1.2 ± 1.7	0.117	1.4 ± 1.3	1.3 ± 1.1	0.642
Native ¹ (n=26)	1.3 ± 1.4	0.9 ± 1.4	0.490	1.1 ± 1.1	1.1 ± 1.1	0.740
Recurrent (n=17)	2.0 ± 2.3	1.8 ± 2.2	0.049	1.9 ± 1.5	1.7 ± 1.1	0.234
Multiple interventions (n=7)						
First intervention	2.3 ± 1.9	1.1 ± 1.2	0.066	1.3 ± 1.1	0.9 ± 0.9	0.317
Second intervention	1.1 ± 1.5	1.5 ± 1.7	0.715	0.9 ± 0.9	1.1 ± 1.2	0.317

Data are presented as mean ± standard deviation. ¹ Concludes index procedure in case of second unplanned procedure, DDD: defined daily dose.

Recurrent versus native CoA

At baseline, no significant differences in demographic data or characteristics of the CoA were found between patients with native and recurrent CoA. Post-intervention, only the difference in residual PG was found to be significant ($p = 0.049$). There was no significant difference between the two groups in reduction of PG, medication or increase of aortic diameter.

Effect of re-intervention on blood pressure regulation

Seven patients underwent a second procedure after the index procedure despite successful relief of obstruction. Blood pressure control proved difficult for these patients, which raised the suspicion of re-stenosis. However, no significant (re)stenosis was seen on computed tomography or cardiac magnetic resonance imaging. On

diagnostic catheterization, either the presence of a significant gradient and/or a clear substrate was an indication to perform re-dilation. In this patient subgroup, the mean PG before re-intervention was 21.9 ± 10.9 mmHg, decreasing to 9.2 ± 10.5 mmHg after re-dilatation ($p = 0.027$). The mean minimal luminal diameter decreased from 13.5 ± 3.4 mm; to 15.8 ± 3.7 mm ($p = 0.077$). Among the patients who underwent re-intervention, the mean systolic blood pressure before the index procedure was 151 ± 18 mmHg, decreasing at first follow-up to a mean of 135 ± 13 mmHg ($p = 0.027$), and was 144 ± 7 mmHg at latest follow up ($p = 0.893$, compared to baseline).

DISCUSSION

In the current contemporary cohort of patients mean diastolic and systolic blood pressure decreased significantly after stenting of the (re)coarctation at first follow up, which sustained at long-term follow-up. No significant differences in effect of treatment were found between native or recurrent CoAs.

To date, only a few studies have been published investigating the effect of stent implantation on hypertension and blood pressure regulation in CoA patients.^{10, 23-25} Most studies on the effects of stent implantation on hypertension also report a decrease in blood pressure, albeit not as large as in our cohort. Moltzer et al. recently reported a decrease in mean systolic blood pressure after stent implantation of 8 mmHg in 24 patients.²⁶ There may be several explanations for the observed differences. First, with only 24 patients, the sample size of this studies is relative small. Second, the patient data used in their study were obtained from 2003 to 2008. It could be that materials and/or implantation techniques used during that time period, were simply not as effective as the materials used nowadays. This may be reflected in the decrease in mean peak-to-peak gradient observed. This decrease was 19 mmHg in their cohort, whereas we observed a decrease of 24 mmHg.

The observed sustained decrease in mean systolic blood pressure of 16 mmHg can be highly clinically relevant. Extrapolating from previous studies, such a decrease in blood pressure would be associated with a reduction of 20% in relative risk of cardiovascular events and a 17% reduction in relative risk of coronary heart disease in particular.^{23, 27, 28}

One might argue that the decrease in systolic blood pressure could simply be the result of a more rigid anti-hypertensive medication regime after stent implantation. However, in our study both the number of pills taken per patient and the DDD decreased after intervention, albeit not statistically significant, but did not increase. Furthermore, the most recent ESC guidelines on hypertension outline how challenging it may be to

achieve a substantial decrease in blood pressure using anti-hypertensive medication alone.¹⁷ For example, angiotensin receptor blockers can only facilitate a reduction in systolic blood pressure up to 10 mmHg²⁹ whereas calcium channel blockers most likely result up to a decrease of about 6 mmHg.³⁰ Thus, achieving a reduction in systolic blood pressure of the magnitude observed in this study (15 mmHg) solely using medication, may be cumbersome.

Multiple studies show a decrease in the number of patients suffering from hypertension after intervention in patients with CoA.^{10, 23-25} Still, around 30% of patients remain hypertensive, even after technically successful stent implantation. In our study, 74% of patients were suffering from arterial hypertension at baseline, while only 27% did so at latest follow up. This amount of reduction is in accordance with the COAST trial.²³ On the other hand, Krasemann et al. reported 45% of patients to be hypertensive at a mean follow up of 41 months.²⁵ In our study, seven patients underwent a second procedure after more than one year after the index procedure. There are two possible explanations for the need for a second intervention in this group of patients. First, in a number of cases, a choice was made to go for a two-step approach. Second, in this group the Adventa V12 stent (Atrium, Mijdrecht, Netherlands) was used. It is now known that this stent has a low radial strength, and a higher incidence of recoil.³¹ Nowadays, this stent is not being used anymore in our hospital.

There are several possible explanations for the difficulties with blood pressure regulation and the residual gradient in patients after successful CoA repair. Histological studies in humans have shown that proximal to the CoA, the stiffness of the aortic wall is increased, due to an increase in collagen and a decrease in smooth muscle cells and elastin.^{32,33} Aortic stiffness may lead to high systolic blood pressure by decreasing aortic compliance. It mainly affects the ascending aorta and aortic arch, and combined with a dilated descending aorta, could cause a gradient to be present without a re-stenosis. However, if this was the case, intervention would not be expected to result in a decrease in PG as we observed. Also, in some cases, CoA is not simply a focal issue, but a disease encompassing the whole aorta. Many patients who have CoA also have a hypoplastic aortic arch, which could also be the cause of a residual gradient and persistent hypertension. Furthermore, age of initial CoA repair is known to be an important risk factor for the development of late hypertension.¹⁶

According to the most recent ESC guidelines, a PG > 20 mmHg or persistent hypertension with a clear substrate are indications for intervention. In this study, 16 patients had a PG < 20 mmHg. Nevertheless, they still underwent stent implantation because of persistent hypertension. When we divide the patient into two groups: patients with a

PG > 20 mmHg and patients with a PG < 20 mmHg, we observed that the decrease in mean systolic blood pressure is similar. The true severity of a CoA cannot be measured by assessing the PG alone, since patients with a longstanding severe CoAs most likely have multiple collateral arteries in use, which might cause a decrease of the PG. Therefore, other factors, like the CoA anatomy, presence of hypertension, and cardiovascular events should also be considered when deciding on treatment option.

Taking into account all the observations we made in this study, we believe that more vigorous imaging and treatment protocols could be of benefit in selected groups of CoA patients. Early diagnosis of re-CoA or suboptimal intervention combined with a more aggressive interventional approach could lead to improvement in blood pressure regulation.

LIMITATIONS

Several limitations of this study should be acknowledged. First, the sample size is limited with a population of 44 patients. However, this number is in line with other studies performed on this subject. Second, due to the retrospective study design there is missing data. Third, follow-up duration is limited, with a mean follow-up duration of 19 months. Also, choice of anti-hypertensive regime was at the discretion of the treating physician and compliance could not be assessed. Last, office blood pressure measurements could give higher readings than in real life due to the “white-coat-effect”. Data on 24-hour blood pressure measurement, which is more reliable than office blood pressure measurements^{34, 35}, were only available for 9 patients.

CONCLUSION

This study showed clinically significant decrease in systolic blood pressure after (re) intervention in CoA patients, which sustained at mid-term follow-up. The number of patients suffering from hypertension decreased significantly, while there was no significant difference in prescribed anti-hypertensive medication. Vigorous imaging and treatment protocols could be of value in selected cases. The sustained decrease of blood pressure can be expected to lead to less future adverse events.



Chapter 5

Safety and efficacy of stenting for aortic arch hypoplasia in patients with coarctation of the aorta

Evangeline G. Warmerdam

Gregor J. Krings

Timion A. Meijs

Anouk C. Franken

Bart W. Driesen

Gertjan Tj. Sieswerda

Folkert J. Meijboom

Pieter A.F. Doevendans

Mirella M.C. Molenschot

Michiel Voskuil

Netherlands Heart Journal. vol. 28,3 (2020): 145-152

ABSTRACT

Background. Despite a successful repair procedure for coarctation of the aorta (CoA), up to two-thirds of patients remain hypertensive. CoA is often seen in combination with abnormal aortic arch anatomy and morphology. This might be a substrate for persistent hypertension. Therefore, we performed endovascular aortic arch stent placement in patients with CoA and concomitant aortic arch hypoplasia or gothic arch morphology. The goal of this retrospective analysis was to investigate the safety and efficacy of aortic arch stenting.

Methods. A retrospective analysis was performed for patients who underwent stenting of the aortic arch at the University Medical Center Utrecht. Measurements collected included office blood pressure, use of antihypertensive medication, invasive peak-to-peak systolic pressure over the arch, and aortic diameters on three-dimensional angiography. Data on follow-up were obtained at the date of most recent outpatient visit.

Results. Twelve patients underwent stenting of the aortic arch. Mean follow-up duration was 14 ± 11 months. Mean peak-to-peak gradient across the arch decreased from 39 ± 13 mm Hg to 7 ± 8 mm Hg directly after stenting ($p < 0.001$). There were no major procedural complications. Mean systolic blood pressure decreased from 145 ± 16 mm Hg at baseline to 128 ± 9 mm Hg at latest follow-up ($p = 0.014$).

Conclusion. This retrospective study shows that stenting of the aortic arch is successful when carried out in a state-of-the-art manner. A direct optimal angiographic and haemodynamic result was shown. No major complications occurred during or after the procedure. At short- to medium-term follow-up a decrease in mean systolic blood pressure was observed.

INTRODUCTION

Coarctation of the aorta (CoA) accounts for approximately 5–8% of all forms of congenital heart disease.¹ It is characterised by a narrowing of the upper descending aorta, most commonly distal to the origin of the left subclavian artery near the insertion of the arterial ligament. CoA can occur as an isolated lesion, but frequently occurs in combination with other lesions such as a bicuspid aortic valve (50% of patients), ventricular septal defect (15% of patients), or a hypoplastic aortic arch (13% of patients).^{1–4} Clinical characteristics depend on the severity of the CoA and may vary from acute congestive heart failure in the neonate to systemic hypertension in late childhood or adulthood. Currently, percutaneous stent placement is the standard of care for adults and older children.⁵

Even after successful CoA repair, residual or late-onset systemic hypertension is not uncommon. It is seen in up to two-thirds of the adult patients after an initial successful repair.^{6,7} Systemic hypertension contributes to a higher morbidity and mortality in these patients, due to an increased incidence of cerebrovascular diseases, heart failure, and acceleration of the progression of coronary artery disease.⁸ Although successful stenting of native or recurrent CoA does not always eliminate the need for treatment with antihypertensive drugs, it can facilitate optimal medical treatment.⁹

A substantial number of patients with CoA have an abnormal aortic arch anatomy or geometry. It is thought that neonatal aortic arch hypoplasia in CoA patients is caused by a decreased flow to the aorta in utero and that catch-up growth of the transverse aortic arch after repair is limited.^{10,11} Several studies have found that aortic arch hypoplasia is associated with late systemic hypertension^{12,13}, even in the absence of an arm-leg blood pressure gradient.⁸

The influence of abnormal aortic arch geometry on systemic hypertension is still a subject of debate. An abnormal aortic flow and increased aortic stiffness have been observed in aortic arches with gothic morphology.¹⁴ Deviating morphology may lead to hypertension.^{15,16} Both systemic hypertension and abnormal blood pressure response to exercise have been reported in this population.^{17,18} A hypoplastic or gothic aortic arch might be a substrate for persistent hypertension and stenting of the aortic arch could be beneficial for this patient cohort. The main objectives of this study were to investigate the safety of this treatment strategy and to investigate the effect on blood pressure regulation of aortic stenting in adolescent and adult patients.

METHODS

Study population

A retrospective review of the cardiac interventional database at the University Medical Center Utrecht (Utrecht, the Netherlands) was performed to identify patients for this study. Patients were selected when they met the following inclusion criteria: (1) diagnosed with CoA; (2) underwent stent implantation that included the aortic arch; (3) a body weight > 50 kg. Arch stenting was defined as stenting between the brachiocephalic trunk and the left subclavian artery. Due to the retrospective nature of this study, an ethics waiver was granted by the local Medical Ethical Committee.

Data acquisition

Data on demography, biometry, blood pressure, medication use, cardiac imaging, and catheterisation procedures were collected from the electronic patient records. Data were collected at two different time points: before stent implantation and at the most recent outpatient visit.

Measurements

The office blood pressure was measured in a seated position in the right upper limb with an automated cuff in accordance with the European Society of Cardiology (ESC) guideline.¹⁹ The ascending and descending aortic pressure were measured during cardiac catheterisation for evaluation of the peak-to-peak systolic pressure over the arch. During catheterisation both two-dimensional angiograms and three-dimensional rotational angiograms were obtained, before and after stent implantation. In three-dimensional rotational angiography the measurements were performed using multi-planar reconstructions. The ascending aorta was measured just before the brachiocephalic trunk, the descending aorta was measured at the level of the diaphragm and the transverse aortic arch was measured at the narrowest diameter. In case the aorta had an 'oval' shape, surface area was calculated using the formula:

$$\text{surface area} = \text{radius } a * \text{radius } b * \pi.$$

Stent implantation technique

All procedures were performed under general anaesthesia. In all patients, vascular access was achieved using the right femoral artery. The DynaCT Artis Zee system (Siemens Healthcare, Erlangen, Germany) was used for performing three-dimensional rotational angiography. The three-dimensional reconstructions gathered with this system were used as an overlay over our fluoroscopy images for optimal procedure

guidance, as previously published.²⁰ The decision to proceed to stent placement was made taking into account several parameters: the peak-to-peak gradient across the aortic arch, the presence of an anatomical substrate, the presence of collaterals, and the presence of hypertension in daily life (preferably confirmed with 24-hours ambulatory blood pressure measurements). Target stent diameter and length were determined based on three-dimensional rotational angiography measurements, conventional two-dimensional angiography measurements of dimensions of the ascending aorta just before the brachiocephalic trunk and the descending aorta at the level of the diaphragm, and balloon interrogation. In complex arch morphology a steerable long sheath (Oscor, 12–13,8 French) as well as rapid pacing were used. Mainly, ev3 Max LD (Medtronic, Plymouth, MN, USA), Andra XXL (Andamed GmbH, Reutlingen, Germany) and Cheatham-Platinum (CP) stent (NuMED Inc., Hopkinton, NY, USA) were used. Strut dilatation to side branches was performed when deemed necessary to enhance left carotid or left subclavian flow. In selected patients with complex aortic morphology two procedures were planned. Stents were placed in the first procedure and consequently dilated further in the second procedure. Major complications were defined as stroke, myocardial infarction, bleeding classified as Bleeding Academic Research Consortium scale (BARC) > 2, or death.

Data analysis

All analyses were performed using SPSS statistical software version 25 (IBM SPSS Data Collection, Chicago, IL, USA). Descriptive statistics were used for demographic data. Quantitative data are presented as mean \pm standard deviation or absolute number (percentage). Group means before and after stent placement were compared using the paired samples t-test. Results were considered statistically significant if the probability value (p-value) was < 0.05.

RESULTS

Demographic data

Between April 2014 and January 2018 a total of 12 patients with a mean age of 24 ± 8 years underwent stenting for aortic arch hypoplasia or gothic arch morphology. Eleven patients previously had some form of CoA repair, one patient had a native CoA. Eleven patients had a hypoplastic aortic arch, one patient had a gothic arch morphology. Ten patients had concomitant congenital cardiac defects. Follow-up data were available for all patients; mean follow-up duration was 14 ± 11 months. Patient characteristics are presented in Table 1.

Table 1. Baseline characteristics.

Parameter	Patients (n=12)
Age (years)	24 ± 8
Male	9 (75%)
Weight (kg)	70 ± 7
BMI (kg/m ²)	23 ± 2
Native CoA	1 (8%)
<i>Concomitant cardiac defects</i>	
Bicuspid aortic valve	6 (50%)
Ventricular septal defect	4 (33%)
Persistent ductus arteriosus	2 (17%)
Transposition of the great arteries	1 (8%)
<i>Previous CoA repair</i>	
End-to-end anastomosis	7 (58%)
Patch angioplasty	4 (33%)
Balloon dilatation	3 (25%)
Stent implantation	5 (42%)
<i>Medication use</i>	
ACE inhibitor	4 (33%)
Angiotensin II receptor blocker	4 (33%)
Beta-blocker	1 (8%)
Calcium-channel blocker	4 (33%)
Diuretics	3 (25%)

Data are presented as number (percentage) or mean ± standard deviation. BMI: body mass index, CoA: coarctation of the aorta, ACE: angiotensin-converting enzyme inhibitor.

Procedural data

Femoral artery sheath sizes ranged from 8–14 French. During the stenting procedure 21 stents were used in a total of 12 patients: the CP stent was used in 6 (50%) patients, the ev3 Max LD stent was used in 5 (42%) patients, the ev3 Mega LD stent was used in 3 (25%) patients, and the Andra XXL stent was used in 1 (8%) patient. The length of the used stents varied from 26–57 mm. After stent implantation, post-dilatation of the stent was performed in 10 patients using the Atlas PTA Balloon (Bard Peripheral Vascular, Tempe, AZ, USA) in six (50%) patients and the Cristal balloon (ab medica, Dusseldorf, Germany) in four (33%) patients, with balloon inflation pressures ranging between 10–24 atm. Aortic arch vessels were crossed in all patients; in six patients the left subclavian

artery was crossed, in two patients the left common carotid artery was crossed, and in four patients both the left subclavian artery and the left common carotid artery were crossed.

Acute angiographic result

The mean peak-to-peak gradient across the aortic arch decreased from 39 ± 13 mmHg to 7 ± 8 mmHg after stent placement ($p < 0.001$). The mean orthogonal diameters at the narrowest point of the transverse aortic arch increased from 12 ± 3 mm \times 13 ± 3 mm to 18 ± 3 mm \times 19 ± 4 mm after stent placement ($p < 0.001$ and $p < 0.001$, respectively). Resulting in an increase in mean surface area of 126 ± 56 mm² to 276 ± 107 mm² ($p < 0.001$). Data are presented in Table 2 and Figure 1.

Table 2. Acute angiographic results. Orthogonal diameters were measured using three-dimensional rotational angiography.

	Pre	Post	p-value
PG (mmHg)	39 ± 13	7 ± 8	< 0.001
Aortic arch narrowest point			
Sagittal diameter (mm)	12 ± 3	18 ± 3	< 0.001
Corresponding orthogonal diameter (mm)	13 ± 3	19 ± 4	< 0.001
Surface area (mm ²)	126 ± 56	276 ± 107	< 0.001
Descending aorta caudal			
Sagittal diameter (mm)	18 ± 5	NA	NA
Corresponding orthogonal diameter (mm)	18 ± 5	NA	NA
Surface area (mm ²)	716 ± 472	NA	NA

Data are presented as mean \pm standard deviation. NA: not applicable, PG: peak gradient measured over the aortic arch during catheterization

Procedural complications

No major complications occurred during the procedure or follow-up, we observed three minor complications. A temporary third-degree atrioventricular block occurred in one patient. During the post-implantation re-dilatation of one of the stents a stent fracture occurred in one patient, which was resolved by placement of a covered stent. One patient experienced minor rebleeding of the access site, which was managed with a simple bandage. No endovascular leaks occurred after stent implantation.

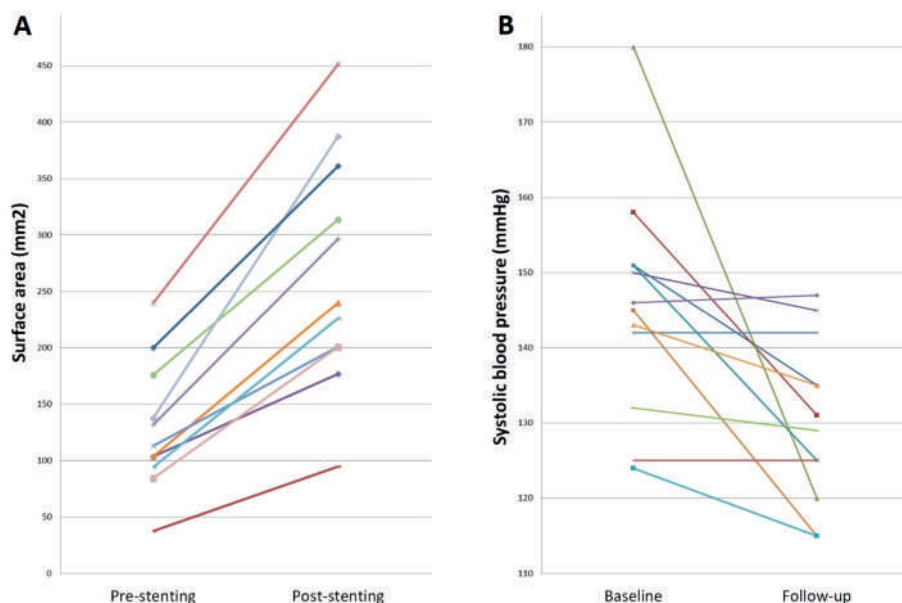


Figure 1. Result of stenting on surface area and systolic blood pressure. a Surface area (mm²) as measured on three-dimensional rotational angiography multiplanar reconstructions pre- and post-stenting. b Systolic blood pressure (mmHg) measured at the right arm at baseline and follow-up

Follow-up

Four patients underwent a planned staged procedure, with successful further dilatation of the stent in the first year after the implantation. Data presented are at baseline (before stent implantation) and at latest follow-up (after further dilatation). No major complications occurred during mean follow-up of 14 ± 11 months.

Blood pressure regulation

There was a decrease in mean systolic blood pressure, measured at the right arm, from 145 ± 16 mm Hg at baseline to 128 ± 9 at latest outpatient visit ($p = 0.014$) (Figure 1). There was no significant decrease in mean diastolic blood pressure ($p = 0.477$). A decrease in the mean number of antihypertensive drug classes used was observed from 1.27 ± 1.10 before stent placement to 0.64 ± 1.03 at the most recent outpatient visit ($p = 0.016$). Data on blood pressure and antihypertensive medication for each individual patient are presented in Table 3.

Table 3. Data on blood pressure and antihypertensive medication for each patient before stent placement and at latest follow-up after stent implantation.

Patient	BP baseline (mmHg)	AHD baseline	BP post stent (mmHg)	AHD post stent
1	151/98	None	135/63	None
2	158/60	Losartan 50 mg Metoprolol 25 mg	131/63	None
3	180/95	Verapamil 240 mg	120/91	None
4	150/74	None	145/85	None
5	151/71	Telmisartan 80 mg	125/75	None
6	145/90	None	115/70	None
7	142/80	Lisinopril 20 mg	142/77	None
8	125/80	Telmisartan 40 mg Amlodipine 5 mg	125/70	Telmisartan 40 mg Amlodipine 5 mg
9	124/57	None	129/69	None
10	124/56	Lercanidipine 5mg Lisinopril 20 mg Hydrochlorothiazide 25 mg	115/57	Lisinopril 20 mg
11	146/55	Ramipril 10 mg	147/68	Ramipril 10 mg
12	143/67	Olmesartan 40mg Amlodipine 10 mg Hydrochlorothiazide 25 mg	135/70	Olmesartan 40mg Amlodipine 10 mg Hydrochlorothiazide 25 mg

AHD: antihypertensive drugs, BP: blood pressure.

DISCUSSION

In this retrospective study we analysed a subset of patients with CoA and a concomitant hypoplastic or gothic aortic arch who underwent stenting of the aortic arch. Stenting of the aortic arch was successful in all selected patients and no complications occurred. The acute angiographic result was excellent, demonstrated by an increase in aortic arch surface area and a decrease in mean peak-to-peak gradient across the aortic arch. Most importantly, a significant decrease in mean systolic blood pressure was observed, with a concomitant decrease in the need for antihypertensive medication.

The target of interventional treatment in CoA is the relief of the obstruction and reduction of the pressure gradient. A large number of patients still suffer from residual or late-onset systemic hypertension despite successful initial percutaneous or surgical therapy. A substantial number of patients who have a CoA also have an abnormal aortic arch anatomy or morphology, which might be a substrate for hypertension. Percutaneous

stent placement has become the standard of care for the treatment of CoA after childhood in the last decade. However, stent placement as treatment for aortic arch hypoplasia has only been described in small series and case reports.²¹⁻²⁵ All reports on aortic arch stenting showed anatomical and physiological relief of obstruction. Boshoff et al. reported no peri-procedural complications²⁴, Holzer et al. reported a relatively high number of adverse events (in 31% of patients), although this was mostly in patients with a weight below 10 kg or with univentricular physiology.²⁵ In a study including 21 patients, Pushparajah et al. reported three major complications in two patients.²¹ Stent migration occurred in two patients, of which one subsequently suffered from an embolic stroke. In these two cases stents were implanted without the use of rapid pacing, which was thought to have increased the risk of stent migration. In our cohort no major complications were observed peri-procedurally or during follow-up.

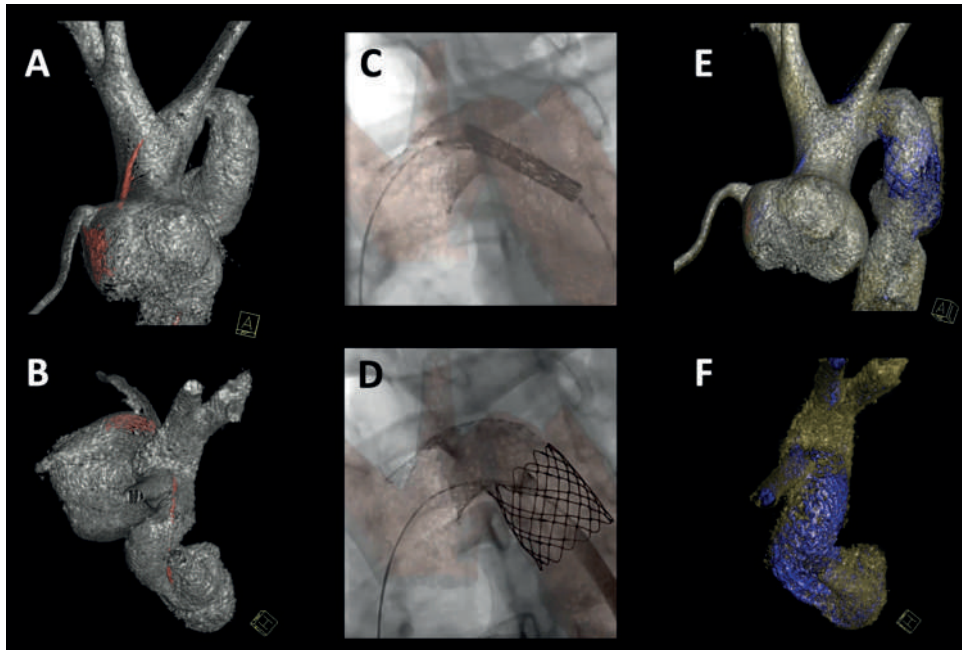


Figure 2. Stent implantation in gothic aortic arch after arterial switch operation. A 36-year-old male with a history of dextro-transposition of the great arteries and coarctation of the aorta. He presented with persisting hypertension late after arterial switch operation. Three ev3 Mega LD stents and one non-covered CP stent were implanted. A, C, D, F: Three-dimensional reconstructions made from three-dimensional angiography data. A: Anterior view before stent implantation. D: Cranial view before stent implantation. B and E: Conventional two-dimensional fluoroscopy images showing stent implantation. C: Anterior view after stent implantation. F: Cranial view after stent implantation.

We believe several steps are important for a safe and successful procedure. Understanding the aortic arch anatomy and morphology is vital, cardiac magnetic resonance imaging (CMR) and computed tomography (CT) are therefore essential in the pre-procedural phase. During the procedure we use reconstructions derived from three-dimensional rotational angiography as an overlay on our fluoroscopy images for optimal guidance (see Figure 2 and 3).

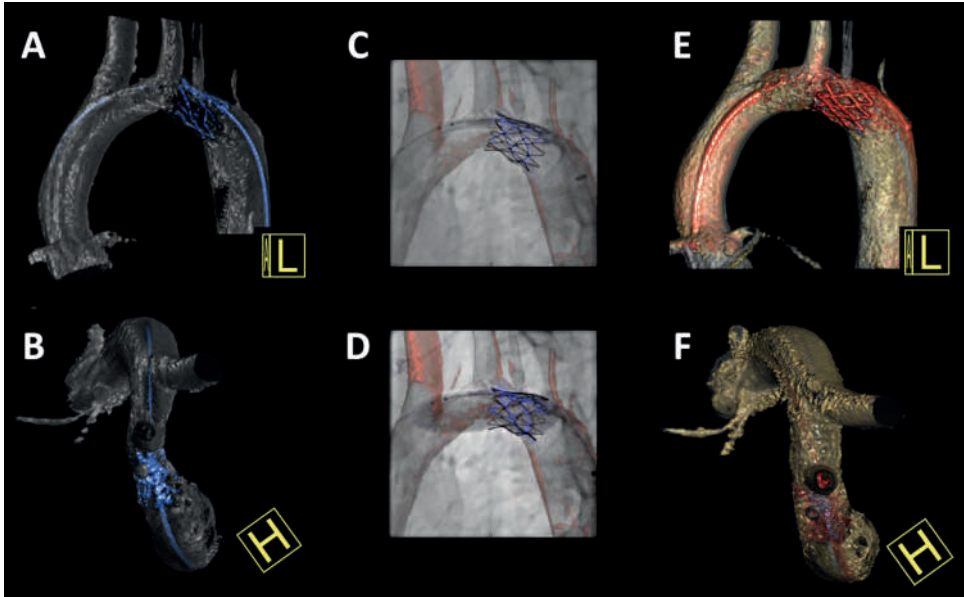


Figure 3. Stent implantation in hypoplastic aortic arch. An 18-year-old female with a history of coarctation of the aorta, for which she underwent surgical coarctation repair (end-to-end anastomosis) as an infant. At the age of seven a CP stent was implanted for re-coarctation. Since she remained hypertensive in the presence of a narrow aortic arch, an ev3 Mega LD stent was implanted in the aortic arch. A, C, D, F: Three-dimensional reconstructions made from three-dimensional angiography data. A: Lateral view before stent implantation. D: Cranial view before stent implantation. B and E: Conventional two-dimensional fluoroscopy images showing stent implantation. C: Lateral view after stent implantation. F: Cranial view after stent implantation

Balloon interrogation can provide information regarding correct stent size, tissue compliance and balloon stability. Rapid pacing and deployment of the stent through a steerable long sheath can enhance positioning effectively and reduce the risk of stent migration. A stent with moderate radial strength and good compliance—such as the ev3 Max LD and ev3 Mega LD—serves best to achieve an ideal aortic arch shape. True open cell design is mandatory to enable strut dilatation when necessary to enhance carotid or subclavian flow. Typically, we aim to position an arch stent between the brachiocephalic

trunk and the left subclavian artery with the proximal and distal part reaching out into the ostia. We believe that this technique results in an optimal distribution of shear stress to reduce intimal trauma of the aortic arch.

Pushparajah et al. investigated the effect of stent implantation on blood pressure and antihypertensive medication at short- and medium-term follow-up. An improvement in blood pressure outcome was seen, with a decrease in median systolic blood pressure from 145 to 128 mmHg.²¹ Antihypertensive medication could be reduced in 13 out of 17 patients.²¹ These results are in line with our results on blood pressure regulation. Even though the goal of stent placement in the aortic arch is not to stop medical therapy, a decrease in antihypertensive medication is beneficial for this patient population. For these relatively young patients lifelong use of multiple medications is very demanding. Therefore, optimal treatment of the underlying substrate seems a sensible approach.

Several mechanisms are thought to increase the risk of systemic hypertension after successful CoA repair. It is hypothesised that these patients have an abnormal baroreceptor function and a decreased aortic compliance. Furthermore, age at initial CoA repair is known to be of great influence on the risk of long-term hypertension.²⁶ A hypoplastic or gothic aortic arch morphology might also be a substrate for persistent hypertension.^{11, 12, 16, 17} The use of three-dimensional rotational angiography changed our understanding of the aortic arch anatomy and helped to accurately diagnose aortic arch hypoplasia and gothic morphology. Biplane angiographic projections as well as lateral and frontal views are not always sufficient; cranial and posterior views are typically essential to detect aortic arch hypoplasia. Such views can only be obtained from pre-procedural CT angiogram or CMR or peri-procedural three-dimensional rotational angiography.

Hypertension after CoA repair is not a benign condition and should be treated, regardless of its aetiology. Strict follow-up using advanced three-dimensional imaging and timely invasive haemodynamic evaluation and, if deemed necessary, intervention/reintervention is important in this patient group. When aortic arch hypoplasia is thought to play an important role in the presence of persistent hypertension, stent implantation should be considered to improve clinical outcome in the long term.

LIMITATIONS

First, due to the retrospective nature of the study there was no clear protocol for the measurements before and after stent implantation, which resulted in missing data. Second, the population size of this study was quite small. Third, very incomplete data

on 24-hour ambulatory blood pressure measurements were available. It is well known that this is a more reliable technique than office blood pressure measurement and gives a more comprehensive assessment of the patient's blood pressure.^{27, 28} Finally, although blood pressure response to exercise would have been an interesting parameter to examine, only a limited number of patients underwent exercise testing. Data on blood pressure response to exercise were therefore omitted.

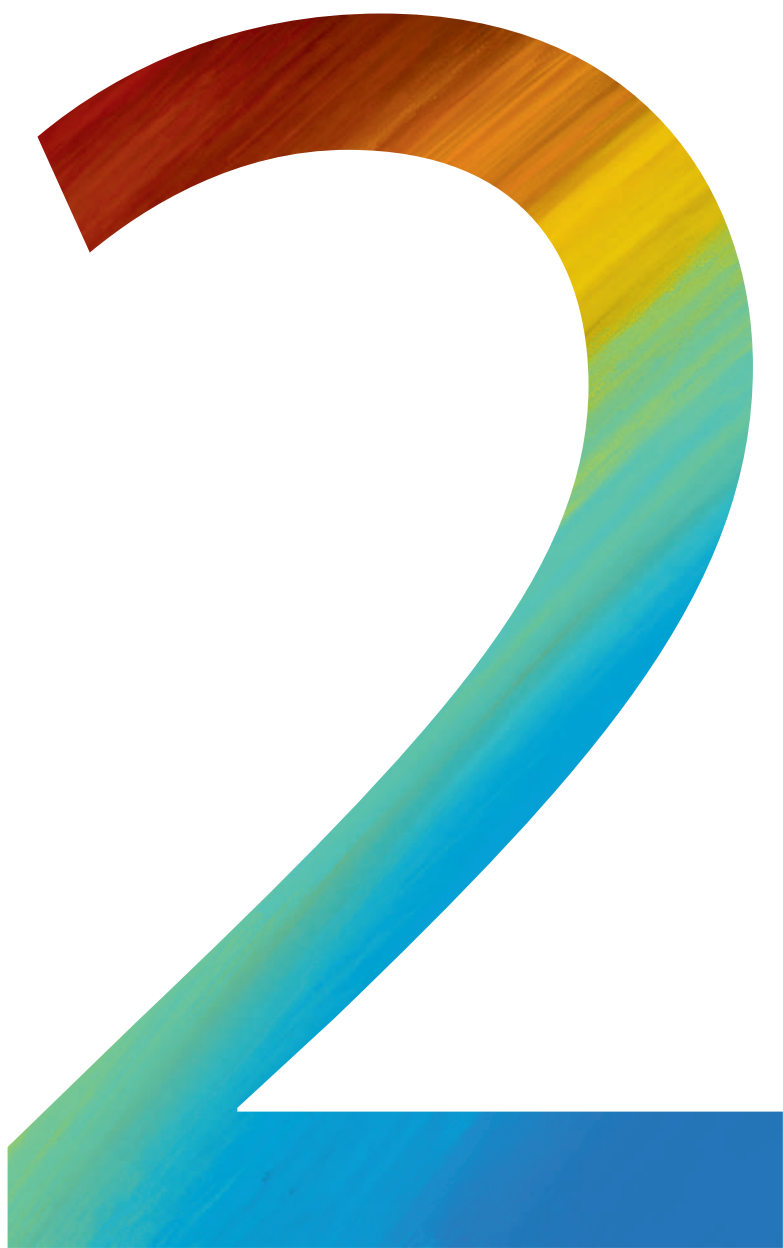
CONCLUSION

The present analysis shows that stenting of the aortic arch is successful when carried out in a state-of-the-art manner. It may lead to improved clinical outcome for this specific patient subset with abnormal aortic arch anatomy or morphology. Stent placement in our cohort achieved a direct optimal angiographic and haemodynamic result. No major complications occurred during or after the procedure. At short- to medium-term follow-up a significant decrease in systolic blood pressure was observed, combined with a parallel decrease in the use of antihypertensive medication.

REFERENCES

1. Ringel RE, Gauvreau K, Moses H, Jenkins KJ. Coarctation of the Aorta Stent Trial (COAST): study design and rationale. *Am Heart J*. 2012;164:7-13.
2. Hamid T, Motwani M, Schneider H, et al. Benefit of endovascular stenting for aortic coarctation on systemic hypertension in adults. *Arch Cardiovasc Dis*. 2015;108:626-33.
3. Keane JF, Flyer DC. Coarctation of the aorta. In: Keane JF, Lock JE, Flyer DC, editors. *Nadas' Pediatric Cardiology*, 2nd edition. Philadelphia: Saunders Elsevier; 2006:627.
4. Campbell M. Natural history of coarctation of the aorta. *Br. Heart J*. 1970;32:633-640.
5. Ovaert C, Benson LN, Nykanen D, Freedom RM. Transcatheter treatment of coarctation of the aorta: a review. *Pediatr Cardiol*. 1998;19:27-44.
6. Brown ML, Burkhart HM, Connolly HM, et al. Coarctation of the aorta: lifelong surveillance is mandatory following surgical repair. *J Am Coll Cardiol*. 2013;10;62:1020-5.
7. Rinnstrom D, Dellborg M, Thilen U, et al. Hypertension in adults with repaired coarctation of the aorta. *Am Heart J*. 2016;181:10-15.
8. Quennelle S, Powell AJ, Geva T, Prakash A. Persistent aortic arch hypoplasia after coarctation treatment is associated with late systemic hypertension. *J Am Heart Assoc*. 2015;25:4-7.
9. Krasemann T, Bano M, Rosenthal E, Qureshi SA. Results of stent implantation for native and recurrent coarctation of the aorta-follow-up of up to 13 years. *Catheter Cardiovasc Interv*. 2011;Sep;1;78(3):405-12
10. Weber HS, Cyran SE, Grzeszczak M, Myers JL, Gleason MM, Baylen BG. Discrepancies in aortic growth explain aortic arch gradients during exercise. *J Am Coll Cardiol*. 1993;15;21:1002-7.
11. Liu JY, Kowalski R, Jones B, et al. Moderately hypoplastic arches: do they reliably grow into adulthood after conventional coarctation repair? *Interact Cardiovasc Thorac Surg*. 2010;10:582-6.
12. Lee MG, Kowalski R, Galati JC, et al. Twenty-four-hour ambulatory blood pressure monitoring detects a high prevalence of hypertension late after coarctation repair in patients with hypoplastic arches. *J Thorac Cardiovasc Surg*. 2012;144:1110-6.
13. Teo LL, Cannell T, Babu-Narayan SV, Hughes M, Mohiaddin RH. Prevalence of associated cardiovascular abnormalities in 500 patients with aortic coarctation referred for cardiovascular magnetic resonance imaging to a tertiary center. *Pediatr Cardiol*. 2011;32:1120-1127.
14. Ou P, Celermajer DS, Rasky O, et al. Angular (gothic) aortic arch leads to enhanced systolic wave reflection, central aortic stiffness, and increased left ventricular mass late after aortic coarctation repair: evaluation with magnetic resonance flow mapping. *J Thorac Cardiovasc Surg*. 2008;135:62-68.
15. Donazzan L, Crepaz R, Stuefer J, Stelling G. Abnormalities of aortic arch shape, central aortic flow dynamics, and distensibility predispose to hypertension after successful repair of aortic coarctation. *World J Pediatr Congenit Heart Surg*. 2014;5:546-53.
16. Dernellis J, Panaretou M. Aortic stiffness is an independent predictor of progression to hypertension in nonhypertensive subjects. *Hypertension*. 2005;45:426-431.

17. Ou P, Mousseaux E, Celermajer DS, et al. Aortic arch shape deformation after coarctation surgery: effect on blood pressure response. *J Thorac Cardiovasc Surg.* 2006;132:1105-11
18. Ou P, Bonnet D, Auriacombe L, et al. Late systemic hypertension and aortic arch geometry after successful repair of coarctation of the aorta. *Eur Heart J.* 2004;25:1853-9.
19. Williams B, Mancia G, Spiering W, et al. 2018 ESC/ESH Guidelines for the management of arterial hypertension. *Eur Heart J.* 2018;39:3021-3104.
20. Starmans NL, Krings GJ, Molenschot MM, et al. Three-dimensional rotational angiography in children with an aortic coarctation. *Neth Heart J.* 2016;24(11):666-674.
21. Pushparajah K, Sadiq M, Brzezinska-Rajszyz G, Thomson J, Rosenthal E, Qureshi SA. Endovascular stenting in Transverse aortic arch hypoplasia. *Catheter Cardiovasc Interv.* 2013;1;82:E491-9.
22. Pihkala J, Pedra CA, Nykanen D, Benson Ln. Implantation of endovascular stents for hypoplasia of the Transverse aortic arch. *Cardiol Young.* 2000;10(1):3-7.
23. Recto MR, Elbl F, Austin E. Use of the new IntraStent for treatment of Transverse arch hypoplasia/coarctation of the aorta. *Catheter Cardiovasc Interv.* 2001;53:499-503.
24. Boshoff D, Budts W, Mertens L, et al. Stenting of hypoplastic aortic segments with mild pressure gradients and arterial hypertension. *Heart.* 2006;92:1661-6.
25. Holzer RJ, Chisolm JL, Hill SL, Cheatham JP. Stenting complex aortic arch obstructions. *Catheter Cardiovasc Interv.* 2008;15;71:375-82.
26. Daniels SR. Repair of Coarctation of the Aorta and Hypertension: Does age matter? *Lancet.* 2001;14;358:89.
27. Mancia G, Parati G. Ambulatory blood pressure monitoring and organ damage. *Hypertension.* 2000;36:894-900.
28. Julia A, Puukka P, Karanko H. Multiple clinic and home blood pressure measurements versus ambulatory blood pressure monitoring. *Hypertension.* 1999;34:261-6.



PART TWO

Tetralogy of Fallot



Chapter 6

Percutaneous Pulmonary Valve Implantation; current status and future perspectives

Bart W. Driesen
Evangeline G. Warmerdam
Gertjan Tj. Sieswerda
Folkert J. Meijboom
Mirella M.C. Molenschot
Pieter A.F. Doevendans
Gregor J. Krings
Arie P. van Dijk
Michiel Voskuil

Current cardiology reviews vol. 15,4 (2019): 262-273

ABSTRACT

Patients with congenital heart disease (CHD) with right ventricle outflow tract (RVOT) dysfunction need sequential pulmonary valve replacements throughout their life in the majority of cases. Since their introduction in 2000, the number of percutaneous pulmonary valve implantations (PPVI) has grown and reached over 10,000 procedures worldwide. Overall, PPVI has been proven safe and effective, but some anatomical variations can limit procedural success. This review discusses the current status and future perspectives of the procedure.

INTRODUCTION

Congenital heart disease (CHD) is the most common of all congenital defects. Almost 1% of live births are affected.¹ Around 20% of these patients have right ventricular outflow tract (RVOT) or pulmonary valve anomalies. These include Fallot's tetralogy (TOF), pulmonary atresia with ventricular septal defect (PA-VSD), double outlet right ventricle (DORV), isolated pulmonary valve stenosis (PS), and truncus arteriosus communis, which are usually corrected surgically early in life. Additionally, RVOT abnormalities are introduced after both the Ross Procedure, used for the correction of congenital aortic valve disease, as well as after surgical correction of complex transposition of the great arteries.

Improvement in surgical techniques has substantially enhanced short- and long-term outcomes in this patient cohort over the last decades. Nowadays, over 90% of affected children will reach adulthood.^{2,3}

Historically, two treatment options for initial (early childhood) surgical repair have been used. Up to the nineties, excision of the dysplastic PV and implantation of a non-valved trans-annular patch were preferentially used, leading to free regurgitation and right ventricular volume overload. Thereafter, surgeons mainly implanted valved conduits such as homografts (human tissue) or grafts with the use of porcine or bovine material (e.g. Contegra, Freestyle, Shelhigh, Sorin, Hancock). Implantation of a valved conduit in early childhood will eventually lead to degeneration, resulting primarily in stenosis and subsequent right ventricular (RV) pressure overload within 15 years after implantation.⁴ Concomitant pulmonary branch stenoses may be present and may need either surgical or transcatheter intervention.

Thus, pulmonary regurgitation (PR) and PS are common problems in patients with congenital heart disease such as TOF, PA-VSD, and DORV, but also in patients post-Ross or post-Rastelli surgery. Most of these patients need multiple RVOT interventions throughout life.

Percutaneous pulmonary valve implantation (PPVI) has been developed as a non-surgical, less invasive alternative for the treatment of RVOT dysfunction. Bonhoeffer et al. performed transcatheter PV implantation for the first time in 2000.⁵ Hereafter, various percutaneous pulmonary valves have been developed. Since then, experience with percutaneous pulmonary valve implantation has grown rapidly and it has become widely accepted for the treatment of RVOT dysfunction. In this review we will discuss the

indications for percutaneous valve replacement, the available devices and techniques, outcomes and complications of the procedure, as well as current developments and future perspectives.

Indications for pulmonary valve replacement

In clinical practice the indication for intervention in the case of stenosis is generally reasonably straightforward, since it is mainly based on the Doppler gradient; a peak instantaneous gradient > 64 mmHg regardless of symptoms, or a peak instantaneous gradient < 64 mmHg with symptoms or decreased RV function is considered an indication for valve replacement in the ESC guideline.⁶ In many centres a mean gradient of 35 mmHg is also used. In the 2018 ACC/AHA guideline, valve replacement in isolated PR is indicated in symptomatic patients with moderate or greater PR with RV dilatation or dysfunction. Valve replacement is appropriate for preservation of ventricular size and function in asymptomatic patients with repaired TOF and ventricular enlargement or dysfunction and moderate or greater PR.⁷

In combined stenosis and regurgitation, debate remains. As the main goal for intervention in the volume overloaded RV is reverse remodelling, research is concentrated on finding thresholds for valve replacement after which reverse remodelling should still take place. Over the years, various thresholds have been suggested for optimal timing of intervention.

Previously, the end-diastolic volume was considered the most important parameter, though no threshold is reported after which RV volumes do not decrease.⁸ RVEDV thresholds of $> 150 \text{ ml/m}^2$ to 170 ml/m^2 were used as cut-off points, because normalization of RVEDV was reported by several authors^{9,10} when valve replacement was performed before these cut-off points. Currently end-systolic volume and RV ejection fraction are used more often as both are markers of RV function. End-systolic volumes (RVESV) of $< 82 \text{ ml/m}^2$ to $< 90 \text{ ml/m}^2$ are used.¹⁰⁻¹⁴ An RV ejection fraction $< 30\%$ is associated with major adverse clinical outcomes.¹⁵

Furthermore, tricuspid regurgitation (TR) has to be taken into account. In moderate or severe TR, combined PPVI with tricuspid valve repair should be considered because PPVI probably will not reduce TR sufficiently.^{16,17} Therefore, in case of significant TR, there might be an indication for surgical pulmonary valve replacement, instead of PPVI, as it can be combined with tricuspid valve plasty.

Electrocardiography parameters like a broadened QRS width of 140 ms to 180 ms, or progression of QRS duration have been used in decision-making.^{10,12, 18-24}

An early intervention strategy will have the most favourable effect on the preservation of RV function. However, such a strategy has to be weighed against the procedural risks of intervention, the risk of endocarditis and the need for repeat interventions. Currently, patients with dilated RVs survive into their sixties. It is unknown if prognosis will improve with earlier intervention and a goal of RV normalization.

Transcatheter Pulmonary Valves

Currently two types of percutaneous implantable pulmonary valves are CE and FDA approved: the Melody transcatheter pulmonary valve (Medtronic, Minneapolis, Minn, USA) for implantation in valved conduits (Figure 1) and the Sapien Edwards XT (Edwards Lifesciences, Irvine, Ca, USA) for implantation in valved conduits and non-conduit (native) RVOT (Figure 2).



Figure 1. The Melody transcatheter pulmonary valve (Medtronic, Minneapolis, Minn, USA)

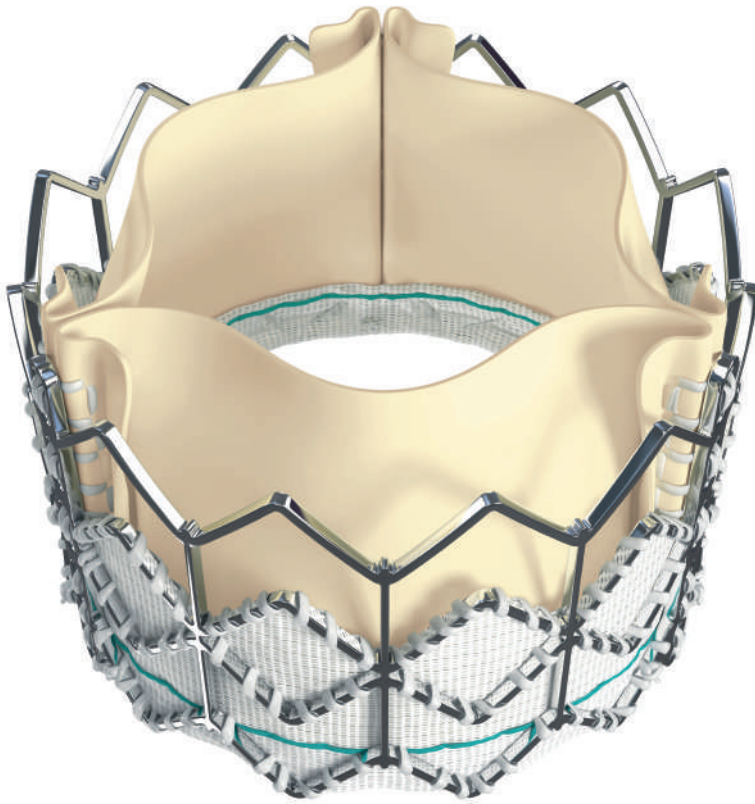


Figure 2. The Edwards Sapien XT (Edwards Lifesciences, Irvine, Ca, USA) for implantation in valved conduits and non-conduit (native) RVOT.

The valvular component of the Melody valve is similar to that of the surgical Contegra (Medtronic) valved conduit and consists of a bovine jugular vein (BJV) valve. The BJV is sutured within a balloon-expandable Cheatham Platinum stent (CP; NuMED, Hopkinton, NY, USA). The valve comes into two sizes: 16 mm (up to 20 mm deployment) and 18 mm (up to 24 mm deployment). The Melody Ensemble transcatheter delivery system comes in three sizes: 18 mm, 20 mm and 22 mm. The valve is crimped on the balloon-in-balloon (BiB) catheter of the Ensemble delivery system. Covered by a flexible 16 French shaft, with a true 22 French outer diameter profile, the valve/balloon combination is advanced to the landing zone over a stiff exchange guidewire. The maximal outside diameter of the Melody valve with fully inflated balloon reaches about 20 mm, 22 mm or 24 mm respectively (for the Ensemble sizes 18, 20 or 22 mm). The 34mm stent length will shorten to about 26 mm, 24 mm or 23 mm after delivery using the Ensemble 18 mm, 20 mm or 22 mm, respectively.

The Edwards SAPIEN XT transcatheter heart valve (Edwards Lifesciences, Irvine, Ca, USA) consists of a tri-leaflet bovine pericardial tissue valve hand-sutured in a balloon expandable cobalt-chromium stent. It is available in sizes 20 mm, 23 mm, 26 mm, and 29 mm, allowing for deployment in RVOTs up to 29 - 30 mm. Similar to the Melody valve, the Sapien XT stent shortens after deployment. For example the cobalt-chromium stent of 26 mm valve shortens 2.9 mm from 20.1 mm to 17.2 mm after implantation. Accordingly, the stent length after deployment is 13.5 mm, 14.3 mm, 17.2 mm and 19.1 mm for the 20 mm, 23 mm, 26 mm, and 29 mm valve, respectively.

The delivery system that is used for the Edwards SAPIEN XT transcatheter heart valve is the NovaFlex+ system (usable length 105 cm) which consists of a 20 French split sheath. This delivery system includes a flex wheel for articulation of the flex catheter, a tapered tip at the distal end of the delivery system to facilitate crossing the valve, and a balloon catheter for deployment of the valve. The handle also contains a flex indicator depicting articulation of the flex catheter and a valve alignment wheel for fine adjustment of the valve during valve alignment. The balloon catheter has radiopaque markers defining the valve alignment position and the working length of the balloon. A radiopaque double marker proximal to the balloon indicates flex catheter position during deployment.

The Edwards Sapien S3 transcatheter heart valve (Edwards Lifesciences, Irvine, Ca, USA) is FDA approved for use in the aortic position. Many centres use the S3 valve also for PPVI. The S3 differs from the XT by an outer skirt at the distal part of the valve which was designed to reduce paravalvular leak. The frame is longer than that of the XT and the delivery catheters (Commander) allow for more precise valve positioning. The delivery system uses 14 or 16 French sheaths designed to reduce access site complications. The S3 valve is available in four sizes: 20 mm, 23 mm, 26 mm and 29 mm.

PROCEDURE

Pre-procedure

It is common to perform PPVI under conscious sedation or general anaesthesia allowing adequate pain control, the use of rapid pacing and ventilation control. Pre-treatment with antibiotics (in our centre cefazolin 2gram) and acetylsalicylic acid (500 mg iv, hereafter 80 - 100 mg daily), and periprocedural heparin (unfractionated heparin 100 IE/kg) is standard care. In case of an extended procedure (> 4 hours), an additional dose of cefazolin can be administered. One extra dose of antibiotics is given 8hours after the procedure. Vascular access site for both devices is commonly the femoral vein, but jugular or subclavian access is also possible. Pre-procedural magnetic resonance angiography

(MRA), computed tomography angiography (CTA) or echocardiography can be used as overlay for roadmapping the procedure, which makes anatomic orientation easier for the operator and enhances safety of the procedure.

Assessment pre-valve implantation

The first step in PPVI after non-invasive pre-procedural imaging is confirming the indication for PPVI by cardiac catheterization for angiography and pressure measurements. The relationships between the main pulmonary artery (MPA), left and right pulmonary arteries, aorta, and coronary arteries should be assessed. It has been shown that approximately 5% of PPVI candidates are at risk for coronary compression.²⁵ Hereby, also special attention should be made to the presence of pulmonary artery branch stenoses, the RVOT landing zone (diameter and support for stenting), and thus the potential for coronary compression. The latter can be avoided by performing balloon interrogation with simultaneous selective coronary angiography. Multiple biplane angiography acquisitions or alternatively, a three-dimensional angiography (3DRA) is needed to acquire a reliable assessment. 3DRA allows for views in every angle while radiation and contrast doses are equal to 2 - 5 biplane acquisitions.²⁶

PPVI in valved conduits

PPVI in conduits follows a different approach than PPVI in native or patched RVOTs. In conduits often multiple balloon dilatations and covered stents are necessary before implanting the valve. After careful assessment, especially for coronary compression, one can proceed by pre-stenting the conduit. For Melody valves, pre-stenting is required to reduce stent fractures.²⁷ Although in Sapien valves stent fractures have not been reported, pre-stenting is generally advised to create a landing zone.

PPVI in native or patched RVOTs

In RVOTs > 25 mm, sizing can be performed by occluding the RVOT with a large (e.g. 30 mm) balloon and infusing contrast in the RV while executing a push-and-pull manoeuvre to ensure a stable position before stent implantation. In patients with native RVOTs, PPVI can be attempted in RVOT diameters < 28 mm measured with balloon testing²⁸, but pre-stenting may be particularly challenging in these cases. Initially, valve implantation was delayed up to several months after pre-stenting ensuring good stent ingrowth and stable position. Subsequently, a combined approach with immediate valve implantation became common practice. Nowadays, more often direct implantation of a Sapien 29 mm is performed without pre-stenting.²⁹

Post-procedure

The access site vessel can be closed with manual compression or with the Perclose ProGlide (Abbott, Illinois, U.S.A) suture-mediated closure system. Alternatively, a subcutaneous suture using the 'figure-of-eight' results in quick haemostasis. Post-interventional observation commonly takes place in telemetry wards and lasts until late afternoon the day after the procedure. An electrocardiogram, chest X-ray and echocardiography are performed to check for valve function and potential complications.

It is of importance to instruct the patient and other health workers to use antibiotic prophylaxis. The use of low-dose acetylsalicylic acid varies among institutions and ranges from no use at all, to a 6 or 12 month period to life-long use. Though evidence is scarce, life-long acetylsalicylic acid use might be warranted. In a prospective study with 86 patients discontinuation of acetylsalicylic acid was found to be a risk factor for the development of infective endocarditis.³⁰

Clinical outcomes

PPVI has proven to be safe over the years. Excellent early and short-term outcomes have been reported³¹⁻³³, which are equal or better than surgical PVR.²⁷ After PPVI, right ventricular parameters, pulmonary regurgitation^{34,35}, left ventricular filling properties³⁶, and exercise capacity^{31,37-40}, improve and electrical remodelling can be seen.⁴¹ PPVI has a lower morbidity than PVR.⁴² There are few re-operations directly after the procedure.⁴³ A recent systematic review showed a pooled peri-procedural mortality of 1.4% in 12 studies with 677 patients.⁴⁴ Freedom from re-intervention was 76% at 5 years in 148 patients studied post-Melody implantation by Cheatham et al.⁴⁵ The presence of a pre-stented conduit and a lower post-interventional RVOT pressure gradient was associated with a longer freedom from re-intervention.

A small conduit diameter (< 16mm) seems to be associated with early valve failure⁴⁶, although the acute haemodynamic results of the Melody implantation were good in these patients.

Besides obvious benefits of percutaneous treatment, such as faster patient recovery and less invasive procedure, cost-benefits have been described as well. Vergales et al. reported a significant cost advantage of PPVI over PVR. In their model, PPVI would only lose its cost effectiveness with an annual PPVI failure rate of 17%.⁴⁷ Currently in-hospital costs are higher for PPVI mainly due to the high costs of the stent and valve. If device costs would be reduced in the future, PPVI would be cost saving even with a device cost of five times that of a surgical valve.⁴⁸

Complications

In the most recent systematic review, procedural complications were limited.⁴⁴ Coronary compression was present in 1.2%, valve embolization in 2.4%, conduit rupture in 2.6% and pulmonary artery obstruction in 1.2%. Earlier studies reported a coronary compression risk of around 5%.^{25,49} Probably the rate of coronary compression is lower in the review by Virk et al., because of improved pre-procedural risk assessment.⁴⁴

Coronary compression

Coronary compression is the most important complication to avoid. In case of coronary compression, urgent surgery or percutaneous coronary intervention may be necessary.⁵⁰⁻⁵² Fatal cases have been described.³⁵ Abnormal coronary anatomy is common in CHD. These patients are at high risk for coronary compression because the coronaries may be close to the RVOT / stent area.

Patients after Ross procedures are of special concern because the coronaries are re-implanted in a more cranial part of the aorta during their initial treatment. The risk of coronary compression might be as high as 22% in abnormal coronaries, versus 1.8% in normal anatomy.²⁵ Pre-procedural MRA or CTA do not allow for reliable risk assessment of this phenomenon because they are both off-line, CTA is static and MRA has low spatial resolution. Another aspect that cannot be anticipated using CTA or MRA alone is the behaviour of the mass between MPA and coronaries. Even if the distance between MPA and coronaries seems enough (> 5 mm), the risk of coronary compression exists, because this mass might not be compressible, especially if it consists of calcified tissue or residues of stents and conduits. So, real-time assessment in the catheterization laboratory as previously described is warranted.

Aortic compression

Similar to coronary compression, compression of the aortic root can occur with or without consequent aortic regurgitation.^{53, 54} In a majority of cases aortic root compression will occur in native or TAP RVOTs⁵⁵, but its clinical significance is unclear. A study by Torres et al. showed no progression of aortic regurgitation during follow-up after PPVI.⁵³ However, attention should be paid for this potential phenomenon during balloon interrogation because it may constitute an important contraindication for PPVI.

Stent fracture

Stent fracture used to be one of the most common complications encountered in the earlier era of Melody valve implantation. Since the use of pre-stenting, the incidence of stent fractures has been significantly reduced.^{45, 56} Stent fracture is only reported

for Melody valves. Commonly it involves the rupture of only one or more stent struts without the loss of stent integrity and therefore usually has no clinical consequences.⁵⁶ However, stent fracture may lead to dysfunction of the valve as well and may necessitate repeat intervention. If stent fracture leads to loss of stent integrity or embolization of stent fragments, re-stenting or surgical intervention might be indicated.

Conduit rupture

The overall incidence of conduit rupture was reported to be 6% in a retrospective analysis by Bishnoi et al., with no significant differences between homografts or other type of conduits. The only identifiable risk factor was a highly elevated RVOT gradient.⁵⁷ Mostly, bleeding is contained by the surrounding scar tissue and only monitoring is necessary, but major bleeding with procedural death can occur. Urgent stenting with covered stents is then indicated.²⁷ Implantation of the NuMED Covered Cheatham-Platinum Stent can be performed without negative impact on the TPV function.⁵⁷ Urgent surgery might be an option too but will often take far more critical time. Pre-stenting severe calcified homografts over the entire length with a covered stent is probably the only way to prevent conduit rupture or cardiac tamponade.

Valve embolization

Embolization or migration of stents and valves is very rare, but cases have been described.^{34, 58} Often surgical intervention will be necessary to explant the device, but transcatheter retrieval has also been reported.⁵⁹ It may be necessary to implant the device in a pulmonary artery branch or vena cava (valve leaflets can be stented to flatten them out).⁶⁰

Tricuspid valve damage

In PPVI with Sapien XT or S3 valves there is a risk of tricuspid valve damage with subsequent tricuspid regurgitation. The valve passes the valve while it is uncovered on the sheath with risk of entrapment in the tricuspid valve apparatus.

Infective endocarditis

Infective endocarditis is a serious concern in PPVI. For Melody valves, high rates of endocarditis are described, whereas for Sapien valves the incidence of infective endocarditis seems low. However, the later introduction of Sapien valves for the pulmonary position has to be taken into account (less valves implanted and shorter follow-up).

Several reports concerning endocarditis in post-PPVI patients treated with Melody valves have been published.^{30, 31, 49, 61, 62} Van Dijck et al. report 7.5% incidence of infective endocarditis in 107 patients with a mean follow-up of 2 years and an annual event rate of 3%. The 5 year endocarditis-free survival was 84,9%. Interestingly, they compared Melody endocarditis to endocarditis in Contegra conduits and homografts, the latter having an annual event rate of only 0.8%.⁶¹ In New-Zealand, higher numbers of endocarditis are reported by O'Donnell et al. After 2.9 years follow-up the incidence of Melody endocarditis was 16% in their cohort.⁶³ The study with the longest follow-up after Melody implantation (7 years) reports a 5-year freedom from infective endocarditis of 89%.⁴⁵

Recently the longest Sapien follow-up to date (mean 3.5 years), showed no endocarditis.⁶⁴ In the prospective multi-institutional COMPASSION trial, freedom from endocarditis at three years was 97.1% with an annualized PPVI related endocarditis of 0.5% per patient per year.⁶⁵ Several other publications with relative short follow-up periods reported a low incidence of endocarditis in Sapien valves in the pulmonary position.⁶⁶⁻⁶⁸ The study of Hascoët et al. showed no cases of endocarditis after 40 months in 47 patients treated with the Sapien valve and a cumulative incidence of endocarditis of 24% in 32 patients treated with the Melody.⁶⁹ In a recent publication of Haas et al. the risk of bacterial endocarditis was 5-8 times higher for Melody valves compared to other valves in a group of 246 patients with all types of pulmonary valves.⁷⁰ There was no bacterial endocarditis in the patients treated with Sapien valves during follow-up.

Aetiology of infective endocarditis post-PPVI is unknown; it is suggested that the type of material might play a role in the risk of developing endocarditis. Melody valves and Contegra conduits compared to pulmonary homografts demonstrate different flow patterns with high shear stress and turbulence, jet lesions or local stress, whilst blood stasis in and around the conduits might contribute to this increased risk. Both systems are composed of bovine material, and the tissue characteristics might contribute to the endocarditis risk as well.^{61,71} This concept is supported by a small in vitro study by Jalal et al. that showed an increased bacterial adhesion of *Staphylococcus Aureus* and *Staphylococcus Sanguis* on healthy Melody valve tissue, which increased after procedural preparation. The authors hypothesized that miniature fractures resulting from procedural preparation provide a bacterial trap and form the preferred location for bacterial adhesion.^{72,73}

Sharma et al. recently reported a higher incidence of endocarditis with BJV valves than other types of RV-to-pulmonary artery conduits. There was no difference in the incidence of endocarditis between catheter-based bovine valves and surgically

implanted bovine valves, suggesting that the substrate for future infection is related to the tissue rather than the method of implantation.⁷⁴ These results are strengthened by the results of Veloso et al.

Adhesion of *Staphylococcus aureus*, *Staphylococcus epidermidis*, and *Streptococcus sanguinis* to bovine pericardium patch, bovine jugular vein, and cryopreserved homograft tissues under static and shear stress conditions indicated similar bacterial adhesion to all tissues. These data provide evidence that the surface composition of BJV and cryopreserved homograft tissues themselves, bacterial surface proteins, and shear forces per se may not be the prime determinant.

One of the major risk factors for infective endocarditis has been shown to be the post-interventional RVOT gradient.^{31, 75} The higher flow velocity might cause endothelial damage with non-bacterial thrombus formation, which might get infected later. This observation might explain the higher rates of endocarditis reported in patients who discontinued acetylic salicylic acid.^{30,49,66} Buber et al. reported male sex, longer procedure time and multiple RVOT stents as risk factors.⁵⁷ Additionally, traditional endocarditis risk factors like previous endocarditis, unprotected dental procedures, skin wounds and personal hygiene (like nail biting), all contribute to endocarditis risk.

When patients present with infective endocarditis, urgent intervention seems warranted, because of a 50% mortality rate as reported by Fraisse et al. Two of their patients died before urgent (next-day) surgery could be performed.⁴⁹

So far, it seems that the risk of infective endocarditis is lower in the Sapien valve as compared to the Melody valve, although no head-to-head comparison has been made up till now. A different patient selection for the 26 to 29 mm Sapien valve, i.e. larger sized conduits and valve implantation in native RVOTs might explain the reported differences in the incidence of infective endocarditis. Future studies, preferably a randomized trial comparing the Melody and the Sapien valves, are needed to definitely answer this issue.

FUTURE PERSPECTIVES

Patient selection and timing

In the last decades knowledge concerning RV volumes and function, and changes in electrocardiographic parameters and exercise parameters has grown. A wide range of thresholds for valve replacement has been proposed, after which reverse remodelling can still take place and right ventricular function recovers. However, little is known

about the RV histopathology and the long-term functional outcomes of pulmonary valve implantation. More research is needed to better define the ideal timing for (repeat) intervention in RVOT dysfunction.

Currently the team is performing a study with magnetic resonance imaging of irreversible RV fibrosis using T1 and T1-rho mapping (The RV-REPAIR study, NL53771.041.15). Strain measurements using speckle-tracking echocardiography and feature tracking cardiac MRI, combined with the investigation of novel biomarkers of RV function will probably aid in a better patient selection, earlier intervention and possibly even improved long-term outcomes. The fact that earlier intervention can lead to improved outcomes, has been shown in a recent study of Pagourelas et al. They reported a more pronounced biventricular remodelling reaching near-normal values in patients with PPVI < 7 years after the last RVOT operation.⁷⁶ Ideally, large cohorts with very long (life-long) follow-up will be created and timing might shift to an earlier intervention in the future.

Advanced imaging in assessment of RV function

Pressure-volume loops would be ideal (load-independent) for the assessment of the RV in RVOT dysfunction. But pressure-volume loops are not routinely used because of several disadvantages including the invasiveness of the procedure. Therefore, non-invasive methods are used to determine the RV function. In clinical practice echocardiography and MRI are the routine diagnostics for follow-up of RVOT dysfunction. Their measurements are load-dependent. Strain and strain-rate are less load dependent than other parameters and therefore increasingly used for assessment of intrinsic function. Different strain and strain rate parameters are associated with volume overloading, RV dyssynchrony and RVEF.^{77, 78} Other authors report significant correlation between RV contractility (RV peak longitudinal systolic strain) and TAPSE.⁷⁹ TAPSE in general is not reliable in post-operative hearts but can be used for follow-up of the longitudinal function when the RV declines. Real-time three-dimensional echocardiographic assessment of RVEF in congenital heart disease has proven to be reliable and feasible in small studies but has to be examined further.⁸⁰

In CMR, T1 mapping is increasingly used to quantify the extracellular volume (ECV). ECV is a validated surrogate marker of diffuse fibrosis. When excess collagen appears in the interstitium, native T1 and ECV increase and post-contrast T1 decreases.⁸¹ ECV has a good correlation with histological global fibrosis⁸² and is correlated with arrhythmia in TOF patients with volume overloading due to PR.⁸¹ With the evolving ability for non-invasive assessment of RV fibrosis, preservation of RV myocardium might take the lead over volumes and pressures in determining the timing of PV replacement.^{81, 83} However, it is unclear how to translate ECV to function and prognosis. Moreover, it is still not possible

to reliably measure T1 in the RV free wall^{83,84} since the spatial resolution approaches the thickness of the myocardium.⁸¹ It is questionable if septal ECV represents fibrosis of the RV since there is a regional difference in RV wall stress due to its complex geometry. Chen et al. did measure ECV of the RV and reported elevated ECV values in TOF patients, these were associated with RV volume overload and arrhythmia.⁸⁵

Another advance in CMR is four-dimensional flow cardiac magnetic resonance (4D flow CMR). This technique can be used to derive advanced haemodynamic measures such as wall shear stress, pressure difference maps, pulse wave velocity, energy loss, turbulent kinetic energy and others⁸⁶ without radiation burden. The use of 4D flow in RVOT dysfunction in the future might result in improved understanding of RV physiology and remodelling.^{87,88}

Advanced imaging in performing PPVI

Computational fluid dynamics (CFD) is a tool to derive the same haemodynamic measurements as 4D flow CMR. This tool calculates flow patterns and pressure changes within a virtual model of the cardiovascular system.⁸⁹ It can predict physiological responses to intervention and compute haemodynamic parameters.⁹⁰ CFD tools may support assessment of pulmonary valve dysfunction and treatment decisions, especially by predicting the post-treatment changes.^{91,92} Recently the use of finite element modelling was described to predict RVOT intervention outcomes and periprocedural risks.⁵⁴

3DRA is used in an increasing number of clinics. Superior imaging quality has been reported⁹³ and may facilitate higher procedural success and decreased risk of serious adverse events by assessment of coronary compression and vessel-airway interactions (see Figure 3).^{94,95} It has been shown that the use of 3DRA does not result in increased radiation or contrast dose^{26,96}, on the contrary lower radiation dose can be achieved.⁹⁷ Furthermore, adequate and safe balloon interrogation in large (native) RVOTs is possible, potentially resulting in more PPVIs in patients with native RVOTs and wide conduits (Figure 4).

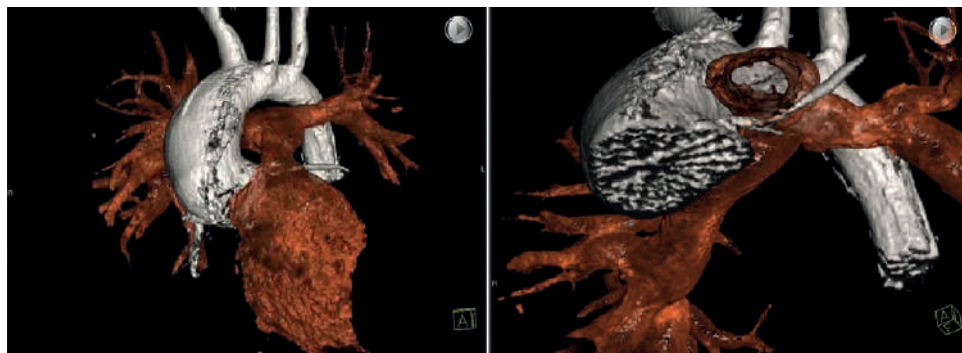


Figure 3. Three-dimensional rotational angiography showing critical proximity of left coronary artery to posterior main pulmonary artery, not suitable for percutaneous pulmonary valve replacement.

3D-models

Three-dimensional printed models may aid in patient education.⁹⁸ In vitro simulation with three-dimensional models might help planning PPVI in native RVOTs.⁹⁹

New device technology

Several devices for the reduction of large diameter (native) RVOTs are being developed and tested to broaden the treatment scope for PPVI. The first-in-man use of the Alterra Adaptive Presept (Edwards Lifesciences, Irvine, CA, USA) was reported recently (see Figure 5).¹⁰⁰ Devices under development are; the Harmony Transcatheter Pulmonary valve (Medtronic, Minneapolis, MN, USA) (see Figure 6), which was formerly known as Native Outflow Tract Device.¹⁰¹ Alternative new devices include the Venus P-valve (MedTech, Shanghai, China)¹⁰², the Pulsta valve by TaeWoong Medical Company (Gyeonggi-do, Republic of Korea)^{103,104}, the RVOT reducer (see Figure 7)¹⁰⁵, and the Downsize stent.¹⁰⁶

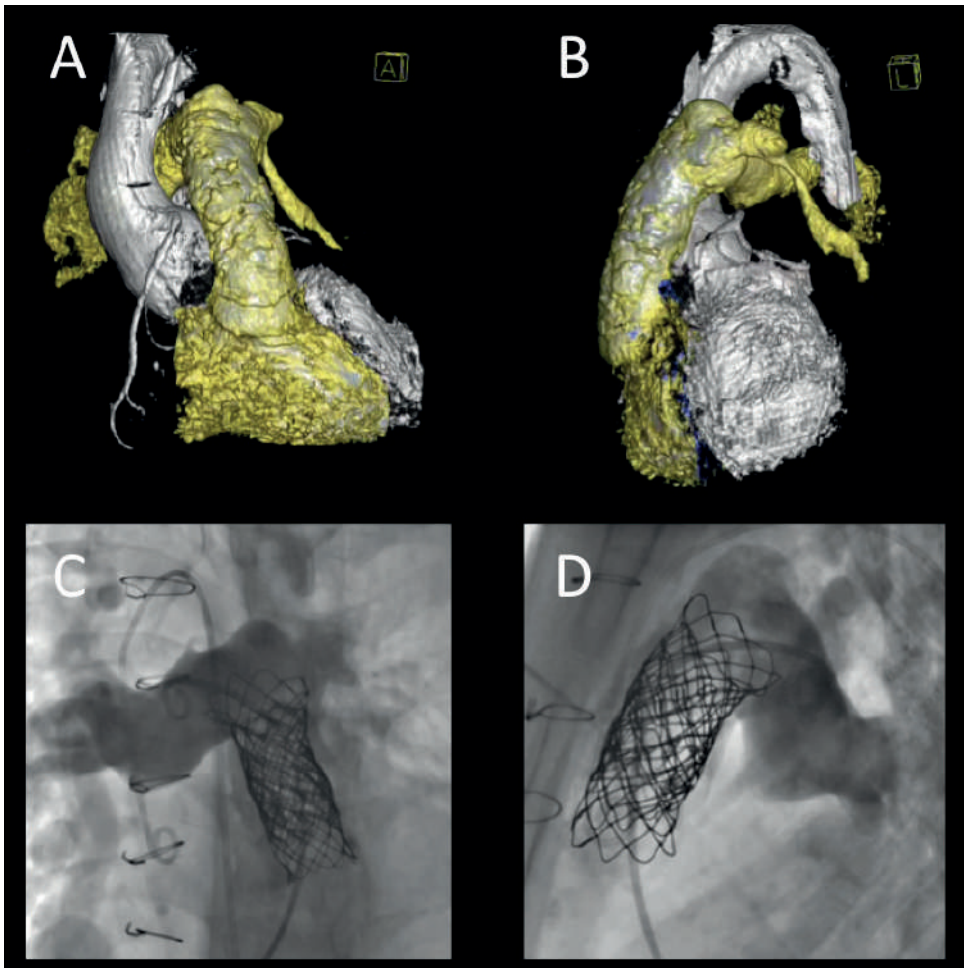


Figure 4. A and B: Three-dimensional rotational angiography in patient with severe homograft stenosis. C and D: angiographic images after implantation of 3 covered CP stents and Sapien 20 mm.

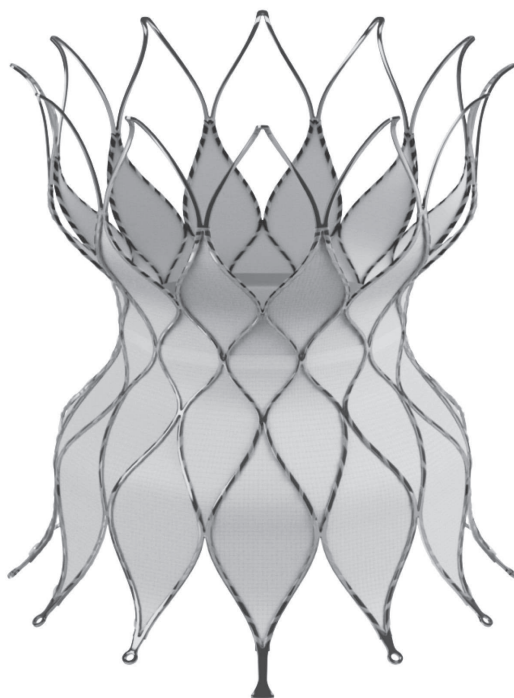


Figure 5. The Alterra Adaptive Pre-stent (Edwards Lifesciences, Irvine, CA, USA).



Figure 6. The Harmony Transcatheter Pulmonary valve (Medtronic, Minneapolis, MN, USA).

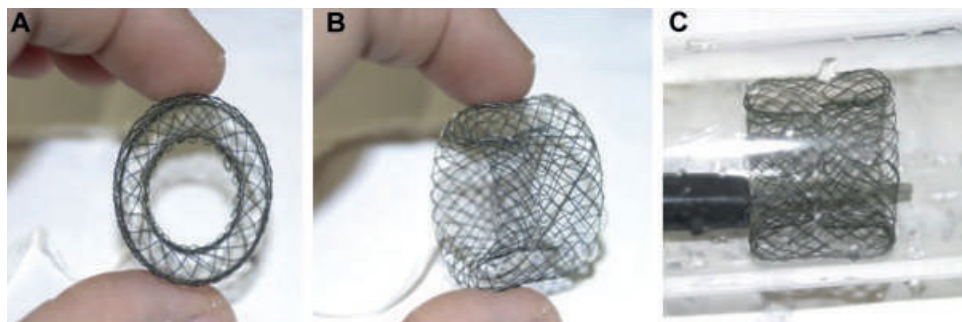


Figure 7. The RVOT reducer device. Courtesy of Y. Boudjemline, permission to re-use granted.

The Harmony valve has an hourglass geometry with the smaller central diameter holding the (porcine pericardium) valve. The system uses a self-expanding nitinol stent with a polymeric graft, which aims to improve the stability of the device in various RVOT anatomies.¹⁰⁵ Recently the results of the first FDA approved early feasibility study were presented, which revealed high procedural success and favourable acute haemodynamics.⁶⁴

The Venus p-valve (MedTech, Shanghai, China) is a self-expanding percutaneous heart valve designed to be implanted in a native patched right ventricle outflow tract. This valve is currently available up to a maximum diameter of 34 mm for use in an RVOT diameter up to 30 – 32 mm. Three studies have been published so far in TOF patients with trans-annular patch repair. Results are encouraging and the use of the Venus p-valve in large (native) RVOTs seems possible.^{102, 107}

A feasibility study of the Pulsta valve (by TaeWoong Medical Company, Korea) was recently reported. The Pulsta self-expandable valve consists of a knitted nitinol wire stent mounted with a treated trileaflet α -Gal-free porcine pericardial valve. Implantation of this valve was feasible and showed short-term effectiveness without serious adverse events.¹⁰³

Besides these innovations, existing valves with a bigger diameter will become available and will be increasingly used. Although the SAPIEN 3 valve (Edwards Lifesciences, Irvine, CA), available in 23 mm, 26 mm, and 29 mm, was designed and FDA approved for the aortic position, this valve is also used in the pulmonary position.¹⁰⁸ Direct implantation (without pre-stenting) of the S3 valve, which has a strong stent frame, is being performed in native RVOTs. With sizes up to 29 mm, clearly the spectrum of patients that can be treated with a percutaneous procedure grows.

As an alternative to percutaneous device techniques, a hybrid plication technique has been reported by Sosnowski et al.¹⁰⁹ After full median sternotomy and minimal dissection of the heart and great vessels, RVOT angiography was performed to measure the main RVOT and pulmonary artery diameter and to determine the extent of plication. A sizing balloon was used for procedural guidance and plication was performed with a pledged longitudinal running suture to provide a more elongated reduction of the RVOT. In case of calcification of a pre-existing RVOT patch, a mattress suture was used to provide focal narrowing of the RVOT size to approximately 22 – 24 mm. After this plication, a PPVI was performed.¹⁰⁹

Decellularized human valves

Small studies with conflicting results have described the use of decellularized human valves.¹¹⁰⁻¹¹² High immunogenic competence in children and young adults contributes to allograft and xenograft (i.e. cryopreserved homografts and bovine jugular vein grafts) degeneration. With heart valve tissue engineering it is possible to eliminate immunogenic cells from the valvular matrix, hereby creating viable, non-immunogenic, and biologically active grafts. Elimination of immunogenic cells from the valvular matrix seems to significantly decrease immunologic response in valve recipients. Reduced re-operation rates compared to cryopreserved homografts and BJVs were reported in preclinical studies and mid-term outcomes of clinical studies.^{110, 111} Another publication reported disappointing results of the use of decellularized valves; abnormal immunologic response leading to significant and long-standing xenograft inflammation appeared to be the reason for graft stenosis and failure early after surgery. Moreover, the asserted endothelialisation of the valve leaflets could not be confirmed by histology.¹¹³

Other innovations are tissue-engineered valves (feasibility in sheep)¹¹⁴, new wire and sheath techniques¹¹⁵, and promising results on valve in valve replacements.¹¹⁶ A double stent technique was reported by Valverde et al.⁹⁸ A 3D print was used to test a double stent implantation in a 36 mm RVOT. Subsequently, two stents were implanted adjacent to each other, after which one stent was used as landing zone for PPVI and the other stent was occluded with a vascular plug.

Infective endocarditis

Further research and long-term outcome results are required to address the risk of endocarditis. Results of the Sapien valves have scarcely been available till now. Results of the currently running COMPASSION trial will give further insight in the infection risk in Sapien valves. The association between endocarditis and bovine material (Contegra and Melody) has to be examined further.⁷² In addition, randomized clinical trials have

to be conducted to investigate whether life-long use of acetylsalicylic acid prevents infective endocarditis. Patient instructions concerning dealing with unexplained fever, aspirin use, dental procedures and personal hygiene (including tattoos and piercings) remain of utmost importance.

SUMMARY

PPVI has become an accepted and widely used technique for treating RVOT dysfunction in several congenital heart disease states, particularly after initial surgical repair. In short- and medium-term follow-up reports, results (outcomes) are excellent. Coronary compression, with possible dramatic consequences, is the most critical complication to avoid. Post-PPVI, infective endocarditis is a concern. In this, a possible predisposition of the Melody valve should be elucidated. In the near future RVOT reducer devices will become available that make PPVI in large (native) RVOTs feasible. Advances in imaging techniques such as 3DRA, 4D flow CMR and CFD will improve understanding of RV (reverse) remodelling and possibly influence the timing of intervention. Larger size studies with long-term follow-up, will also contribute to improved timing of pulmonary valve replacement.

REFERENCES

1. Krasuski RA, Bashore TM. Congenital Heart Disease Epidemiology in the United States: Blindly Feeling for the Charging Elephant. *Circulation*. 2016;134(2):110-3.
2. Moons P, Bovijn L, Budts W, Belmans A, Gewillig M. Temporal trends in survival to adulthood among patients born with congenital heart disease from 1970 to 1992 in Belgium. *Circulation*. 2010;122(22):2264-72.
3. van der Bom T, Bouma BJ, Meijboom FJ, Zwinderman AH, Mulder BJ. The prevalence of adult congenital heart disease, results from a systematic review and evidence based calculation. *Am Heart J*. 2012;164(4):568-75.
4. Davlouros PA, Karatza AA, Gatzoulis MA, Shore DF. Timing and type of surgery for severe pulmonary regurgitation after repair of tetralogy of Fallot. *Int J Cardiol*. 2004;97 Suppl 1:91-101.
5. Bonhoeffer P, Boudjemline Y, Saliba Z, Merckx J, Aggoun Y, Bonnet D, et al. Percutaneous replacement of pulmonary valve in a right-ventricle to pulmonary-artery prosthetic conduit with valve dysfunction. *Lancet*. 2000;356(9239):1403-5.
6. Baumgartner H, Bonhoeffer P, De Groot NM, de Haan F, Deanfield JE, Galie N, et al. ESC Guidelines for the management of grown-up congenital heart disease (new version 2010). *Eur Heart J*. 2010;31(23):2915-57.
7. Stout KK, Daniels CJ, Aboulhosn JA, Bozkurt B, Broberg CS, Colman JM, et al. 2018 AHA/ACC Guideline for the Management of Adults With Congenital Heart Disease: Executive Summary: A Report of the American College of Cardiology/American Heart Association Task Force on Clinical Practice Guidelines. *J Am Coll Cardiol*. 2018.
8. Ferraz Cavalcanti PE, Sa MP, Santos CA, Esmeraldo IM, de Escobar RR, de Menezes AM, et al. Pulmonary valve replacement after operative repair of tetralogy of Fallot: meta-analysis and meta-regression of 3,118 patients from 48 studies. *J Am Coll Cardiol*. 2013;62(23):2227-43.
9. Quail MA, Frigiola A, Giardini A, Muthurangu V, Hughes M, Lurz P, et al. Impact of pulmonary valve replacement in tetralogy of Fallot with pulmonary regurgitation: a comparison of intervention and nonintervention. *Ann Thorac Surg*. 2012;94(5):1619-26.
10. Oosterhof T, van Straten A, Vliegen HW, Meijboom FJ, van Dijk AP, Spijkerboer AM, et al. Preoperative thresholds for pulmonary valve replacement in patients with corrected tetralogy of Fallot using cardiovascular magnetic resonance. *Circulation*. 2007;116(5):545-51.
11. Alvarez-Fuente M, Garrido-Lestache E, Fernandez-Pineda L, Romera B, Sanchez I, Centella T, et al. Timing of Pulmonary Valve Replacement: How Much Can the Right Ventricle Dilate Before it Loses Its Remodelling Potential? *Pediatr Cardiol*. 2016;37(3):601-5.
12. Geva T. Repaired tetralogy of Fallot: the roles of cardiovascular magnetic resonance in evaluating pathophysiology and for pulmonary valve replacement decision support. *J Cardiovasc Magn Reson*. 2011;13:9.

13. Henkens IR, van Straten A, Hazekamp MG, SchaliJ MJ, de Roos A, van der Wall EE, et al. Preoperative determinants of recovery time in adult Fallot patients after late pulmonary valve replacement. *Int J Cardiol.* 2007;121(1):123-4.
14. Lee C, Kim YM, Lee CH, Kwak JG, Park CS, Song JY, et al. Outcomes of pulmonary valve replacement in 170 patients with chronic pulmonary regurgitation after relief of right ventricular outflow tract obstruction: implications for optimal timing of pulmonary valve replacement. *J Am Coll Cardiol.* 2012;60(11):1005-14.
15. Bokma JP, Geva T, Sleeper LA, Babu Narayan SV, Wald R, Hickey K, et al. A propensity score-adjusted analysis of clinical outcomes after pulmonary valve replacement in tetralogy of Fallot. *Heart.* 2018;104(9):738-44.
16. Tanase D, Ewert P, Georgiev S, Meierhofer C, Pabst von Ohain J, McElhinney DB, et al. Tricuspid Regurgitation Does Not Impact Right Ventricular Remodelling After Percutaneous Pulmonary Valve Implantation. *JACC Cardiovasc Interv.* 2017;10(7):701-8.
17. Boudjemline Y. Percutaneous pulmonary valve implantation: what have we learned over the years? *EuroIntervention.* 2017;13(AA):AA60-AA7.
18. Frigiola A, Tsang V, Bull C, Coats L, Khambadkone S, Derrick G, et al. Biventricular response after pulmonary valve replacement for right ventricular outflow tract dysfunction: is age a predictor of outcome? *Circulation.* 2008;118(14 Suppl):S182-90.
19. Therrien J, Provost Y, Merchant N, Williams W, Colman J, Webb G. Optimal timing for pulmonary valve replacement in adults after tetralogy of Fallot repair. *Am J Cardiol.* 2005;95(6):779-82.
20. Buechel ER, Dave HH, Kellenberger CJ, Dodge-Khatami A, Pretre R, Berger F, et al. Remodelling of the right ventricle after early pulmonary valve replacement in children with repaired tetralogy of Fallot: assessment by cardiovascular magnetic resonance. *Eur Heart J.* 2005;26(24):2721-7.
21. Henkens IR, van Straten A, SchaliJ MJ, Hazekamp MG, de Roos A, van der Wall EE, et al. Predicting outcome of pulmonary valve replacement in adult tetralogy of Fallot patients. *Ann Thorac Surg.* 2007;83(3):907-11.
22. Frigiola A, Redington AN, Cullen S, Vogel M. Pulmonary regurgitation is an important determinant of right ventricular contractile dysfunction in patients with surgically repaired tetralogy of Fallot. *Circulation.* 2004;110(11 Suppl 1):II153-7.
23. van Straten A, Vliegen HW, Lamb HJ, Roes SD, van der Wall EE, Hazekamp MG, et al. Time course of diastolic and systolic function improvement after pulmonary valve replacement in adult patients with tetralogy of Fallot. *J Am Coll Cardiol.* 2005;46(8):1559-64.
24. Gengsakul A, Harris L, Bradley TJ, Webb GD, Williams WG, Siu SC, et al. The impact of pulmonary valve replacement after tetralogy of Fallot repair: a matched comparison. *Eur J Cardiothorac Surg.* 2007;32(3):462-8.
25. Morray BH, McElhinney DB, Cheatham JP, Zahn EM, Berman DP, Sullivan PM, et al. Risk of coronary artery compression among patients referred for transcatheter pulmonary valve implantation: a multicenter experience. *Circ Cardiovasc Interv.* 2013;6(5):535-42.
26. Peters M, Krings G, Koster M, Molenschot M, Freund MW, Breur JM. Effective radiation dosage of three-dimensional rotational angiography in children. *Europace.* 2015;17(4):611-6.

27. Holzer RJ, Hijazi ZM. Transcatheter pulmonary valve replacement: State of the art. *Catheter Cardiovasc Interv.* 2016;87(1):117-28.
28. Georgiev S, Tanase D, Ewert P, Meierhofer C, Hager A, von Ohain JP, et al. Percutaneous pulmonary valve implantation in patients with dysfunction of a "native" right ventricular outflow tract - Mid-term results. *Int J Cardiol.* 2018;258:31-5.
29. Morgan GJ, Sadeghi S, Salem MM, Wilson N, Kay J, Rothman A, et al. SAPIEN valve for percutaneous transcatheter pulmonary valve replacement without "pre-stenting": A multi-institutional experience. *Catheter Cardiovasc Interv.* 2018.
30. Malekzadeh-Milani S, Ladouceur M, Patel M, Boughenou FM, Iserin L, Bonnet D, et al. Incidence and predictors of Melody(R) valve endocarditis: a prospective study. *Arch Cardiovasc Dis.* 2015;108(2):97-106.
31. McElhinney DB, Hellenbrand WE, Zahn EM, Jones TK, Cheatham JP, Lock JE, et al. Short- and medium-term outcomes after transcatheter pulmonary valve placement in the expanded multicenter US melody valve trial. *Circulation.* 2010;122(5):507-16.
32. Lurz P, Nordmeyer J, Giardini A, Khambadkone S, Muthurangu V, Schievano S, et al. Early versus late functional outcome after successful percutaneous pulmonary valve implantation: are the acute effects of altered right ventricular loading all we can expect? *J Am Coll Cardiol.* 2011;57(6):724-31.
33. Asoh K, Walsh M, Hickey E, Nagiub M, Chaturvedi R, Lee KJ, et al. Percutaneous pulmonary valve implantation within bioprosthetic valves. *Eur Heart J.* 2010;31(11):1404-9.
34. Butera G, Milanesi O, Spadoni I, Piazza L, Donti A, Ricci C, et al. Melody transcatheter pulmonary valve implantation. Results from the registry of the Italian Society of Pediatric Cardiology. *Catheter Cardiovasc Interv.* 2013;81(2):310-6.
35. Eicken A, Ewert P, Hager A, Peters B, Fratz S, Kuehne T, et al. Percutaneous pulmonary valve implantation: two-centre experience with more than 100 patients. *Eur Heart J.* 2011;32(10):1260-5.
36. Lurz P, Puranik R, Nordmeyer J, Muthurangu V, Hansen MS, Schievano S, et al. Improvement in left ventricular filling properties after relief of right ventricle to pulmonary artery conduit obstruction: contribution of septal motion and interventricular mechanical delay. *Eur Heart J.* 2009;30(18):2266-74.
37. Bonhoeffer P, Boudjemline Y, Qureshi SA, Le Bidois J, Iserin L, Acar P, et al. Percutaneous insertion of the pulmonary valve. *J Am Coll Cardiol.* 2002;39(10):1664-9.
38. Khambadkone S, Coats L, Taylor A, Boudjemline Y, Derrick G, Tsang V, et al. Percutaneous pulmonary valve implantation in humans: results in 59 consecutive patients. *Circulation.* 2005;112(8):1189-97.
39. Khambadkone S, Bonhoeffer P. Percutaneous pulmonary valve implantation. *Semin Thorac Cardiovasc Surg Pediatr Card Surg Annu.* 2006:23-8.
40. Vezmar M, Chaturvedi R, Lee KJ, Almeida C, Manlhiot C, McCrindle BW, et al. Percutaneous pulmonary valve implantation in the young 2-year follow-up. *JACC Cardiovasc Interv.* 2010;3(4):439-48.

41. Plymen CM, Bolger AP, Lurz P, Nordmeyer J, Lee TY, Kabir A, et al. Electrical remodelling following percutaneous pulmonary valve implantation. *Am J Cardiol*. 2011;107(2):309-14.
42. Nordmeyer J, Coats L, Bonhoeffer P. Current experience with percutaneous pulmonary valve implantation. *Semin Thorac Cardiovasc Surg*. 2006;18(2):122-5.
43. Lurz P, Gaudin R, Taylor AM, Bonhoeffer P. Percutaneous pulmonary valve implantation. *Semin Thorac Cardiovasc Surg Pediatr Card Surg Annu*. 2009:112-7.
44. Virk SA, Liou K, Chandrakumar D, Gupta S, Cao C. Percutaneous pulmonary valve implantation: A systematic review of clinical outcomes. *Int J Cardiol*. 2015;201:487-9.
45. Cheatham JP, Hellenbrand WE, Zahn EM, Jones TK, Berman DP, Vincent JA, et al. Clinical and hemodynamic outcomes up to 7 years after transcatheter pulmonary valve replacement in the US melody valve investigational device exemption trial. *Circulation*. 2015;131(22):1960-70.
46. Bensemlali M, Malekzadeh-Milani S, Mostefa-Kara M, Bonnet D, Boudjemline Y. Percutaneous pulmonary Melody(R) valve implantation in small conduits. *Arch Cardiovasc Dis*. 2017.
47. Vergales JE, Wanchek T, Novicoff W, Kron IL, Lim DS. Cost-analysis of percutaneous pulmonary valve implantation compared to surgical pulmonary valve replacement. *Catheter Cardiovasc Interv*. 2013;82(7):1147-53.
48. Andresen B, Mishra V, Lewandowska M, Andersen JG, Andersen MH, Lindberg H, et al. In-hospital cost comparison between percutaneous pulmonary valve implantation and surgery. *Eur J Cardiothorac Surg*. 2017;51(4):747-53.
49. Fraisse A, Aldebert P, Malekzadeh-Milani S, Thambo JB, Piechaud JF, Aucoururier P, et al. Melody (R) transcatheter pulmonary valve implantation: results from a French registry. *Arch Cardiovasc Dis*. 2014;107(11):607-14.
50. Mauri L, Frigiola A, Butera G. Emergency surgery for extrinsic coronary compression after percutaneous pulmonary valve implantation. *Cardiol Young*. 2013;23(3):463-5.
51. Kostolny M, Tsang V, Nordmeyer J, Van Doorn C, Frigiola A, Khambadkone S, et al. Rescue surgery following percutaneous pulmonary valve implantation. *Eur J Cardiothorac Surg*. 2008;33(4):607-12.
52. Divekar AA, Lee JJ, Tymchak WJ, Rutledge JM. Percutaneous coronary intervention for extrinsic coronary compression after pulmonary valve replacement. *Catheter Cardiovasc Interv*. 2006;67(3):482-4.
53. Torres AJ, McElhinney DB, Anderson BR, Turner ME, Crystal MA, Timchak DM, et al. Aortic Root Distortion and Aortic Insufficiency During Balloon Angioplasty of the Right Ventricular Outflow Tract Prior to Transcatheter Pulmonary Valve Replacement. *J Interv Cardiol*. 2016;29(2):197-207.
54. Caimi A, Sturla F, Pluchinotta FR, Giugno L, Secchi F, Votta E, et al. Prediction of stenting related adverse events through patient-specific finite element modelling. *J Biomech*. 2018;79:135-46.
55. Lindsay I, Aboulhosn J, Salem M, Levi D. Aortic root compression during transcatheter pulmonary valve replacement. *Catheter Cardiovasc Interv*. 2016;88(5):814-21.

56. Nordmeyer J, Khambadkone S, Coats L, Schievano S, Lurz P, Parenzan G, et al. Risk stratification, systematic classification, and anticipatory management strategies for stent fracture after percutaneous pulmonary valve implantation. *Circulation*. 2007;115(11):1392-7.
57. Bishnoi RN, Jones TK, Kreutzer J, Ringel RE. NuMED Covered Cheatham-Platinum Stent for the treatment or prevention of right ventricular outflow tract conduit disruption during transcatheter pulmonary valve replacement. *Catheter Cardiovasc Interv*. 2015;85(3):421-7.
58. Kenny D, Hijazi ZM, Kar S, Rhodes J, Mullen M, Makkar R, et al. Percutaneous implantation of the Edwards SAPIEN transcatheter heart valve for conduit failure in the pulmonary position: early phase 1 results from an international multicenter clinical trial. *J Am Coll Cardiol*. 2011;58(21):2248-56.
59. Suradi HS, Hijazi ZM. Percutaneous pulmonary valve implantation. *Glob Cardiol Sci Pract*. 2015;2015(2):23.
60. Khambadkone S. Percutaneous pulmonary valve implantation. *Ann Pediatr Cardiol*. 2012;5(1):53-60.
61. Van Dijk I, Budts W, Cools B, Eyskens B, Boshoff DE, Heying R, et al. Infective endocarditis of a transcatheter pulmonary valve in comparison with surgical implants. *Heart*. 2015;101(10):788-93.
62. Malekzadeh-Milani S, Ladouceur M, Iserin L, Bonnet D, Boudjemline Y. Incidence and outcomes of right-sided endocarditis in patients with congenital heart disease after surgical or transcatheter pulmonary valve implantation. *J Thorac Cardiovasc Surg*. 2014;148(5):2253-9.
63. O'Donnell C, Holloway R, Tilton E, Stirling J, Finucane K, Wilson N. Infective endocarditis following Melody valve implantation: comparison with a surgical cohort. *Cardiol Young*. 2017;27(2):294-301.
64. Wilson WM, Benson LN, Osten MD, Shah A, Horlick EM. Transcatheter Pulmonary Valve Replacement With the Edwards Sapien System: The Toronto Experience. *JACC Cardiovasc Interv*. 2015;8(14):1819-27.
65. Kenny D, Rhodes JF, Fleming GA, Kar S, Zahn EM, Vincent J, et al. 3-Year Outcomes of the Edwards SAPIEN Transcatheter Heart Valve for Conduit Failure in the Pulmonary Position From the COMPASSION Multicenter Clinical Trial. *JACC Cardiovasc Interv*. 2018;11(19):1920-9.
66. Patel M, Malekzadeh-Milani S, Ladouceur M, Iserin L, Boudjemline Y. Percutaneous pulmonary valve endocarditis: incidence, prevention and management. *Arch Cardiovasc Dis*. 2014;107(11):615-24.
67. Hascoet S, Jalal Z, Baruteau A, Mauri L, Chalard A, Bouzguenda I, et al. Stenting in paediatric and adult congenital heart diseases: A French multicentre study in the current era. *Arch Cardiovasc Dis*. 2015;108(12):650-60.
68. Vollroth M, Daehnert I, Kostelka M, Wagner R. First case of blood-culture proven *Staphylococcus aureus* endocarditis of a Sapien(R) XT valve after percutaneous pulmonary valve implantation. *Eur J Cardiothorac Surg*. 2015;48(6):e124-5.

69. Hascoet S, Mauri L, Claude C, Fournier E, Lourtet J, Riou JY, et al. Infective Endocarditis Risk After Percutaneous Pulmonary Valve Implantation With the Melody and Sapien Valves. *JACC Cardiovasc Interv.* 2017;10(5):510-7.
70. Haas NA, Bach S, Vcasna R, Laser KT, Sandica E, Blanz U, et al. The risk of bacterial endocarditis after percutaneous and surgical biological pulmonary valve implantation. *Int J Cardiol.* 2018;268:55-60.
71. Uebing A, Rigby ML. The problem of infective endocarditis after transcatheter pulmonary valve implantation. *Heart.* 2015;101(10):749-51.
72. Jalal Z, Galmiche L, Lebeaux D, Villemain O, Brugada G, Patel M, et al. Selective propensity of bovine jugular vein material to bacterial adhesions: An in-vitro study. *Int J Cardiol.* 2015;198:201-5.
73. Malekzadeh-Milani S, Houeijeh A, Jalal Z, Hascoet S, Bakloul M, Aldebert P, et al. French national survey on infective endocarditis and the Melody valve in percutaneous pulmonary valve implantation. *Arch Cardiovasc Dis.* 2018.
74. Sharma A, Cote AT, Hosking MCK, Harris KC. A Systematic Review of Infective Endocarditis in Patients With Bovine Jugular Vein Valves Compared With Other Valve Types. *JACC Cardiovasc Interv.* 2017;10(14):1449-58.
75. Buber J, Bergersen L, Lock JE, Gauvreau K, Esch JJ, Landzberg MJ, et al. Bloodstream infections occurring in patients with percutaneously implanted bioprosthetic pulmonary valve: a single-center experience. *Circ Cardiovasc Interv.* 2013;6(3):301-10.
76. Pagourelas ED, Daraban AM, Mada RO, Duchenne J, Mirea O, Cools B, et al. Right ventricular remodelling after transcatheter pulmonary valve implantation. *Catheter Cardiovasc Interv.* 2017;90(3):407-17.
77. Yu HK, Li SJ, Ip JJ, Lam WW, Wong SJ, Cheung YF. Right ventricular mechanics in adults after surgical repair of tetralogy of fallot: insights from three-dimensional speckle-tracking echocardiography. *J Am Soc Echocardiogr.* 2014;27(4):423-9.
78. Focardi M, Cameli M, Carbone SF, Massoni A, De Vito R, Lisi M, et al. Traditional and innovative echocardiographic parameters for the analysis of right ventricular performance in comparison with cardiac magnetic resonance. *Eur Heart J Cardiovasc Imaging.* 2015;16(1):47-52.
79. Kempny A, Fernandez-Jimenez R, Orwat S, Schuler P, Bunck AC, Maintz D, et al. Quantification of biventricular myocardial function using cardiac magnetic resonance feature tracking, endocardial border delineation and echocardiographic speckle tracking in patients with repaired tetralogy of Fallot and healthy controls. *J Cardiovasc Magn Reson.* 2012;14:32.
80. van der Zwaan HB, Helbing WA, McGhie JS, Geleijnse ML, Luijnenburg SE, Roos-Hesselink JW, et al. Clinical value of real-time three-dimensional echocardiography for right ventricular quantification in congenital heart disease: validation with cardiac magnetic resonance imaging. *J Am Soc Echocardiogr.* 2010;23(2):134-40.
81. Messroghli DR, Moon JC, Ferreira VM, Grosse-Wortmann L, He T, Kellman P, et al. Clinical recommendations for cardiovascular magnetic resonance mapping of T1, T2, T2* and

- extracellular volume: A consensus statement by the Society for Cardiovascular Magnetic Resonance (SCMR) endorsed by the European Association for Cardiovascular Imaging (EACVI). *J Cardiovasc Magn Reson*. 2017;19(1):75.
82. Zile MR, Gregg D. Is Biventricular Fibrosis the Mediator of Late Complications in Tetralogy of Fallot? *JACC Cardiovasc Imaging*. 2016;9(1):11-3.
83. Broberg CS, Chugh SS, Conklin C, Sahn DJ, Jerosch-Herold M. Quantification of diffuse myocardial fibrosis and its association with myocardial dysfunction in congenital heart disease. *Circ Cardiovasc Imaging*. 2010;3(6):727-34.
84. Plymen CM, Sado DM, Taylor AM, Bolger AP, Lambiase PD, Hughes M, et al. Diffuse myocardial fibrosis in the systemic right ventricle of patients late after Mustard or Senning surgery: an equilibrium contrast cardiovascular magnetic resonance study. *Eur Heart J Cardiovasc Imaging*. 2013;14(10):963-8.
85. Chen CA, Dusenberry SM, Valente AM, Powell AJ, Geva T. Myocardial ECV Fraction Assessed by CMR Is Associated With Type of Hemodynamic Load and Arrhythmia in Repaired Tetralogy of Fallot. *JACC Cardiovasc Imaging*. 2016;9(1):1-10.
86. Markl M, Schnell S, Barker AJ. 4D flow imaging: current status to future clinical applications. *Curr Cardiol Rep*. 2014;16(5):481.
87. Kamphuis VP, Westenberg JJM, van der Palen RLF, Blom NA, de Roos A, van der Geest R, et al. Unravelling cardiovascular disease using four dimensional flow cardiovascular magnetic resonance. *Int J Cardiovasc Imaging*. 2017;33(7):1069-81.
88. Dyverfeldt P, Bissell M, Barker AJ, Bolger AF, Carlhall CJ, Ebberts T, et al. 4D flow cardiovascular magnetic resonance consensus statement. *J Cardiovasc Magn Reson*. 2015;17:72.
89. DeCampi WM, Argueta-Morales IR, Divo E, Kassab AJ. Computational fluid dynamics in congenital heart disease. *Cardiol Young*. 2012;22(6):800-8.
90. Morris PD, Narracott A, von Tengg-Kobligh H, Silva Soto DA, Hsiao S, Lungu A, et al. Computational fluid dynamics modelling in cardiovascular medicine. *Heart*. 2016;102(1):18-28.
91. Slesnick TC. Role of Computational Modelling in Planning and Executing Interventional Procedures for Congenital Heart Disease. *Can J Cardiol*. 2017;33(9):1159-70.
92. Goubergrits L, Riesenkampff E, Yevtushenko P, Schaller J, Kertzscher U, Hennemuth A, et al. MRI-based computational fluid dynamics for diagnosis and treatment prediction: clinical validation study in patients with coarctation of aorta. *J Magn Reson Imaging*. 2015;41(4):909-16.
93. Aldoss O, Fonseca BM, Truong UT, Bracken J, Darst JR, Guo R, et al. Diagnostic Utility of Three-Dimensional Rotational Angiography in Congenital Cardiac Catheterization. *Pediatr Cardiol*. 2016;37(7):1211-21.
94. Truong UT, Fagan TE, Deterding R, Ing RJ, Fonseca BM. Use of rotational angiography in assessing relationship of the airway to vasculature during cardiac catheterization. *Catheter Cardiovasc Interv*. 2015;86(6):1068-77.

95. Pockett CR, Moore JW, El-Said HG. Three dimensional rotational angiography for assessment of coronary arteries during melody valve implantation: introducing a technique that may improve outcomes. *Neth Heart J*. 2017;25(2):82-90.
96. Haddad L, Waller BR, Johnson J, Choudhri A, McGhee V, Zurakowski D, et al. Radiation Protocol for Three-Dimensional Rotational Angiography to Limit Procedural Radiation Exposure in the Pediatric Cardiac Catheterization Lab. *Congenit Heart Dis*. 2016;11(6):637-46.
97. Goreczny S, Moszura T, Dryzek P, Lukaszewski M, Krawczuk A, Moll J, et al. Three-dimensional image fusion guidance of percutaneous pulmonary valve implantation to reduce radiation exposure and contrast dose: A comparison with traditional two-dimensional and three-dimensional rotational angiographic guidance. *Neth Heart J*. 2017;25(2):91-9.
98. Valverde I, Sarnago F, Prieto R, Zunzunegui JL. Three-dimensional printing in vitro simulation of percutaneous pulmonary valve implantation in large right ventricular outflow tract. *Eur Heart J*. 2017;38(16):1262-3.
99. Poterucha JT, Foley TA, Taggart NW. Percutaneous pulmonary valve implantation in a native outflow tract: 3-dimensional DynaCT rotational angiographic reconstruction and 3-dimensional printed model. *JACC Cardiovasc Interv*. 2014;7(10):e151-2.
100. Zahn EM, Chang JC, Armer D, Garg R. First human implant of the Alterra Adaptive PreStent(TM) : A new self-expanding device designed to remodel the right ventricular outflow tract. *Catheter Cardiovasc Interv*. 2018;91(6):1125-9.
101. Bergersen L, Benson LN, Gillespie MJ, Cheatham SL, Crean AM, Hor KN, et al. Harmony Feasibility Trial: Acute and Short-Term Outcomes With a Self-Expanding Transcatheter Pulmonary Valve. *JACC Cardiovasc Interv*. 2017;10(17):1763-73.
102. Garay F, Pan X, Zhang YJ, Wang C, Springmuller D. Early experience with the Venus pvalve for percutaneous pulmonary valve implantation in native outflow tract. *Neth Heart J*. 2017;25(2):76-81.
103. Kim GB, Song MK, Bae EJ, Park EA, Lee W, Lim HG, et al. Successful Feasibility Human Trial of a New Self-Expandable Percutaneous Pulmonary Valve (Pulsta Valve) Implantation Using Knitted Nitinol Wire Backbone and Trileaflet alpha-Gal-Free Porcine Pericardial Valve in the Native Right Ventricular Outflow Tract. *Circ Cardiovasc Interv*. 2018;11(6):e006494.
104. Kim GB, Kwon BS, Lim HG. First in human experience of a new self-expandable percutaneous pulmonary valve implantation using knitted nitinol-wire and tri-leaflet porcine pericardial valve in the native right ventricular outflow tract. *Catheter Cardiovasc Interv*. 2017;89(5):906-9.
105. Jalal Z, Thambo JB, Boudjemline Y. The future of transcatheter pulmonary valvulation. *Arch Cardiovasc Dis*. 2014;107(11):635-42.
106. Boudjemline Y, Agnoletti G, Bonnet D, Sidi D, Bonhoeffer P. Percutaneous pulmonary valve replacement in a large right ventricular outflow tract: an experimental study. *J Am Coll Cardiol*. 2004;43(6):1082-7.
107. Promphan W, Prachasilchai P, Siripornpitak S, Qureshi SA, Layangool T. Percutaneous pulmonary valve implantation with the Venus P-valve: clinical experience and early results. *Cardiol Young*. 2016;26(4):698-710.

108. Rockefeller T, Shahanavaz S, Zajarias A, Balzer D. Transcatheter implantation of SAPIEN 3 valve in native right ventricular outflow tract for severe pulmonary regurgitation following tetralogy of fallot repair. *Catheter Cardiovasc Interv.* 2016;88(1):E28-33.
109. Sosnowski C, Matella T, Fogg L, Ilbawi M, Nagaraj H, Kavinsky C, et al. Hybrid pulmonary artery plication followed by transcatheter pulmonary valve replacement: Comparison with surgical PVR. *Catheter Cardiovasc Interv.* 2016;88(5):804-10.
110. Cebotari S, Tudorache I, Ciubotaru A, Boethig D, Sarikouch S, Goerler A, et al. Use of fresh decellularized allografts for pulmonary valve replacement may reduce the reoperation rate in children and young adults: early report. *Circulation.* 2011;124(11 Suppl):S115-23.
111. Sarikouch S, Horke A, Tudorache I, Beerbaum P, Westhoff-Bleck M, Boethig D, et al. Decellularized fresh homografts for pulmonary valve replacement: a decade of clinical experience. *Eur J Cardiothorac Surg.* 2016;50(2):281-90.
112. d'Udekem Y. Decellularized homografts: in fashion or really superior? *Eur J Cardiothorac Surg.* 2016;50(2):291-2.
113. Voges I, Brasen JH, Entenmann A, Scheid M, Scheewe J, Fischer G, et al. Adverse results of a decellularized tissue-engineered pulmonary valve in humans assessed with magnetic resonance imaging. *Eur J Cardiothorac Surg.* 2013;44(4):e272-9.
114. Priestestersbach H, Prudlo A, Bartosch M, Sanders B, Radtke T, Baaijens FP, et al. First percutaneous implantation of a completely tissue-engineered self-expanding pulmonary heart valve prosthesis using a newly developed delivery system: a feasibility study in sheep. *Cardiovasc Interv Ther.* 2017;32(1):36-47.
115. Shah RR, Poommipanit P, Law MA, Amin Z. Anchor balloon, buddy wire, and wire and sheath techniques to deploy percutaneous pulmonary valves in tetralogy of fallot patients. *Catheter Cardiovasc Interv.* 2017.
116. Tarzia P, Conforti E, Giamberti A, Varrica A, Giugno L, Micheletti A, et al. Percutaneous management of failed bioprosthetic pulmonary valves in patients with congenital heart defects. *J Cardiovasc Med (Hagerstown).* 2017;18(6):430-5.



Chapter 7

Four-dimensional flow CMR in tetralogy of Fallot: current perspectives

Evangeline G. Warmerdam*

Rosalie L. Neijzen*

Michiel Voskuil

Tim Leiner

Heynric B. Grotenhuis

* These authors contributed equally

Submitted

ABSTRACT

Tetralogy of Fallot is the most common cyanotic congenital heart defect, accounting for 10% of all CHD. Despite most patients now surviving well into adulthood, morbidity and mortality rates continue to be high. Surgical and percutaneous pulmonary valve replacement are procedures that are performed to prevent long-term complications from occurring. Unfortunately, pulmonary valve replacement based on current CMR criteria does not prevent postoperative ventricular arrhythmia, heart failure, and sudden cardiac death. Thus, a more advanced and comprehensive haemodynamic evaluation is needed to better understand right ventricular (dys)function in tetralogy of Fallot patients and to optimize the timing of valve replacement. Recently, four-dimensional flow CMR has emerged as a promising and non-invasive imaging technique that can provide comprehensive quantitative evaluation of flow in an entire volume within the chest in a single imaging session. With velocity-encoding in all three spatial directions throughout the complete cardiac cycle, it can provide analysis of cardiac, pulmonary artery and aortic flow volumes, flow velocities, flow patterns, as well as more advanced haemodynamic parameters. Four-dimensional flow CMR could therefore provide insights into the complex haemodynamics of tetralogy of Fallot and could potentially provide novel criteria for pulmonary valve replacement in these patients. The aim of this review is to provide an overview of available research on four-dimensional flow CMR research in tetralogy of Fallot patients.

INTRODUCTION

Tetralogy of Fallot (TOF) is the most common cyanotic congenital heart defect (CHD), accounting for 10% of all CHD.¹ TOF consists of a combination of a ventricular septal defect (VSD), overriding of the aorta, right ventricular outflow tract (RVOT) obstruction, and right ventricular (RV) hypertrophy.² Surgical repair, consisting of VSD closure and RVOT reconstruction, is usually performed during infancy. Major advances in surgical techniques and perioperative care have resulted in survival rates of over 90% up to 20 years after surgical repair for patients with TOF.³ Despite most patients now surviving well into adulthood, morbidity and mortality rates continue to be high during the third and fourth postoperative decades.^{3,4,5} These decreased survival rates are related to postoperative sequelae such as residual RVOT obstruction, pulmonary regurgitation (PR), and RV dilation or hypertrophy, which ultimately can lead to a negative cascade of RV dysfunction, congestive heart failure, arrhythmias, and sudden cardiac death.⁶

Surgical and percutaneous pulmonary valve replacement (PVR) are procedures that are performed to prevent these long-term complications from occurring. Unfortunately, the indication guidelines for PVR in TOF patients are not clear-cut. With the current cardiac magnetic resonance (CMR) criteria for PVR, such as increased indexed ventricular volumes and reduced ejection fraction, only measures of a late expression of RV dysfunction are taken into account. Although PVR may allow for reduced RV volumes and can improve symptoms, recent research shows that PVR based on current CMR criteria unfortunately does not prevent postoperative ventricular arrhythmia, heart failure, and sudden cardiac death.⁷ Thus, a more advanced and comprehensive haemodynamic evaluation is needed to better understand RV (dys)function in TOF patients and to optimize the timing of PVR in TOF.

Recently, four-dimensional flow CMR (4D flow CMR) has emerged as a promising and non-invasive imaging technique that can provide comprehensive quantitative evaluation of flow in an entire volume within the chest in a single short CMR imaging session. With velocity-encoding in all three spatial directions throughout the complete cardiac cycle, it can provide analysis of flow volumes, flow velocities, and flow patterns, as well as more advanced haemodynamic parameters such as kinetic energy, energy loss, helicity, vorticity, and wall shear stress.⁸ With these new advanced flow parameters available, 4D flow CMR could provide insights into the complex haemodynamics of TOF and could potentially provide novel criteria for PVR in TOF patients. The aim of this review is to provide an overview of available research on 4D flow CMR research in TOF patients.

IMAGING IN TETRALOGY OF FALLOT

Currently, echocardiography and CMR are the imaging modalities of choice for follow-up of TOF patients. Both modalities can provide a wide range of anatomical and functional parameters, but both also have a number of limitations. Echocardiography can provide information on anatomy and physiology, while qualitative flow assessment can be performed by colour Doppler. Image quality is strongly dependent on the acoustic window and operator skills.⁹ Especially the RV and PAs can be difficult to visualize in older children and adults, given the limited acoustic window due to the retrosternal positioning.

CMR can provide a completely non-invasive three-dimensional evaluation of cardiovascular anatomy, volumes and function. Flow can be analysed using two-dimensional phase-contrast (2D PC) CMR, which can provide flow volumes and velocity measurements perpendicular to a single plane placed in the vessel of interest. To obtain flow measurements each plane of interest has to be individually planned and separate breath-holding scans need to be performed. Furthermore, 2D PC CMR suffers from errors in flow quantification due to motion of the heart relative to the imaging plane and may give an incomplete assessment of blood flow due to technical limitations, especially in complex CHD.

4D FLOW VERSUS 2D FLOW

With 4D flow CMR, all data are acquired in a single free-breathing acquisition, so any location or plane of interest can be analysed retrospectively. Thus, there is no need for multiple breath-holds as is the case in 2D PC CMR, which also requires planning of each individual imaging plane. Furthermore, valvular flow can be measured using retrospective valve tracking, which takes into account and can correct for through-plane motion of the valve and flow angulation (Figure 1).¹⁰

The first comparison of 4D flow CMR and 2D PC CMR in patients with TOF was performed by van der Hulst et al. (Table 1).¹¹ In this study, 4D flow CMR was compared to 2D PC CMR for the evaluation of flow across the pulmonary valve (PV) and tricuspid valve (TV). The investigators found 4D flow CMR to be more accurate in the quantification of forward flow across the TV and regurgitant flow across the PV when compared to 2D PC CMR. Moreover, 4D flow CMR showed better agreement with RV stroke volumes measured in multi slice short axis cine images compared to 2D PC CMR. These results were confirmed in a more recent study by Isorni et al.¹² In this study, pulmonary and aortic flow

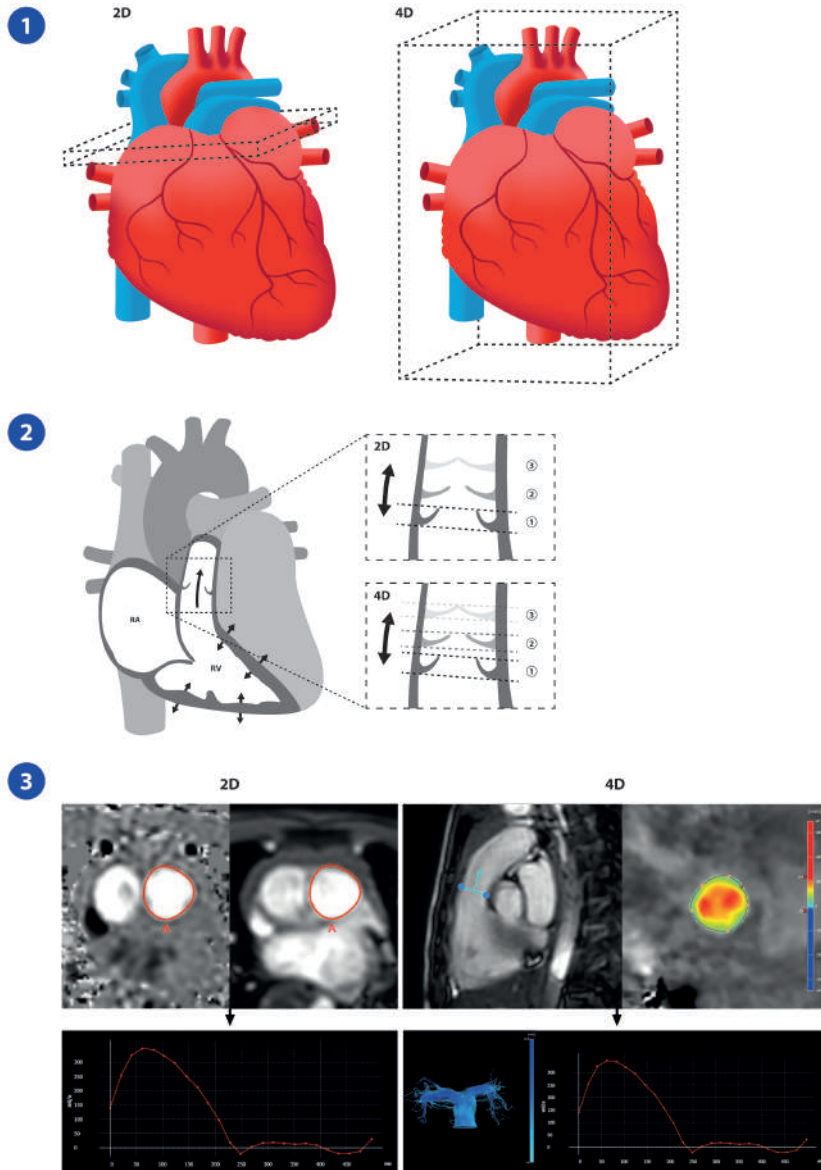


Figure 1. Valve analyses by 2D PC CMR versus 4D flow CMR. (A) For 2D PC CMR, imaging planes for flow measurements have to be individually prescribed, and separate breath-holding scans need to be performed for each acquisition. For 4D flow CMR, all data are acquired in a single acquisition, so any plane of interest can be analysed retrospectively to study the haemodynamic status of the individual patient. (B) In 2D PC CMR, information on valvular blood flow has to be obtained from one static plane, so flow assessment is hampered by the through-plane motion of the valve during the cardiac cycle. 4D flow CMR provides retrospective valve tracking, making it more accurate than 2D PC CMR due to its ability to correct for valvular through-plane motion and flow angulation. (C) After identification of the valve area, both 2D PC CMR and 4D flow CMR provide information on basic flow parameters. However, 4D flow CMR can also visualise both the forward and, if present, backward flow over the valve. 2D, two-dimensional; 4D, four-dimensional; CMR, cardiac magnetic resonance; PC, phase contrast; RA, right atrium, RV, right ventricle.

measurements by 4D flow CMR and 2D PC CMR were compared for paediatric and adult patients with TOF. Isorni et al. found 4D flow CMR to be more reliable and consistent due to the better correlation between pulmonary and aortic flow measurements when compared to 2D PC CMR. Another recent study, by Jakobs et al., also found 4D flow CMR had a better correlation between net flow across the PV and AV when compared to 2D PC CMR.¹³ Overall, 4D flow CMR has consistently shown to be more accurate compared to 2D PC CMR for measuring PV flow and is therefore ideally suited for the evaluation of degree of PR in TOF patients. The impact of 4D flow CMR measurements on clinical decision making however, has yet to be investigated.

RIGHT VENTRICLE

Functional assessment of the RV can be challenging due to its complex shape and often dyssynchronous contraction pattern. Since RV function is often impaired in TOF patients, accurate evaluation of RV function is crucial. Multi-slice short axis images obtained with routine CMR scans can provide routine parameters to assess RV function, such as ejection fraction, end-diastolic volume, and end-systolic volume. Indexation for body surface should be performed in the paediatric population, to correct for body composition and size. The aim of PVR is improvement of RV dimensions and function, which, according to current guidelines, can be achieved when preoperative RV end-diastolic volumes are $< 160 \text{ mL/m}^2$ or RV end-systolic volumes are $< 82 \text{ mL/m}^2$.¹⁴

Several studies have investigated flow patterns and advanced flow parameters in the RV using 4D flow CMR. Francois et al. found increased vortex flow in TOF patients compared to controls in the right atrium and RV during diastole.¹⁵ Similar results were found by Hirtler et al., as they found that the degree of PR (Figure 2) was associated with a higher degree of vorticity in the right atrium and the RV.¹⁶ These right sided vortices may represent energy loss and a less efficient circulation, which can potentially be harmful for the RV in TOF with impaired contractile capacity and could potentially serve to refer patients for early intervention.

One of the advanced parameters that can be measured with 4D flow CMR is kinetic energy, which is the mean energy content per mass unit blood flow. Kinetic energy measurements represent the amount of energy required for ventricular contraction and are therefore a good marker of ventricular efficiency. Kinetic energy is increased when ventricular efficacy is reduced, since more energy is required to achieve circulatory demand. Jeong et al. used 4D flow CMR to investigate flow energetics in the RV in TOF patients and healthy controls. They found kinetic energy in the RV to be increased in the TOF patients compared to healthy controls.¹⁷ Similar results were found in two other

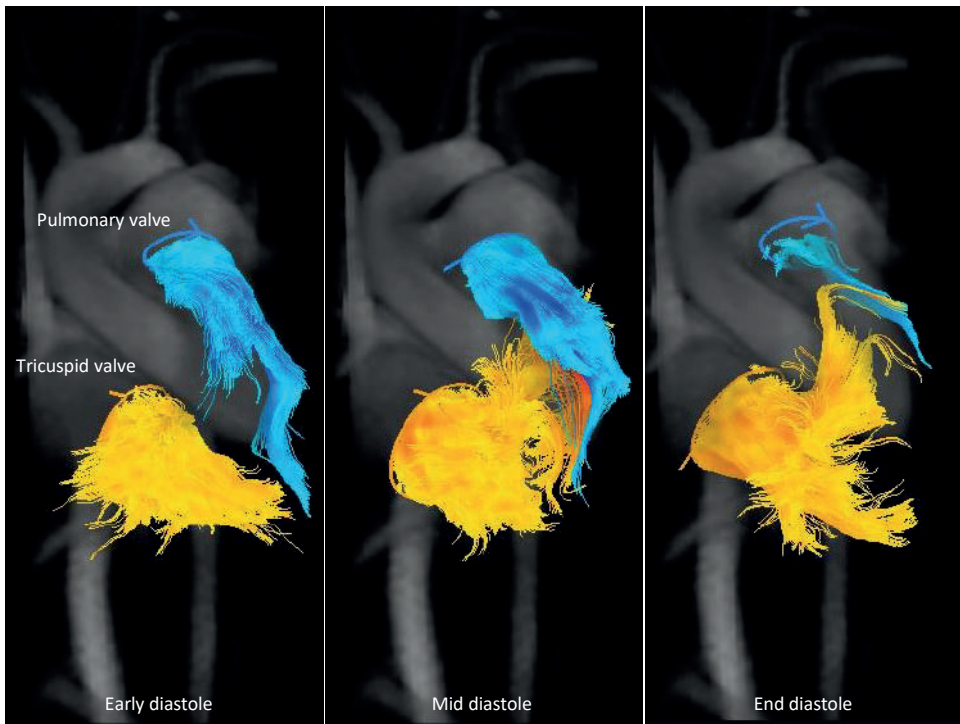


Figure 2. Visualisation of flow through the tricuspid valve (orange) and the pulmonary valve (blue). It is clear that the severe pulmonary regurgitation impairs the normal inflow of blood through the tricuspid valve in the right ventricle. Image was created using CAAS 4D flow CMR software (Pie Medical, Maastricht, The Netherlands)

studies by Sjöberg et al. and Frederiksson et al.^{18,19} Sjöberg et al., who evaluated RV kinetic energy over the entire cardiac cycle in patients with TOF with moderate to severe PR (> 20%) compared to healthy controls. They found RV diastolic peak kinetic energy to be increased in TOF patients compared to healthy controls, especially in patients with non-restrictive RV physiology.¹⁸ Frederiksson et al. found increased turbulent kinetic energy in the RV of patients with TOF and PR compared to healthy controls. High values of turbulent kinetic energy were located predominantly in the RVOT. Furthermore, they found that turbulent kinetic energy had a stronger relationship to indices of RV remodelling, as expressed by PR volumes and fractions, compared to conventional 2D CMR parameters such as RV dimensions.¹⁹ These findings of increased kinetic energy in the RV suggest that circulation in the RV is less efficient in TOF patients compared to healthy controls. Moreover, kinetic energy could potentially serve as an important indicator of RV performance, which is often impaired in patients with TOF due to chronic volume overload.

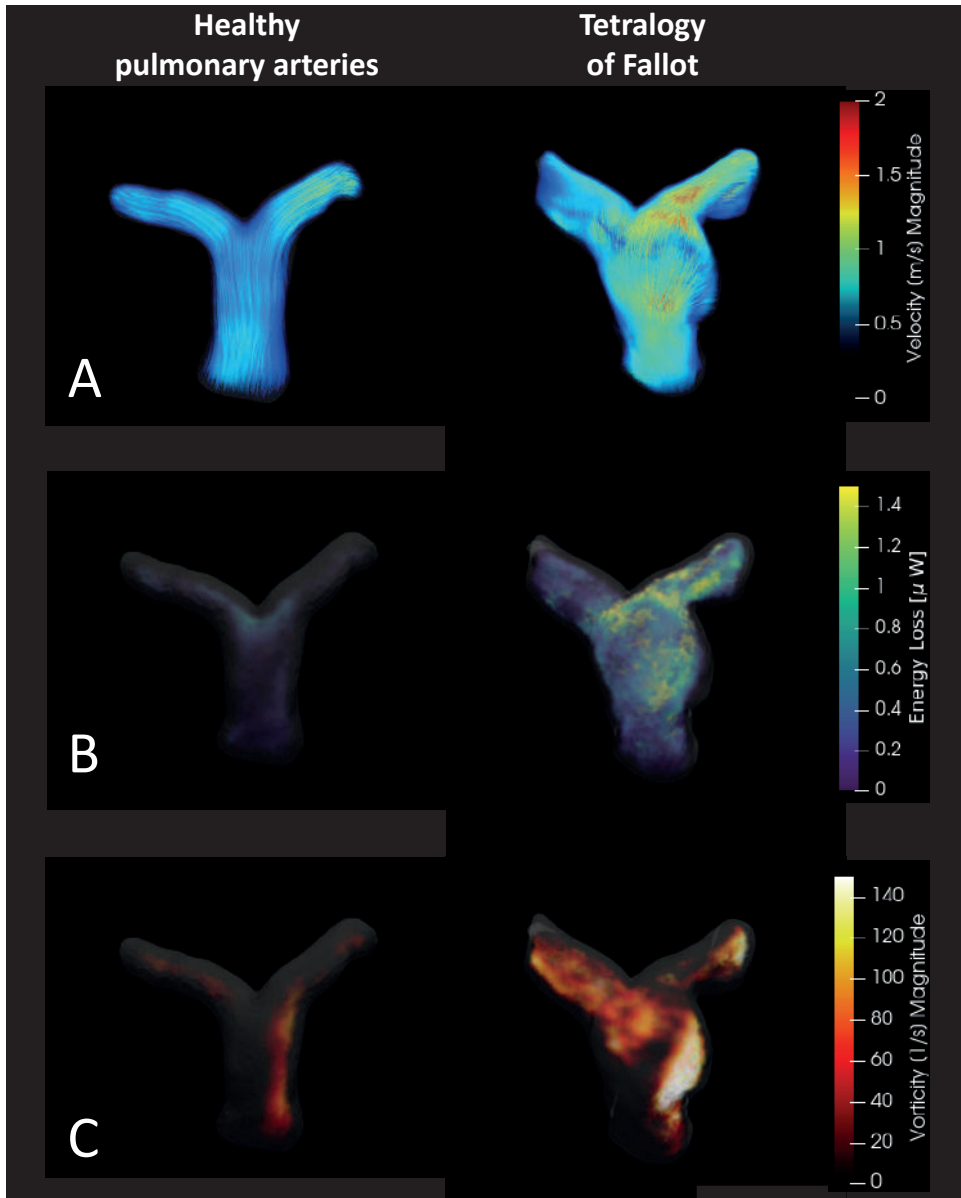


Figure 3. 4D flow CMR visualisation of the pulmonary arteries from a healthy volunteer and a TOF patient. Panel A shows flow patterns and flow velocities using colour-coded streamlines. The TOF patient shows dilatation of the main pulmonary artery and clear areas of increased flow velocity and abnormal flow patterns. Panel B shows a visual representation of the energy loss, a marker of efficiency of the circulation, within the pulmonary arteries. In healthy pulmonary arteries with normal flow patterns, only a minimal amount of energy loss is seen just before the bifurcation. For the TOF patient, increased levels of energy loss are seen, especially in the areas with non-laminar flow and increased velocity. Panel C shows a visual representation of vorticity, a parameter describing the local flow rotation, in the pulmonary arteries. The TOF patients clearly has higher vorticity values compared to the healthy volunteer. Overall, the TOF patient shows abnormal flow patterns and clearly has a less efficient pulmonary circulation compared to the healthy volunteer.

PULMONARY ARTERIES

Patients with TOF can suffer from varying degrees of PR, PV stenosis and PA branch stenosis. Therefore, flow in the PAs can exhibit complex patterns (Figure 3). As a consequence, PA flow analysis based on a single 2D flow CMR plane is often incomplete and prone to errors. Geiger et al. and Francois et al. have used 4D flow CMR to investigate blood flow patterns in the PAs. They found that TOF patients can exhibit helical flow patterns in the PAs and frequently demonstrate extensive vortex formation.^{15,20}

Hu et al. performed an analysis of helical and vortical flow patterns in the PAs of TOF patients.²¹ They found vortices to be present predominantly in the main PA, which is most likely related to increased main PA diameters as a result of prior surgical repair. Helical flow patterns were mainly found in the right PA. The mechanism for helical flow is not very well understood, but it might be a more efficient way of driving blood through a stenotic vessel.²² Furthermore, Hu et al. found systolic energy loss in the right PA to be associated with increased RV dimensions, which is suggestive of impaired ventricular-arterial coupling. In order to investigate whether 4D flow CMR measurements of haemodynamic inefficiency are associated with disease severity in TOF patients, Robinson et al. compared 4D flow CMR measurements to conventional CMR parameters used for the monitoring of disease progression such as RV volumes and ejection fraction.²³ The researchers found that kinetic energy in the PAs was increased in TOF patients compared to healthy controls and that these kinetic energy measurements were correlated with traditional measurements of disease severity, such as ventricular volumes and the degree of PR. Especially interesting were the strong and positive correlations between increased kinetic energy in the PAs and larger RV dimensions. With 4D flow CMR, parameters of haemodynamic (in)efficiency in the PAs can be measured, and these parameters could therefore serve as early markers of disease progression in TOF patients and, potentially, earlier intervention.

LEFT VENTRICLE AND AORTA

Although follow-up of TOF is primarily focused on the right heart, the status of the left heart also needs to be considered during follow-up of these patients. A substantial number of TOF patients suffer from aortic root dilatation and aortic stiffness, which can result in volume or pressure overload of the LV, respectively.²⁴ Three studies have investigated the LV and aorta in patients with TOF using 4D flow CMR. Sjoberg et al. investigated LV kinetic energy for the entire cardiac cycle in TOF patients with moderate to severe PR and healthy controls.¹⁸ They found a significant decrease in LV systolic

kinetic energy in TOF patients compared to healthy controls. Possible explanations could be decreased preload of the LV due to RV impairment, septal dyssynchrony (with the septum moving towards the RV during systole), and adverse RV-LV interaction in the setting of RV dysfunction. Schäfer et al. used 4D flow CMR to assess aortic wall characteristics and aortic flow haemodynamics in pre-adolescent and adolescent TOF patients who underwent early repair (age < 1 year) and compared these findings to age-matched controls.²⁵ They found elevated wall shear stress values throughout the entire aorta and increased aortic stiffness in the ascending and proximal descending aorta. In a different study, Schäfer et al. found abnormal helical flow patterns in the aorta in TOF patients, whereas none of the control patients showed abnormal flow patterns. In TOF patients, these abnormal flow patterns were found to be associated with increased energy loss and this energy loss was subsequently found to be associated with reduced LV function and volumes.²⁶ These findings suggest LVOT abnormalities due to initial TOF repair could result in abnormal flow patterns in the aorta which in turn could lead to impaired LV function.

FUTURE PERSPECTIVES

4D flow CMR enables comprehensive evaluation of blood flow within the cardiopulmonary circulation of patients with repaired TOF. In studies comparing 4D flow CMR to 2D PC CMR, 4D flow CMR has been found to be more accurate than 2D PC CMR for measurements of valvular flow. Since precise evaluation of PR is important, evaluation of valvular flow in TOF patients is better performed using 4D flow CMR. Abnormal flow patterns can be visualized with 4D flow CMR and this can be insightful for both physicians and patients. Furthermore, advanced flow parameters such as vorticity and helicity provide the opportunity to precisely quantify these abnormal blood flow patterns. Further research could help to provide insights into the complex interplay between vessel anatomy and blood flow patterns. Advanced flow parameters that can better assess the haemodynamic consequences of altered postoperative anatomy as well as improved prediction of which patient will develop valvular or arterial stenosis would be of great use in determining follow-up frequency and identifying patients at risk of reintervention. Advanced flow parameters that are markers of efficiency of the circulation, such as kinetic energy and energy loss, have been found to be abnormal in TOF patients compared to healthy controls. The abovementioned research suggests that these parameters could potentially serve as markers for disease progression or even become predictors of cardiovascular outcome.

Table 1. An overview of all available articles, including patient characteristics and results, on four-dimensional flow CMR in tetralogy of Fallot.

First author Year	Patients	Controls	Area of interest	Parameters	Conclusion
Hu 2020	n = 25 Age 8.44 ± 4.52 years	n = 10 Age 8.2 ± 1.22 years	RV, PAs	Flow, WSS, EL	Increased peak WSS and viscous energy are associated with pulmonary haemodynamic changes.
Jakobs 2020	n = 34 Age 15.6 ± 3.6 years	-	PV, PAs	Flow, volumetry	4D flow CMR is more accurate than 2D PC CMR for flow measurements.
Isorni 2019	n = 50 Age 18.2 (2-54) years	-	PAs, aorta	Flow	4D flow CMR is more accurate than 2D PC CMR for flow measurements.
Rizk, 2019	n = 37 Age 27 (18-35) years	n = 11 Age 26 (24-27) years	PAs	WSS	WSS is increased in patients with PS.
Robinson 2019	n = 21 Age 13.8 ± 8.2 years	n = 24 Age 15.8 ± 3.0 years	RV, PAs	KE	KE is abnormal in TOF patients and has a direct relationship with traditional measures of disease severity.
Schäfer 2019	n = 41 Age 14 (10-21) years	n = 15 Age 10 (10-18) years	Aorta	EL	Abnormal aortic flow patterns are associated with increased EL. EL is associated with LV volumes and function.
Frederiksson 2018	N = 17	n = 10 Age 31 ± 11 years	RV	Flow, TKE	RV TKE is increased in TOF patients. RV TKE has a stronger association with RV remodelling than 2D PC CMR measurements.
Schäfer 2018	n = 18 Age 10.3 ± 3.2 years	n = 18 Age 11.6 ± 3.4 years	Aorta	Flow, WSS	TOF patients have increased aortic WSS, increased aortic stiffness and abnormal aortic flow during systole.
Sjöberg 2018	n = 15 Age 29 ± 12 years	n = 14 Age 30 ± 7 years	LV and RV	KE	TOF patients with PR > 20% and preserved LV function have disturbed KE in the LV and RV.
Hirtler 2016	n = 24; Age 11.7 ± 5.8 years	n = 12 Age 23.3 ± 1.6 years	RV, PAs	Flow, vorticity	TOF patients have increased RV vorticity. Higher PR fraction is associated with increased RV vorticity.
Jeong 2015	n = 10 Age 20.6 ± 12.2 years	n = 9 Age 38.9 ± 15.1 years	LV, RV, PAs, aorta	KE	TOF patients have increased RV KE.

Table 1. Continued.

First author Year	Patients	Controls	Area of interest	Parameters	Conclusion
Francois 2012	n = 11 Age 20.1 ± 12.4 years	n = 10 Age 34.2 ± 13.4 years	SVC, IVC, RV, PAs	Flow, WSS	TOF patients have increased vortical flow in the RA and RV and have increased helical and vortical flow in the PAs.
Geiger 2011	n = 10 Age 12.1 ± 8.1 years	n = 4 Age 26 ± 0.8 years	PAs, aorta	Flow, vorticity	TOF patients can have helical flow and severe vortices in the PAs.
Van der Hulst 2010	n = 25 Age 13.1 ± 2.7 years	n = 19 Age 14.1 ± 2.4 years	TV, RV, PV	Flow	4D flow CMR is more accurate than 2D PC CMR for valvular flow measurements and evaluation of RV diastolic function.

2D PC CMR: two-dimensional phase-contrast cardiac magnetic resonance, 4D flow CMR: four-dimensional flow cardiac magnetic resonance, EL: energy loss, IVC: inferior caval vein, KE: kinetic energy, LV: left ventricle, PA: pulmonary artery, PV: pulmonary valve, RV: right ventricle, SVC: superior caval vein, TV: tricuspid valve, WSS: wall shear stress.

Timing of PVR in TOF patients has been subject of academic debate for decades. Unfortunately, recent research shows that, using current CMR criteria, PVR does not prevent postoperative ventricular arrhythmia, heart failure, and sudden cardiac death in a significant portion of patients.⁷ Using 4D flow CMR, a more accurate assessment of PV regurgitation flow can be obtained, which could lead to better timing of PVR. Furthermore, 4D flow CMR provides a wealth of advanced flow parameters which could be used to assess ventricular and vascular function in TOF patients. Research using 4D flow CMR in large cohorts of TOF patients with a long follow-up period could potentially validate these novel indicators in decision making for PVR.

Thus, 4D flow CMR provides a unique opportunity to investigate abnormal blood flow in TOF due to (repaired) defects and study flow phenomena and arterial-ventricular interaction. Further research could potentially identify parameters suitable for the prediction of outcomes in patients with repaired TOF and for refining timing of PVR.

CONCLUSION

A substantial body of research shows 4D flow CMR is more accurate in measuring pulmonary flow and especially valvular regurgitation fraction compared to 2D PC CMR. Furthermore, 4D flow CMR provides the opportunity to analyse a wide range of

advanced haemodynamic parameters not accessible with any other method. Compared to healthy controls, patients with TOF have increased kinetic energy and vortex flow in the RV and PAs and increased wall shear stress and abnormal flow patterns in the aorta, all of which are indicative of a less efficient circulation. Further research into advanced flow parameters in patients with TOF could potentially validate parameters suitable for prediction of outcomes in patients with repaired TOF and for refining timing of PVR.

REFERENCES

1. Villafane J, Feinstein JA, Jenkins KJ, Vincent RN, Walsh EP, Dubin AM, et al. Hot topics in tetralogy of Fallot. *J Am Coll Cardiol* 2013;Dec;10;62(23):2155-66
2. Fallot E. Contribution a l'anatomie pathologique de la maladie bleue (cyanose cardiaque). *Mars Med*. 1888;25:77ff
3. Cuypers JAAE, Menting ME, Konings EEM, Opic P, Utens EMW, Helbing WA, et al. Unnatural history of tetralogy of Fallot: prospective follow-up of 40 years after surgical correction. *Circulation*. 2014 Nov 25;130(22):1944-53. doi: 10.1161/CIRCULATIONAHA.114.009454.
4. Murphy JG, Bersh BJ, Mair DD, Fuster V, McGoon MD, Ilstrup DM, et al. Long-term outcome in patients undergoing surgical repair of tetralogy of Fallot. *N Engl J Med*. 1993 Aug 26;329(9):593-9. doi: 10.1056/NEJM199308263290901.
5. Nollert G, Fischlein T, Bouterwek S, Böhmer C, Klinner W, Reichart B. Long-term survival in patients with repair of tetralogy of Fallot: 36-year follow-up of 490 survivors of the first year after surgical repair. *J Am Coll Cardiol*. 1997 Nov 1;30(5):1374-83. doi: 10.1016/s0735-1097(97)00318-5.
6. Gatzoulis MA, Balaji S, Webber SA, Siu SC, Hokanson JS, Poile C, et al. (2000) Risk factors for arrhythmia and sudden cardiac death late after repair of tetralogy of Fallot: a multicentre study. *Lancet* 356:975–981
7. Bokma JP, Geva T, Sleeper LA, Narayan SVB, Wald R, Hickey K, et al. A propensity score-adjusted analysis of clinical outcomes after pulmonary valve replacement in tetralogy of Fallot. *Heart*. 2018 May;104(9):738-744. doi: 10.1136/heartjnl-2017-312048.
8. Dyverfeldt P, Bissell M, Barker AJ, Bolger AF, Carlhäll CJ, Ebberts T, et al. 4D flow cardiovascular magnetic resonance consensus statement. *J Cardiovasc Magn Reson*. 2015 Aug 10;17(1):72. doi: 10.1186/s12968-015-0174-5. PMID: 26257141; PMCID: PMC4530492.
9. Lai WW, Gauvreau K, Rivera ES, Saleeb S, Powell AJ, Geva T. Accuracy of guideline recommendations for two-dimensional quantification of the right ventricle by echocardiography. *Int J Cardiovasc Imaging*. 2008; 24: 691–698
10. Roes SD, Hammer S, van der Geest RJ, Marsan NA, Bax JJ, Lamb HJ, et al. Flow assessment through four heart valves simultaneously using 3-dimensional 3-directional velocity-encoded magnetic resonance imaging with retrospective valve tracking in healthy volunteers and patients with valvular regurgitation. *Invest Radiol*. 2009;44:669–75.
11. Van der Hulst AE, Westenberg JJM, Kroft LJM, Bax JJ, Blom NA, de Roos A, et al. Tetralogy of fallot: 3D velocity-encoded MR imaging for evaluation of right ventricular valve flow and diastolic function in patients after correction. *Radiology*. 2010 Sep;256(3):724-34. doi: 10.1148/radiol.10092269.
12. Isorni MA, Martins D, Ben Moussa N, Monnot S, Boddaert N, Bonnet D, et al. 4D flow MRI versus conventional 2D for measuring pulmonary flow after Tetralogy of Fallot repair. *Int J Cardiol*. 2020 Feb 1;300:132-136. doi: 10.1016/j.ijcard.2019.10.030.

13. Jakobs KG, Chan FP, Cheng JY, Vasanawala SS, Maskatia SA. 4D flow vs. 2D cardiac MRI for the evaluation of pulmonary regurgitation and ventricular volume in repaired tetralogy of Fallot: a retrospective case control study. *Int J Cardiovasc Imaging*. 2020 Apr;36(4):657-669. doi: 10.1007/s10554-019-01751-1.
14. Oosterhof T, van Straten A, Vliegen HW, Meijboom FJ, van Dijk APJ, Spijkerboer AM, et al. Preoperative thresholds for pulmonary valve replacement in patients with corrected tetralogy of Fallot using cardiovascular magnetic resonance. *Circulation*. 2007 Jul 31;116(5):545-51. doi: 10.1161/CIRCULATIONAHA.106.659664
15. Francois CJ, Srinivasan S, Schiebler ML, Reeder SB, Niespodzany E, Landgraf BR, et al. 4D cardiovascular magnetic resonance velocity mapping of alterations of right heart flow patterns and main pulmonary artery haemodynamics in tetralogy of Fallot. *J Cardiovasc Magn Reson*. 2012. doi: 10.1186/1532-429X-14-16
16. Hirtler D, Garcia J, Barker AJ, Geiger J. Assessment of intracardiac flow and vorticity in the right heart of patients after repair of tetralogy of Fallot by flow-sensitive 4D MRI. *Eur Radiol*. 2016 Oct;26(10):3598-607. doi: 10.1007/s00330-015-4186-1.
17. Jeong D, Anagnostopoulos PV, Roldan-Alzate A, Srinivasan S, Schiebler ML, Wieben O, et al. Ventricular kinetic energy may provide a novel noninvasive way to assess ventricular performance in patients with repaired tetralogy of Fallot. *J Thorac Cardiovasc Surg*. 2015 May;149(5):1339-47. doi: 10.1016/j.jtcvs.2014.11.085.
18. Sjöberg P, Bidhult S, Bock J, Heiberg E, Arheden H, Gufstafsson R, et al. Disturbed left and right ventricular kinetic energy in patients with repaired tetralogy of Fallot: pathophysiological insights using 4D-flow MRI. *Eur Radiol*. 2018; 28(10): 4066–4076. doi: 10.1007/s00330-018-5385-3
19. Fredriksson A, Trzebiatowska-Krzynska A, Dyverfeldt P, Engvall J, Ebbers T, Carlhäll CJ. Turbulent kinetic energy in the right ventricle: Potential MR marker for risk stratification of adults with repaired Tetralogy of Fallot. *J Magn Reson Imaging*. 2018 Apr;47(4):1043-1053. doi: 10.1002/jmri.25830.
20. Geiger J, Markl M, Jung B, Grohmann J, Stiller B, Langer M, et al. 4D-MR flow analysis in patients after repair for tetralogy of Fallot. *Eur Radiol*. 2011 Aug;21(8):1651-7. doi: 10.1007/s00330-011-2108-4.
21. Hu L, Ouyang R, Sun A, Wang Q, Guo C, Peng Y, et al. Pulmonary artery haemodynamic assessment of blood flow characteristics in repaired tetralogy of Fallot patients versus healthy child volunteers. *Quant Imaging Med Surg*. 2020 May;10(5):921-933. doi: 10.21037/qims.2020.03.23.
22. Liu X, Sun A, Fan Y, Deng X. Physiological significance of helical flow in the arterial system and its potential clinical applications. *Ann Biomed Eng*. 2015 Jan;43(1):3-15. doi: 10.1007/s10439-014-1097-2.
23. Robinson JD, Rose MJ, Joh M, Jarvis K, Schnell S, Barker AJ, et al. 4-D flow magnetic-resonance-imaging-derived energetic biomarkers are abnormal in children with repaired tetralogy of Fallot and associated with disease severity. *Pediatr Radiol*. 2019 Mar;49(3):308-317. doi: 10.1007/s00247-018-4312-8

24. Cheun YF, Ou X, Wong SJ. Central and peripheral arterial stiffness in patients after surgical repair of tetralogy of Fallot: implications for aortic root dilatation. *Heart*. 2006 Dec; 92(12): 1827–1830. doi: 10.1136/hrt.2006.091199
- 25 Schäfer M, Browne LP, Morgan GJ, Barker AJ, Fonseca B, Ivy DD, et al. Reduced proximal aortic compliance and elevated wall shear stress after early repair of tetralogy of Fallot. *J Thorac Cardiovasc Surg*. 2018 Dec;156(6):2239-2249. doi: 10.1016/j.jtcvs.2018.08.081.
26. Schäfer M, Barker AJ, Jaggars J, Morgan GJ, Stone ML, Truong U, et al. Abnormal aortic flow conduction is associated with increased viscous energy loss in patients with repaired tetralogy of Fallot. *Eur J Cardiothorac Surg*. 2020 Mar 1;57(3):588-595. doi: 10.1093/ejcts/ezz246
27. Warmerdam E, Krings GJ, Leiner T, Grotenhuis HB. Three-dimensional and four-dimensional flow assessment in congenital heart disease. *Heart*. 2020 Mar;106(6):421-426. doi: 10.1136/heartjnl-2019-315797. Epub 2019 Dec 19. PMID: 31857355.



PART THREE

Transposition of the Great Arteries



Chapter 8

Head-to-head comparison between computational fluid dynamics and four-dimensional flow CMR of the pulmonary arteries in congenital heart disease

Maartje Conijn *

Evangeline G. Warmerdam*

Jos J.M. Westenberg

Felix Haas

Tim Leiner

Julio Sotelo

Sergio Uribe

Arno A.W. Roest

Friso M. Rijnberg

Hildo J. Lamb

Michiel Voskuil

Gregor J. Krings**

Heynric B. Grotenhuis**

* These authors contributed equally

** These authors contributed equally

Submitted

ABSTRACT

Background. Life-long follow-up is required for many congenital heart disease patients. A non-invasive imaging modality that provides comprehensive haemodynamic evaluation is therefore crucial. Computational fluid dynamics (CFD) and four-dimensional flow (4D flow) cardiac magnetic resonance (CMR) are increasingly used in these patients. Both modalities have different strengths and limitations for the assessment of the pulmonary arteries, but a direct comparison has not been performed before. Therefore, the aim of this study was to compare CFD with 4D flow CMR for haemodynamic evaluation of the pulmonary arteries in transposition of the great arteries patients.

Methods. Three patients with transposition of the great arteries were studied with CFD and 4D flow CMR: one patient without pulmonary artery stenosis, one with unilateral, and one with bilateral branch stenosis. Comparison was made to one control with normal pulmonary arteries. For this study we numerically compared peak velocities and flow volumes, and visually compared flow patterns and wall shear stress distribution.

Results. Maximum velocities and flow distribution were similar for CFD and 4D flow CMR in all cases. Flow patterns were broadly comparable for all cases. Wall shear stress values were lower for CMR measurements, but wall shear stress distribution was similar for all cases.

Conclusion. Haemodynamic assessment of the pulmonary arteries was comparable between CFD and 4D flow CMR in all subjects. Due to differences in spatial and temporal resolution, absolute wall shear stress values provided by CMR provided were consistently lower when compared to CFD.

INTRODUCTION

Congenital heart disease is the most common congenital defect, with an incidence of 8 per 1000 births.¹ Major advances in surgical techniques and perioperative care have greatly improved the survival rate of congenital heart disease patients. Nowadays, 95% of infants with congenital heart disease will survive into adulthood.² Unfortunately this increased survival rate goes hand in hand with an increased rate of long-term morbidity. The majority of congenital heart disease patients will therefore require lifelong follow-up and many of the more complex entities will require (repeat) intervention at some point in life.

With a growing group of congenital heart disease patients who need lifelong monitoring, non-invasive diagnostic modalities are essential. Patients with congenital heart disease often have abnormal blood flow patterns, either due to their cardiac defect or as a consequence of required intervention(s). Research shows that abnormal blood flow patterns may contribute to a decline in cardiovascular functioning.³ Imaging techniques that provide visualization and quantification of blood flow could therefore improve our understanding of the often-complex haemodynamics in these patients and could potentially guide the timing and nature of interventions. Two different (but complementary) diagnostic modalities provide a comprehensive assessment of blood flow: computational fluid dynamics (CFD) and 4D flow cardiac magnetic resonance (4D flow CMR). Both modalities allow for flow visualization and assessment of a broad range of parameters for flow quantification, including important advanced blood flow parameters such as wall shear stress, kinetic energy, energy loss, helicity and vorticity.

CFD is a specialized area of mathematics and a branch of fluid mechanics, often used in engineering to study complex flow patterns. It can be used to evaluate blood flow in the cardiovascular system of patients in a reconstructed 3D model of the patients anatomy. CFD has several advantages: the high spatial and temporal resolution, the potential to perform virtual surgery or stent implantation, and the ability to simulate different loading conditions, i.e. rest and exercise. However, outcomes are always an approximation of reality and are highly dependent on the quality of the reconstructed anatomy images and the applied boundary conditions.^{4, 5} Furthermore, processing time can be extensive ranging between hours up to several days depending on the complexity of the case.

4D flow CMR is the term used for time-resolved phase-contrast CMR with flow-encoding in all three spatial directions.^{6,7} Using 4D flow CMR, qualification and quantification of flow over an entire volume can be obtained. This technique has been available for several

decades now, however only in the last years acquisition time has reached acceptable levels for clinical application.⁸ Despite other limitations such as limited spatial and temporal resolution, 4D flow CMR is currently the only non-invasive imaging technique available to analyse and quantify blood flow in vivo.

In this study, CFD analyses of the pulmonary arteries of patients with transposition of the great arteries after the arterial switch operation with various degrees of pulmonary artery stenosis are compared with 4D flow CMR measurements. The aim of this study is to identify potential differences between both modalities and to explore the appropriate indications for each modality.

METHODS

Patients

Imaging data of three patients with transposition of the great arteries who underwent the arterial switch operation were used in this study: one patient without pulmonary artery stenosis, one with unilateral pulmonary artery stenosis, and one with bilateral branch stenosis. Comparison was made to one control with normal pulmonary arteries with a history of coarctation of the aorta. All study participants underwent CMR as part of routine follow-up care. In the same session 4D flow CMR was performed for study purposes. Approval from the local Medical Ethical Committee was granted for this study (number 16-197 and 18-200, respectively). Written informed consent was obtained from all patients and, if applicable, their guardians.

CMR acquisition

A visual summary of CFD and 4D flow methods can be found in Figure 1. CMR imaging was performed on a 3.0 Tesla MR scanner (Ingenia R5.6.1, Philips Healthcare, Best, The Netherlands). A 3D non-contrast end diastolic scan with prospective ECG-triggering and respiratory navigator-gating was performed to visualize cardiovascular anatomy. Imaging parameters for the 3D non-contrast scan were as follows: spatial resolution = 0.92 mm², FOV = 294 mm², slice thickness = 1.5 - 3 mm, echo time: 1.31 ms, repetition time: 3.7 - 4.1 ms, flip angle = 10°, bandwidth = 1085 Hz/pixel. Scan times were typically 10 minutes per scan. 4D flow CMR acquisition was performed with retrospective ECG and respiratory navigator-gating. The acquired volume covered the entire pulmonary arteries. The 4D flow CMR was a respiratory navigator-gated scan, parameters were as follows: spatial resolution = 2.5 mm³, FOV = 300 mm², slice thickness = 2.5 mm, temporal

resolution = 32.8 – 46.1 ms, TE = 2.1 – 2.4 ms, TR: 3.9 – 4.2 ms, flip angle = 8°, venc = 200 – 380 cm/s, TFE factor = 3, SENSE = 2.5 (AP) and 1.5 (RL). Acquisition times were typically 8–12 minutes per scan.

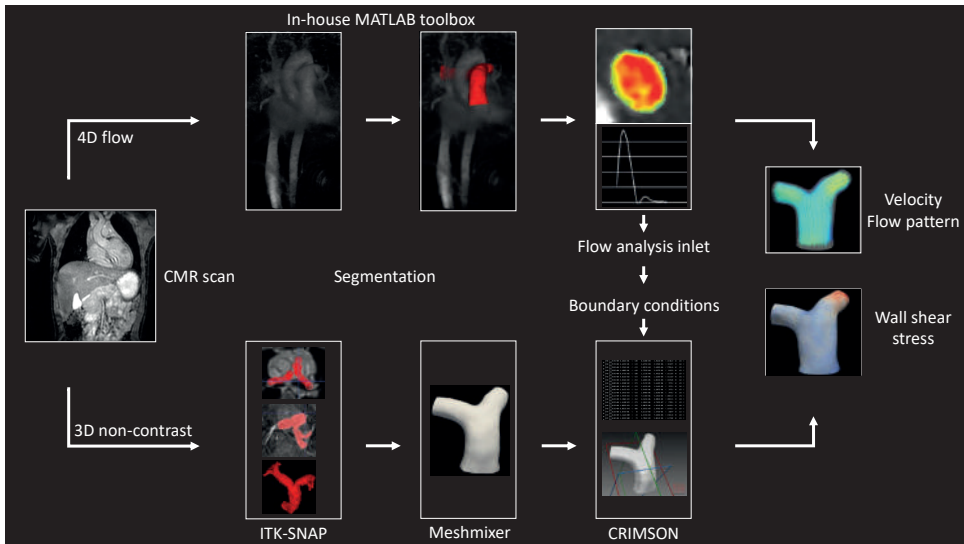


Figure 1. Visual summary of methods used for computational fluid dynamics and 4D flow CMR measurements. For both modalities, segmentation of the vessel of interest is the first step. Subsequently, flow waveform and volumes in the main pulmonary artery just above the pulmonary valve are measured using 4D-flow CMR, which will be used as inlet boundary condition for the computational fluid dynamics analysis. For both modalities, peak velocities and flow volumes are measured in the right and left pulmonary artery. Flow patterns and wall shear stress are visualized using Paraview software.

CMR post-processing

The 4D Flow CMR images were processed using an in-house MATLAB toolbox (The MathWorks, Natick, MA, USA)⁹ which included the segmentation of the pulmonary artery, the generation of the tetrahedral finite element mesh and the quantification of the wall shear stress as detailed in previous reports.^{10, 11, 12} To process the 4D Flow CMR images, the angiographic image was segmented at peak systole using thresholding, labelling, and manual separation of the vessels, based on the angiographic image generated by the velocity field.¹³ The tetrahedral finite element mesh was created using the iso2mesh MATLAB toolbox.¹⁴ Once the mesh was constructed, the velocity values were transferred to each node of the mesh from the 4D Flow CMR using a cubic interpolation. Finally, the wall shear stress was calculated, using a finite element method based on a Least Square

Stress Projection Method, as previously published.¹⁰ The finite element method is well known by obtaining more precision and better representation of the geometry, gaining great interest in recent studies.^{10, 11, 12}

CFD method

The end-diastolic 3D non-contrast CMR scan of each patient was used to construct a 3D model of the pulmonary arteries from the pulmonary valve up to the right and left pulmonary artery. Segmentation was performed with ITK-SNAP software (<http://itksnap.org/>). The Surface Tessellation Language mesh was manually smoothened in Meshmixer software (Autodesk Inc, San Rafael, USA). A tetrahedral mesh with a total of 5 boundary layers was created using CRIMSON software (Cardiovascular Integrated Modelling and Simulation (CRIMSON; available at <http://www.crimson.software/>). To ensure numerical outcomes independent of mesh size, a grid independence test was performed. The solution was considered mesh independent in case of < 1 mmHg difference in pressure outcomes, < 0.5 mmHg in wall shear stress and < 1 ml in flow split outcomes. The final simulation was performed with a mesh of respectively 884,536, 1,010,000, 1,004,000 and 1,000,000 elements for case A, B, C and D.

The acquired 4D flow CMR scan was used to define patient-specific boundary conditions. Patient-specific mass flow, flow waveform and cardiac frequency derived from 4D flow CMR were used as inlet boundary conditions for the CFD analysis together with a generic parabolic inlet velocity profile. A three-element windkessel was coupled to each outlet consisting of a proximal- and distal resistor and a capacitor. The windkessel parameters were calculated as previously published.¹⁵ As no patient-specific invasive pressure measurements were available, pulmonary artery pressures were assumed to be around 20 mmHg in the pulmonary periphery.

CRIMSON software was used to perform the numerical studies and several conditions were set as follows: the wall was assigned an overall compliance with a Young's modulus of 0.26 MPa and a Poisson ratio of 0.5.¹⁶ The wall thickness was set to be 0.5 mm. Blood was assumed to behave as a Newtonian fluid with a blood density of 1060 kg/m³ and a viscosity of 0.004 kg/ms. Four cardiac cycles with a time step size of 0.001s were simulated. The last simulated cardiac cycle was used for analysis. The solution was considered converged when residuals dropped below 10⁻⁴.

Comparison of CMR and CFD

The peak-systolic phase was used for comparison between both modalities. Streamlines, wall shear stress and velocity were visually compared with color-coded streamlines in

Paraview software.¹⁷ Paraview software was also used to calculate maximum velocities in the right and left pulmonary artery. Furthermore, the right-left pulmonary artery flow split was calculated. Wall shear stress distribution was compared qualitatively and absolute values of maximal wall shear stress on the right and left pulmonary artery were compared. Due to the compliant arterial wall used in the numerical analysis the anatomy changed during the cardiac cycle by expanding during systole. The wall shear stress and colour-coded streamlines results are shown within the systolic anatomy calculated by CFD.

RESULTS

Patient characteristics are shown in Table 1. None of the patients underwent reintervention after initial repair of their cardiac defect. All patients had good biventricular function on echocardiography. None of the patients suffered from pulmonary regurgitation. Geometries and inlet waveforms for all cases can be found in Figure 2.

Flow distribution

Flow distribution comparison between CFD and 4D flow CMR are shown in Figure 2. In all cases the distribution of flow between the right and left pulmonary artery was comparable. The differences for flow distribution ranged between 0% and 6% for the both the right and left pulmonary artery.

Flow pattern and peak velocity

The velocity streamlines were similar for both modalities in all four cases (Figure 3) and areas with high flow velocities were in high agreement between both modalities in all subjects. The absolute values for peak velocities in the right and left pulmonary artery were similar in all cases for both modalities (Figure 3). The differences in peak velocity ranged from 0.0 m/s to 0.4 m/s for both the right and left pulmonary artery. Visually some differences can be observed. In general, CMR displays a more extensive area with low flow velocities in the area of the vessel wall when compared to CFD. Also, CFD results showed marked turbulence in the main pulmonary artery for case C (unilateral pulmonary artery stenosis), whereas 4D flow CMR demonstrated a more laminar flow pattern within the main pulmonary artery. In case D (bilateral branch pulmonary artery stenosis), the highly stenotic right pulmonary artery displayed an area of high flow velocity in the CFD results which was not observed in the CMR case.

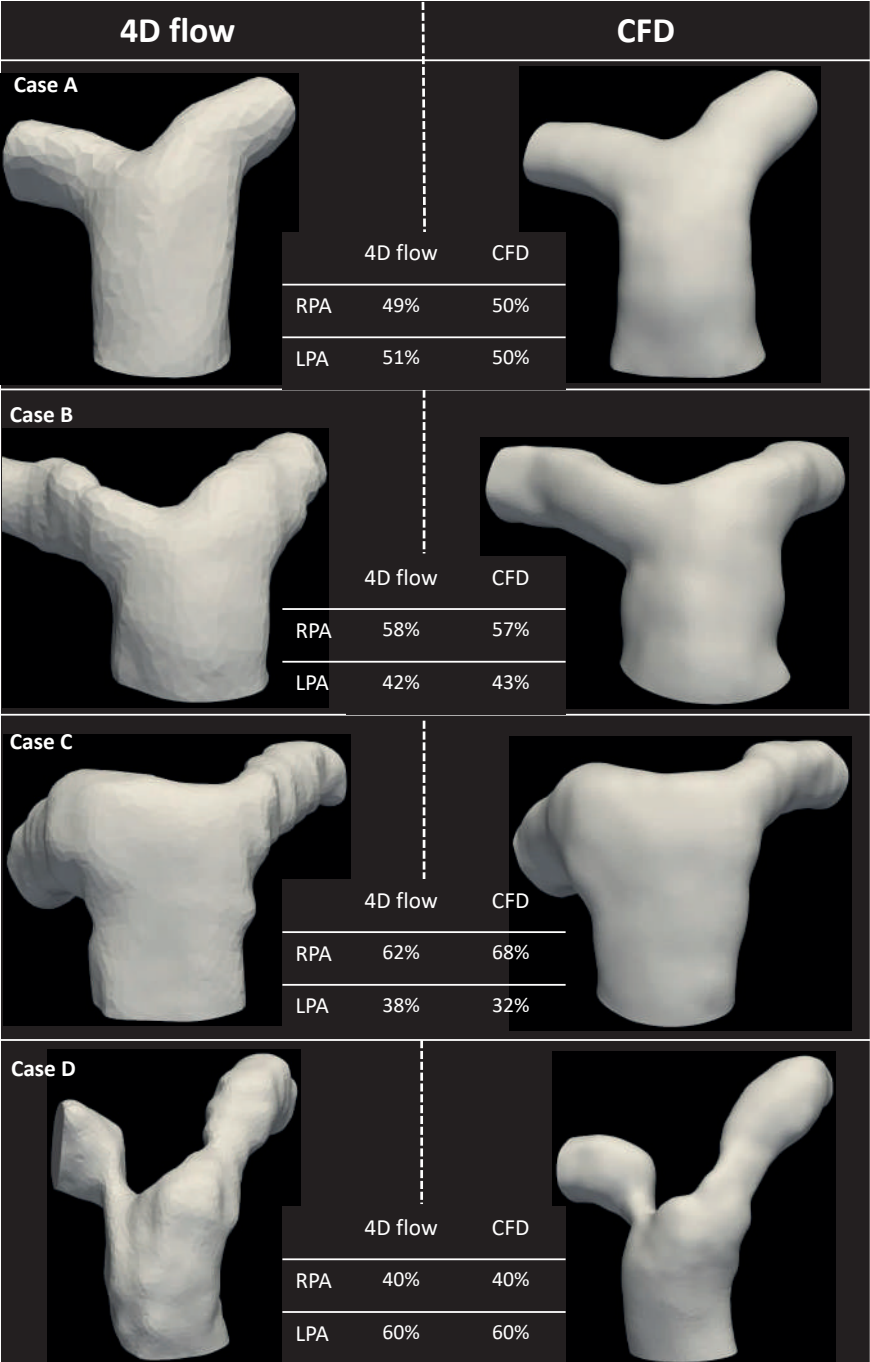


Figure 2. Mesh, inlet flow profiles and flow distributions for the right and left pulmonary arteries for all cases. 4D flow: four-dimensional flow CMR, CFD: computational fluid dynamics, LPA: left pulmonary artery, RPA: right pulmonary artery.

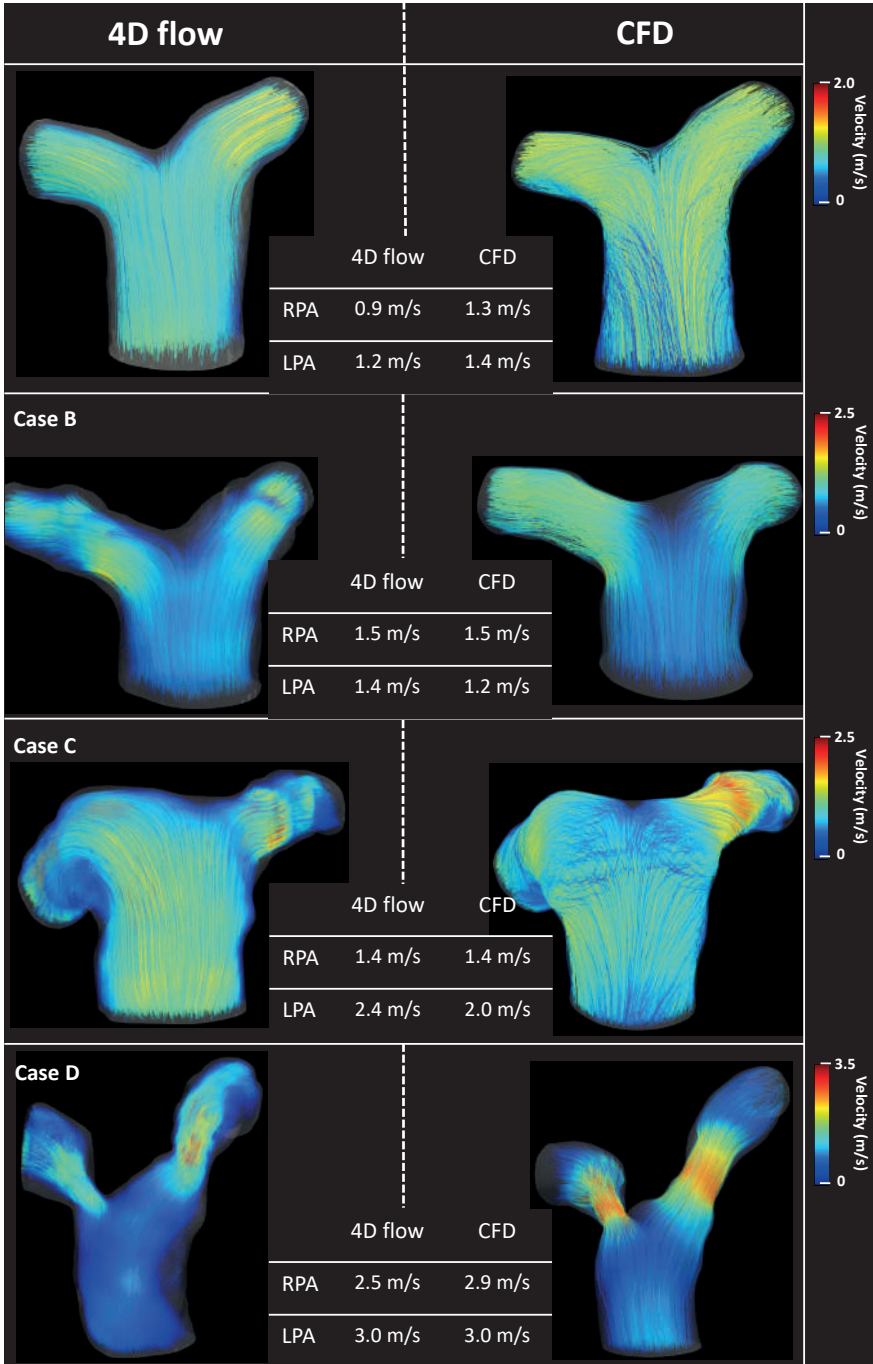


Figure 3. Visual assessment of flow patterns and flow velocities using color-coded streamlines and numerical comparison of the peak velocity in the right and left pulmonary arteries.

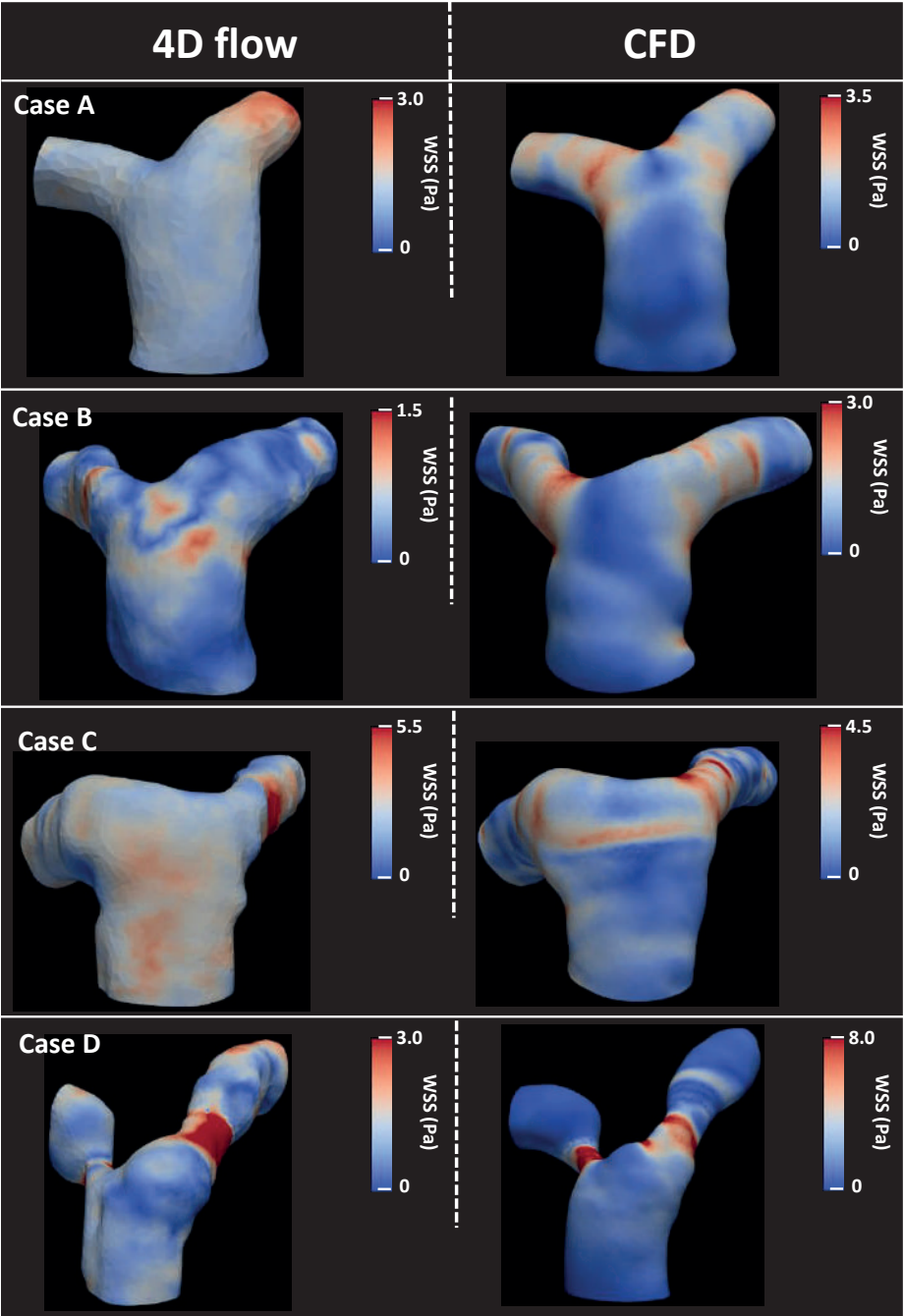


Figure 4. Visual and numerical assessment of wall shear stress as measured by four-dimensional flow cardiac magnetic resonance and computational fluid dynamics. The numerical values displayed represent the maximal values of wall shear stress in respectively the right- and left pulmonary artery.

Wall shear stress

The wall shear stress distribution in case C and D (branch pulmonary artery stenosis) was visually comparable (Figure 4). In both cases, the areas with high wall shear stress values were similar for both CMR and CFD. The absolute values of the peak wall shear stress located in the stenotic areas differed up to tenfold between 4D flow CMR and CFD. In patients without branch stenosis (case A and B), larger differences in wall shear stress distribution were found between CFD and 4D flow. In the control subject (A), CMR identified a region with high wall shear stress in the left pulmonary artery, whereas CFD analyses calculated high wall shear stress in the bifurcation and ostia of the right and left pulmonary artery. The maximal wall shear stress was twice as high in the CFD results when compared to the 4D flow CMR measurements. 4D flow CMR showed a maximal wall shear stress of 3 Pa in both cases A and D. In case D, CFD results gave a maximal wall shear stress almost three times higher for the stenotic case (case D) as compared to case A.

DISCUSSION

CFD and 4D flow CMR are emerging imaging modalities for haemodynamic evaluation of patients with congenital heart disease. To the best of our knowledge, this was the first study to compare results of flow analysis using CFD and 4D flow CMR in normal and diseased pulmonary arteries. The main findings of this study are:

1. CFD and 4D flow CMR demonstrate good agreement for absolute values of peak velocities and flow distribution in the pulmonary arteries.
2. Flow patterns within the pulmonary arteries, visually assessed using color-coded streamlines, were comparable for CFD and 4D flow CMR.
3. Although CFD and 4D flow CMR display similar distribution areas of increased wall shear stress, absolute values of wall shear stress are consistently lower by 4D flow CMR.

Peak velocities and flow distribution

Peak velocities and flow distribution are of great importance in the clinical evaluation of pulmonary artery branch stenosis. In clinical practice, peak velocities are obtained using Doppler echocardiography or two-dimensional phase-contrast CMR (2D PC CMR). Both modalities use a single plane for measurements in the region of interest and thus may not provide an accurate peak velocity measurement. Furthermore, the limited acoustic window in older or obese children and adults can make visualization and velocity measurements of the branch pulmonary arteries can be a challenge or even

impossible. Previous research has clearly shown that 2D PC CMR often underestimates peak velocities in the pulmonary artery branches of transposition of the great arteries patients, thereby underestimating the number of transposition of the great arteries patients suitable for intervention.¹⁸

The distribution of flow between the right and left pulmonary artery and the degree of perfusion mismatch between the left and right lung is also an important measure for pulmonary artery branch stenosis, as a substantial perfusion mismatch might be an indication for intervention. Reduction of ipsilateral lung perfusion to < -35% is considered a reason for intervention of the stenosed pulmonary artery branch.¹⁹ The ability to assess the entire volume of the pulmonary arteries is therefore key and 2D-PC CMR often underestimates the individual flow of the affected branch pulmonary artery. For the cases described in this study, results from CFD analyses and 4D flow CMR were comparable for peak velocities and flow distribution in the pulmonary artery branches, suggesting that both modalities are suitable for clinical evaluation of pulmonary artery branch peak velocities and flow distribution.

Flow patterns within the pulmonary arteries

Due to the unlimited spatial and temporal resolution, CFD provides excellent visualization of secondary flow phenomena and flow behaviour close to the arterial wall. In contrast, the relatively low spatial resolution of 4D flow CMR results in less accurate capture of flow patterns close to the arterial wall and secondary flow phenomena. With 4D flow CMR, substantial areas of low velocities close to the wall are depicted with underestimation of flow velocities in highly stenotic branches, exemplified by case D (transposition patient with bilateral pulmonary artery stenosis). In case A (normal pulmonary arteries) and case C (unilateral pulmonary artery branch stenosis), CFD clearly demonstrated secondary flow phenomena close to the arterial wall. Due to the high density of the mesh close to the wall, CFD is able to capture these complex flow patterns. In 4D flow CMR the velocity in the area of the vessel wall is set to zero to allow for WSS values calculation. Due to the low spatial resolution of CMR, this results in a relatively large area of zero velocity close to the arterial wall. This makes it impossible for 4D flow CMR to accurately capture flow behaviour in the direct vicinity of the arterial wall.

The results of a patient-specific CFD analysis are highly dependent on the quality of the 3D reconstruction of the anatomy. CFD therefore always depends on the spatial and temporal resolution of the imaging techniques available and the quality of the segmentation performed. Even small differences in geometry used for the CFD analysis can have great impact the numerical outcomes. In our study, the pulmonary arteries were segmented using the 3D non-contrast CMR (spatial resolution 0.92 x 0.92 x 2

mm) rather than the 4D flow CMR (spatial resolution 2.5 x 2.5 x 2.5 mm). By using the higher spatial resolution source for the anatomic reconstruction, the accuracy of the numerical outcomes was improved. However, the 3D non-contrast CMR represented the end-diastolic anatomy and the 4D flow CMR the peak-systolic anatomy. Although a compliant vessel was used for numerical analyses, differences in velocity and wall shear stress results, i.e. in case A (normal pulmonary arteries) and case C (unilateral pulmonary artery stenosis), might be explained by differences between the *in silico* and *in vivo* anatomy and the different expansion of the *in silico* arterial wall as compared to the *in vivo* arterial wall.

Wall shear stress

The overall wall shear stress distribution in the two stenotic patients was comparable. However, numerical analysis gave higher absolute values when compared to the 4D flow measurements. Since wall shear stress calculations are based on the velocity gradient, this difference is most likely explained by the lower spatial resolution of 4D flow CMR and, consequently, the limited number of measurements near the wall. Besides the lower spatial resolution of the 4D flow CMR, the lower temporal resolution also influences the wall shear stress results. The temporal resolution of 4D flow CMR was between 33 and 46 ms. In contrast, the temporal resolution of CFD is more than one order of magnitude higher at approximately 1 ms. The 4D flow CMR velocity measurements are therefore averaged over a longer period resulting in lower absolute values of wall shear stress calculations. As a consequence, even small differences of the velocity measurements near the wall have great impact on wall shear stress calculations. Previous studies comparing wall shear stress in the aorta and carotid arteries have shown similar results, with comparable wall shear stress patterns between 4D flow CMR and CFD, but with 4D flow CMR consequently underestimating the absolute values of the wall shear stress.²⁰⁻²³

Both CFD and 4D flow CMR show great potential for visualization and quantification of often-complex haemodynamics in congenital heart disease. Currently 4D flow CMR is the only modality able to measure blood flow in all spatial directions *in vivo* without invasive measurements or radiation burden. 4D flow CMR is therefore ideally suited for patients whose cardiovascular anatomy is yet unknown, and in patients with an abnormal aortic (bicuspid) or pulmonary valves, the presence of collateral vessels, or dissection of a vascular wall. Four-dimensional flow CMR does not allow for flow evaluation in patients with stents or pacemakers due to flow artefacts. Also, the low spatial and temporal resolution limits the application in patients with severe stenosis or in small children. CFD has a wide range of applications due to its unlimited spatial and temporal resolution and the possibility for exercise simulation and virtual treatment

planning. Furthermore, it is not hampered by artefacts created by stent and pacemakers. However, as CFD is a simulation, it is always an approximation of reality and the reliability of the outcomes greatly depend on the accuracy of the boundary conditions and the reconstructed anatomy. Therefore, both modalities could be used complementary in the clinical evaluation of flow in patients with pulmonary artery stenosis. Four-dimensional flow CMR is able to provide initial flow and anatomy assessment in patients with clinical suspicion of pulmonary artery pathology and pathological valves. It also offers the patient-specific boundary conditions necessary for an accurate numerical analysis. CFD is then able to perform in-depth flow analysis in patients with severe stenosis or stents in situ, and enables exercise assessment and patient-specific virtual treatment planning.

LIMITATIONS

There are several limitations that need to be taken into account for this study. First, only four cases were evaluated, of which only two cases had significant pulmonary artery branch stenosis. A larger group size is required for further statistical comparison of the results. Second, for analysis of flow patterns, peak velocities, and wall shear stress distribution, only measurements for the peak-systolic phase were taken into account, disregarding the rest of the systole and the complete diastole. Third, no interobserver comparison was performed, segmentations were performed by only one experienced observer (MC: CFD, EW: 4D flow CMR). Segmentation and analysis by multiple observers could have made the results more robust. Last, although patient-specific mass flow, waveform and heart frequency were used as inlet boundary conditions, generic values were used for the inlet velocity profile and compliance of the vessel. Due to the exploratory nature of this study and limitations of the software, we were unable to align two-dimensional phase-contrast flow acquisitions or 4D flow acquisitions of the vessel inlet with the segmentations of the anatomy made for the numerical analysis. Therefore it was impossible to use patient-specific inlet velocity profiles. Since all of the presented cases had normal functioning valves, this probably did not influence our results. However, in case of valvular regurgitation or an anatomically abnormal valve, thus abnormal inlet profiles, patient-specific velocity profiles will likely be necessary to achieve comparable results.

CONCLUSION

CFD and 4D flow CMR provide comparable results in evaluation of peak velocities, flow distribution, flow patterns and wall shear stress distribution for patients with and without pulmonary artery branch stenosis. Absolute wall shear stress values were consistently lower for 4D flow CMR. More research is warranted in larger patients groups to identify the prognostic value and clinical application of both imaging techniques.

REFERENCES

1. Hoffman JL, Kaplan S. The incidence of congenital heart disease. *J Am Coll Cardiol* 2002;12:1890-900.
2. Oster ME, Lee KA, Honein MA, et al. Temporal trends in survival among infants with critical congenital heart defects. *Pediatrics* 2013;5:1502-8.
3. Vanderlaan RD, Caldarone CA, Backx PH. Heart failure in congenital heart disease: the role of genes and hemodynamics. *Eur J Physiol* 2014;466:1025.
4. Boccadifuoco, A. Mariotti, S. Celi, N. Martini, M.V. Salvetti, Impact of uncertainties in outflow boundary conditions on the predictions of hemodynamic simulations of ascending thoracic aortic aneurysms. *Computers & Fluids* 2018;165:96-115.
5. DeCampi, W., Argueta-Morales, I., Divo, E., & Kassab, A. Computational fluid dynamics in congenital heart disease. *Cardiology in the Young* 2012;6, 800-808.
6. Markl M, Harloff A, Bley TA, et al. Time-resolved 3D MR velocity mapping at 3T: improved navigator-gated assessment of vascular anatomy and blood flow. *J Magn Reson Imaging* 2007;4:824-831.
7. Uribe S, Beerbaum P, Sørensen TS, et al. Four-dimensional (4D) flow of the whole heart and great vessels using real-time respiratory self-gating. *Magn Reson Med* 2009;4:984-992.
8. Sierra-Galan, L.M., François, C.J. Clinical Applications of MRA 4D-Flow. *Curr Treat Options Cardio Med* 2019;21:58.
9. Sotelo J, Mura J, Hurtado D, Uribe S. A novel MATLAB Toolbox for processing 4D Flow MRI data. *Proc Intl Soc Mag Reson Med* 2019;27:1956
10. Sotelo J, Urbina J, Valverde I, et al. 3D Quantification of Wall Shear Stress and Oscillatory Shear Index Using a Finite-Element Method in 3D CINE PC-MRI Data of the Thoracic Aorta. *IEEE Trans Med Imaging* 2016;6:1475-87.
11. Sotelo J, Urbina J, Valverde I, et al. Three-dimensional quantification of vorticity and helicity from 3D cine PC-MRI using finite-element interpolations. *Magn Reson Med* 2018;1:541-553.
12. Sotelo J, Dux-Santoy L, Guala A, Rodríguez-Palomares J, et al. 3D axial and circumferential wall shear stress from 4D flow MRI data using a finite element method and a laplacian approach. *Magn Reson Med* 2018;5:2816-2823.
13. Bock J, Frydrychowicz A, Stalder AF et al. 4D phase contrast MRI at 3 T: effect of standard and blood-pool contrast agents on SNR, PC-MRA, and blood flow visualization. *Magn Reson Med* 2010;2:330-8
14. Qianqian F, Boas DA. 2009. Tetrahedral Mesh Generation from Volumetric Binary and Gray-Scale Images. In Proceedings of the 6th IEEE International Conference on Symposium on Biomedical Imaging: From Nano to Macro, Boston, Massachusetts, USA: 1142-1145.
15. Conijn M, Krings GJ. Understanding stenotic pulmonary arteries: can computational fluid dynamics help us out?
16. Huang W, Yen RT. Zero-stress states of human pulmonary arteries and veins. *J Appl Physiol* 1985;3:867-73.

17. Ayachit, Utkarsh, *The ParaView Guide: A Parallel Visualization Application*, Kitware, 2015, ISBN 978-1930934306
18. Jarvis K, Vonder M, Barker AJ, et al. Hemodynamic evaluation in patients with transposition of the great arteries after the arterial switch operation: 4D flow and 2D phase contrast cardiovascular magnetic resonance compared with Doppler echocardiography. *J Cardiovasc Magn Reson* 2016;1:59.
19. Timothy F. Feltes, Emile Bacha, Robert H. Beekman et al. *Indications for Cardiac Catheterization and Intervention in Pediatric Cardiac Disease* 2011;123:2607-2652.
20. Isoda H, Ohkura Y, Kosugi T, et al. Comparison of hemodynamics of intracranial aneurysms between MR fluid dynamics using 3D cine phase-contrast MRI and MR-based computational fluid dynamics. *Neuroradiology* 2010;10:913-20.
21. Sjaizer J, Ho-Shon K. A comparison of 4D flow MRI-derived wall shear stress with computational fluid dynamics methods for intracranial aneurysms and carotid bifurcations - A review. *Magn Reson Imaging* 2018;48:62-69.
22. Miyazaki S, Itatani K, Furusawa T, et al. Validation of numerical simulation methods in aortic arch using 4D Flow MRI. *Heart Vessels*. 2017;8:1032-1044.
23. Cibis M, Potters WV, Gijzen FJH, et al. Wall shear stress calculations based on 3D cine phase contrast MRI and computational fluid dynamics: a comparison study in healthy carotid arteries. *NMR Biomed* 2014;7:826-34.



Chapter 9

Head-to-head comparison of 4D flow CMR, 2D phase-contrast CMR and Doppler echocardiography for the detection of pulmonary artery stenosis in patients after the arterial switch operation

Evangeline G. Warmerdam

Jos J.M. Westenberg

Michiel Voskuil

Hans C. van Assen

Friso M. Rijnberg

Arno A.W. Roest

Hildo J. Lamb

Bram van Wijk

Gertjan Tj. Sieswerda

Pieter A.F. Doevendans

Henriette ter Heide

Gregor J. Krings

Tim Leiner

Heynric B. Grotenhuis

Submitted

ABSTRACT

Background. Pulmonary artery (PA) stenosis is the most common complication after the arterial switch operation (ASO) for transposition of the great arteries (TGA). Four-dimensional flow CMR provides the ability to quantify flow and velocities within an entire volume instead of a single plane. The aim of this study was to compare PA maximum velocities and stroke volumes between 4D flow CMR, two-dimensional phase-contrast (2D PC CMR) and echocardiography.

Methods. A prospective study including TGA patients after ASO was performed between December 2018 and October 2020. All patients underwent echocardiography and CMR, including 2D PC and 4D flow acquisition. Maximum velocities and stroke volumes were measured in the main, right, and left PA.

Results. A total of 39 patients aged 20 ± 8 years were included. Maximum velocities in the main, left, and right PA measured by 4D flow CMR were significantly higher compared to 2D PC CMR ($p < 0.001$ for all). PA assessment by echocardiography was not possible in the majority of patients. 4D flow CMR maximum velocity measurements were consistently higher than those by 2D PC CMR with a mean difference of 65 cm/s for the main PA, and 77 cm/s for both the right and left PA. Stroke volumes showed good agreement between 4D flow and 2D PC CMR.

Conclusion. Maximum velocities in the PAs after ASO for TGA are consistently lower by 2D PC CMR, while echocardiography only allows for PA assessment in a minority of cases. Stroke volumes showed good agreement between 4D flow and 2D PC CMR.

INTRODUCTION

Transposition of the great arteries (TGA) is a common cyanotic congenital heart defect (CHD), accounting for 5-8% of all CHD.¹ In TGA, the aorta arises from the right ventricle (RV) and the pulmonary artery from the left ventricle, for which the arterial switch operation (ASO) combined with the LeCompte manoeuvre is standard of care.² Although the ASO results in an excellent survival rate, frequent complications occur such as dilation of the ascending aorta and pulmonary artery stenosis (PS).² Branch PS is the most common cause for reintervention after ASO, with an incidence of up to 20% of ASO patients.^{2,3} Stretching of the pulmonary arteries with the LeCompte manoeuvre, dynamic systolic compression due to the close anatomical relationship with an often dilated ascending aorta, scar formation at the anastomosis site and atherosclerosis due to altered shear stress distribution are all thought to cause PS after ASO.⁴ Frequent and robust non-invasive evaluation of the pulmonary arteries is therefore crucial for appropriate follow-up of these patients.

Standard non-invasive haemodynamic evaluation of the pulmonary arteries after ASO is currently performed with Doppler echocardiography and two-dimensional phase-contrast cardiovascular magnetic resonance (2D PC CMR).⁵ Flow assessment with 2D PC CMR relies on measurements from a single fixed imaging plane and thus may not give an accurate representation of the peak velocity or flow volume in the vessel if not appropriately aligned with the blood vessel. Although echocardiography has the benefit of a high temporal resolution for peak velocity measurements, it is greatly dependent on the acoustic window, which can make visualization of the branch pulmonary arteries challenging or even impossible, especially in older children and adults.

Four-dimensional flow CMR (4D flow CMR) provides the opportunity for quantification of flow in an entire volume throughout the complete cardiac cycle. Previous studies have demonstrated that 4D flow CMR is a reliable tool for flow and velocity measurements.^{6,7} 4D flow CMR may therefore provide a more comprehensive evaluation of the presence and severity of local or even multilevel PS than Doppler echocardiography or 2D PC CMR, as the complete region of the pulmonary arteries can be assessed within a single imaging session. The aim of this study was therefore to compare maximum velocities and stroke volumes measured by 4D flow CMR with 2D PC CMR and Doppler echocardiography in TGA patients after ASO.

METHODS

Population

For this study TGA patients after ASO aged between 8 to 40 years were prospectively recruited between December 2018 and September 2020. Exclusion criteria were presence of a stent in the pulmonary arteries, presence of a cardiac pacemaker and all other contra-indications for CMR, including claustrophobia and pregnancy. Patients underwent CMR according to the routine TGA protocol of our centre, with the addition of 4D flow CMR. Routine echocardiography was preferably performed on the same day as CMR. Written informed consent was obtained for all patients and/or their guardians (for patients under 16 years of age). This study was approved by the local Medical Ethical Committee (study number 18-200).

CMR acquisition

CMR imaging was performed on a 3.0 T scanner (Ingenia R5.6.1, Philips Healthcare, Best, The Netherlands). Velocity encoded 2D PC CMR scans with ECG-triggering and a single breath-hold were acquired for the main PA (MPA), left PA (LPA) and right PA (RPA). The plane was positioned at the site where the vessel diameter was considered the narrowest, which was assessed visually on axial and coronal views. Imaging parameters for the 2D PC CMR were as follows: spatial resolution = $1.25 \times 1.25 \text{ mm}^2$, FOV = $320 \times 320 \text{ mm}^2$, slice thickness: 5 mm, number of cardiac phases: 25, echo time = 2.8 – 3.4 ms, repetition time = 4.9 – 5.5 ms, flip angle = 10° , bandwidth = 479 Hz/pixel, venc = 180–350 cm/s. Scan times were typically around one minute per scan. All scans were checked for velocity-aliasing directly after the end of each scan and repeated with altered venc if necessary.

4D flow CMR acquisition was performed with prospective ECG and respiratory navigator-gating. The acquired volume covered the entire MPA, LPA and RPA. Imaging parameters for the 4D flow CMR were as follows: spatial resolution = $2.5 \times 2.5 \times 2.5 \text{ mm}^3$, FOV = $300 \times 300 - 350 \times 350 \text{ mm}^2$, temporal resolution = 32.8 – 46.1 ms, echo time = 2.1 – 2.5 ms, repetition time = 3.9 – 4.5 ms, flip angle = 10° , venc = 200–450 cm/s, TFE factor 3, SENSE: 2.5 (AP) and 1.5 (RL). Concomitant gradient correction and local phase correction were performed using standard available scanner software. Scan times were typically 8 – 12 minutes per scan.

CMR post-processing

Post-processing for 2D PC acquisitions was performed with 2D PC software (CAAS MR Solutions, version 5.0-5.1, Pie Medical Imaging, Maastricht, the Netherlands). The

region of interest was manually segmented by one observer (EW). From these regions of interest, peak velocity, forward flow and regurgitant flow were collected. Stroke volume was defined as forward flow minus regurgitant flow and calculated for the MPA, LPA, and RPA.

4D flow data was processed using automatic background and velocity aliasing correction (CAAS MR Solutions, version 5.0-5.1, Pie Medical Imaging, Maastricht, the Netherlands). If aliasing artefacts could not be corrected, patients were excluded from this study. In case of minimal aliasing (defined as one or two voxels), the measurements were performed in the next plane without artefacts. Segmentation of the vessel was performed automatically, and subsequent manual correction was done by a single observer with two years of experience in arterial segmentation of 4D flow scans (EW). Maximum velocity regions were determined by retrospective placement of 2D planes at the region of suspected maximum velocity, which was determined visually using color-coded streamlines visualization and velocity overlay for the region of interest within the plane. The plane was repositioned until the region with the maximum velocity was identified. For the regions of interest, peak velocity, forward flow and regurgitant flow were collected and stroke volumes were calculated. Aliasing correction was validated using flow mapping in a region proximal and distal to the plane and comparing the flow to the flow in the plane of interest.

Echocardiography

Echocardiography was performed by an experienced cardiac sonographer using General Electric (GE Healthcare, Wauwatosa, Wisconsin, USA) ultrasound systems, using the optimal transducer for patient size. Parameters collected for this study were maximum instantaneous velocities from Doppler images for the MPA, LPA and RPA.

Statistical analyses

Statistical analysis was performed using R version 3.6.3⁸, and figures were produced using the package ggplot2.⁹ All data were assessed for normality using histograms, QQ-plots and the Shapiro-Wilk test. The paired Student's t-test or Wilcoxon matched-paired signed rank test was used to compare measurements from the different modalities, depending on data distribution (normal or non-normal). Agreement between the different modalities was assessed using Bland-Altman analyses. To assess the proportion of patients with PS in our cohort, we dichotomized patients into two groups based on the peak velocities measured in the RPA and LPA. A peak velocity > 250 cm/s was classified as clinically relevant PS; a lower peak velocity was considered to be normal. Results were considered statistically significant in case of a probability value (p-value) of < 0.05.

RESULTS

A total of 45 patients were included between December 2018 and October 2020. Four patients were excluded from analysis due to insufficient quality of the 4D flow CMR acquisition, due to severe aliasing which could not be corrected or motion artefacts. Two patients were excluded due to severe aliasing in the 2D PC CMR scan. Thus, data for 39 patients were analysed with a mean age of 20 ± 8 years. Median age at ASO was 8 (IQR: 7 - 12) days. The most common concomitant cardiac defect was a ventricular septal defect, present in 10 (26%) patients. One patient had undergone aortic valve replacement for severe aortic valve regurgitation, and one had undergone surgery for branch PA stenosis. All baseline characteristics are presented in Table 1.

Table 1. Baseline characteristics.

Characteristic	
Age (years)	20 ± 8
Male	31 (79%)
Height (cm)	171 ± 16
Weight (kg)	64 ± 22
Body mass index (kg/m^2)	22 ± 5
Age at arterial switch operation (days)	7 (IQR: 8 - 12)
<i>Concomitant cardiac defect</i>	
Aberrant coronary artery	2 (5%)
Atrial septal defect	4 (10%)
Bicuspid aortic valve	1 (3%)
Coarctation of the aorta	4 (10%)
Hypoplastic aortic arch	1 (3%)
Ventricular septal defect	10 (26%)
<i>Reintervention</i>	
Aortic valve replacement	1 (3%)
Pulmonary artery plasty	1 (3%)
None	37

Data are presented as number (percentage), mean \pm standard deviation or median (interquartile range).

Median time between CMR and echocardiography examinations was 20 (IQR: 0 – 69) days. For Doppler echocardiography, velocity measurements of the MPA were not available for 18 patients, for the RPA in 24 patients, and for the LPA in 23 patients. CMR and echocardiography demonstrated preserved biventricular function in all but two patients (LVEF was 49% for these two patients). Mean LVEF was $56 \pm 5\%$ and a mean RVEF was $56 \pm 5\%$ on CMR, mean TAPSE was 19 ± 3 mm on echocardiography. All data on biventricular function is presented in Table 2.

Table 2. Cardiac magnetic resonance and echocardiography parameters on biventricular function.

Imaging parameter	
LVEDV _i (ml/m ²)	108 ± 25
LVESV _i (ml/m ²)	48 ± 14
LVSV _i (ml/m ²)	60 ± 13
LVEF (%)	56 ± 5
LVCQ _i (L/m ²)	4.3 ± 0.8
RVEDV _i (ml/m ²)	102 ± 19
RVESV _i (ml/m ²)	45 ± 11
RVSV _i (ml/m ²)	60 ± 18
RVEF (%)	56 ± 5
RVCO _i (ml/m ²)	4.1 ± 0.7
TAPSE (mm)	19 ± 3

i: indexed for body surface area, LVCQ: left ventricular cardiac output, LVEDV: left ventricular end-diastolic volume, LVEF: left ventricular ejection fraction, LVESV: left ventricular end-systolic volume, LVSV: left ventricular stroke volume, RVCO: right ventricular cardiac output, RVEDV: right ventricular end-diastolic volume, RVEF: right ventricular ejection fraction, RVESV: right ventricular end-systolic volume, RVSV: right ventricular stroke volume. Data are presented as mean ± standard deviation.

Maximum velocities as measured by 4D flow CMR were significantly higher compared to 2D PC CMR measurements in the MPA, RPA and LPA ($p < 0.001$ for all, respectively) (Table 3, Figure 1). There was no significant difference between maximum velocities as measured by 4D flow CMR and by Doppler echocardiography (Table 4). Bland-Altman plots (Figure 2) showed 4D flow CMR peak velocity measurements were consistently higher than those by 2D PC CMR with a mean difference of 65 cm/s for the MPA and a mean difference of 77 cm/s for both the RPA and LPA. Bland-Altman plots comparing peak velocity measurements by 4D flow CMR and echocardiography (Figure 2) showed good agreement with a mean difference of 11 cm/s for the MPA, 18 cm/s for the RPA, and 27 cm/s for the LPA.

Table 3. Comparison of maximum velocities between four-dimensional flow cardiac magnetic resonance and two-dimensional phase contrast cardiac magnetic resonance.

Location	Peak velocity 4D (cm/s)	Peak velocity 2D (cm/s)	p-value
MPA	197 (169 – 244)	135 (118 – 162)	< 0.001
RPA	229 (180 – 274)	154 (124 – 188)	< 0.001
LPA	230 (201 – 305)	166 (145 – 203)	< 0.001

Data are presented as median (interquartile range). 2D: two-dimensional, 4D: four-dimensional, MPA: main pulmonary artery, LPA: left pulmonary artery, RPA: right pulmonary artery.

Table 4. Comparison of maximum velocities between four-dimensional flow cardiac magnetic resonance and Doppler echocardiography.

Location	Peak velocity 4D (cm/s)	Peak velocity echo (cm/s)	p-value
MPA (n=21)	195 (154 – 235)	170 (135 – 222)	0.394
RPA (n=15)	224 (187 – 255)	200 (165 – 240)	0.277
LPA (n=16)	226 (173 – 277)	200 (160 – 238)	0.065

Data are presented as median (interquartile range). 2D: two-dimensional, 4D: four-dimensional, MPA: main pulmonary artery, LPA: left pulmonary artery, RPA: right pulmonary artery.

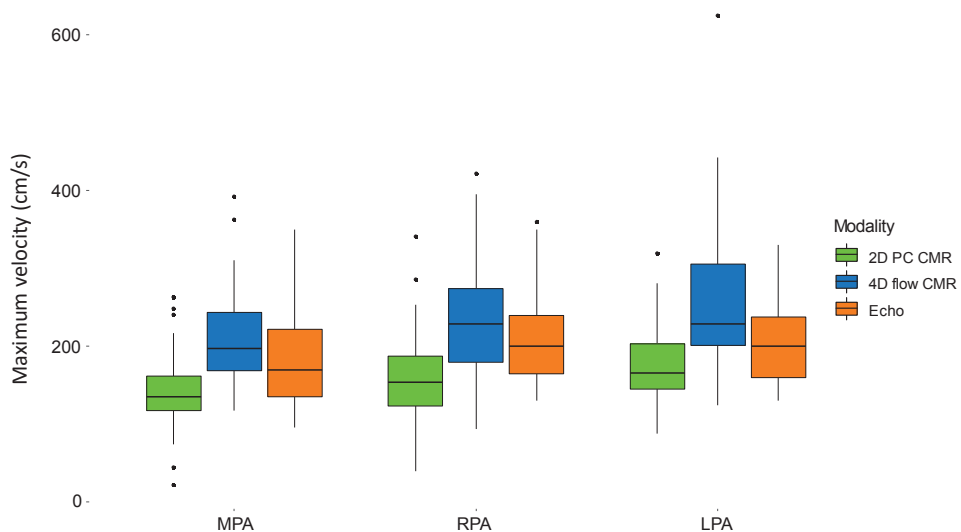


Figure 1. Comparison of maximum velocities in the main, right, and left pulmonary artery as measured by two-dimensional flow phase-contrast cardiac magnetic resonance, four-dimensional flow cardiac magnetic resonance and Doppler echocardiography. 2D PC CMR: two-dimensional phase-contrast cardiac magnetic resonance, 4D flow CMR: four-dimensional flow cardiac magnetic resonance, MPA: main pulmonary artery, LPA: left pulmonary artery, RPA: right pulmonary artery.

We dichotomized patients into two groups based on the maximum velocities measured in the RPA and LPA; a peak velocity > 250 cm/s was classified as clinically relevant PS, a lower peak velocity was considered to be normal. 4D flow measurements identified a substantially higher number of patients with PS than 2D PC CMR measurements. For the LPA, 14 patients (36%) were identified as having PS based on 4D flow measurements, versus only 2 patients (5%) based on 2D PC CMR measurements. Similarly, 14 patients (36%) had PS of the RPA based on 4D flow measurements, compared to only 3 patients (8%) based on 2D PC CMR measurements.

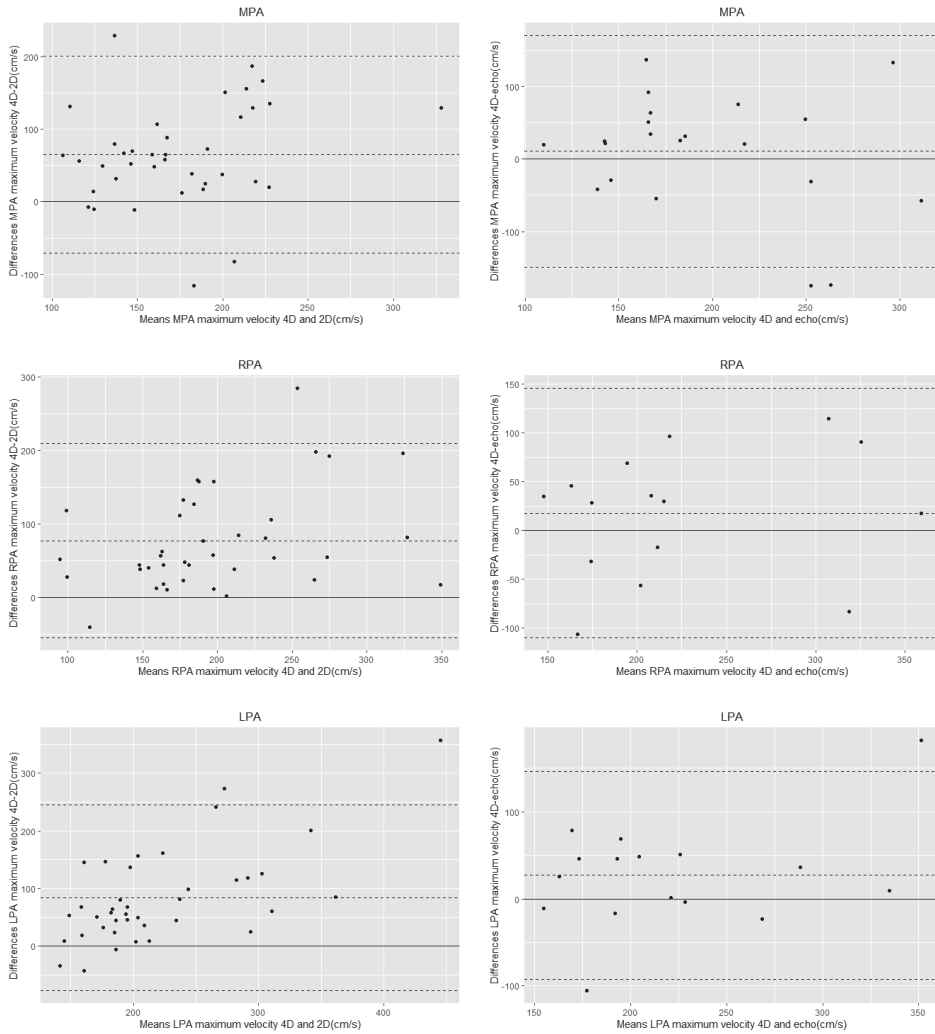


Figure 2. Agreement between four-dimensional flow cardiac magnetic resonance and two-dimensional phase-contrast cardiac magnetic resonance and agreement between four-dimensional flow cardiac magnetic resonance and Doppler echocardiography for measurement of maximum velocities in the main, right, and left pulmonary artery. 2D: two-dimensional phase-contrast cardiac magnetic resonance, 4D: four-dimensional flow.

Stroke volumes measured by 4D flow CMR were not significantly different when compared to 2D PC CMR in the MPA, LPA and RPA. (Table 5). Bland-Altman plots (Figure 4) showed good agreement between 4D flow CMR and 2D PC CMR measurements of flow volumes, with a mean difference of -1.8 ml for the MPA, 3.1 ml for the RPA, and 3.8 ml for the LPA.

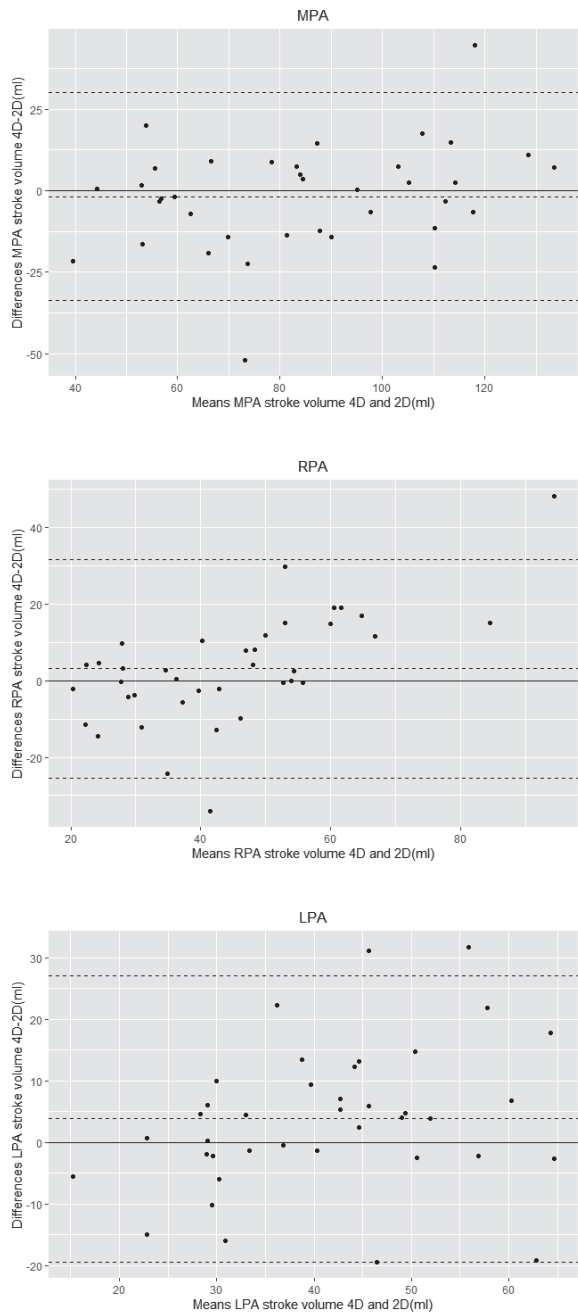


Figure 3. Agreement between four-dimensional flow cardiac magnetic resonance and two-dimensional phase-contrast cardiac magnetic resonance for measurement of stroke volumes (forward flow – regurgitant flow) in the main, right, and left pulmonary artery. 2D: two-dimensional phase-contrast cardiac magnetic resonance, 4D: four-dimensional flow cardiac magnetic resonance, MPA: main pulmonary artery, LPA: left pulmonary artery, RPA: right pulmonary artery.

Table 5. Comparison of stroke volumes (forward – regurgitant flow) between four-dimensional flow cardiac magnetic resonance and two-dimensional phase-contrast cardiac magnetic resonance.

Location	Stroke volume 4D (ml)	Stroke volume 2D (ml)	p-value
MPA	85 ± 29	85 ± 24	0.503
RPA	46 ± 22	43 ± 13	0.196
LPA	48 ± 24	43 ± 13	0.102

Data are presented as mean ± standard deviation. 2D: two-dimensional phase-contrast CMR, 4D: four-dimensional flow CMR, MPA: main pulmonary artery, LPA: left pulmonary artery, RPA: right pulmonary artery.

DISCUSSION

The goal of this study was to compare maximum velocities and stroke volumes in the PAs between 4D flow CMR, 2D PC CMR and Doppler echocardiography and conveys the following findings:

1. Maximum velocities measured by 4D flow CMR are significantly higher than maximum velocities measured by 2D PC CMR, but similar to maximum velocities by Doppler echocardiography.
2. Maximum velocities in the MPA and branch PAs could be evaluated in almost all TGA patients with 4D flow CMR and 2D PC CMR. In contrast, the branch PAs for the majority of TGA patients could not be visualized using echocardiography.
3. Stroke volumes measured by 2D PC CMR were not significantly different compared to stroke volumes measured by 4D flow CMR for the MPA and branch PAs.

We found 4D flow CMR to be superior to 2D PC CMR for identification of PS in our TGA study cohort. There are several reasons for the underestimation of the maximum velocities by conventional 2D PC CMR. First, the positioning of the 2D imaging planes was done based on visual assessment of the PAs and placed where the diameter was considered to be the narrowest. The peak velocity can only be measured in that specific plane, whereas 4D flow CMR provides the opportunity to measure maximum velocities along the entire length of the pulmonary vessel. Second, the 2D PC CMR plane is positioned by the operator based on 2D anatomical images and flow is measured in one direction: orthogonal to this plane. When the plane has not been positioned exactly perpendicular to the vessel, this can give an underestimation of the velocity magnitude.^{10,11} With 4D flow CMR, the plane for analysis can be positioned retrospectively and with use of three-dimensional anatomical data and visualization of the flow to ensure the plane is positioned exactly perpendicular to the vessel and the blood flow.

Last, since 2D PC CMR only measures flow in one direction, it does not take into account turbulent flow, which is often present in patients with CHD. With the three-dimensional velocity-encoding of 4D flow CMR, eccentric flow can be taken into account, resulting in higher maximum velocities.^{12,13}

To our knowledge, only one prior study compared maximum velocities as measured by 4D flow CMR, 2D PC CMR and Doppler echocardiography in patients after the arterial switch operation.¹² Jarvis et al. found significantly higher velocities using 4D flow CMR in the MPA and RPA, but not in the LPA, and no difference in maximum velocities between Doppler echocardiography and 4D flow CMR. Their results are thus partially in line with our results. However, there are important differences between our study population and theirs. Our population was considerably older: 20 ± 8 years (range 8 – 37 years) versus 13 ± 9 years (range: 1 – 25 years). Furthermore, we most likely included more patients with branch PS, as comparison of maximum velocities in our study versus Jarvis et al. revealed 2.1 ± 0.8 versus 1.8 ± 0.6 m/s for the RPA and 2.4 ± 1.0 versus 1.7 ± 0.5 m/s for the LPA. Since visualization of PAs on echocardiography becomes more difficult with increasing age, 4D flow CMR is especially suitable for older children and adults.

To assess the clinical impact of the haemodynamic evaluation of 4D flow CMR versus 2D PC CMR, we analysed the proportion of patients that would be classified as having PS in our centre based on peak velocity as measured by both modalities. When using 250 cm/s as the cut-off value for the diagnosis of substantial PS, we found an increase in the proportion of patients with PS when comparing 2D PC CMR with 4D flow CMR. Since there is no literature available on the cut-off value of significant stenosis in these patients, we chose the cut-off value generally used in our centre. Due to the lack of evidence on cut-off values, Jarvis et al. decided not to perform such an analysis.¹² Therefore, these results need to be interpreted with caution. Furthermore, since evidence for intervention for PS is lacking, the impact of our findings on (re)intervention in this patient group warrant further investigation.

We found no significant differences between maximum velocities measured by 4D flow CMR and Doppler echocardiography. However, in the majority of patients, the PAs could not be visualized using echocardiography. It is well known that the acoustic window severely limits the ability to visualize PAs in older children and adults, especially in patients after ASO, with a retrosternal position of the PAs.¹⁴ Echocardiography is often the imaging modality of choice for follow-up of these patients due to it being widely available, cost-effective and non-invasive. Based on the results of this study, 4D flow CMR should be considered when imaging quality of echocardiography is insufficient.

We found no significant difference in stroke volumes in the main and branch PAs when comparing 4D flow CMR and 2D PC CMR. Our results are in line with a previous study by Nordmeyer et al. in healthy volunteers and CHD patients, in which no differences were found when comparing flow volumes measured by 4D flow CMR and 2D PC CMR.¹⁵

In general, 4D flow CMR has several important advantages over 2D PC CMR for the evaluation of PS in patients after ASO: the ability to position planes of interest exactly perpendicular to the vessels at any point within the scanned volume, the fact that it has velocity encoding in all three spatial directions and the ability to visualize the blood flow. We believe that 4D flow CMR will be an important tool in the haemodynamic assessment of TGA patients after ASO, with a clear need for comprehensive serial evaluation of the cardiovascular system.

LIMITATIONS

There are several limitations that need to be taken into account for this study. First, the CMR and echocardiography were not always performed on the same day. We included echocardiography up to one year prior to CMR to limit the effect of development of PS over time. Second, 4D flow CMR has a limited spatial and temporal resolution, a relatively long acquisition time and time and skill required for post-processing.¹⁶ These limitations currently hamper widespread clinical implementation for the follow-up of patients after ASO, although recent improvements in CMR techniques have provided shorter acquisition times and more user-friendly postprocessing software.

CONCLUSION

This study shows that 4D flow CMR detects higher maximum velocities in the PAs of TGA patients when compared to 2D PC CMR, while echocardiography only allows for PA assessment in a minority of cases. In our cohort, a substantial number of patients would be classified as having PS based on 4D flow CMR measurements, in contrast to 2D PC CMR measurements. No differences were found between stroke volumes in the PAs measured by 4D flow CMR compared to 2D PC CMR.

REFERENCES

1. Brickner ME, Hillis LD, Lange RA. Congenital heart disease in adults. Second of two parts. *N Engl J Med* 2000;342:334–342.
2. Ruys TP, Van der Bosch AE, Cuypers JA, et al. Long term Outcome and quality of life after arterial switch operation: a prospective study with a historical comparison. *Congenit Heart Dis.* 2013;May-Jun;8(3):203-10
3. Choi BS, Kwon BS, Kim BG, et al. Long-Term Outcomes After an Arterial Switch Operation for Simple Complete Transposition of the Great Arteries. *Korean Circ J* 2010;Jan;40(1):23-30
4. Morgan CT, Mertens L, Grotenhuis H, Yoo SJ, Seed M, Grosse-Wortmann L. Understanding the mechanism for branch pulmonary artery stenosis after the arterial switch operation for transposition of the great arteries. *Eur Heart J Cardiovasc Imaging.* 2017;18(2):180-185. doi:10.1093/ehjci/jew046
5. Baumgartner H, De Backer J, Babu-Narayan SV, et al. 2020 ESC Guidelines for the management of adult congenital heart disease. *Eur Heart J.* 2020 Aug 29;ehaa554. doi: 10.1093/eurheartj/ehaa554.
6. Summers PE, Holdsworth DW, Nikolov HN, Rutt BK, Drangova M. Multisite trial of MR flow measurement: phantom and protocol design. *J Magn Reson Imaging.* 2005;21:620–31.
7. Van Ooij P, Powell AL, Potters WV, Carr JC, Markl M, Barker AJ. Reproducibility and interobserver variability of systolic blood flow velocity and 3D wall shear stress derived from 4D flow MRI in the healthy aorta. *J Magn Reson Imaging.* 2016;43:236–48.
8. R Core Team (2020). R: A language and environment for statistical computing. R Foundation for Statistical Computing, Vienna, Austria. URL <https://www.R-project.org/>
9. Wickham H (2016). *ggplot2: Elegant Graphics for Data Analysis*. Springer-Verlag New York. ISBN 978-3-319-24277-4, <https://ggplot2.tidyverse.org>
10. Gabbour M, Schnell S, Jarvis K, et al. 4-D flow magnetic resonance imaging: blood flow quantification compared to 2-D phase-contrast magnetic resonance imaging and Doppler echocardiography. *J Cardiovasc Magn Reson.* 2016 Sep 22;18(1):59. doi: 10.1186/s12968-016-0276-8.
11. Rose MJ, Jarvis K, Chowdhary V, et al. Efficient method for volumetric assessment of peak blood flow velocity using 4D flow MRI. *J Magn Reson Imaging.* 2016. doi:10.1002/jmri.25305.
12. Jarvis K, Vonder M, Barker AJ, et al. Hemodynamic evaluation in patients with transposition of the great arteries after the arterial switch operation: 4D flow and 2D phase contrast cardiovascular magnetic resonance compared with Doppler echocardiography. *J Cardiovasc Magn Reson.* 2016 Sep 22;18(1):59. doi: 10.1186/s12968-016-0276-8.
13. Sieren MM, Berlin C, Oechtering TH, et al. Comparison of 4D Flow MRI to 2D Flow MRI in the pulmonary arteries in healthy volunteers and patients with pulmonary hypertension. *PLoS One.* 2019; 14(10): e0224121. doi: 10.1371/journal.pone.0224121

14. Gutberlet M, Boeckel T, Hosten N, et al. Arterial switch procedure for D-transposition of the great arteries: quantitative midterm evaluation of hemodynamic changes with cine MR imaging and phase-shift velocity mapping-initial experience. *Radiology*. 2000 Feb; 214(2):467-75.
15. Nordmeyer S, Riesenkampff E, Crelier G, Khasheei A, Schnackenburg B, Berger F, et al. Flow-sensitive four-dimensional cine magnetic resonance imaging for offline blood flow quantification in multiple vessels: a validation study. *J Magn Reson Imaging*. 2010;32:677–683. doi: 10.1002/jmri.22280.
16. Dyverfeldt P, Bissel M, Barker AJ, et al. 4D flow cardiovascular magnetic resonance consensus statement. *J Cardiovasc Magn Reson*. 2015 Aug 10;17(1):72. doi: 10.1186/s12968-015-0174-5.



Chapter 10

Echocardiography and MRI parameters associated with exercise capacity in patients after the arterial switch operation

Evangeline G. Warmerdam*

Francesca Magni*

Tim Leiner

Pieter A.F. Doevendans

Gertjan T. Sieswerda

Sebastiaan W. van Wijk

Hans M. Breur

Bart W. Driesen

Heynric B. Grotenhuis**

Tim Takken**

* These authors contributed equally

** These authors contributed equally

Journal of cardiology vol. 76,3 (2020): 280-286

ABSTRACT

Background. The arterial switch operation (ASO) for transposition of the great arteries has excellent survival, but a substantial number of patients have a reduced exercise capacity. The goal of this study was to identify imaging parameters associated with a reduced exercise capacity in patients after ASO.

Methods. A retrospective analysis was performed of ASO patients who underwent cardiopulmonary exercise testing (CPET) between 2007 and 2017. Reduced exercise performance was defined as a reduced workload peak (W_{peak}) with Z-score < -2 or a peak oxygen uptake indexed for weight ($\text{VO}_{2\text{peak}}/\text{kg}$) with Z-score < -2 . Data on echocardiography and cardiac magnetic resonance (CMR) performed within one year of the CPET were collected for comparison.

Results. A total of 81 ASO patients (age 17 ± 7 years) were included. Reduced exercise performance was found in 22 patients (27%) as expressed by either a reduced W_{peak} and / or a reduced $\text{VO}_{2\text{peak}}/\text{kg}$. Main pulmonary artery gradient and tricuspid regurgitation gradient by echocardiography were found to be associated with reduced W_{peak} ($p = 0.031$; $p = 0.020$, respectively). The main pulmonary artery gradient and tricuspid regurgitation gradient by echocardiography were found to be associated with reduced $\text{VO}_{2\text{peak}}/\text{kg}$ ($p = 0.009$; $p = 0.019$, respectively). No left ventricular parameters were found to be associated with abnormal exercise performance.

Conclusion. This study demonstrates that ASO patients frequently experience reduced exercise capacity. Echocardiographic evidence of main pulmonary artery stenosis and increased right ventricular pressure were associated with reduced exercise capacity and are therefore important to monitor during serial follow-up of ASO patients.

INTRODUCTION

Transposition of the great arteries (TGA) is the second most common cyanotic congenital heart defect, accounting for 5-8% of all congenital heart defects.¹ A major improvement in the treatment of TGA was the arterial switch operation (ASO), introduced in 1976 by Jatene.² With the ASO, the normal arrangement of the circulation is restored by detaching the aorta and pulmonary arteries (PAs) from their roots and reattach them to the correct ventricle. Nowadays, ASO is combined with the Lecompte manoeuvre, bringing the main pulmonary artery (MPA) and the pulmonary bifurcation anterior to the aorta.³ ASO has excellent long-term results: patients have a good life expectancy, preserved left ventricular function, and favourable quality of life.⁴ Despite these good long term results, ASO patients often have a reduced exercise capacity when compared to their healthy peers.⁴ Complications that may influence exercise capacity are pulmonary stenosis (PS), right ventricular (RV) dysfunction, aortic regurgitation and coronary artery abnormalities.⁴ Of these complications, PS is a typical late sequelae after ASO and is the most common indication for intervention after ASO.⁴⁻⁶ Regular follow-up with echocardiography, cardiac magnetic resonance (CMR) and cardiopulmonary exercise testing (CPET) is therefore crucial to detect complications at an early stage and, if necessary, to assess the optimal timing for intervention. However, routine exercise testing in all ASO patients would imply a significant patient burden. Currently, imaging parameters associated with abnormal exercise performance are lacking. Therefore, the aim of the current study was to identify imaging parameters that are associated with a reduced exercise capacity in patients late after ASO. Furthermore, we wanted to investigate whether ASO patients who underwent an intervention for PS have a reduced exercise capacity.

METHODS

Study population

A retrospective analysis was performed on patients with simple TGA after ASO who underwent CPET between 2007 and 2017 in our centre. Data on echocardiography and CMR performed within one year of the CPET were collected from the electronic patient files, as well as data on patient demographics and clinical status. Due to the retrospective nature of this study, an ethics waiver was granted by the local Medical Ethical Committee. Several patients included for this study were part of a separate prospective study executed in our centre. This study was approved by the local Medical Ethical Committee (study number 10-289).⁷

Cardiopulmonary exercise testing

All CPETs were conducted on a bicycle ergometer. After 3 minutes of warming-up - consisting of unloaded cycling - the workload increased in a ramp fashion by 10-15-20-25 W/min, to assure a test duration between 8-12 minutes. The CPET was stopped when the patient reached exhaustion or if ECG changes were observed. During the CPET, respiratory gas exchange was monitored using a ZAN 600 (ZAN Messgerate, Obterthulba, Germany) or a Geratherm Respiratory Ergostik (Geratherm, Bad Kissingen, Germany). The exercise test parameters obtained for this study were: heart rate at peak exercise (HR_{peak}), peak oxygen uptake (VO_{2peak}), VO_{2peak} indexed for weight (VO_{2peak}/kg), VO_2 at ventilatory anaerobic threshold as a percentage of VO_{2peak} (%), workload peak (W_{peak}), W_{peak} indexed for weight (W_{peak}/kg), O_2 pulse and peak systolic blood pressure (SBP_{peak}). W_{peak} was used to as one of the parameters to determine exercise capacity since it includes both aerobic and anaerobic work capacity. Reference values for each exercise test parameter were calculated using equations based on age and sex.⁸ Z-scores were calculated for patient-specific outcomes. Reduced exercise performance was defined as a reduced W_{peak} with Z-score < -2 or a VO_{2peak}/kg with Z-score < -2. In a normal population only 2.3% of people would be expected to have a Z-score < -2, hence we chose a Z-score of -2 as our cut-off value.

Echocardiography

Echocardiography was performed using General Electric (GE Healthcare, Wauwatosa, Wisconsin, USA) ultrasound systems. In our centre, diagnosis of valvular disease is made based upon the definitions of the European Society of Echocardiography recommendations for the assessment of valve stenosis and valve regurgitation.^{9,10} Parameters collected for this study were: left ventricular (LV) ejection fraction (LVEF), LV shortening fraction, LV end-diastolic diameter, LV end-systolic diameter, end-diastolic interventricular septal diameter, end-diastolic LV posterior wall diameter, MPA pressure gradient, left pulmonary artery (LPA) pressure gradient, right pulmonary artery (RPA) pressure gradient, tricuspid regurgitation (TR) gradient, RV end-diastolic area, RV end-systolic area, and RV Fractional Area Change values. In order to assess echocardiography data in patients of different ages, all data were expressed as Z-scores if applicable.

Cardiac Magnetic Resonance Imaging

CMR imaging was performed on a 1.5 T scanner (Ingenia R5.1.7. and R5.3.1. Philips Healthcare, Best, The Netherlands). The following CMR parameters were assessed: end-diastolic volume (EDV) and end-systolic volume (ESV) for the LV and RV (absolute and indexed for body surface area), LVEF, RVEF, aortic regurgitation, MPA regurgitation, RPA

regurgitation, LPA regurgitation, peak velocities across the aortic and pulmonary valves, and stroke volumes of the MPA, LPA and RPA. In order to assess volumes measured by CMR in patients of different ages, we used volumes indexed for body surface area.

Intervention

The decision to proceed to stent placement was based on several parameters: the RV pressure, the pressure gradient across the PAs, the presence of an anatomical substrate of PS, and the flow distribution in the PAs.

Statistics

All statistical analyses were performed using IBM SPSS statistics, version 25 (International Business Machines Corporation, Armonk, New York, United States). Descriptive statistics were used for demographic and other descriptive data. Quantitative data are presented as mean \pm standard deviation or absolute numbers with percentages. An independent Student's t-test was used to compare echocardiography and CMR parameters between patients with normal (Z-score > -2) and abnormal (Z-score < -2) CPET results. Linear regression analyses were performed for each individual imaging parameter for which a significant difference or when a trend towards significance was found between patients with normal and abnormal CPET results. The Z-scores of the CPET results (W_{peak} and VO_{2peak} /kg) were set as dependent variable, whereas the imaging parameters were set as independent variable. Results were considered statistically significant if the probability value (p-value) was < 0.05 . Due to the exploratory nature of this study, correction for multiple testing was not performed.

RESULTS

A total of 81 ASO patients were included in this study (Table 1). Median age at ASO was 7 days (range: 1 – 320 days), of whom 19 (23%) also underwent VSD closure. Out of the 81 patients, 73 patients underwent echocardiography within one year from CPET (58 ± 85 days from CPET) and 60 patients had a CMR within 1 year from the CPET (52 ± 92 days from CPET). Mean age of TGA patients was 17 ± 7 years at time of CPET. Between ASO and CPET, 17 ASO patients (21%) underwent one or more interventions after ASO. Thirteen patients underwent surgery: seven for PS, four for aortic regurgitation, one for residual ventricular septum defect, and one for coarctation of the aorta. Seven patients underwent balloon dilatation and five underwent stent placement for PA branch stenosis. Median age at first intervention was 6 years (range: 0 – 30 years). At

latest follow-up, 23 (28%) of patients had PS (Figure 1), aortic stenosis was present in 2 patients (2%) and mild to moderate aortic regurgitation in 11 patients (14%), based on echocardiography.

CPET results, expressed both as absolute values and Z-scores, are shown in table 2. Reduced exercise performance was found in a total of 22 patients (27%): 10 patients (12%) had a decreased W_{peak} and a decreased $VO_{2peak/kg}$ (Z-score < -2), 7 patients (9%) had only a decreased W_{peak} , and 5 patients (6%) a decreased $VO_{2peak/kg}$. The ventilatory anaerobic threshold could be determined in all patients. Four patients experienced dyspnoea during peak exercise, while in one case the CPET was stopped by the exercise physiologist due to a rapid increase in systolic blood pressure. None of the patients developed ischemia during the test. No limitations were observed due to peripheral musculature or lung conditions.

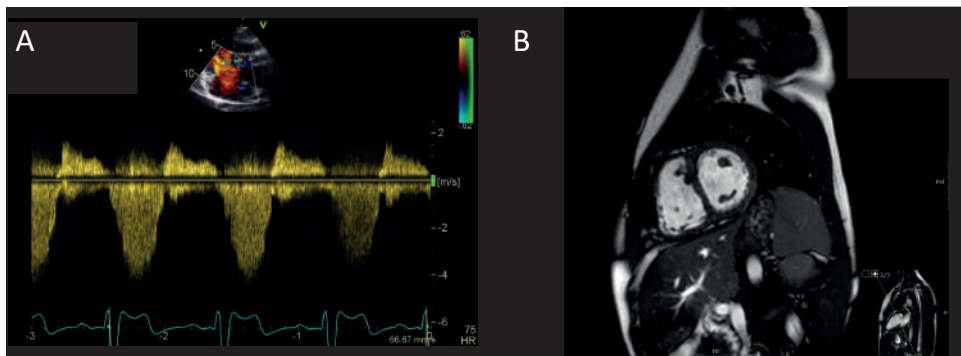


Figure 1. A 13 year-old patient with transposition of the great arteries for which an arterial switch operation was performed at the age of 10 days. This patient developed a stenosis in the left pulmonary artery, resulting in an increased right ventricular pressure. A: echocardiographic evaluation of the tricuspid regurgitation jet (peak tricuspid regurgitation gradient 53 mmHg). B: short axis view on CMR showing flattening of the interventricular septum (D-shaped left ventricle).

Table 1. Demographic data.

	All patients (n=81)
Age (years)	17 ± 7
Height (cm)	165 ± 18
Weight (kg)	57 ± 21
BMI (kg/m ²)	20 ± 5
Age at ASO (days)	7 (range: 1 - 320)
<i>Concomitant defects</i>	
VSD	19 (23%)
<i>Coronary artery pattern</i>	
Usual	60 (74%)
LCX from RCA	11 (14%)
Single RCA	3 (4%)
Inverted RCA and LCX	3 (4%)
Absent LCX	2 (3%)
Unknown	2 (3%)
<i>Complications</i>	
PS	23 (28%)
Valvular stenosis	4 (5%)
MPA stenosis	4 (5%)
LPA stenosis	10 (12%)
RPA stenosis	10 (12%)
AR	11 (14%)
AS	2 (2%)
<i>Interventions</i>	
Surgery	13 (16%)
PS	7 (9%)
AR	4 (5%)
Residual VSD	1 (1%)
CoA	1 (1%)
Balloon dilatation*	7 (9%)
Stent placement*	5 (6%)

Data are presented as mean ± standard deviation, median (range), or absolute number (percentage). ASD: atrial septum defect, ASO: arterial switch operation, AR: aortic regurgitation, AS: aortic stenosis, BMI: body mass index, CoA: coarctation of the aorta, LCX: left circumflex coronary artery, PDA: persistent ductus arteriosus, PS: pulmonary stenosis, RCA: right coronary artery, VSD: ventricular septum defect. * All interventions were performed for pulmonary artery stenosis.

Table 2. CPET results in absolute values and in Z-scores.

	All patients (n=81)	Z-scores
W_{peak} (Watt)	187 ± 67	-1.15 ± 1.89
W_{peak}/kg (Watt/kg)	3.37 ± 0.20	-0.79 ± 1.64
HR_{peak} (bpm)	179 ± 15	-0.97 ± 1.52
SBP_{peak} (mmHg)	179 ± 27	0.24 ± 1.18
O_2 pulse (ml/beat)	13 ± 4	-0.78 ± 1.27
VO_{2peak} at VAT (%)	59 ± 13	0.19 ± 1.90
VO_{2peak} (l/min)	2.24 ± 0.79	-1.33 ± 1.39
VO_{2peak}/kg (ml/min/kg)	41 ± 10	-0.84 ± 1.52

Data are expressed as mean ± standard deviation. Bpm: beats per minute, HR: heart rate, SBP: systolic blood pressure, VAT: ventilatory anaerobic threshold, VO_{2peak} : peak oxygen uptake, VO_{2peak}/kg : peak oxygen uptake indexed for weight, W: workload.

Echocardiography results are presented in table 3. Normal biventricular function and dimensions were found, with increased gradients across the MPA (22 ± 17 mmHg), LPA (21 ± 14 mmHg), and RPA (21 ± 14 mmHg).

Table 3. Echocardiography results.

TTE parameter	All patients (n=73)
LVEF (%)	60 ± 8
LVSF (%)	34 ± 8
RVFAC (%)	46 ± 7
MPA gradient (mmHg)	22 ± 17
LPA gradient (mmHg)	21 ± 14
RPA gradient (mmHg)	21 ± 14
TR gradient (mmHg)	33 ± 17
LVIDd (mm)	49 ± 7
IVSd (mm)	8 ± 2
LVPWd (mm)	7 ± 2

Data are expressed as mean ± standard deviation. IVSd: interventricular septal end-diastole, LPA: left pulmonary artery, LVEF: left ventricular ejection fraction, LVIDd: left ventricular internal diameter end-diastole, LVPWd: left ventricular posterior wall end-diastole, LVSF: left ventricular shortening fraction, MPA: main pulmonary artery, RPA: right pulmonary artery, RVFAC: right ventricle fraction area change, TR: tricuspid regurgitation.

CMR results are presented in Table 4. CMR demonstrated preserved biventricular function and volumes. Mean peak velocities across the MPA (141 ± 49 cm/s), LPA (179 ± 56 cm/s), and RPA (167 ± 53 cm/s) were found to be increased. Mean stroke volume in the LPA (35 ± 11 ml) was slightly less when compared to mean stroke volume in the RPA (43 ± 11 ml) but within normal range.

Table 4. MRI results disaggregated for normal and reduced VO_2/kg .

TTE parameter	Normal W_{peak}	Reduced W_{peak}	P-value	Normal VO_2/kg	Reduced VO_2/kg	P-value
LVEF (%)	60 ± 7	61 ± 11	0.891	60 ± 7	63 ± 8	0.916
LVSF (%)	34 ± 7	31 ± 10	0.159	34 ± 8	30 ± 10	0.498
RVFAC (%)	47 ± 7	42 ± 8	0.147	46 ± 8	48 ± 5	0.163
MPA gradient (mmHg)	18 ± 10	35 ± 28	0.007*	18 ± 10	36 ± 28	0.024 *
LPA gradient (mmHg)	20 ± 15	25 ± 11	0.520	20 ± 15	23 ± 11	0.716
RPA gradient (mmHg)	20 ± 15	29 ± 3	0.297	2 ± 15	23 ± 9	0.746
TR gradient (mmHg)	27 ± 12	46 ± 24	0.004*	28 ± 12	49 ± 7	0.004 *
LVIDd (mm)	48 ± 7	51 ± 8	0.171	49 ± 7	49 ± 7	0.805
IVSd (mm)	8 ± 2	9 ± 2	0.056	8 ± 2	9 ± 1	0.239
LVPWd (mm)	7 ± 2	7 ± 1	0.740	7 ± 2	7 ± 1	0.299

Data are expressed as mean \pm standard deviation. AV: aortic valve, EDV: end diastolic volume, ESV: end systolic volume, LPA: left pulmonary artery, LPR: left pulmonary artery regurgitation, LVEF: left ventricular ejection fraction, MPA: main pulmonary artery, MPR: main pulmonary artery regurgitation, RPA: right pulmonary artery, RPR: right pulmonary artery regurgitation, RVEF: right ventricular ejection fraction.

Imaging parameters were compared between ASO patients with a normal or decreased exercise capacity as expressed by Z-scores < -2 for $\text{VO}_{2\text{peak}}/\text{kg}$ and W_{peak} (Table 5, 6). ASO patients with a decreased W_{peak} demonstrated an increased MPA gradient and TR gradient by echocardiography ($p = 0.007$, $p = 0.004$; respectively), an increased MPA, LPA, and RPA regurgitation fraction ($p = 0.006$, $p < 0.001$, $p < 0.001$; respectively) by CMR and a decreased MPA stroke volume by CMR ($p = 0.031$) when compared to patients with normal exercise capacity. ASO patients with a decreased $\text{VO}_{2\text{peak}}/\text{kg}$ demonstrated an increased MPA gradient and TR gradient by echocardiography ($p = 0.024$, $p = 0.004$; respectively) and a reduced LV EDV index and LV ESV index by CMR ($p = 0.012$, $p = 0.045$; respectively) when compared to patients with normal exercise capacity.

Table 5. Echocardiography results disaggregated for normal and reduced $\text{VO}_{2\text{peak}}$ and W_{peak} .

MRI parameter	All patients (n=60)
LVEF (%)	56 ± 6
RVEF (%)	53 ± 6
Left EDV index (ml/m ²)	106 ± 23
Left ESV index (ml/m ²)	47 ± 13
Right EDV index (ml/m ²)	108 ± 17
Right ESV index (ml/m ²)	59 ± 66
RPR (%)	6 ± 5
LPR (%)	7 ± 11
MPR (%)	5 ± 8
RPA peak velocity (cm/s)	167 ± 53
LPA peak velocity (cm/s)	179 ± 56
MPA peak velocity (cm/s)	141 ± 49
AV peak velocity (cm/s)	115 ± 28
LPA stroke volume (ml)	35 ± 11
RPA stroke volume (ml)	43 ± 11
MPA stroke volume (ml)	82 ± 19

Data are expressed as mean ± standard deviation. IVSd: interventricular septal end-diastole, LPA: left pulmonary artery, LVEF: left ventricular ejection fraction, LVIDd: left ventricular internal diameter end-diastole, LVPWd: left ventricular posterior wall end-diastole, LVSF: left ventricular shortening fraction, MPA: main pulmonary artery, RPA: right pulmonary artery, RVFAC: right ventricle fraction area change, TR: tricuspid regurgitation. *: $p < 0.05$.

Regression analysis demonstrated that reduced W_{peak} was associated with increased MPA gradient and increased TR gradient by echocardiography ($p = 0.031$; $p = 0.020$, respectively), as displayed in Table 7. Reduced $\text{VO}_{2\text{peak}}$ /kg was associated with increased MPA gradient and increased TR gradient by echocardiography ($p = 0.009$; $p = 0.019$, respectively).

Table 6. MRI results disaggregated for normal and reduced VO_2/kg and W_{peak} *

MRI parameter	Normal W_{peak}	Reduced W_{peak}	P-value	Normal VO_2/kg	Reduced VO_2/kg	P-value
LVEF (%)	57 ± 6	54 ± 6	0.773	56 ± 6	56 ± 5	0.956
RVEF (%)	54 ± 6	52 ± 6	0.691	53 ± 6	53 ± 4	0.819
Left EDV index (ml/m ²)	105 ± 22	110 ± 28	0.470	109 ± 23	87 ± 9	0.012*
Left ESV index (ml/m ²)	46 ± 12	51 ± 16	0.487	48 ± 13	7 ± 2	0.045*
Right EDV index (ml/m ²)	107 ± 16	116 ± 23	0.216	109 ± 16	100 ± 22	0.145
Right ESV index (ml/m ²)	60 ± 72	56 ± 15	0.625	61 ± 70	47 ± 12	0.588
RPR (%)	5 ± 4	9 ± 10	0.006 *	6 ± 5	6 ± 5	0.726
LPR (%)	5 ± 5	18 ± 24	< 0.001 *	6 ± 9	11 ± 20	0.275
MPR (%)	3 ± 2	14 ± 18	< 0.001 *	4 ± 7	10 ± 15	0.199
RPA peak velocity (cm/s)	172 ± 53	132 ± 34	0.280	168 ± 52	155 ± 56	0.564
LPA peak velocity (cm/s)	181 ± 57	163 ± 48	0.814	183 ± 57	152 ± 40	0.206
MPA peak velocity (cm/s)	143 ± 52	130 ± 19	0.447	137 ± 26	193 ± 162	0.054
AV peak velocity (cm/s)	116 ± 29	105 ± 18	0.637	115 ± 30	111 ± 16	0.745
LPA stroke Volume (ml)	35 ± 11	30 ± 13	0.921	35 ± 12	31 ± 7	0.405
RPA stroke Volume (ml)	44 ± 12	39 ± 7	0.439	43 ± 12	41 ± 8	0.588
MPA stroke Volume (ml)	82 ± 21	80 ± 8	0.031 *	84 ± 18	68 ± 23	0.113

Data are expressed as mean ± standard deviation. AV: aortic valve, EDV: end diastolic volume, ESV: end systolic volume, LPA: left pulmonary artery, LPR: left pulmonary artery regurgitation, MPA: main pulmonary artery, MPR: main pulmonary artery regurgitation, RPR: right pulmonary artery regurgitation, LVEF: left ventricular ejection fraction, RPA: right pulmonary artery, RVEF: right ventricular ejection fraction.

Table 7. Results of univariate regression for each individual imaging parameter for which a significant difference or when a trend towards significance was found between patients with normal and abnormal CPET results.

CPET parameter	Imaging modality	Imaging parameter	R	P-value
W_{peak}	Echocardiography	MPA gradient	0,345	0.031 *
W_{peak}	Echocardiography	TR gradient	0,392	0.020 *
W_{peak}	MRI	RPA regurgitation	0,100	0.460
W_{peak}	MRI	LPA regurgitation	0,141	0.273
W_{peak}	MRI	MPA regurgitation	0,155	0.351
W_{peak}	MRI	MPA stroke volume	0,255	0.135
VO_2/kg	Echocardiography	MPA gradient	0,414	0.009 *
VO_2/kg	Echocardiography	TR gradient	0,394	0.019 *
VO_2/kg	MRI	RPA regurgitation	0,105	0.442
VO_2/kg	MRI	LPA regurgitation	0,202	0.137
VO_2/kg	MRI	MPA regurgitation	0,207	0.213
VO_2/kg	MRI	MPA stroke volume	0.000	0.975

MPA: main pulmonary artery, LPA: left pulmonary artery, RPA: right pulmonary artery, TR: tricuspid regurgitation, * $p < 0.05$.

DISCUSSION

The ASO has excellent long-term survival, but a substantial number of ASO patients have a reduced exercise capacity. The goal of the present study was to identify imaging parameters associated with exercise capacity. It conveys the following findings:

1. In our ASO cohort, one in five paediatric and adolescent patients suffers from a reduced exercise capacity.
2. MPA gradient and TR gradient by echocardiography were associated with reduced exercise capacity of ASO patients.

Our finding that one in four ASO patients suffers from a reduced exercise capacity is in line with other reports in literature.^{4,7-10} Data on exercise capacity throughout life is highly relevant, since a decreased exercise capacity has been associated with a decreased quality of life¹¹ and an adverse prognosis in patients with congenital heart disease.¹² Prior studies investigating exercise capacity in patients after ASO also showed a mildly reduced exercise capacity in this patient group.^{4,11-14} The course of reduced exercise capacity after ASO over time is not completely clear, as data available for younger patients is somewhat conflicting. Giardini et al. studied a cohort of 60 patients with a mean age of 13.3 ± 3.4 years and found no relationship between age at CPET and VO_{2peak} .¹⁷ In contrast, Kuebler et al. found VO_{2peak} to decline over time on serial assessment, in a ASO cohort with a mean age of 17 ± 1 years, although this decline only slightly exceeded the normal decline with ageing.¹⁸

Echocardiographic parameters of MPA stenosis and increased RV pressure were associated with reduced exercise capacity. Similarly, Giardini et al. reported RV outflow tract obstruction to be related with a reduced VO_{2peak} in a cohort of 60 ASO patients¹⁷, while Kuebler et al. found a significant relationship between MPA stenosis or branch PA stenosis and VO_{2peak} in a cohort of 113 patients after ASO.¹⁸

Twenty-eight per cent of patients in our cohort demonstrated significant MPA and PA branch stenosis, similar to other reports.^{8,19,20} Large cohort studies consistently report that PS is the most common cause for intervention, with up to 20% of patients requiring a reintervention for PS after ASO.^{4,11,20}

PS in patients after ASO is thought to be a multifactorial process. Stretching of the PAs with the Lecompte manoeuvre, dynamic compression of the PAs due to the often dilated neo-aorta, scar formation at the anastomosis site and atherosclerosis due to altered wall shear stress distribution are all thought to lead to proximal PS after ASO.^{6,21} During

exercise, the PAs distend, and pulmonary vascular resistance drops to accommodate the increase in pulmonary blood flow due to increased cardiac output. In healthy subjects, only a slight increase in PA pressure is observed during exercise.²² However, ASO patients with a smaller and stiffer pulmonary vascular bed may not be able to accommodate this increase in blood flow during exercise, resulting in an increased PA pressure - hence an increased afterload for the RV - thereby limiting overall exercise performance. A similar mechanism, albeit more profound, is observed in TGA patients after the atrial switch operation, the surgical approach that preceded the ASO. The rigid atrial baffle systems in these patients limit the blood flow during exercise, resulting in a decreased exercise capacity. Importantly, studies comparing the exercise capacity of patients after ASO and atrial switch have consistently shown that atrial switch patients are more limited in their exercise capacity than ASO patients.^{23,24} Furthermore, similar results are observed in studies investigating patients with tetralogy of Fallot: patients with RV outflow tract obstruction had a significantly lower VO_{2peak} compared to patients without RV outflow tract obstruction.²⁵ The fact that similar results were found in different patient groups substantiates the hypothesis that obstruction in the RV outflow tract, or more distally in the PAs, leads to a diminished exercise capacity.

We observed an overall good RV function in our cohort. A limited number of studies have focused on RV performance after ASO. Taylor et al. demonstrated preserved global RV function at 10 years after ASO²⁶, similar to Haas et al.²⁷ and Grotenhuis et al.²¹ Given the impact of increased RV afterload related to PS, monitoring of RV function during follow-up appears to be important after ASO. RV hypertrophy can develop in response to preserve RV systolic function, but with increased RV stiffness related to increased myocardial thickness, diastolic dysfunction and subsequent systolic dysfunction may develop.²¹ Systolic and diastolic dysfunction of the RV are known to be strong indicators of impaired prognosis in patients with congestive heart failure.²⁸

Fourteen per cent of patients in our cohort suffered from aortic regurgitation, which is in agreement with results from previous studies.^{4,11} Although aortic root dilatation is present in the majority of patients late after ASO, severe aortic regurgitation is rare and when present, often a result of previous concomitant cardiac defects, such as the Taussig-Bing anomaly.²⁹ We did not find a correlation between the exercise capacity of TGA patients and measures of aortic stenosis or regurgitation on echocardiography or CMR. This observation appears to be somewhat inconsistent with findings of previous studies. The study by Kuebler et al. found a significant correlation between moderate to severe aortic regurgitation and reduced VO_{2peak} .¹⁸ However, our patients only suffered

from mild regurgitation, whereas the cohort of Kuebler et al. included several patients with moderate or severe aortic regurgitation, which probably explains the difference in findings.

In the univariate linear regression analyses, we did not find any significant associations between function parameters of the left-sided heart and exercise capacity. This is in line with findings in patients with congestive heart failure, where the LVEF is repeatedly found not to be associated with abnormal exercise capacity.^{30,31} Furthermore, studies show LV function is usually preserved in patients after ASO.^{4,11} Interestingly, we found a significantly lower left EDV index and left ESV index in patients with a reduced exercise capacity. Research suggests that patients with a decreased exercise capacity have smaller left ventricle chamber size³², which could be the explanation for the combination of decreased left EDV and ESV index with preserved left ventricular function in our patient group.

TGA patients often have an abnormal coronary flow reserve after ASO.³³ When the coronary blood flow is disturbed to a degree where the increased demand for oxygen during exercise cannot be met, myocardial ischemia can occur, thereby limiting exercise capacity. In our cohort none of the patients developed ischemia during CPET and no coronary abnormalities were seen on CMR. This is in line with other studies: patients after ASO rarely have symptoms and ECG, echocardiography, and CMR seldom demonstrate evidence of myocardial ischemia.^{33,34}

Regular clinical evaluation of patients after ASO is necessary to assess (progression of) complications and determine the need for intervention. To minimize patient burden, only investigations that are necessary should be performed regularly. We believe a CPET is indicated when the patient complains of reduced exercise tolerance or when echocardiography or CMR suggests MPA stenosis or when an increased TR gradient is found. We would advise to perform a CPET before and after intervention for PS, to provide an objective evaluation of the effect of the PS intervention on individual exercise capacity. Furthermore, we would advise regular follow-up with echocardiography and CPET after intervention to assess the long term results of the intervention.

Advanced imaging techniques, such as four-dimensional flow CMR, could be of use to obtain a more comprehensive evaluation of the pulmonary haemodynamics in this patient group. More research on the underlying mechanisms and the influence of an abnormal pulmonary circulation on exercise capacity in ASO patients is warranted to completely understand this phenomenon.

LIMITATIONS

The main limitation of this study was the retrospective nature, and missing data. Second, all patients in our cohort were referred for CPET on clinical indication, which may have resulted in selection bias and an increased incidence of abnormal findings. Third, this study covered a long time span, changes in management and imaging technics may have influenced the outcomes. Last, we did not take into consideration possible comorbidities and the physical activity level of the patients, all factors which could have influenced results of the CPET.

CONCLUSION

This study demonstrates that patients after ASO frequently have reduced exercise capacity. Imaging parameters of MPA stenosis and increased RV pressure were associated with reduced exercise capacity and are therefore key to monitor during serial follow-up of these patients.

REFERENCES

1. Brickner ME, Hillis LD, Lange RA. Congenital heart disease in adults. Second of two parts. *N Engl J Med* 2000;342:334–342.
2. Jatene AD, Fontes VF, Paulista PP, Souza LC, Neger F, Galantier M, et al. Anatomic correction of transposition of the great vessels. *J Thorac Cardiovasc Surg* 1976;72:364–370.
3. Lecompte Y, Neveux JY, Leca F, Zannini L, Tu TV, Dubois Y, et al. Reconstruction of the pulmonary outflow tract without prosthetic conduit. *J Thorac Cardiovasc Surg* 1982;84(5):727–731.
4. Ruys TP, Van der Bosch AE, Cuypers JA, Witsenburg M, Helbing WA, Bogers AJ, et al. Long term Outcome and quality of life after arterial switch operation: a prospective study with a historical comparison. *Congenit Heart Dis* 2013;May-Jun;8(3):203–10.
5. Choi BS, Kwon BS, Kim BG, et al. Long-Term Outcomes After an Arterial Switch Operation for Simple Complete Transposition of the Great Arteries. *Korean Circ J* 2010;Jan;40(1):23–30
6. Morgan CT, Mertens L, Grotenhuis H, Yoo SJ, Seed M, Grosse-Wortmann L. Understanding the mechanism for branch pulmonary artery stenosis after the arterial switch operation for transposition of the great arteries. *Eur Heart J Cardiovasc Imaging*. 2017;18(2):180–185. doi:10.1093/ehjci/jew046
7. van Wijk SW, Driessen MMP, Meijboom FJ, Takken T, Doevendans PA, Breur JM. Evaluation of Left Ventricular Function Long Term After Arterial Switch Operation for Transposition of the Great Arteries. *Pediatr Cardiol* 2019;Jan;40(1):188–193. doi: 10.1007/s00246-018-1977-6.
8. Van de Poppe DJ, Hulzebos E, Takken T, Low-Land Fitness Registry Study group. Reference values for maximum work rate in apparently healthy Dutch/Flemish adults: data from the LowLands fitness registry. *Acta Cardiol* 2018;Jun 22:1–8.
9. Baumgartner H, Hung J, Bermejo J, Chambers JB, Evangelista A, Griffin BP, et al. Echocardiographic assessment of valve stenosis: EAE/ASE recommendations for clinical practice. *J Am Soc Echocardiogr* 2009;Jan;22(1):1–23; quiz 101–2.
10. Lancellotti P, Moura L, Pierard LA, Agricola E, Popescu BA, Tribouilloy C, et al. European Association of Echocardiography recommendations for the assessment of valvular regurgitation. Part 2: mitral and tricuspid regurgitation (native valve disease). *Eur J Echocardiogr* 2010;May;11(4):307–32. doi: 10.1093/ejechocard/jeq031.
11. Choi BS, Kwon BS, Kim BG, Bae EJ, Noh CI, Choi JY, et al. Long-Term Outcomes After an Arterial Switch Operation for Simple Complete Transposition of the Great Arteries. *Korean Circ J* 2010;Jan;40(1): 23–30
12. van Beek E, Binkhorst M, de Hoog M, de Groot P, van Dijk AP, Schokking M, et al. Exercise performance and activity level in children with transposition of the great arteries treated by the arterial switch operation. *Am J Cardiol* 2010;Feb 1;105(3):398–403
13. Losay J, Touchot A, Serraf A, Litvinova A, Lambert V, Piot JD, et al. Late outcome after arterial switch operation for transposition of the great arteries. *Circulation* 2001;Sep;18;104(12;Suppl 1):1121–6.

14. Khairy P, Clair M, Fernandes S, Blume ED, Powell AJ, Newburger JW, et al. Cardiovascular outcomes after the arterial switch operation for D-transposition of the great arteries clinical perspective. *Circulation* 2013;Jan;22;127(3):331-9. doi:10.1161/CIRCULATIONAHA.112.135046.
15. Amedro P, Picot MC, Moniotte S, Dorka R, Bertet H, Guillaumont S, et al. Correlation between cardio-pulmonary exercise test variables and health-related quality of life among children with congenital heart diseases. *Int J Cardiol* 2016;203:1052–60. doi:10.1016/j.ijcard.2015.11.028
16. Inuzuka R, Diller GP, Borgia F, Benson L, Tay EL, Alonso-Gonzalez R, et al. Comprehensive use of cardiopulmonary exercise testing identifies adults with congenital heart disease at increased mortality risk in the medium term. *Circulation* 2012;Jan;17;125(2):250-9. doi: 10.1161/CIRCULATIONAHA.111.058719
17. Giardini A, Hager A, Lammers AE, Derrick G, Müller J, Diller GP, et al. Ventilatory efficiency and aerobic capacity predict event-free survival in adults with atrial repair for complete transposition of the great arteries. *J Am Coll Cardiol* 2009;Apr 28;53(17):1548-55. doi: 10.1016/j.jacc.2009.02.005.
18. Kuebler JD, Chen MH, Alexander ME, Rhodes J. Exercise Performance in Patients with D-Loop Transposition of the Great Arteries After Arterial Switch Operation: Long-Term Outcomes and Longitudinal Assessment. *Pediatr Cardiol* 2016;Feb;37(2):283-9. doi: 10.1007/s00246-015-1275-5.
19. Hutter P, Kreb D, Mantel S, Hitchcock JF, Meijboom EJ, Bennink GBWE. Twenty-five years' experience with the arterial switch operation. *J Thorac Cardiovasc Surg* 2002;124:790–7.
20. Tobler D, Williams WG, Jegatheeswaran A, Van Arsdell GS, McCrindle BW, Greutmann M, et al. Cardiac outcomes in young adult survivors of the arterial switch operation for transposition of the great arteries. *J Am Coll Cardiol* 2010;56:58–64.
21. Grotenhuis HB, Kroft LJM, van Elderen SGC, Westenberg JJM, Doornbos J, Hazekamp MG, et al. Right ventricular hypertrophy and diastolic dysfunction in arterial switch patients without pulmonary artery stenosis. *Heart* 2007;Dec;93(12):1604–1608.
22. Giardini A, Khambadkone S, Rizzo N, Riley G, Pace Napoleone C, Muthialu N, et al. Determinants of exercise capacity after arterial switch operation for transposition of the great arteries. *Am J Cardiol* 2009;104:1007–12
23. Reybroeck T, Eyskens B, Mertens L, Defoor J, Daenen W, Gewillig M. Cardiorespiratory exercise function after the arterial switch operation for transposition of the great arteries. *Eur Heart J* 2001;22:1052–9.
24. Fredriksen PM, Pettersen E, Thaulow E. Declining aerobic capacity of patients with arterial and atrial switch procedures. *Pediatr Cardiol* 2009;Feb;30(2):166-71. doi: 10.1007/s00246-008-9291-3.
25. Freling HG, Willems TP, van Melle JP, van Slooten YJ, Bartelds B, Berger RM, et al. Effect of right ventricular outflow tract obstruction on right ventricular volumes and exercise capacity in patients with repaired tetralogy of fallot. *Am J Cardiol* 2014;Feb;113(4):719-23. doi: 10.1016/j.amjcard.2013.10.049.

26. Taylor AM, Dymarkowski S, Hamaekers P, Razavi R, Gewillig M, Mertens L, et al. MR coronary angiography and late-enhancement myocardial MR in children who underwent arterial switch surgery for transposition of great arteries. *Radiology* 2005;Feb;234(2):542-7.
27. Haas F, Wottke M, Poppert H, Meisner H. Long-term survival and functional follow-up in patients after the arterial switch operation. *Ann Thorac Surg* 1999;68:1692-7.
28. Meluzin J, Spinarova L, Hude P, Krejčí J, Dusek L, Vítovec J, et al. Combined right ventricular systolic and diastolic dysfunction represents a strong determinant of poor prognosis in patients with symptomatic heart failure. *Int J Cardiol* 2005;Nov 2;105(2):164-73.
29. McMahon CJ, Ravekes WJ, Smith EO, Denfield SW, Pignatelli RH, Altman CA, et al. Risk factors for neo-aortic root enlargement and aortic regurgitation following arterial switch operation. *Pediatr Cardiol* 2004;Jul-Aug;25(4):329-35.
30. Task Force of the Italian Working Group on Cardiac Rehabilitation Prevention; Working Group on Cardiac Rehabilitation and Exercise Physiology of the European Society of Cardiology, Piepoli MF, Corrà U, Agostoni PG, Belardinelli R, Cohen-Solal A, Hambrecht R, Vanhees L. Statement on cardiopulmonary exercise testing in chronic heart failure due to left ventricular dysfunction: recommendations for performance and interpretation. Part I: definition of cardiopulmonary exercise testing parameters for appropriate use in chronic heart failure. *Eur J Cardiovasc Prev Rehabil* 2006;Apr;13(2):150-64.
31. Di Salvo TG, Mathier M, Semigran MJ, Dec GW. Preserved Right Ventricular Ejection Fraction Predicts Exercise Capacity and Survival in Advanced Heart Failure. *J Am Coll Cardiol* 1995;Apr;25(5):1143-53.
32. Franciosa JA, Baker BJ, Seth L. Pulmonary versus systemic hemodynamics in determining exercise capacity of patients with chronic left ventricular failure. *Am Heart J* 1985;Oct;110(4):807-13.
33. Pedra SR, Pedra CA, Abizaid AA, Braga SL, Staico R, Arrieta R, et al. Intracoronary ultrasound assessment late after the arterial switch operation for transposition of the great arteries. *J Am Coll Cardiol* 2005;Jun;21;45(12):2061-8.
34. Ou P, Mousseaux E, Azarine A, Dupont P, Agnoletti G, Vouhé P et al. Detection of coronary complications after the arterial switch operation for transposition of the great arteries: first experience with multislice computed tomography in children. *J Thorac Cardiovasc Surg* 2006;Mar;131(3):639-43.



Chapter 11

Abnormal vortex formation in the right pulmonary artery after the arterial switch operation

Evangeline G. Warmerdam

Hans C. van Assen

Julio Sotelo

Heynric B. Grotenhuis

European heart journal. Case reports, 5(1), ytaa549

CASE DESCRIPTION

Transposition of the great arteries (TGA) is a common cyanotic congenital heart defect, accounting for 5-8% of all congenital heart defects.¹ Currently, the arterial switch operation (ASO) combined with the LeCompte manoeuvre is the most used surgical procedure to correct TGA. Although pulmonary artery (PA) stenosis is the most common late complication after ASO², flow disturbances such as vortex formation can also be observed in patients without obvious PA stenosis. Energy loss (EL) may then be a good marker of an inefficient circulation.

We present a 20 year-old male with TGA who underwent an ASO and ventricular septal defect closure at the age of 7 days. The patient had no complaints and underwent echocardiography, cardiac magnetic resonance (CMR), and exercise testing for research purposes. Echocardiography showed diastolic flattening of the intraventricular septum, indicative of mild right ventricular pressure overload. PAs could not be visualized. The exercise test revealed a decreased exercise capacity with a VO_2/kg at 75% of predicted. CMR showed preserved biventricular function, normal flow distribution between the branch PAs, and a right PA diameter of 27x16 mm. Four-dimensional flow CMR revealed a significant vortex flow in the right PA (Figure 1). To assess haemodynamic impact of this flow disturbance, peak-systolic EL was calculated and visualized (Figure 2) for the PAs. EL in the right PA at peak-systole was 4.33 mW, 38% of total EL measured in the PAs, which may be associated with the reduced exercise capacity of this TGA patient.

This case highlights the value of four-dimensional flow CMR, allowing for visualization of flow and quantification of haemodynamic parameters in the cardiovascular system. Since TGA patients require lifelong follow-up, a non-invasive imaging modality that allows for improved understanding of the often complex haemodynamics in these patients may prove of important value.

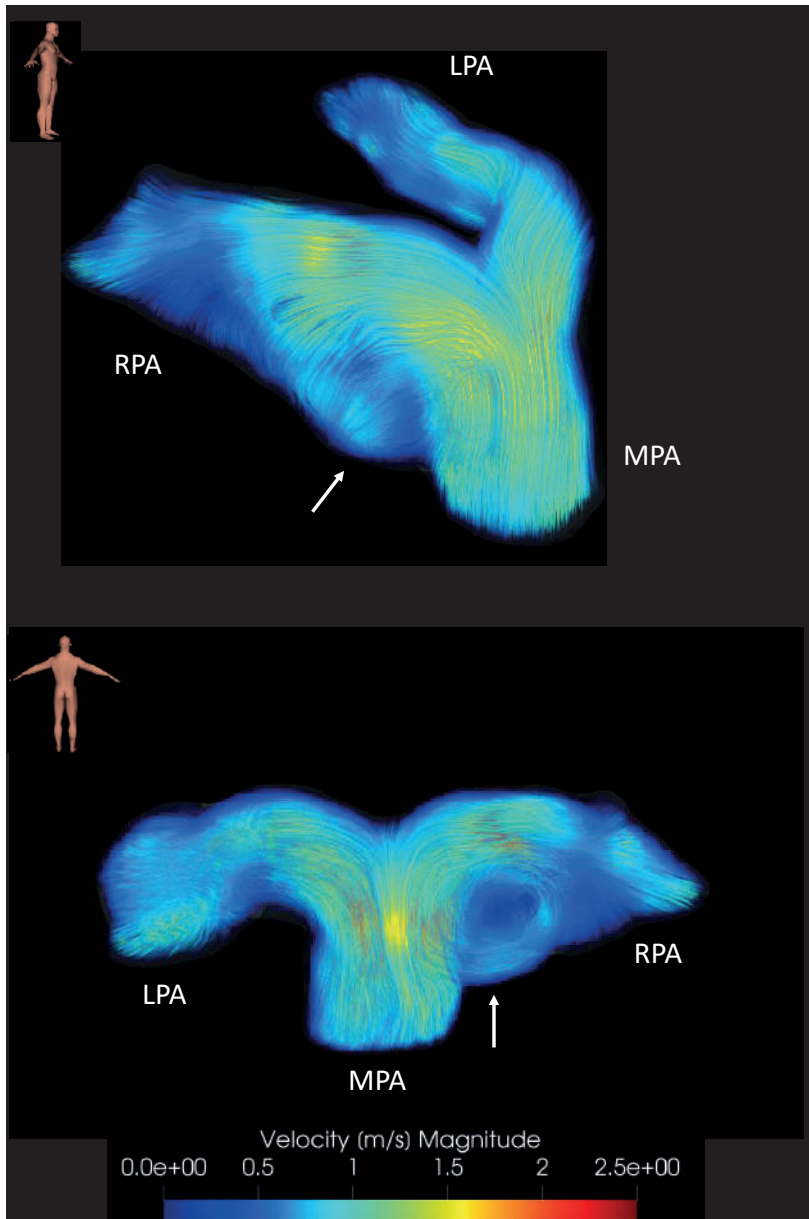


Figure 1. Visualisation of blood flow in the pulmonary arteries at peak-systole with colour-coded streamlines obtained from a four-dimensional flow CMR scan. Four-dimensional flow CMR is the term used for time-resolved phase-contrast CMR with flow-encoding in all three spatial directions. Using four-dimensional-flow CMR, qualification and quantification of flow over an entire volume can be obtained. This figure shows vortex flow in the right pulmonary artery, indicated by the arrow. MPA: main pulmonary artery, LPA: left pulmonary artery, RPA: right pulmonary artery. This four-dimensional flow CMR was acquired a 3.0T scanner (Ingenia R5.6.1, Philips Healthcare, Best, The Netherlands), with the following scan parameters: spatial resolution $2.5 \times 2.5 \times 2.5 \text{ mm}^3$, FOV $350 \times 350 \text{ mm}^2$, temporal resolution 65.5 ms, echo time 2.44 ms, repetition time 4.28 ms, flip angle 10° , venc 200 cm/s, TFE factor 3.

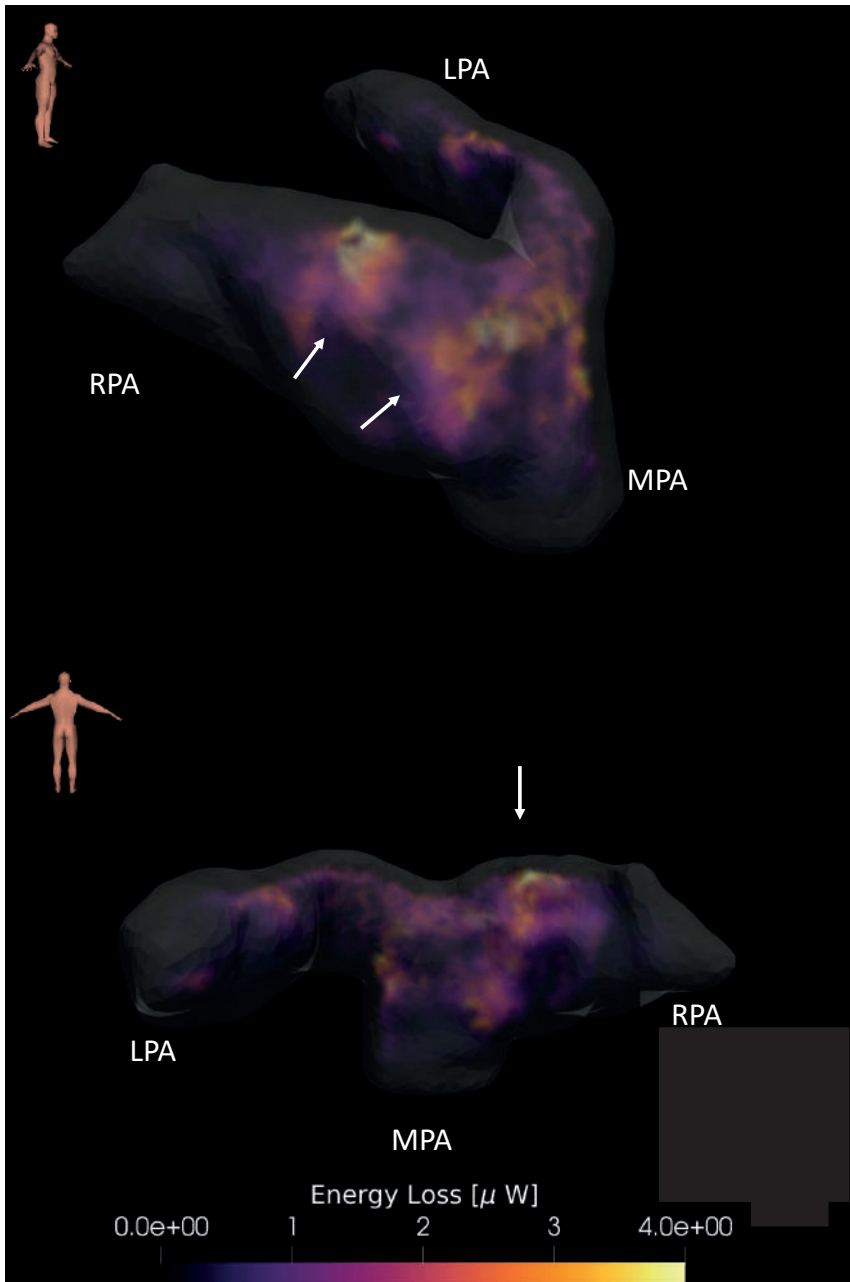


Figure 2. Visualisation of energy loss in the pulmonary arteries at peak-systole. Energy loss is a quantitative measure of the mechanical kinetic energy irreversibly lost to thermal energy, due to friction forces between viscous fluids and the adjacent wall. Minimal energy loss is required for an optimal cardiovascular circulation. Therefore, loss may be a good marker of an inefficient circulation. Increased values of energy loss can be seen at the location of the vortex flow, indicated by the arrow. MPA: main pulmonary artery, LPA: left pulmonary artery, RPA: right pulmonary artery.

REFERENCES

1. Brickner ME, Hillis LD, Lange RA. Congenital heart disease in adults. Second of two parts. *N Engl J Med* 2000;342:334–342.
2. Ruys TPE, Van der Bosch AE, Cuypers JAAE, Witsenburg M, Helbing WA, Bogers AJJC, et al. Long term Outcome and quality of life after arterial switch operation: a prospective study with a historical comparison. *Congenit Heart Dis*. 2013;May-Jun;8(3):203-10



Chapter 12

Impact of pulmonary haemodynamics on exercise performance in patients after the arterial switch operation

Evangeline G. Warmerdam

Tim Takken

Hans C. van Assen

Jos J.M. Westenberg

Pim van Ooij

Gregor J. Krings

Arno A.W. Roest

Friso M. Rijnberg

Hildo J. Lamb

Hans M.P. Breur

Heleen B. van der Zwaan

Michiel Voskuil

Tim Leiner

Heynric B. Grotenhuis

In preparation

ABSTRACT

Background. Pulmonary stenosis (PS) and decreased exercise capacity are common complications after the arterial switch operation (ASO) for transposition of the great arteries. Four-dimensional flow (4D flow) cardiac magnetic resonance (CMR) can provide a comprehensive quantitative haemodynamic evaluation. We hypothesized that 4D flow CMR parameters measured in the pulmonary arteries (PAs) may be associated with exercise capacity after ASO.

Methods. A prospective study including patients after ASO was performed between December 2018 and October 2020. All patients underwent cardiopulmonary exercise testing (CPET) and CMR, including 4D flow acquisition. From CPET predicted peak oxygen uptake corrected for sex, age and weight ($\text{predVO}_{2\text{peak}}/\text{kg}$) was calculated for each patient. Decreased exercise capacity was defined as $\text{predVO}_{2\text{peak}}/\text{kg} < 80\%$. 4D flow CMR was used to calculate energy loss, kinetic energy, helicity and vorticity in the main, right, and left PA.

Results. A total of 36 patients were included with a mean age of 20 ± 8 years. Decreased $\text{predVO}_{2\text{peak}}/\text{kg}$ was found in 42% of patients. In the main PA, energy loss was found to have an association with $\text{predVO}_{2\text{peak}}/\text{kg}$ ($p=0.0499$). In the left PA, energy loss, kinetic energy, and vorticity were all found to have an association with $\text{predVO}_{2\text{peak}}/\text{kg}$ ($p=0.0196$, $p=0.0283$, $p=0.0056$, respectively). No associations were found between flow parameters in the right PA and $\text{predVO}_{2\text{peak}}/\text{kg}$.

Conclusion. The 4D flow CMR parameters energy loss, kinetic energy and vorticity in the PAs of TGA patients had a negative association with exercise capacity.

INTRODUCTION

Transposition of the great arteries (TGA) is the second most common cyanotic congenital heart disease.¹ In TGA, the aorta arises from the right ventricle (RV) and the pulmonary artery from the left ventricle (LV), for which the arterial switch operation (ASO) combined with the LeCompte manoeuvre is standard of care.² With the ASO, the normal arrangement of the circulation is restored by detaching the aorta and pulmonary arteries (PAs) from their roots and reattach them to the correct ventricle. Nowadays, ASO is combined with the LeCompte manoeuvre, bringing the main pulmonary artery (MPA) and the pulmonary bifurcation anterior to the aorta.³ ASO has excellent long term results: patients have a good life expectancy and preserved LV function.⁴ Despite these good long term results, ASO patients often have a reduced exercise capacity when compared to their healthy peers.⁴

Complications after the ASO that may influence exercise capacity are pulmonary stenosis (PS), RV dysfunction, aortic regurgitation, chronotropic incompetence and coronary artery abnormalities.⁴ Of these complications, PS is a typical late sequelae after ASO and is the most common indication for intervention after ASO.^{4,5} In order to detect possible PS in time and – if necessary – intervene to prevent ventricular dysfunction, lifelong follow-up is recommended for these patients.⁶ Currently, non-invasive imaging modalities used for follow-up are echocardiography and cardiac magnetic resonance (CMR).⁶ In recent years, the scope of CMR has been expanded with four-dimensional flow (4D flow) CMR. This technique allows for flow assessment over an entire volume. Due to the fact flow is measured within a volume rather than in a single plane, 4D flow CMR is able to provide a variety of novel haemodynamic parameters and thus give a qualitative and quantitative analysis of the entire PAs within an entire imaging session.^{7,8}

In this study, we hypothesized that potentially abnormal pulmonary blood flow could have a negative impact on the exercise capacity of TGA patients. The aim was therefore to investigate if there is a relationship between haemodynamics in the PAs as measured by 4D flow CMR and exercise capacity in TGA patients after the ASO.

METHODS

Population

For this study patients with TGA who previously underwent ASO aged 8 to 40 years were prospectively recruited between December 2018 and October 2020. Exclusion criteria included presence of a stent in the pulmonary arteries, presence of a cardiac pacemaker

and all contra-indications for CMR including claustrophobia and pregnancy. Patients underwent CMR according to the local TGA CMR protocol, with the addition of 4D flow CMR and also underwent routine cardiopulmonary exercise testing (CPET). Written informed consent was obtained for all patients and/or their guardians (for patients < 16 years of age). This study was approved by the local Medical Ethical Committee (study number 18-200).

Cardiopulmonary exercise testing

All CPETs were conducted on a bicycle ergometer. After 3 minutes of warming-up - consisting of unloaded cycling - the workload increased in a ramp fashion by 10-15-20-25 W/min, to assure a test duration between 8-12 minutes. The CPET stopped when the patient reached exhaustion or if ECG changes were observed. During the CPET, respiratory gas exchange was monitored using a ZAN 600 (ZAN Messgerate, Obterthulba, Germany) or a Geratherm Respiratory Ergostik (Geratherm, Bad Kissingen, Germany). Only patients who reached a gas exchange ratio > 1.0 were included. The CPET parameters obtained for this study were: heart rate at peak exercise, percentage of predicted maximum heart rate, workload peak, percentage of predicted workload peak, peak oxygen pulse, peak systolic blood pressure, peak oxygen uptake (VO_{2peak}) and VO_{2peak} indexed for weight (VO_{2peak}/kg). To be able to compare patients, the predicted VO_{2peak}/kg value was calculated for each individual patient. The following formulas, previously published by Takken et al. were used: $-0,0049 * age^2 + 0,0884 * age + 48,263$ for males and $-0,0021 * age^2 - 0,1407 * age + 43,066$ for females.⁹ The individually calculated percentage obtained of predicted VO_{2peak}/kg ($predVO_{2peak}/kg$) was used for further analysis. Reduced exercise performance was defined as a $predVO_{2peak}/kg$ of < 80%.

CMR acquisition

All patients underwent CMR in accordance with the local TGA CMR protocol, which was analysed by a specialized cardiovascular radiologist, with the addition of 4D flow acquisition. Our local TGA CMR protocol consists of (amongst others) a three-dimensional non-contrast scan acquired at end-diastole used to measure vascular dimensions, multi-slice short axis cine images to measure biventricular function and dimensions. The following parameters were collected for this study: LV cardiac output, LV end-diastolic volume, LV ejection fraction, LV end-systolic volume, LV stroke volume, RV cardiac output, RV end-diastolic volume, RV ejection fraction, RV end-systolic volume, RV stroke volume, right PA (RPA) narrowest diameter, left PA (LPA) narrowest diameter. All ventricular parameters were indexed for body surface area. For branch PA diameters Z-scores were calculated based on height and weight as described previously.¹⁰

The 4D flow scan was processed and analysed by the investigators. CMR imaging was performed on a 3.0 T scanner (Ingenia R5.6.x, Philips Healthcare, Best, The Netherlands). 4D flow CMR acquisition was performed with retrospective ECG- and respiratory navigator-gating. The acquired volume covered the entire MPA, LPA and RPA. Imaging parameters for the 4D flow CMR were as follows: spatial resolution = $2.5 \times 2.5 \times 2.5 \text{ mm}^3$, FOV = $300 \times 300 - 350 \times 350 \text{ mm}^2$, temporal resolution = $32.8 - 46.1 \text{ ms}$, echo time = $2.1 - 2.5 \text{ ms}$, repetition time = $3.9 - 4.5 \text{ ms}$, flip angle = 10° , venc = $200 - 450 \text{ cm/s}$, TFE factor 3, SENSE: 2.5 (AP) and 1.5 (RL). Scan times were typically 8–12 minutes per scan.

4D flow CMR post processing

Concomitant gradient correction and local phase correction were performed from standard available scanner software. An aliased voxel was detected by a sign jump with the previous time frame (negative to positive velocity or vice-versa) of which the absolute velocity difference was higher than 0.75 times the VENC. The velocity in this voxel was corrected by adding or subtracting two times the VENC (MATLAB, R2018b, the MathWorks, Natick, Massachusetts).

Segmentation of the vessel was performed semi-automatically using commercially available 4D flow software (CAAS MR Solutions, version 5.0 - 5.1, Pie Medical Imaging, Maastricht, the Netherlands). The segmentation of the PAs was divided into three parts: MPA, LPA, RPA. Within the boundaries of these segmentations the following 4D flow parameters were calculated using in-house developed software: energy loss, kinetic energy, vorticity, and absolute helicity. Energy loss is the mechanical kinetic energy irreversibly lost (converted) to thermal energy due to frictional forces induced by fluid viscosity and no-slip condition^{11,12} and is calculated as follows:

$$E_L = \mu \phi_{\vec{v}} V$$

In this equation viscosity (μ) = $0.004 \text{ Pa}\cdot\text{s}$, assuming blood as a Newtonian fluid, represents the rate of viscous energy dissipation per unit volume, \vec{v} is the velocity vector and V is the voxel volume.^{11,12} Kinetic energy (KE) was calculated as follows:

$$KE = \frac{1}{2} \rho |\vec{v}|^2$$

In this equation blood is assumed an incompressible fluid with density $\rho = 1025 \text{ kg/m}^3$. Flow vorticity (ω) was defined as the vector that describes the flow rotation^{11,12} and calculated as follows:

$$\vec{\omega} = \vec{\nabla} \times \vec{v}$$

In this equation $\vec{\nabla}$ represents Nabla. Flow helicity (H) was defined as the dot-product of the vorticity with the three-dimensional flow vector^{11,12} and calculated as follows:

$$H = \vec{v} \cdot (\vec{\nabla} \times \vec{v})$$

Subsequently all 4D flow parameters were indexed for the volume (in ml) of the segmentations. The indexed parameters were used for further analysis.

Statistical analyses

Statistical analysis was performed using R version 3.6.3¹³, and figures were produced using the package ggplot2.¹⁴ Continuous data were assessed for normality using histograms, QQ-plots and the Shapiro-Wilk test. Quantitative data are presented as mean \pm standard deviation, median (interquartile range) or absolute number (percentage). Linear regression was used to assess the correlation between 4D flow parameters and $\text{predVO}_{2\text{peak}}/\text{kg}$ and the correlation between PA diameter Z-scores and 4D flow parameters. Results were considered statistically significant if the probability value (p-value) did not exceed or was not equal to 0.05. Due to the exploratory nature of this study, correction for multiple testing was not performed.¹⁵

RESULTS

A total of 45 patients were studied between December 2018 and October 2020. Nine patients were excluded from the study due to insufficient imaging quality of the 4D flow CMR acquisition. The majority of excluded cases were young children with motion artefacts in the scans. Therefore, data for 36 patients were analysed, with a mean age of 20 ± 8 years (range: 8 – 37 years) and of which 30 patients (83%) were male. Mean time between CMR and CPET was 13 ± 61 days. Median age at ASO was 9 (IQR: 7 - 14) days. The most common concomitant cardiac defect was a ventricular septal defect, present in 9 (25%) patients. One patient previously underwent aortic valve replacement for severe aortic valve regurgitation, none of the patients underwent (re)interventions on the PAs or pulmonary valve. All baseline characteristics are presented in Table 1.

Reduced exercise performance, defined as a $\text{predVO}_{2\text{peak}}/\text{kg}$ of $< 80\%$ was found in a total of 15 (42%) patients. Mean $\text{VO}_{2\text{peak}}/\text{kg}$ was 37 ± 8 ml/min/kg with a $\text{predVO}_{2\text{peak}}/\text{kg}$ of 82 ± 16 %. The ventilatory anaerobic threshold could be determined in all patients. Patients were not limited by other comorbidities (e.g. decreased peripheral musculature

capacity, lung conditions). None of the patients developed ischemia or arrhythmias, and none of the patients experienced desaturation during the test. No limitations were observed due to peripheral musculature or lung conditions.

Table 1. Baseline characteristics.

Characteristic	
Age (years)	20 ± 8
Male	30 (83%)
Height (cm)	171 ± 17
Weight (kg)	63 ± 21
Body mass index (kg/m ²)	21 ± 4
Age at arterial switch operation (days)	9 (IQR: 7 – 14)
<i>Concomitant cardiac defect</i>	
Aberrant coronary artery	2 (6%)
Atrial septal defect	4 (11%)
Bicuspid aortic valve	1 (3%)
Coarctation of the aorta	1 (3%)
Hypoplastic aortic arch	1 (3%)
Ventricular septal defect	9 (25%)
<i>Reintervention</i>	
Aortic valve replacement	1 (3%)
None	35 (97%)

Data are presented as number (percentage), mean ± standard deviation or median (interquartile range). IQR: interquartile range.

Table 2. CPET results in absolute values and in Z-scores.

	Value	Predicted (%)
W_{peak} (Watt)	209 ± 65	100 ± 22
HR_{peak} (bpm)	180 ± 18	94 ± 6
SBP_{peak} (mmHg)	182 ± 25	-
O_2 pulse (ml/beat)	13 (IQR: 9 – 17)	-
VO_2 at AT (ml/min/kg)	23 ± 7	-
VO_{2peak} (ml/min)	2275 ± 696	85 ± 18
VO_{2peak}/kg (ml/min/kg)	37 ± 8	82 ± 16

Data are expressed as mean ± standard deviation. Bpm: beats per minute, HR_{peak} : peak heart rate, SBP_{peak} : peak systolic blood pressure, VO_{2peak}/kg : peak oxygen uptake indexed for weight, W_{peak} : peak workload.

All biventricular and pulmonary CMR parameters are listed in Table 3. A summary on 4D flow parameters in the PAs are described in Table 4. CMR showed normal biventricular function in all patients with a mean LV ejection fraction of $56 \pm 5\%$ and a mean RV

ejection fraction of $56 \pm 5\%$. Biventricular dimensions were also preserved, as expressed by normal end-diastolic and end-systolic volumes. Mean peak velocity was 208 ± 66 cm/s in the MPA, 254 ± 82 cm/s in the LPA, and 240 ± 75 cm/s in the RPA.

Table 3. Cardiac magnetic resonance parameters on biventricular function.

CMR parameter	
LVEDV _i (ml/m ²)	106 ± 23
LVESV _i (ml/m ²)	48 ± 12
LVSV _i (ml/m ²)	59 ± 12
LVEF (%)	56 ± 5
LVCO _i (L/m ²)	4.2 ± 0.7
RVEDV _i (ml/m ²)	99 ± 18
RVESV _i (ml/m ²)	44 ± 11
RVSV _i (ml/m ²)	57 ± 13
RVEF (%)	56 ± 5
RVCO _i (ml/m ²)	4.0 ± 0.7
Aortic regurgitation (%)	2.0 (IQR: 1.0 – 3.7)
LPA diameter Z-score	-1.6 (IQR: -3.3 – 2.2)
RPA diameter Z-score	-2.5 (IQR: -4.5 – -1.3)

Data are presented as mean ± standard deviation or median (interquartile range). CMR: cardiac magnetic resonance, i: indexed for body surface area, IQR: interquartile range, LVCO: left ventricular cardiac output, LVEDV: left ventricular end-diastolic volume, LVEF: left ventricular ejection fraction, LPA: left pulmonary artery LVESV: left ventricular end-systolic volume, LVSV: left ventricular stroke volume, RPA: right pulmonary artery, RVCO: right ventricular cardiac output, RVEDV: right ventricular end-diastolic volume, RVEF: right ventricular ejection fraction, RVESV: right ventricular end-systolic volume, RVSV: right ventricular stroke volume.

Using linear regression analyses several associations were found between 4D flow parameters and $\text{predVO}_{2\text{peak}}/\text{kg}$. In the MPA, increased energy loss was found to be associated with a decreased exercise capacity ($p = 0.0499$) (Table 5, Figure 1). In the LPA, increased energy loss, kinetic energy, and vorticity were all found to be associated with a decreased exercise capacity ($p = 0.0196$, $p = 0.0283$, $p = 0.0056$, respectively). In Figure 2 examples are shown for energy loss, kinetic energy and vorticity in three different TGA patients with decreased exercise capacity.

Table 4. 4D flow CMR parameters for the pulmonary arteries.

4D flow parameter	Location	Value
Peak velocity (cm/s)	MPA	208 ± 66
Peak velocity (cm/s)	LPA	254 ± 82
Peak velocity (cm/s)	RPA	240 ± 75
Energy loss (mW/ml)	MPA	217 (IQR: 127 – 270)
Energy loss (mW/ml)	LPA	287 (IQR: 210 – 352)
Energy loss (mW/ml)	RPA	240 (IQR: 162 – 455)
Kinetic energy (mJ/ml)	MPA	387 (IQR: 274 – 579)
Kinetic energy (mJ/ml)	LPA	340 (IQR: 265 – 486)
Kinetic energy (mJ/ml)	RPA	266 (IQR: 184 – 352)
Vorticity (s ⁻¹ ml ⁻¹)	MPA	52803 (IQR: 45178 – 61047)
Vorticity (s ⁻¹ ml ⁻¹)	LPA	67217 (IQR: 54766 – 73570)
Vorticity (s ⁻¹ ml ⁻¹)	RPA	62221 (IQR: 51006 – 84310)
Absolute helicity (ml ⁻¹)	MPA	2421 (IQR: 1075 – 7580)
Absolute helicity (ml ⁻¹)	LPA	7332 (IQR: 4933 – 13449)
Absolute helicity (ml ⁻¹)	RPA	6185 (IQR: 2288 – 12815)

Data are presented as median (interquartile range). LPA: left pulmonary artery, MPA: main pulmonary artery, RPA: right pulmonary artery, IQR: interquartile range.

Table 5. Results for linear regression analyses between predVO₂peak/kg and four-dimensional parameters.

4D flow parameter	Location	Intercept	Coefficient	R	p-value
Energy loss (mW/ml)	MPA	91.32	-0.0389	0.3339	0.0499 *
Energy loss (mW/ml)	LPA	94.28	-0.0393	0.3928	0.0196 *
Energy loss (mW/ml)	RPA	85.35	-0.0095	0.1549	0.3750
Kinetic energy (mJ/ml)	MPA	92.26	-0.0235	0.3270	0.0552
Kinetic energy (mJ/ml)	LPA	92.97	-0.0284	0.3709	0.0283 *
Kinetic energy (mJ/ml)	RPA	82.69	-0.0015	0.0173	0.9220
Vorticity (s ⁻¹ ml ⁻¹)	MPA	96.87	-0.0002	0.3030	0.0768
Vorticity (s ⁻¹ ml ⁻¹)	LPA	107.6	-0.0004	0.4585	0.0056 *
Vorticity (s ⁻¹ ml ⁻¹)	RPA	89.77	-0.0001	0.1863	0.2840
Absolute helicity (ml ⁻¹)	MPA	85.47	-0.0007	0.1852	0.2870
Absolute helicity (ml ⁻¹)	LPA	86.98	-0.0004	0.3033	0.0765
Absolute helicity (ml ⁻¹)	RPA	83.44	-0.0002	0.0678	0.7000

4D flow: four-dimensional flow, LPA: left pulmonary artery, MPA: main pulmonary artery, RPA: right pulmonary artery, *: statistically significant result.

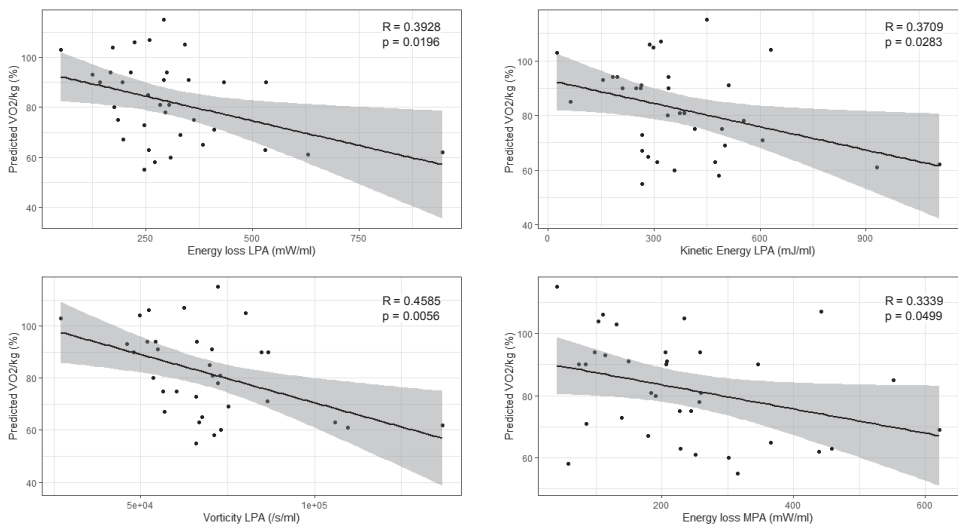


Figure 1. Plots for linear regression analyses with significant results. MPA: main pulmonary artery, LPA: left pulmonary artery, VO2/kg: peak oxygen uptake.

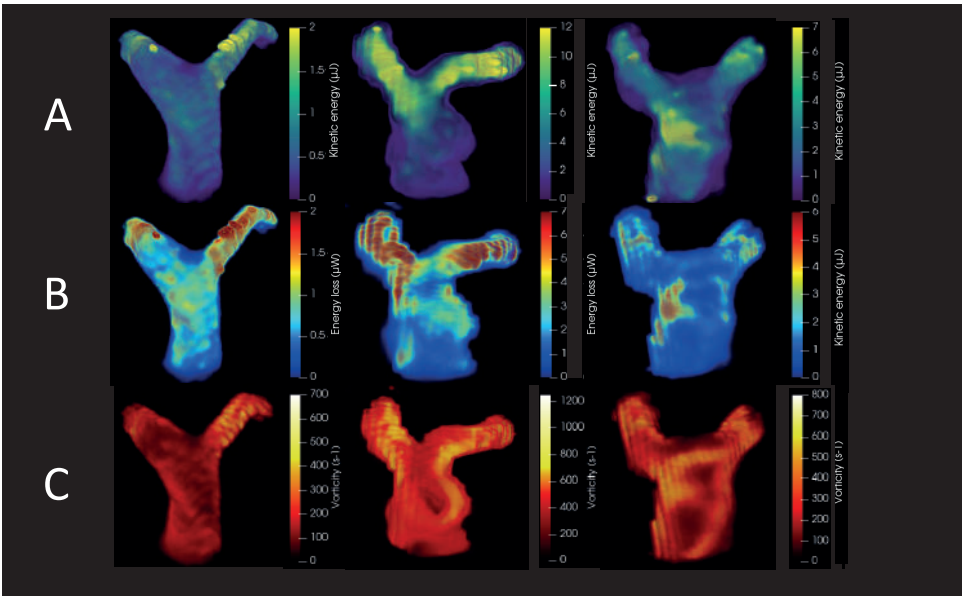


Figure 2. Four-dimensional flow CMR results at peak-systole in the pulmonary arteries from three patients with transposition of the great arteries. Panel A shows a visual representation of the kinetic energy. Panel B shows a visual representation of the energy loss. Panel C shows a visual representation of vorticity, in the pulmonary arteries. In all three patients, there is similarity in the patterns of kinetic energy, energy loss and vorticity.

To investigate whether there is an association between PA diameter Z-scores and 4D flow parameters, linear regression analyses was used. RPA diameters Z-scores were found to have a negative association with energy loss in the LPA and RPA ($p = 0.0087$, $p = 0.0079$, respectively) and vorticity in the LPA and RPA ($p = 0.0058$, $p = 0.0069$, respectively), see also Table 6. No significant associations were found for LPA diameter Z-scores and 4D flow parameters.

Table 6. Results with significant associations for linear regression analyses between pulmonary artery branch diameter Z-scores and four-dimensional flow parameters.

4D flow parameter	Location	Diameter Z-score	Intercept	Coefficient	R	p-value
Energy loss	LPA	RPA	213.19	-32.56	0.4370	0.00865
Energy loss	RPA	RPA	179.80	-49.66	0.4419	0.00787
Vorticity	LPA	RPA	56451	-4062	0.4571	0.00577
Vorticity	RPA	RPA	52532	-5207	0.4487	0.00686

LPA: left pulmonary artery, RPA: right pulmonary artery.

DISCUSSION

Decreased exercise capacity after the ASO for TGA is a common long term complication. We investigated whether decreased exercise capacity related to haemodynamic parameters in the PAs assessed with 4D flow CMR. The study conveys the following findings:

1. In our cohort, 42% of patients have a $\text{predVO}_{2\text{peak}}/\text{kg} < 80\%$.
2. Increased energy loss in the MPA and LPA is associated with a decreased exercise capacity.
3. Increased kinetic energy and increased vorticity in the LPA are associated with a decreased exercise capacity.
4. RPA diameter Z-scores were associated with energy loss and vorticity in both the LPA and RPA

We found that 42% of our cohort has a decreased exercise capacity, with a mean $\text{predVO}_{2\text{peak}}/\text{kg}$ of $82 \pm 16\%$. These findings on exercise capacity are in line with previous studies in patients who underwent ASO for TGA.^{4, 16, 17} Ruys et al. report that 53% of their cohort has a $\text{predVO}_{2\text{peak}}/\text{kg} < 85\%$, van Beek et al. report a mean $\text{predVO}_{2\text{peak}}/\text{kg}$ of $81.4 \pm 10.9\%$ and Giardini et al report a mean $\text{predVO}_{2\text{peak}}/\text{kg}$ of $84 \pm 15\%$. Studies demonstrating

a higher $\text{predVO}_{2\text{peak}}/\text{kg}$ in patients after the ASO did not include adults, but only young children.^{18, 19} Factors thought to be of influence on the exercise capacity of TGA patients who underwent ASO are (amongst others) chronotropic incompetence, RV dysfunction, coronary abnormalities, aortic valve regurgitation and PS. In our cohort, none of our patients suffered from chronotropic incompetence or biventricular dysfunction, median percentage of aortic regurgitation was 2.0% (IQR: 1 – 3.7%). Furthermore, only two patients had an aberrant coronary artery pattern and no patients showed signs of ischemia during the CPET. These findings suggest that decreased exercise capacity in our cohort could be related to PS.

With 4D flow CMR, several hemodynamic parameters can be calculated within the PAs. Energy loss is a quantitative measure of the mechanical kinetic energy irreversibly lost to thermal energy, due to friction forces between viscous fluids and the adjacent wall¹⁰ and may be a marker of an inefficient circulation. We found increased energy loss in the MPA and LPA to be associated with a decreased exercise capacity. Although the clinical significance of energy loss has not been investigated in TGA patients before, results are in line with previous studies in patients with Fontan circulation.^{20, 21} Khiabani et al. and Tang et al. used computational fluid dynamics simulations to calculate energy loss in the total cavopulmonary connection in Fontan patients and both found a significant negative relationship between energy loss and exercise capacity.^{20, 21}

Besides energy loss, we found increased kinetic energy and vorticity in the LPA to be associated with a decreased exercise capacity. Kinetic energy represents the amount of energy required for the blood to circulate. Kinetic energy is increased when more energy is required to achieve circulatory demand. Vorticity is a quantification of the local flow rotation (spin) rate of the blood flow. These parameters have not been investigated in TGA patients before, but our results are in line with previous research in patients with Fontan circulation. Kamphuis et al. investigated Fontan patients who underwent 4D flow CMR before and after dobutamine infusion. Dobutamine stress caused an increase in kinetic energy, vorticity, and energy loss averaged over the complete cardiac cycle. These increases in kinetic energy, vorticity, and energy loss all showed a negative correlation to $\text{VO}_{2\text{peak}}$.²² Furthermore, vortex flow has been previously described in patients with repaired tetralogy of Fallot and patients with pulmonary hypertension.^{23, 24} Although the clinical relevance of vortices in the pulmonary arteries remains to be investigated, flow vortices in general are associated with alterations in the wall shear stress of the vessel which has a negative impact on the endothelial function.^{25, 26}

Our results show multiple significant associations between RPA diameter Z-scores and 4D flow parameters in both the LPA and RPA, but no associations between advanced

flow parameters in the RPA and exercise capacity. Interestingly, we found multiple significant associations between RPA diameter Z-scores and 4D flow parameters in both the LPA and RPA, but no associations between LPA diameter Z-scores and 4D flow parameters. One explanation could be that RPA stenosis, causing abnormal flow patterns and flow acceleration in the RPA, results in abnormal flow in the MPA and LPA, and thus also influences 4D flow parameters there. These results are interesting, since it is often hypothesized that, due to the usually more rightward position of the neo-pulmonary root, the LPA is stretched more and also has to cross the aortic root, which is frequently dilated after ASO. This could lead to more cases of stenosis in the LPA. This is confirmed by Morgan et al., who showed that patients with a rightward neo-pulmonary root and/or a dilated aortic root had a smaller LPA area.²⁷ Furthermore, in a cohort of 400 patients assessed by Khairy et al., PA intervention was required 1.5 times more for the LPA compared to the RPA.²⁸ Our results suggest that the RPA diameter has influence on haemodynamics in both the LPA and the RPA, which in turn could have consequences for the clinical status of patients. Further research into interplay between the RPA and LPA and the influence of PS on pulmonary haemodynamics is warranted.

One of the great advantages of 4D flow CMR is that it provides us with a wide range of novel advanced flow parameters. Furthermore, 4D flow CMR provides opportunity for retrospective valve tracking and retrospective position of planes to measure flow and velocities throughout the complete PAs. 4D flow parameters can give us more insight into the often-complex circulation in patients with congenital heart disease. As is the case with all novel imaging parameters, the clinical significance needs to be investigated. This study is a first step towards determining the clinical relevance of 4D flow CMR in TGA patients. We believe that 4D flow CMR will be an important tool in the haemodynamic assessment of patients with congenital heart disease, with a clear need for comprehensive serial evaluation of the cardiovascular system.

LIMITATIONS

There are several limitations that need to be taken into account. First, CMR and CPET were not always performed on the same day. We included CPETs up to one year prior to CMR to limit the effect of age or lifestyle changes on exercise capacity. Second, 4D flow CMR has a limited spatial and temporal resolution, a relatively long acquisition time and time and skill required for post-processing.²⁹ These limitations currently hamper widespread clinical implementation for the follow-up of patients after ASO, although recent improvements in CMR techniques have provided shorter acquisition times and more user-friendly postprocessing software.

CONCLUSION

We show that multiple advanced 4D flow parameters in the PAs of TGA patients have negative association with exercise capacity, including energy loss, kinetic energy and vorticity. These parameters may therefore be important to monitor during serial follow-up with 4D flow CMR of these patients. Furthermore, in the future, they may be helpful in decision making for the timing of potential (repeat) interventions. The advanced parameters provided by 4D flow CMR may provide novel methods to investigate haemodynamics and clinical status in TGA patients. Further research in larger groups of patients is warranted to determine the clinical significance of our findings.

REFERENCES

1. Brickner ME, Hillis LD, Lange RA. Congenital heart disease in adults. Second of two parts. *N Engl J Med* 2000;342:334–342.
2. Jatene AD, Fontes VF, Paulista PP, Souza LC, Neger F, Galantier M, et al. Anatomic correction of transposition of the great vessels. *J Thorac Cardiovasc Surg* 1976;72:364–370.
3. Lecompte Y, Neveux JY, Leca F, Zannini L, Tu TV, Dubois Y, et al. Reconstruction of the pulmonary outflow tract without prosthetic conduit. *J Thorac Cardiovasc Surg* 1982;84(5):727–731.
4. Ruys TP, van der Bosch AE, Cuypers JA, Witsenburg M, Helbing WA, Bogers AJ, et al. Long-term outcome and quality of life after arterial switch operation: a prospective study with a historical comparison. *Congenit Heart Dis.* 2013 May-Jun;8(3):203–10. doi: 10.1111/chd.12033.
5. Choi BS, Kwon BS, Kim BG, et al. Long-Term Outcomes After an Arterial Switch Operation for Simple Complete Transposition of the Great Arteries. *Korean Circ J* 2010;Jan;40(1):23–30
6. Baumgartner H, De Backer J, Babu-Narayan SV, et al. 2020 ESC Guidelines for the management of adult congenital heart disease. *Eur Heart J.* 2020 Aug 29;ehaa554. doi: 10.1093/eurheartj/ehaa554.
7. Bender R, Lange S. Adjusting for multiple testing—when and how? *J Clin Epidemiol.* 2001 Apr;54(4):343–9. doi: 10.1016/s0895-4356(00)00314-0.
8. Warmerdam E, Krings GJ, Leiner T, Grotenhuis HB. Three-dimensional and four-dimensional flow assessment in congenital heart disease. *Heart.* 2020 Mar;106(6):421–426. doi: 10.1136/heartjnl-2019-315797.
9. van der Steeg GE, Takken T. Reference values for maximum oxygen uptake relative to body mass in Dutch/Flemish subjects aged 6–65 years: the LowLands Fitness Registry. *Eur J Appl Physiol.* 2021 Feb 1. doi: 10.1007/s00421-021-04596-6.
10. Pettersen MD, Du W, Skeens ME, Humes RA. Regression equations for calculation of z scores of cardiac structures in a large cohort of healthy infants, children, and adolescents: an echocardiographic study. *J Am Soc Echocardiogr.* 2008 Aug;21(8):922–34. doi: 10.1016/j.echo.2008.02.006.
11. Barker AJ, van Ooij P, Bandi K, Garcia J, Albaghdadi M, McCarthy P, Bonow RO, Carr J, Collins J, Malaisrie SC, Markl M. Viscous energy loss in the presence of abnormal aortic flow. *Magn Reson Med.* 2014 Sep;72(3):620–8. doi: 10.1002/mrm.24962.
12. Kamphuis VP, Westenberg JJM, van der Palen RLF, van den Boogaard PJ, van der Geest RJ, de Roos A, Blom NA, Roest AAW, Elbaz MSM. Scan-rescan reproducibility of diastolic left ventricular kinetic energy, viscous energy loss and vorticity assessment using 4D flow MRI: analysis in healthy subjects. *Int J Cardiovasc Imaging.* 2018 Jun;34(6):905–920. doi: 10.1007/s10554-017-1291-z.
13. R Core Team (2017). R: A language and environment for statistical computing. R Foundation for Statistical Computing, Vienna, Austria. URL <https://www.R-project.org/>.
14. H. Wickham. ggplot2: Elegant Graphics for Data Analysis. Springer-Verlag New York, 2009.

15. Bender R, Lange S. Adjusting for multiple testing--when and how? *J Clin Epidemiol.* 2001 Apr;54(4):343-9. doi: 10.1016/s0895-4356(00)00314-0.
16. van Beek E, Binkhorst M, de Hoog M, de Groot P, van Dijk AP, Schokking M, et al. Exercise performance and activity level in children with transposition of the great arteries treated by the arterial switch operation. *Am J Cardiol* 2010;Feb 1;105(3):398-403
17. Giardini A, Khambadkone S, Rizzo N, Riley G, Pace Napoleone C, Muthialu N, et al. Determinants of exercise capacity after arterial switch operation for transposition of the great arteries. *Am J Cardiol.* 2009 Oct 1;104(7):1007-12. doi: 10.1016/j.amjcard.2009.05.046.
18. Reybrouck T, Eyskens B, Mertens L, Defoor J, Daenen W, Gewillig M. Cardiorespiratory exercise function after the arterial switch operation for transposition of the great arteries. *Eur Heart J.* 2001;22:1052–1059.
19. Samos F, Fuenmayor G, Hossri C, Elias P, Ponce L, Souza R, Jatene I. Exercise Capacity Long-Term after Arterial Switch Operation for Transposition of the Great Arteries. *Congenit Heart Dis.* 2016 Mar-Apr;11(2):155-9. doi: 10.1111/chd.12303.
20. Khiabani RH, Whitehead KK, Han D, Restrepo M, Tang E, Bethel J, Paridon SM, Fogel MA, Yoganathan AP. Exercise capacity in single-ventricle patients after Fontan correlates with haemodynamic energy loss in TCPC. *Heart.* 2015 Jan;101(2):139-43. doi: 10.1136/heartjnl-2014-306337.
21. Tang E, Wei ZA, Whitehead KK, Khiabani RH, Restrepo M, Mirabella L, Bethel J, Paridon SM, Marino BS, Fogel MA, Yoganathan AP. Effect of Fontan geometry on exercise haemodynamics and its potential implications. *Heart.* 2017 Nov;103(22):1806-1812. doi: 10.1136/heartjnl-2016-310855.
22. Kamphuis VP, Elbaz MSM, van den Boogaard PJ, Kroft LJM, Lamb HJ, Hazekamp MG, Jongbloed MRM, Blom NA, Helbing WA, Roest AAW, Westenberg JJM. Stress increases intracardiac 4D flow cardiovascular magnetic resonance -derived energetics and vorticity and relates to VO2max in Fontan patients. *J Cardiovasc Magn Reson.* 2019 Jul 25;21(1):43. doi: 10.1186/s12968-019-0553-4.
23. Geiger J, Markl M, Jung B, Grohmann J, Stiller B, Langer M, et al. 4D-MR flow analysis in patients after repair for tetralogy of Fallot. *Eur Radiol.* 2011 Aug;21(8):1651-7. doi: 10.1007/s00330-011-2108-4.
24. Schäfer M, Barker AJ, Kheyfets V, Stenmark KR, Crapo J, Yeager ME, et al. Helicity and Vorticity of Pulmonary Arterial Flow in Patients With Pulmonary Hypertension: Quantitative Analysis of Flow Formations. *J Am Heart Assoc.* 2017 Dec 20;6(12):e007010. doi: 10.1161/JAHA.117.007010.
25. Davies PF. Flow-mediated endothelial mechanotransduction. *Physiol Rev.* 1995 Jul;75(3):519-60. doi: 10.1152/physrev.1995.75.3.519.
26. Chien S, Li S, Shyy YJ. Effects of mechanical forces on signal transduction and gene expression in endothelial cells. *Hypertension.* 1998 Jan;31(1 Pt 2):162-9. doi: 10.1161/01.hyp.31.1.162.

27. Morgan CT, Mertens L, Grotenhuis H, Yoo SJ, Seed M, Grosse-Wortmann L. Understanding the mechanism for branch pulmonary artery stenosis after the arterial switch operation for transposition of the great arteries. *Eur Heart J Cardiovasc Imaging*. 2017 Feb;18(2):180-185. doi: 10.1093/ehjci/jew046.
28. Khairy P, Clair M, Fernandes SM, Blume ED, Powell AJ, Newburger JW et al. Cardiovascular outcomes after the arterial switch operation for D-transposition of the great arteries. *Circulation* 2013;127:331–9.
29. Dyverfeldt P, Bissel M, Barker AJ, et al. 4D flow cardiovascular magnetic resonance consensus statement. *J Cardiovasc Magn Reson*. 2015 Aug 10;17(1):72. doi: 10.1186/s12968-015-0174-5.



Chapter 13

General discussion and
future perspectives

GENERAL DISCUSSION

Major advances in diagnostics, perioperative care and surgical techniques have improved the survival rate of CHD patients dramatically. Conversely, although approximately 90% of infants with CHD survive into adulthood¹, the rate of long-term morbidity has increased, which often requires (repeat) intervention. Thereby, the timing of intervention is often difficult. Too early intervention may lead to an unnecessary increase in the number of interventions during adulthood. However, too late intervention may lead to irreversible damage. Thus, there is a great need for advanced non-invasive diagnostic modalities for optimal timing of intervention, and innovative percutaneous treatment options. In this thesis we investigate different imaging techniques and evaluate several percutaneous treatment options for different CHD groups.

In **chapter 2** we present an overview of the possibilities for haemodynamic evaluation in CHD patients of four-dimensional flow CMR (4D flow CMR) and computational fluid dynamics (CFD). 4D flow CMR is the term used for time-resolved phase-contrast CMR with flow-encoding in all three spatial directions. Using 4D-flow CMR, qualification and quantification of flow over an entire volume can be obtained. The major benefit of 4D flow CMR is that it is currently the only modality that can give an advanced quantitative evaluation of blood flow in vivo. The drawbacks are the limited spatial and temporal resolution and relatively long acquisition time.

CFD is a specialized area of mathematics and a branch of fluid mechanics, often used in engineering to study complex flow patterns. It can be used to evaluate blood flow in the cardiovascular system of patients in a reconstructed 3D model of the patient's anatomy. Due to the fact CFD relies on calculations rather than in-vivo measurements, it has several advantages: the unlimited spatial and temporal resolution, the potential to perform virtual surgery or stent implantation and the ability to simulate different loading conditions. However, CFD outcomes are always an approximation of reality and are highly dependent on the quality of the reconstructed anatomy images and the applied boundary conditions. We conclude in our review that, although further research is warranted, both modalities show great potential to evaluate haemodynamic parameters in CHD patients and can help to improve our understanding of the complex circulation in CHD.

PART ONE – COARCTATION OF THE AORTA

Despite successful initial repair, patients with coarctation of the aorta (CoA) often develop hypertension later in life.² Due to the risk of long-term complications because of hypertension or recurrent CoA, lifelong follow-up is warranted for patients with (repaired) CoA.³ Regular blood pressure evaluation and cardiac imaging are recommended. Because of the need for repeated imaging throughout life, the preferred advanced imaging modality for follow-up is cardiac magnetic resonance (CMR). Furthermore, CMR provides a non-invasive assessment of left ventricular (LV) function and dimensions, and a comprehensive overview of cardiovascular anatomy. Over the last years, the scope of CMR has been expanded with 4D flow CMR. 4D flow CMR allows for extensive evaluation of cardiovascular flow within an entire volume. Previous studies investigating CoA patients using 4D flow CMR have shown abnormal flow phenomena in patients with CoA and after successful CoA repair.⁴⁻⁶ In **chapter 3** we present the results of the 4D-FLOAT study (four-dimensional flow cardiac magnetic resonance imaging for the assessment of coarctation of the aorta). This was the first 4D flow CMR study in our centre, in which we investigated the relationship between advanced 4D flow parameters and LV function, volume and mass in patients suspected of (recurrent) CoA. We found several 4D flow parameters to have a significant relationship with LV characteristics. Local flow rotation, as expressed by maximum vorticity, in the descending aorta was found to be related to LV end-diastolic volume. Local flow orientation, as expressed by maximum axial angle, in the ascending aorta was found to be related to LV mass. Pulse wave velocity measured by 4D flow CMR was also found to be related to LV mass. Several patients in this study had a bicuspid aortic valve (BAV). The abnormal arrangement of the aortic valve leaflets in BAV generates an abnormal flow pattern in the aorta. To determine whether the correlations found in this study were not solely driven by the presence of patients with BAV in our cohort, we performed a comparison of the values of 4D flow CMR parameters found to have a significant association with LV parameters for patients with BAV and normal, tricuspid, aortic valve. No significant differences were found between the two groups. We conclude that 4D flow CMR may provide novel parameters to assess haemodynamics and the interaction between the aorta and the LV in patients with (recurrent) CoA.

As of the 1990s, percutaneous treatment became widely accepted as treatment option for CoA. Nowadays, placement of a balloon-expandable stent is the treatment of choice for older children and adults with CoA. Percutaneous stent placement as treatment for CoA leads to fewer acute complications than surgical repair and has acute angiographic and long-term results comparable with surgical repair.⁴ However, despite successful initial repair, blood pressure control in adults with (a history of) CoA proves to be

suboptimal in many cases.⁴ Furthermore, only a handful of studies have investigated the effect of stent placement on blood pressure control in adult patients. We conducted a retrospective study at our centre, presented in **chapter 4**, to investigate the effect of CoA stenting on blood pressure control in adult CoA patients. Mean systolic blood pressure decreased significantly after stent implantation and remained at this level at follow-up. The number of hypertensive patients also decreased significantly. There was no significant difference in defined daily dose of medication or number of pills taken per patient at baseline and follow up post-intervention. Thus, stent placement for CoA led to a sustained decrease in blood pressure, while there was no significant difference in prescribed antihypertensive medication. Taking into account all the observations in this study, we believe that more vigorous imaging and treatment protocols could be beneficial in selected groups of CoA patients. Early diagnosis of recurrent CoA or suboptimal intervention combined with a more aggressive interventional approach could lead to improvement in blood pressure regulation.

There are several reasons why patients can suffer from hypertension late after CoA repair. Around 10% of patients with CoA have a concomitant hypoplastic aortic arch. Both systemic hypertension and abnormal blood pressure response to exercise have been reported in patients with a hypoplastic aortic arch.^{5,6} Although research on this procedure is limited, this patient group might benefit from stent placement in the aortic arch. In **chapter 5** of this thesis, we present a retrospective study at our centre to evaluate the safety and efficacy of aortic arch stenting in patients with CoA and a concomitant hypoplastic aortic arch. We found the procedure to be safe; no major complications occurred during the procedure or follow-up. The immediate angiographic result was excellent, the mean peak-to-peak gradient over the aortic arch dropped significantly, as did the mean systolic blood pressure. We believe that when aortic arch hypoplasia is thought to play an important role in the presence of persistent hypertension after CoA repair, stent implantation should be considered to improve clinical outcome in the long term.

PART TWO – TETRALOGY OF FALLOT

Due to improved treatment options, 90% of the patients with tetralogy of Fallot (TOF) are alive 20 years after initial repair.⁷ However, survival of TOF patients decreases substantially during the third and fourth decades of life.⁷ This decrease in survival is mainly caused by long term sequelae associated with surgical repair. Right ventricular (RV) dysfunction related to pulmonary insufficiency and / or stenosis is the most common long-term complication in TOF and responsible for RV failure, arrhythmias and sudden

cardiac death.⁸⁻¹⁰ Surgical and percutaneous pulmonary valve replacement (PVR) are procedures which can lead to a decrease in RV volumes and improved symptoms^{11,12}, but emerging data show that, using current CMR criteria, they unfortunately do not prevent postoperative ventricular arrhythmias, heart failure, and sudden death.¹³

The timing of PVR has been subject of academic debate for decades and will most likely remain a controversial topic in the future. To summarize the longstanding discussion on pulmonary valve replacement, we provide an overview in **chapter 6** on the current status and future perspectives of percutaneous pulmonary valve replacement (PPVI). PPVI has become an accepted and widely used technique for treating RV outflow tract dysfunction in several CHDs, particularly after initial surgical repair. Research shows excellent results on short- and medium-term follow-up. The most important complications are coronary artery compression during the procedure and in the long term, infective endocarditis. In the near future the scope of PPVI could be expanded when RV outflow tract reducer devices will become available, that make PPVI feasible in large (native) RV outflow tracts. Furthermore, advances in imaging techniques such as 4D flow CMR and CFD could provide more insights in the complex interplay of increased loading conditions and intrinsic myocardial (dys)function of the heart in TOF, and could potentially contribute to optimal timing of PVR in TOF. In **chapter 7** of this thesis we provide a comprehensive review of available research on 4D flow CMR in TOF patients. We conclude that 4D flow CMR is more accurate in measuring pulmonary flow and especially valvular regurgitation fraction compared to 'regular' two-dimensional phase contrast CMR (2D PC CMR). Furthermore, compared to healthy controls, patients with TOF exhibit increased kinetic energy and vortex flow in the RV and pulmonary arteries (PAs) and increased wall shear stress and abnormal flow patterns in the aorta. These findings indicate a less efficient circulation in TOF. We believe that further research into advanced flow parameters in patients with TOF could potentially identify parameters suitable for the prediction of outcomes in patients with repaired TOF and perhaps even refine timing of PVR.

PART THREE – TRANSPOSITION OF THE GREAT ARTERIES

The current treatment of choice for transposition of the great arteries (TGA) is the arterial switch operation (ASO) combined with the Lecompte manoeuvre.^{14,15} Although the ASO has an excellent survival rate, frequent complications occur such as dilation of the ascending aorta and PA stenosis (PS).¹⁶ Branch PS is the most common cause for reintervention after ASO, with an incidence of up to 20% of ASO patients.^{16,17} The degree of PS can be determined by the dimensions of the branch PAs, the distribution of blood

flow to left and right PA, and maximum velocities in the PAs. The maximum velocity can be determined by several imaging modalities such as Doppler echocardiography, 2D PC CMR, 4D flow CMR, and can be simulated used CFD. 4D flow CMR and CFD have the advantage that they can give an evaluation of the blood flow within an entire volume instead of a single slice, which is the case for 2D PC CMR. Furthermore, both 4D flow CMR and CFD are non-invasive and do not require the administration of iodine contrast, which greatly reduces risks and burden for the patient, compared to CT and cardiac catheterization. Since TGA patients need lifelong follow-up, a non-invasive modality that does not require contrast and can give a comprehensive evaluation of the cardiovascular status would be ideal. In **chapter 8**, we present a head-to-head comparison of 4D flow CMR and CFD analysis in healthy pulmonary arteries and TGA patients. We evaluate four different cases: a patient with 'normal' PAs, a TGA patient without branch PS, a TGA patient with unilateral branch PS, and a patient with bilateral branch PS. We found that CFD and 4D flow CMR provided comparable results in evaluation of peak velocities, flow distribution, flow patterns and wall shear stress distribution for patients with and without PS. We only found substantial differences for absolute wall shear stress values; these were consistently lower for 4D flow CMR. We believe more research is warranted to identify the prognostic value and clinical application of both imaging techniques. In **chapter 9** we compare maximum velocities measured by 4D flow CMR with 2D PC CMR and Doppler echocardiography. We show that maximum velocities measured by 4D flow CMR are significantly higher compared to maximum velocities measured by 2D PC CMR. Maximum velocities for 4D flow CMR and Doppler echocardiography were comparable. However, for the majority of patients, the branch PAs could not be visualized using echocardiography, making it impossible to perform velocity measurements. The results of this study show that 4D flow CMR is better fit to investigate the presence and severity of PS in patients after ASO than 2D PC CMR and Doppler echocardiography.

Patients after ASO often have a reduced exercise capacity when compared to their healthy peers.¹⁸ Regular clinical evaluation of patients after ASO is therefore necessary to assess (progression of) exercise intolerance and determine the need for intervention. In **chapter 10** we investigate which CMR and echocardiographic imaging parameters are associated with a reduced exercise capacity in patients late after ASO. In our cohort, one in five patients suffered from a reduced exercise capacity. We found the main PA gradient and tricuspid regurgitation gradient by echocardiography to be associated with reduced exercise capacity. Based on these results, a cardiopulmonary exercise test would be indicated when the patient complains of reduced exercise tolerance or when echocardiography or CMR suggests main PA stenosis or when an increased tricuspid regurgitation gradient is found. With 4D flow CMR, we can obtain a wide range of novel advanced flow parameters. In **chapter 11** we present a case of a TGA patient with a

decreased exercise capacity, in whom 4D flow CMR reveals vortex flow in the right PA and increased energy loss in this region. His decreased exercise capacity may be related to this energy loss. To date, the clinical relevance of most 4D flow parameters is still unclear. To determine which parameters could be useful in the follow-up of TGA patients after ASO, we investigate in **chapter 12** which advanced 4D flow parameters are associated with exercise capacity. We found increased energy loss in the main and left PA and increased kinetic energy and increased vorticity in the left PA to be associated with a decreased exercise capacity. Results of this study show that abnormal haemodynamics in the PAs after ASO have implications for the clinical status of patients.

FUTURE PERSPECTIVES

The increased survival of CHD patients means this patient group will continue to grow, and physicians will be confronted with novel long-term complications. Innovation in the field of diagnostics and interventions for CHD is therefore crucial. In this thesis, we investigate the role of 4D flow CMR and several different percutaneous treatment strategies for CHD.

There are several reasons why 4D flow CMR is ideally suited for haemodynamic evaluation in CHD patients. First, it is a non-invasive modality and does not require the administration of iodinated contrast. This means the burden for the patient is low, which is important when there is a need for lifelong follow-up. Second, the ability of retrospective valve-tracking eliminates through-plane motion of the valve, making 4D flow CMR superior to 2D PC CMR in evaluating valvular flow, as we report in chapter 7. Regurgitation fraction and peak gradient (calculated from peak velocity) are important indicators in evaluating the need for valve replacement. It is therefore crucial to have serial measurements that are as precise as possible. Third, the ability to analyse a complete volume and retrospectively identify an area of interest compared to analysing single pre-defined planes is a great advantage and leads to a more accurate analysis of the blood flow, as we see in chapter 8. This is due to the fact that 2D PC CMR only measures flow in a single direction (orthogonal to the acquired plane) and thus does not take into account non-laminar flow, which is often present in patients with CHD. Furthermore, when planning the plane for analysis of 2D PC CMR, it is often difficult to position the plane perpendicular to the vessel, whereas the ability of 4D flow CMR to retrospectively position the plane of interest ensures that plane is positioned exactly right. This is important, since positioning the plane not exactly perpendicular to the vessel can give an underestimation of the velocity magnitude. Finally, the fact that 4D flow CMR acquires a complete volume instead of a single plane, means that it can

provide a wide range of advanced flow parameters, such as wall shear stress, energy loss and vorticity. As is the case with all novel imaging parameters, the clinical significance of these parameters needs to be investigated.

There are several practical and technical limitations that currently make it challenging to incorporate 4D flow CMR in CMR protocols for regular patient care. Most important limitations are the relatively long acquisition time and the limited temporal and spatial resolution. Since innovation in the field of CMR is rapidly evolving, the aforementioned limitations are likely to be solved in the near future. With these practical issues out of the way, serial assessment with 4D flow CMR is likely to become of great importance to improve our understanding of complex congenital heart disease. Furthermore, it could help to optimize timing of interventions and prevent progression of cardiovascular deterioration.

In the last decades, the scope of percutaneous interventions for CHD has widened to include valve replacement, stent placement for relief of arterial stenosis, closure of collateral vessels and closure of septal defects. In the future, we expect the scope to widen even further to the development of novel stents and devices. Evidence for the safety and efficacy of most percutaneous interventions for CHD is limited, even for procedures that are widely accepted and often performed. For example, closure of a patent ductus arteriosus in case of left ventricular volume overload, CoA stenting in case of hypertension and a peak-to-peak aortic gradient of > 20 mmHg, and pulmonary valve replacement in TOF patients with severe pulmonary regurgitation and at least moderate RV outflow tract obstruction, are all class I indications, with level of evidence C (expert opinion) in the most recent European Society of Cardiology guidelines.¹⁹ The reasons for this lack of evidence are clear: CHD is a relatively small group within the population of cardiovascular disease and it is a heterogeneous population. However, this does not mean the need for evidence-based medicine is somehow less in this patient group, or that novel treatment strategies do not require thorough evaluation. Obviously, retrospective single-centre studies (as presented in this thesis) will not solve this issue. They can, however, be a first step towards a multicentre or national collaboration to investigate treatment strategies. In the future, more prospective, protocolized multicentre research is warranted for treatment of CHD and academic medical centres should initiate this research and collaborate to ultimately provide optimal care for the growing group of CHD patients.

REFERENCES

1. Oster ME, Lee KA, Honein MA, et al. Temporal trends in survival among infants with critical congenital heart defects. *Pediatrics*. 2013;May;131(5):e1502-8.
2. Rinnstrom D, Dellborg M, Thilen U, et al. Hypertension in adults with repaired coarctation of the aorta. *Am Heart J*. 2016;181:10–5.3. Brown ML, Burkhart HM, Connolly HM, et al. Coarctation of the aorta: lifelong surveillance is mandatory following surgical repair. *J Am Coll Cardiol*. 2013 Sep 10;62(11):1020-1025.
3. Brown ML, Burkhart HM, Connolly HM, et al. Coarctation of the aorta: lifelong surveillance is mandatory following surgical repair. *J Am Coll Cardiol*. 2013;62:1020–5.
4. Hope MD, Meadows AK, Hope TA, et al. Clinical evaluation of aortic coarctation with 4D flow MR imaging. *J Magn Reson Imaging*. 2010 Mar;31(3):711-8.
5. Senzaki H, Iwamoto Y, Ishido H, Masutani S, Taketazu M, Kobayashi T, et al. Ventricular-vascular stiffening in patients with repaired coarctation of aorta. *Circulation* 2008;118:S191–8.
6. Hope MD, Meadows AK, Hope TA, et al. Images in cardiovascular medicine. Evaluation of bicuspid aortic valve and aortic coarctation with 4D flow magnetic resonance imaging. *Circulation*. 2008 May 27;117(21):2818-9. doi: 10.1161/CIRCULATIONAHA.107.760124.
4. Hu ZP, Wang ZW, Dai XE et al. Outcomes of surgical versus balloon angioplasty treatment for native coarctation of the aorta: a meta-analysis. *Ann Vasc Surg*. 2014 Feb;28(2):394-403.
5. Ou P, Mousseaux E, Celermajer DS, et al. Aortic arch shape deformation after coarctation surgery: effect on blood pressure response. *J Thorac Cardiovasc Surg*. 2006;132:1105–11.
6. Ou P, Bonnet D, Auriacombe L, et al. Late systemic hypertension and aortic arch geometry after successful repair of coarctation of the aorta. *Eur Heart J*. 2004;25:1853–9.
7. Dennis M, et al. Adults with repaired tetralogy: low mortality but high morbidity up to middle age. *Open Heart* 2017 Mar 1;4(1):e000564
8. Gatzoulis MA, et al. Risk factors for arrhythmia and sudden cardiac death late after repair of tetralogy of Fallot: a multicentre study. *Lancet*. 2000 Sep 16;356(9234):975-81.
9. Hickey EJ, et al. Late risk of outcomes for adults with repaired tetralogy of Fallot from an inception cohort spanning four decades. *Eur J Cardiothorac Surg*. 2009 Jan;35(1):156-64
10. Chaturvedi RR, et al. Pulmonary regurgitation in congenital heart disease. *Heart*. 2007 Jul; 93(7): 880– 889.
11. Alkashkari, et al. Transcatheter Pulmonary Valve Replacement: Current State of Art. *Curr Cardiol Rep*. 2018 Mar 15;20(4):27
12. Ferraz Cavalcanti PE, et al. Pulmonary valve replacement after operative repair of tetralogy of Fallot: meta-analysis and meta-regression of 3,118 patients from 48 studies. *J Am Coll Cardiol*. 2013 Dec 10;62(23):2227-43.
13. Bokma JP, et al. A Propensity Score-Adjusted Analysis of Clinical Outcomes After Pulmonary Valve Replacement in Tetralogy of Fallot. *Heart*. 2018 May;104(9):738-744
14. Jatene AD, Fontes VF, Paulista PP, Souza LC, Neger F, Galantier M, et al. Anatomic correction of transposition of the great vessels. *J Thorac Cardiovasc Surg* 1976;72:364–370.

15. Lecompte Y, Neveux JY, Leca F, Zannini L, Tu TV, Dubois Y, et al. Reconstruction of the pulmonary outflow tract without prosthetic conduit. *J Thorac Cardiovasc Surg* 1982;84(5):727-731.
16. Ruys TP, Van der Bosch AE, Cuypers JA, et al. Long term Outcome and quality of life after arterial switch operation: a prospective study with a historical comparison. *Congenit Heart Dis*. 2013;May-Jun;8(3):203-10
17. Choi BS, Kwon BS, Kim BG, et al. Long-Term Outcomes After an Arterial Switch Operation for Simple Complete Transposition of the Great Arteries. *Korean Circ J* 2010;Jan;40(1):23-30
18. Ruys TP, Van der Bosch AE, Cuypers JA, et al. Long term Outcome and quality of life after arterial switch operation: a prospective study with a historical comparison. *Congenit Heart Dis*. 2013;May-Jun;8(3):203-10
19. Baumgartner H, De Backer J, Babu-Narayan SV, et al.; ESC Scientific Document Group. 2020 ESC Guidelines for the management of adult congenital heart disease. *Eur Heart J*. 2020 Aug 29;ehaa554. doi: 10.1093/eurheartj/ehaa554. Epub ahead of print. PMID: 32860028.



Appendix

Nederlandse samenvatting

List of publications

Review committee

Dankwoord

Curriculum vitae

NEDERLANDSE SAMENVATTING

Aangeboren hartafwijkingen zijn wereldwijd de meest voorkomende aangeboren afwijking. Naar schatting zijn er in Nederland zo'n 25.000 kinderen en meer dan 25.000 volwassenen met een aangeboren hartafwijking.¹ De afgelopen decennia zijn er grote ontwikkelingen geweest in de behandeling en diagnostiek van aangeboren hartafwijkingen. Door deze ontwikkelingen, met name binnen de hartchirurgie en interventiecardiologie, is de overleving voor patiënten met een aangeboren hartafwijking sterk toegenomen. Waar vroeger de meerderheid van de patiënten met aangeboren hartafwijkingen de volwassenheid niet haalde, is dat tegenwoordig meer dan 90%.² Helaas betekent deze verbetering in overleving wel dat patiënten vaker langetermijncomplicaties ondervinden en dat er in de loop van het leven vaker (opnieuw) interventies nodig zijn. Het is daarom van groot belang om diagnostische technieken te hebben die complicaties vroeg op kunnen sporen en interventietechnieken waarmee deze complicaties voorkomen of behandeld kunnen worden. In dit proefschrift onderzoeken we dan ook geavanceerde beeldvormende technieken en interventiestrategieën voor patiënten met verschillende aangeboren hartafwijkingen.

Vier dimensionele flow MRI (4D flow MRI) is een nieuwe MRI-techniek waarmee we gedetailleerd in drie dimensies over de tijd de bloedstroming kunnen analyseren. Met computational fluid dynamics (CFD) kan een simulatie van de cardiovasculaire bloedstroming in een patiënt gemaakt worden. In **hoofdstuk 2** van dit proefschrift geven we een overzicht van de mogelijkheden die 4D flow MRI en CFD bieden voor patiënten met aangeboren hartafwijkingen. De grote kracht van 4D flow MRI is dat het op dit moment de enige niet-invasieve methode is waarmee we metingen aan de bloedstroming van de patiënt kunnen doen. Het nadeel is dat het (net als andere MRI-technieken), niet voor iedereen geschikt is en dat patiënten lang stil moeten liggen voor de scan. Met CFD kunnen simulaties van de bloedstroming in het hart en de vaten van de patiënt gemaakt worden. Met deze techniek kunnen dus veel verschillende situaties doorgerekend worden, zonder dat het belastend is voor de patiënt: inspanning, het virtueel plaatsen van een stent en virtuele operaties. Een nadeel van een CFD-analyse is dat die arbeidsintensief is en veel rekenkracht nodig heeft. Beide technieken kunnen helpen cardiovasculaire complicaties bij patiënten met aangeboren hartafwijkingen op te sporen en meer inzicht te krijgen in de ontstaansmechanismen van deze complicaties.

DEEL 1 – COARCTATIE VAN DE AORTA

Coarctatie van de aorta (CoA) is een aangeboren vernauwing van de aorta.³ Door deze vernauwing kan er een te hoge bloeddruk (hypertensie) ontstaan en kunnen patiënten te maken krijgen met de gevolgen van langdurige hypertensie; zoals hartfalen, een hartinfarct of een herseninfarct. Om dit te voorkomen kan de vernauwing opgeheven worden door middel van een operatie of het plaatsen van een stent. Helaas krijgen veel patiënten, ondanks het succesvol opheffen van de vernauwing, later in het leven hypertensie. Daarnaast krijgt een klein deel opnieuw een vernauwing van de aorta.⁴ Patiënten met een CoA staan daarom meestal levenslang onder controle bij de cardioloog, om hun bloeddruk te monitoren en te controleren of er niet opnieuw een vernauwing in de aorta ontstaat.⁵ In eerdere onderzoeken met 4D flow MRI wordt een verstoorde bloedstroming gezien bij patiënten met een CoA. Het hebben van een CoA ook kan leiden tot een verminderde functie van de linkerhartkamer (linkerventrikel). In **hoofdstuk 3** onderzoeken we daarom de relatie tussen geavanceerde 4D flow MRI-parameters en de functie, volumina en massa van het linkerventrikel. Hierbij vonden we dat de afwijkingen in de bloedstroming (axiale hoek, energieverlies en polsgolfsnelheid) in de aorta gerelateerd zijn aan de volumina en massa van het linkerventrikel in patiënten met (recidief) CoA. We concluderen dan ook dat 4D flow MRI de potentie heeft om de effecten van de afwijkende bloedstroming bij CoA op het hart te onderzoeken.

Voor oudere kinderen en volwassenen met een CoA is het plaatsen van een stent de meest gebruikte behandeling. Ondanks een succesvolle correctie van de CoA krijgen veel patiënten later toch last van hypertensie. Het effect van stentplaatsing bij volwassen CoA-patiënten op de bloeddruk is nog niet vaak onderzocht. Daarom onderzoeken we in **hoofdstuk 4** wat de effecten zijn van het plaatsen van een stent in de aorta op latere (volwassen) leeftijd bij patiënten met (recidief) CoA. We zagen bij deze patiënten een duidelijk effect van het plaatsen van de stent op de bloeddruk, de bovendruk (systolische bloeddruk) daalde significant na stentimplantatie. Deze bloeddrukdaling bleek langdurig; ook na gemiddeld twintig maanden follow-up bleef de gemiddelde systolische bloeddruk op hetzelfde niveau. Het plaatsen van een stent voor (recidief) CoA blijkt ook op latere leeftijd dus nog effectief. Patiënten met CoA hebben regelmatig ook andere afwijkingen aan het hart of de vaten. Sommige patiënten hebben naast hun CoA ook een nauwe (hypoplastische) aortaboog.⁶ In dat geval kan het zijn dat alleen het corrigeren van de CoA niet voldoende is en dat patiënten door de hypoplastische aortaboog nog steeds hypertensie blijven houden. Deze patiënten zouden baat kunnen hebben bij het plaatsen van één of meerdere stents in de aortaboog. Er is echter nog weinig bekend over deze behandeltechniek. In **hoofdstuk 5** onderzoeken we de veiligheid en effectiviteit van stentplaatsing in de aortaboog bij CoA-patiënten die ook

een hypoplastische aortaboog hebben. Tijdens en na de procedure traden er geen ernstige complicaties op. De drukgradiënt over de aortaboog nam significant af, net als de systolische bloeddruk. Stentplaatsing in de aortaboog is dus een veilige procedure is (mits correct uitgevoerd) en geeft een significante bloeddrukdaling.

DEEL 2 – TETRALOGIE VAN FALLOT

Tetralogie van Fallot (TOF) is de meest voorkomende cyanotische aangeboren hartafwijking.⁷ Er is sprake van vier verschillende aanlegstoornissen: er zit een gat in het tussenschot van de linker- en rechterkamer (ventrikelseptumdefect), de longslagader is vernauwd, de aorta staat schuin boven de beide hartkamers en de hartspeer van de rechterkamer (rechterventrikel) is verdikt (hypertrofie).⁸ Hierdoor is het hart niet goed in staat het bloed naar de longen te pompen, waardoor er een zuurstoftekort (cyanose) ontstaat. Vanwege de ernst van de aandoening moeten kinderen met TOF al in de eerste levensjaren een openhartoperatie ondergaan. Met het ouder worden kan het zo zijn dat door lekken van deze klep of doordat het stroomgebied van de klep juist vernauwt, onherstelbare schade aan het hart optreedt door overbelasting.⁹ Om het optreden van deze schade te voorkomen, moet in de loop van het leven bij veel patiënten met TOF de longslagaderklep op een zeker moment worden vervangen. Als we patiënten selecteren voor een klepvervangings op basis van de huidige MRI-criteria, blijkt dat een klepvervangings wel zorgt voor verbetering van klachten, maar niet de ernstige langetermijengevolgen, zoals hartfalen en ritmestoornissen, kan voorkomen. Welke TOF-patiënten baat hebben bij een klepvervangings en wanneer de klepvervangings gedaan moet worden is al decennialang onderwerp van discussie. In **hoofdstuk 6** geven we een samenvatting van deze discussie en bespreken we de huidige status en toekomstige perspectieven van percutane klepvervangings bij patiënten met TOF. Met 4D flow MRI kunnen we veel metingen aan de bloedstroming doen die eerder niet mogelijk waren. We hopen dat we met 4D flow MRI uiteindelijk nieuwe criteria voor klepvervangings kunnen vinden. In **hoofdstuk 7** geven we een uitgebreid overzicht van het beschikbare onderzoek met 4D flow MRI in patiënten met TOF tot nu toe. We zien dat 4D flow MRI preciezer de lekkage van de klep kan meten dan de ‘traditionele’ 2D MRI meting. Verder zien we in de verschillende onderzoeken dat patiënten met TOF vergeleken met gezonde controles vaker een afwijkende bloedstroming en een minder efficiënte circulatie hebben. We weten alleen nog niet wat het effect is van deze afwijkende bloedstromingen, hoe ze veranderen na vervangings van de longslagaderklep en of ze wellicht kunnen voorspellen welke patiënten baat hebben bij klepvervangings.

TRANSPOSITIE VAN DE GROTE VATEN

Transpositie van de grote vaten (TGA) is na TOF de meest voorkomende aangeboren hartafwijking met cyanose.¹⁰ Bij TGA ontspringt de aorta uit het rechterventrikel en de longslagader uit het linkerventrikel. Op dit moment wordt dit meestal gecorrigeerd op babyleeftijd door middel van de arteriële switchoperatie (ASO) gecombineerd met de LeCompte manoeuvre.^{11,12} Met de arteriële switch operatie worden de grote vaten losgehaald en teruggezet op het 'correcte' ventrikel.¹¹ Met de LeCompte manoeuvre wordt de longslagader voor de aorta geplaatst.¹² De ASO heeft een uitstekende overleving en patiënten hebben vaak een goede kwaliteit van leven na de operatie.^{13,14} Toch treden bij deze operatieve correctie op de lange termijn ook complicaties op. De meest voorkomende complicatie is vernauwing (stenose) van de longslagaders.^{13,14} De ernst van deze stenose bepalen we onder andere aan de hand van de stroomsnelheid van het bloed op de plek van de stenose (pieksnelheid) en de verdeling van het bloedvolume tussen de linker en rechter longslagader. We kunnen de pieksnelheid en de volumina met verschillende technieken meten: Doppler echocardiografie, 2D flow MRI, 4D flow MRI en CFD. Het voordeel van 4D flow MRI en CFD is dat deze technieken metingen kunnen doen in een geheel volume (driedimensionaal). Dit in tegenstelling tot echo en 2D flow MRI, waarbij er alleen gemeten wordt in één vlak (tweedimensionaal). In **hoofdstuk 8** vergelijken we de metingen van 4D flow MRI en CFD in 'gezonde' longslagaders en longslagaders van TGA-patiënten. We concluderen dat beide technieken zeer goed overeenkomen met betrekking tot de metingen van pieksnelheid en volumina. In de waarden van de vaatwandspanning zien we wel verschillen tussen 4D flow MRI en CFD. In **hoofdstuk 9** vergelijken we de pieksnelheden in de longslagaders van TGA-patiënten gemeten met 4D flow MRI, 2D flow MRI en Doppler echocardiografie. We zien dat 4D flow MRI veel hogere pieksnelheden geeft dan 2D flow MRI. De pieksnelheden van 4D flow MRI en echocardiografie zijn vergelijkbaar, maar bij veel (vooral volwassen) patiënten was het onmogelijk de longslagaders in beeld te brengen met echo. Wij concluderen dan ook dat 4D flow MRI beter geschikt is voor het meten van pieksnelheden in de longslagaders van TGA-patiënten dan 2D flow MRI en echocardiografie. Patiënten met TGA hebben vergeleken met gezonde leeftijdsgenoten vaak een verminderde inspanningscapaciteit.¹³ In **hoofdstuk 10** onderzoeken we welke echocardiografie- en MRI-parameters gerelateerd zijn aan een verminderde inspanningscapaciteit. We zagen hier dat een verhoogde druk in het rechter ventrikel en een verhoogde druk in de longslagader gerelateerd waren aan een verminderde inspanningscapaciteit. In **hoofdstuk 11** beschrijven we een TGA-patiënt die een 4D flow MRI onderging en waarop we een kolkende bloedstroming en energieverlies in de rechter longslagader zien. Deze patiënt had ook een verminderde inspanningscapaciteit. Mogelijk speelt de inefficiënte kolkende bloedstroming een rol

bij de verminderde inspanningscapaciteit. In **hoofdstuk 12** onderzoeken we welke 4D flowparameters geassocieerd zijn met een verminderde inspanningscapaciteit na de ASO. We zien dat verhoging van energieverlies, kinetische energie en vortciteit in de linker longslagader gerelateerd zijn aan een vermindering van de inspanningscapaciteit. Abnormale bloedstroming in de longslagader kan dus mogelijk gevolgen hebben voor de inspanningscapaciteit van de patiënt.

CONCLUSIE

Dankzij grote vooruitgang in de zorg voor patiënten met een aangeboren hartafwijking is de overleving sterk verbeterd. Dit zorgt er ook voor dat deze patiëntengroep steeds groter wordt. Om deze steeds groeiende groep patiënten de optimale zorg te kunnen bieden, is het belangrijk dat we blijven innoveren, zowel op diagnostisch als therapeutisch gebied. Gelukkig kunnen er steeds meer interventies percutaan verricht worden, zoals het stenten van een CoA of hypoplastische aortaboog. Ook is het percutaan plaatsen van een longslagaderklep voor steeds meer patiënten een optie. Op diagnostisch gebied is de 4D flow MRI een veelbelovende techniek. De mogelijkheid om het gehele vat (in plaats van slechts één doorsnede) te kunnen analyseren blijkt zeer waardevol. Daarnaast zijn er verschillende geavanceerde flowparameters die in de toekomst wellicht kunnen helpen bij de indicatiestelling voor interventie, of om te evalueren hoe de circulatie van een patiënt verandert over de tijd.

REFERENTIES

1. van der Velde ET, Vriend JW, Mannens MM, Uiterwaal CS, Brand R, Mulder BJ. CONCOR, an initiative towards a national registry and DNA-bank of patients with congenital heart disease in the Netherlands: rationale, design, and first results. *Eur J Epidemiol.* 2005;20(6):549-57.
2. Oster ME, Lee KA, Honein MA, et al. Temporal trends in survival among infants with critical congenital heart defects. *Pediatrics.* 2013;May;131(5):e1502-8.
3. Torok RD, Campbell MJ, Fleming GA, Hill KD. Coarctation of the aorta: Management from infancy to adulthood. *World J Cardiol.* 2015 Nov 26;7(11):765-775.
4. Hager A, Kanz S, Kaemmerer H, Schreiber C, Hess J. Coarctation Long-term Assessment (COALA): significance of arterial hypertension in a cohort of 404 patients up to 27 years after surgical repair of isolated coarctation of the aorta, even in the absence of restenosis and prosthetic material. *J Thorac Cardiovasc Surg.* 2007 Sep;134(3):738-745.
5. Brown ML, Burkhart HM, Connolly HM, Dearani JA, Cetta F, Li Z, et al. Coarctation of the aorta: lifelong surveillance is mandatory following surgical repair. *J Am Coll Cardiol.* 2013 Sep 10;62(11):1020-1025.
6. Ou P, Bonnet D, Auriacombe L et al. Late systemic hypertension and aortic arch geometry after successful repair of coarctation of the aorta. *Eur Heart J.* 2004 Oct;25(20):1853-1859.
7. Villafane J, Feinstein JA, Jenkins KJ, et al. Hot topics in tetralogy of Fallot. *J Am Coll Cardiol.* 2013;Dec;10;62(23):2155-66
8. Fallot E. Contribution a l'anatomie pathologique de la maladie bleue (cyanose cardiaque). *Mars Med.* 1888;25:77ff
9. Gatzoulis MA, Balaji S, Webber SA et al. (2000) Risk factors for arrhythmia and sudden cardiac death late after repair of tetralogy of Fallot: a multicentre study. *Lancet.* 356:975-981
10. Brickner ME, Hillis LD, Lange RA. Congenital heart disease in adults. Second of two parts. *N Engl J Med.* 2000;342:334-342.
11. Jatene AD, Fontes VF, Paulista PP, Souza LC, Neger F, Galantier M, et al. Anatomic correction of transposition of the great vessels. *J Thorac Cardiovasc Surg.* 1976;72:364-370.
12. Lecompte Y, Neveux JY, Leca F, Zannini L, Tu TV, Dubois Y, et al. Reconstruction of the pulmonary outflow tract without prosthetic conduit. *J Thorac Cardiovasc Surg.* 1982;84(5):727-731.
13. Ruys TP, Van der Bosch AE, Cuypers JA, Witsenburg M, Helbing WA, Bogers AJ, et al. Long term Outcome and quality of life after arterial switch operation: a prospective study with a historical comparison. *Congenit Heart Dis.* 2013;May-Jun;8(3):203-10.
14. Choi BS, Kwon BS, Kim BG, et al. Long-Term Outcomes After an Arterial Switch Operation for Simple Complete Transposition of the Great Arteries. *Korean Circ J.* 2010;Jan;40(1):23-30
15. Grotenhuis HB, Kroft LJM, van Elderen SGC, Westenberg JJM, Doornbos J, Hazekamp MG, et al. Right ventricular hypertrophy and diastolic dysfunction in arterial switch patients without pulmonary artery stenosis. *Heart.* 2007;Dec;93(12):1604-1608.

LIST OF PUBLICATIONS

Warmerdam EG, van Assen HC, Sotelo J, Grotenhuis HB. Abnormal vortex formation in the right pulmonary artery after the arterial switch operation. *Eur Heart J Case Rep*. 2021 Jan 15;5(1):ytaa549.

Warmerdam EG, Magni F, Leiner T, Doevendans PA, Sieswerda GT, van Wijk SW, Breur HM, Driesen BW, Grotenhuis HB*, Takken T*. Echocardiography and MRI parameters associated with exercise capacity in patients after the arterial switch operation. *J Cardiol*. 2020 Sep;76(3):280-286.

Warmerdam EG, Krings GJ, Leiner T, Grotenhuis HB. Three-dimensional and four-dimensional flow assessment in congenital heart disease. *Heart*. 2020 Mar;106(6):421-426.

Warmerdam EG, Krings GJ, Meijs TA, Franken AC, Driesen BW, Sieswerda GT, Meijboom FJ, Doevendans PAF, Molenschot MMC, Voskuil M. Safety and efficacy of stenting for aortic arch hypoplasia in patients with coarctation of the aorta. *Neth Heart J*. 2020 Mar;28(3):145-152.

Meijs TA, **Warmerdam EG**, Slieker MG, Krings GJ, Molenschot MMC, Meijboom FJ, Sieswerda GT, Doevendans PA, Bouma BJ, de Winter RJ, Mulder BJM, Voskuil M. Medium-term systemic blood pressure after stenting of aortic coarctation: a systematic review and meta-analysis. *Heart*. 2019 Oct;105(19):1464-1470.

van Setten J, **Warmerdam EG**, Groot OQ, de Jonge N, Keating B, Asselbergs FW. Non-HLA Genetic Factors and Their Influence on Heart Transplant Outcomes: A Systematic Review. *Transplant Direct*. 2019 Jan 21;5(2):e422.

Driesen BW, **Warmerdam EG**, Sieswerda GJ, Meijboom FJ, Molenschot MMC, Doevendans PA, Krings GJ, van Dijk APJ, Voskuil M. Percutaneous Pulmonary Valve Implantation: Current Status and Future Perspectives. *Curr Cardiol Rev*. 2019;15(4):262-273.

van der Burg JJ, **Warmerdam EG**, Krings GJ, Meijboom FJ, van Dijk AP, Post MC, Veen G, Voskuil M, Sieswerda GT. Effect of stent implantation on blood pressure control in adults with coarctation of the aorta. *Cardiovasc Revasc Med*. 2018 Dec;19(8):944-950.

Driesen BW, **Warmerdam EG**, Sieswerda GT, Schoof PH, Meijboom FJ, Haas F, Stella PR, Kraaijeveld AO, Evens FCM, Doevendans PAFM, Krings GJ, van Dijk APJ, Voskuil M.

Anomalous coronary artery originating from the opposite sinus of Valsalva (ACAOS), fractional flow reserve- and intravascular ultrasound-guided management in adult patients. *Catheter Cardiovasc Interv.* 2018 Jul;92(1):68-75.

Warmerdam EG, Toorop RJ, Abrahams AC, Berger P. An indwelling urethral catheter knotted around a double-j ureteral stent: an unusual complication after kidney transplantation. *Case Rep Nephrol.* 2011;2011:672326.

MANUSCRIPTS IN PREPARATION

Warmerdam EG*, Neijzen RL*, Voskuil M, Leiner T, Grotenhuis HB. Four-dimensional flow CMR in tetralogy of Fallot: current perspectives. *Submitted*

Warmerdam EG, Westenberg JJM, Voskuil M, van Assen HC, Roest A, van Wijk B, Sieswerda GT, ter Heide HH, Krings GJ, Leiner T, Grotenhuis HB. Head-to-head comparison of 4D flow CMR 2D flow CMR and Doppler echocardiography for the detection of pulmonary artery stenosis in patients after the arterial switch operation. *Submitted*

Conijn M*, **Warmerdam EG***, Westenberg JJM, Haas F, Leiner T, Sotelo J, Uribe S, Voskuil M, Krings GJ*, Grotenhuis HB*. Head-to-head comparison between computational fluid dynamics and four-dimensional flow CMR of the pulmonary arteries in congenital heart disease. *Submitted*

Warmerdam EG, Sotelo, J, Driesen BW, Uribe S, Westenberg JJM, Leiner T, Krings GJ, Voskuil M, Grotenhuis HB. Abnormal aortic flow related to left ventricular mass and volume in coarctation: a four-dimensional flow CMR study. *Submitted*

Warmerdam EG, Takken T, van Assen HC, Westenberg JJM, van Ooij P, Krings GJ, Roest AAW, Rijnberg FM, Breur JMP, van der Zwaan HB, Voskuil M, Leiner T, Grotenhuis HB. Impact of pulmonary haemodynamics on exercise performance in patients after the arterial switch operation. *In preparation*

* Shared first/last authorship

